

Modeling the Impacts of Land Use Activities on the Subsurface Flow Regime of the Upper Roanoke River Watershed

Victoria Ann Barone

Thesis submitted to the Faculty of the
Virginia Polytechnic Institute and State University
in partial fulfillment of the requirements for the degree of

Master of Science
in
Biological Systems Engineering

Dr. Saied Mostaghimi, Chair
Dr. Thomas Burbey
Dr. David Kibler

January 21, 2000
Blacksburg, Virginia

Keywords: Groundwater Modeling, Simulation, MODFLOW, Fractured Bedrock, Upper
Roanoke River Watershed

Copyright 2000, Victoria Ann Barone

Modeling the Impacts of Land Use Activities on the Subsurface Flow Regime of the Upper Roanoke River Watershed

Victoria Ann Barone

(ABSTRACT)

The goal of this study was to determine the impact of land use activities on the subsurface flow regime in the Upper Roanoke River Watershed in Virginia to determine the impacts of land use change on the subsurface flow system, and to provide a tool for future management decisions. Land use activities can impact the groundwater system in two ways. The volume of water recharging the groundwater system can be reduced due to an increase in low permeable areas. It is assumed in this investigation that the input recharge values reflect the increase of low permeability zones that may occur due to land use activities. Increased water withdrawal associated with an increase in population can be another impact of land use change. This possible increase in water withdrawal is explicitly simulated in this investigation.

MODFLOW, the USGS , three-dimensional, finite-difference, groundwater flow model was used to develop a regional conceptualization of the flow system. The fractured bedrock aquifer system consists of three sloping geohydrologic units: the Ordovician to Mississippian clastics, the Cambrian and Ordovician carbonates, and the Precambrian and Cambrian metamorphics and clastics. The 575 mi² study area was divided into cells with dimensions of 0.25 miles by 0.25 miles and containing four layers. The upper model layer was used to simulate the saturated unconsolidated deposits that lie on top of the fractured bedrock and serve primarily as a recharge reservoir. The second layer simulated shallow flow driven by recharge and the withdrawal of water by pumping wells. The bottom two layers were used to simulate deep regional flow within the system and account for possible vertical flow that may be occurring through deep fractures.

Several simplifying assumptions were made during the conceptualization of groundwater flow in the study area: (1) Flow through fractures is approximately equivalent to flow through a porous medium; (2) Darcy's Law is applicable from a regional perspective; (3) Hydraulic

properties are homogeneous and isotropic for an area that is represented by a model cell; and (4) Groundwater flow divides correspond to surface-water flow divides. Although these assumptions are probably valid for parts of the study area, the validity of each assumption is mostly unknown. Therefore, the model results are considered to be conceptual and should be interpreted carefully.

The groundwater flow model was calibrated using UCODE, a USGS code for universal inverse modeling. Parameter estimation was conducted using UCODE for a total of 18 parameters, including hydraulic conductivities, river bottom conductance values, and recharge rates. The model was calibrated to observed hydraulic head information from 1969-1970. Due to the limited data availability, however, the calibrated values are at best, approximate. Nonetheless, several inferences can be made regarding flow in the province.

The calibrated recharge values indicate that approximately 28% of the total precipitation recharges the aquifer system. This is consistent with previous estimates performed in the study area (Rutledge, Mesko, 1996). The Cambrian and Ordovician carbonates were found generally to have the highest hydraulic conductivity in each layer which reflects the notion that due to dissolution, this geohydrologic unit contains more fractures than the other two units. The calibrated values of hydraulic conductivity for the Cambrian and Ordovician carbonates ranged from 0.89m/d in layer 2 to 0.0011m/d in layer 4. The calibrated values of hydraulic conductivity for the Precambrian and Cambrian metamorphics and clastics ranged from 0.013m/d in layer 2 to 0.708E-3m/d in layer 4, and for the Ordovician to Mississippian clastics followed a similar trend in layers 2 and 3, with values of 0.390m/d in layer 2 and 0.242E-4m/d in layer 3.

The streambed conductance values reflected both the variation in streambed thickness, which ranges from nonexistent in some areas to several feet thick in others, and streambed material, which ranges from sandy material with relatively high conductivity values to silty material with lower hydraulic conductivity values. The streambed conductance values range from 4.79 m²/d in the upland reaches to 234.13 m²/d in reaches closer to the outlet.

Present pumping conditions were simulated with the groundwater flow model to establish a “baseline simulation” to which all future scenarios could be compared. Three future scenarios were developed based on the projected increase in population for Roanoke County through the year 2010. Each scenario represented a distinct settlement pattern within the watershed. Development scenario 1 simulated the impacts of the increased population if settled in the same

areas as present development. Development scenario 2 simulated the impacts of the increased population if half settled in areas of present development and the other half in the western half of the watershed. Development scenario 3 simulated the impacts of the increased population if half of the population increase settled in areas of present development and the other half settled in the Tinker Creek sub-watershed. Development scenario 2 resulted in a drastic change in hydraulic head values, and the volume of water discharged from the streams was, on average, reduced by 56%, whereas, for both scenarios 1 and 2, these reductions were less than 1%.

Results indicate that flow in the system is predominantly horizontal. There is no deep vertical flow from possible deep fractures. There may be shallow vertical flow occurring that is driven by recharge, however due to the resolution of the model, this flow is not simulated. In general, the simulation of horizontal flow follows the overall trend of the hydraulic gradient from west to east, which also follows the overall topographic trend. Therefore, upland regions in the province are recharging down-gradient areas. However, simulations indicate that the hydraulic head values in the eastern part of the study area are relatively insensitive to this horizontal recharge contribution from the west.

The most sensitive areas in the basin to increased water withdrawal are the upland areas in the west side of the study area that are receiving no horizontal flow contribution from other places in the watershed. These areas are only being recharged by precipitation, and are the first to react to regional flow changes. Since the resolution of the model is such that local variations in the flow system are not simulated and the model represents regional trends, inferences can only be made about regional impacts. Therefore, if increased withdrawals are so great as to impact the regional system, the west- side of the study area will be affected before all other areas in the watershed.

The study results include estimates of hydraulic properties, direction of regional flow, possible impacts from land use change, and a discussion of the results with respect to gaining a more complete understanding of the subsurface flow system. Perhaps this work will be the first step in learning more about the subsurface flow system of the Upper Roanoke River Watershed, and provide a useful tool to manage and properly plan future land use changes to minimize the impacts on the groundwater resources of the basin.

Acknowledgements

The author would like to sincerely thank all of the people who have offered their encouragement and help during the work on this thesis. Special thanks to her committee chairman, Dr. Saied Mostaghimi for his support, guidance, encouragement, and most of all, for believing in her. Appreciation also goes to Dr. Thomas Burbey and Dr. David Kibler for their guidance, counsel, and time as committee members.

The author would also like to acknowledge all those who assisted in the collection of data, and who offered technical support throughout the investigation. Without their help, this thesis would not have been possible. Many thanks to friends for their support and encouragement, but most of all for listening. Special thanks to Jason Bestimt for his programming support and constant encouragement. Finally, the author would like to thank her parents for their unconditional love, support and encouragement.

Table of Contents

1.0 Introduction.....	1
1.1 Background.....	1
1.2 Goal and Objectives	3
2.0 Literature Review	4
2.1 Introduction	4
2.2 Urban Growth.....	4
2.3 Positive Impacts of Urbanization	5
2.4 Negative Impacts of Urbanization.....	5
2.4.1 Fuel/Energy Consumption.....	5
2.4.2 Industrial Pollutants.....	6
2.4.3 Wastes.....	6
2.4.4 Nutrient Loading.....	7
2.4.5 Urban Runoff.....	7
2.5 Groundwater	7
2.6 Groundwater Models	8
2.7 MODFLOW	9
2.7.1 Mathematical Model.....	10
2.7.2 Discretization.....	11
2.7.3 Finite Difference Equation	12
2.7.4 Iteration.....	16
2.7.5 Boundary Conditions.....	17
2.7.6 Program Structure.....	18
2.7.7 The Basic Package.....	20
2.7.7.1 The IUNIT Array.....	21

2.7.7.2	The IBOUND Array	21
2.7.7.3	Initial Conditions	21
2.7.7.4	Time Discretization	21
2.7.7.5	Output	22
2.7.7.6	Budget Calculations.....	23
2.7.8	The Block-Centered Flow Package	23
2.7.8.1	Basic Conductance Equations	23
2.7.8.2	Horizontal Conductance	24
2.7.8.3	Vertical Conductance	26
2.7.8.4	Storage Formulation	29
2.7.9	The River Package.....	31
2.7.10	The Recharge Package.....	33
2.7.11	The Well Package.....	34
2.7.12	The General-Head Boundary Package	35
2.7.13	The Streamflow-Routing Package.....	36
2.7.14	Limitations of MODFLOW.....	37
2.7.15	Steady-State vs. Transient Models	37
2.8	Applications of MODFLOW	38
2.8.1	Managing Existing Problems in a Groundwater System.....	38
2.8.2	Evaluating Effects of Proposed Water Withdrawal.....	39
2.8.3	Evaluating the Effects of Land Development.....	41
2.9	UCODE	43
2.9.1	UCODE Program Structure	43
2.9.2	Calculation of Sensitivities.....	46
2.9.3	Weighted Least-Squares Objective Function	48

2.9.4 Modified Gauss-Newton Optimization	49
2.9.4.1 Normal Equations and the Marquardt Parameter	49
2.9.5 Convergence Criteria.....	50
2.10 Visual MODFLOW	51
2.11 Summary of the Literature Review	51
3.0 Methodology	53
3.1 The Study Area.....	53
3.1.1 Climate	54
3.1.2 Land Use.....	56
3.1.3 Population and Household Size.....	57
3.1.4 Groundwater Use In the Study Area.....	59
3.1.5 Groundwater Level and Movement.....	60
3.1.6 Geohydrologic Units	60
3.1.7 Available Data.....	66
3.2 Conceptual Model	69
3.2.1 Model Assumptions.....	69
3.2.2 Representation of the System as a Four Layer Model.....	74
3.2.3 Modeling Approach.....	75
3.2.3.1 Creating the Model Grid.....	75
3.2.3.2 Adjusting the Data.....	81
3.2.3.3 Initial Hydraulic Head Data.....	81
3.2.3.4 River Input Values.....	82
3.2.3.5 Hydraulic Conductivities.....	84
3.2.3.6 Recharge	87
3.2.4 Summary of the Conceptual Model.....	89

3.3 Calibration	89
3.3.1 Calibration Data.....	89
3.3.2 Calibration Results	93
3.3.2.1 River Bottom Conductance Values	95
3.3.2.2 Hydraulic Conductivities.....	96
3.3.2.3 Sensitivity Analysis	97
3.3.2.4 Recharge.....	99
3.3.3 Recalibration with Stream Routing	99
3.3.4 Summary of the Model Calibration.....	105
4.0 Results and Discussion	108
4.1 Introduction	108
4.2 Simulation Results.....	108
4.2.1 Storage Values.....	109
4.2.2 Hydraulic Head Contours	110
4.2.2.1 Dry Cells.....	110
4.2.2.2 Vertical Flow	113
4.2.2.3 Model Performance Evaluation through Hydraulic Head Contour Comparision	115
4.2.3 Information on Horizontal Flow Direction.....	117
4.2.4 Surface-Water-Groundwater Interaction	118
4.2.4.1 Explanation of Discharge Results	119
4.2.4.2 Discharge Trend	123
4.3 Model Application.....	124
4.3.1 Baseline Simulation.....	125
4.3.1.1 Baseline Simulation Results	128
4.3.2 Future Development Scenarios.....	132

4.3.2.1 Development Scenario 1.....	135
4.3.2.2 Development Scenario 2.....	141
4.3.2.3 Development Scenario 3.....	148
4.4 Zone Budget Analysis	154
4.5 Summary of the Results and Discussion	156
5.0 Summary and Conclusions	159
6.0 Recommendations for Future Studies	164
7.0 References.....	166
Appendices	172
Appendix A - MODFLOW and Visual MODFLOW model files.....	172
Appendix B - Observed Hydraulic Heads	173
Appendix C – C++ Programs	176
Appendix D - Regression Analysis	177
Appendix E – UCODE files	179
Appendix F – MODFLOW and HSPF Interaction.....	180
Vita.....	184

List of Figures

Figure 1. Discretized hypothetical aquifer system in MODFLOW (McDonald and Harbaugh, 1988).....	12
Figure 2. Cell i,j,k and indices for the six adjacent cells in MODFLOW (McDonald and Harbaugh, 1988).....	13
Figure 3. Hydrograph for cell i,j,k in MODFLOW (McDonald and Harbaugh, 1988)	16
Figure 4. Overall MODFLOW program structure (McDonald and Harbaugh, 1988).....	19
Figure 5. Organization of modules in MODFLOW by procedures and packages (McDonald and Harbaugh, 1988).....	20
Figure 6. Example of the boundary layer (IBOUND) for a single layer in MODFLOW (McDonald and Harbaugh, 1988).....	22
Figure 7. Division of simulation time into stress periods and time steps in MODFLOW (McDonald and Harbaugh, 1988).....	23
Figure 8. Prism of porous material illustrating Darcy's law (McDonald and Harbaugh, 1988)...	25
Figure 9. Calculation of conductance through several prisms in series in MODFLOW (McDonald and Harbaugh, 1988).....	26
Figure 10. Calculation of conductance between nodes using transmissivity and dimensions of cells in MODFLOW (McDonald and Harbaugh, 1988)	27
Figure 11. Diagram for calculation of vertical leakance, V_{cont} , between two nodes which fall within a single geohydrologic unit (McDonald and Harbaugh, 1988).....	28
Figure 12. Diagram for calculation of vertical leakance, V_{cont} , between nodes located at the midpoints of vertically adjacent geohydrologic units	29
Figure 13. Diagram for calculation of vertical leakance, V_{cont} , between two nodes located at the midpoints of aquifers which are separated by a semiconfining unit (McDonald and Harbaugh, 1988).....	30
Figure 14. (a) Cross section of an aquifer containing a stream and (b) Conceptual representation of stream-aquifer interconnection in simulation (McDonald and Harbaugh, 1988) ...	32
Figure 15. Plot of flow, $QRIV$, from a stream into a cell as a function of head, h , in the cell where $RBOT$ is the elevation of the streambed and $HRIV$ is the head in the stream (McDonald and Harbaugh, 1988).....	33

Figure 16. Flow chart of UCODE UCODE (Hill and Poeter, 1998)	44
Figure 17. Location of study area in the state of Virginia (Waller, 1976).....	54
Figure 18. Physiographic and cultural features, Upper Roanoke River Basin (Waller, 1976)	55
Figure 19. Population Growth and Projections – Roanoke County	58
Figure 20. Population growth and projections – Greater Roanoke Valley	59
Figure 21. Geohydrologic units of the Upper Roanoke River Basin (Waller, 1976).....	64
Figure 22. Major geologic structures of the Upper Roanoke River Basin (Waller, 1976)	72
Figure 23. Conceptual model of the Upper Roanoke River Watershed.....	72
Figure 24. Cross-sectional view of Roanoke County (Breeding and Dawson, 1976)	73
Figure 25. Location of cross sections within Roanoke County (Breeding and Dawson, 1976) ..	73
Figure 26. Model domain represented in Visual MODFLOW	77
Figure 27A. Location of the cross-sectional column in Visual MODFLOW	79
Figure 27B. Cross section of model domain along highlighted column in Figure 27A	79
Figure 28A. Location of the cross-sectional row in Visual MODFLOW	80
Figure 28B. Cross section of model domain along highlighted row in Figure 28A	80
Figure 29. River overlay in Visual MODFLOW (.DXF file)	83
Figure 30. General-Head Boundaries represented in Visual MODFLOW	83
Figure 31. Sections of different river bottom conductance values represented in Visual MODFLOW	84
Figure 32. Distribution of hydraulic conductivity of layer 2	85
Figure 33. Distribution of hydraulic conductivity of layer 3	86
Figure 34. Distribution of hydraulic conductivity of layer 4	86
Figure 35. DXF overlay distinguishing recharge areas.....	87
Figure 36. Recharge distribution in MODFLOW	88

Figure 37. Location of known hydraulic heads used for calibration (Waller, 1976)	91
Figure 38. Observed well data locations within the study area (Waller (1976), and Montgomery Co. Health Dept.)	103
Figure 39. Observed vs. calculated hydraulic head values for observation points in Figure 38.	104
Figure 40. Sections of river assigned constant conductance values.....	105
Figure 41. Transient simulation results, layer 1 hydraulic head contours (20m intervals).....	111
Figure 42. Transient simulation results, layer 2 hydraulic head contours (20m intervals).....	112
Figure 43. Transient simulation results, layer 3 hydraulic head contours (20m intervals).....	112
Figure 44. Transient simulation results, layer 4 hydraulic head contours (20m intervals).....	113
Figure 45. Interpolated hydraulic head surface from hydraulic head observations in Figure 39 (ArcView).....	116
Figure 46. Transient simulation results, layer 2 hydraulic head contours (selected intervals, m)	116
Figure 47. Transient simulation - general direction of horizontal flow in layer 2	117
Figure 48. Surface-water-groundwater interaction dictated by the gradient between the two systems	118
Figure 49. Segment numbers and locations (defined in Streamflow-Routing Package) (Prudic,1989).....	120
Figure 50. Transient simulation average flux (m ² /day) for segments 1-23 (Figure 49).....	121
Figure 51. Model resolution and its effects on detailed output.....	123
Figure 52. Trend of average discharge vs. distance from outlet	124
Figure 53. Roanoke County wells pumping as of year 1996 – baseline simulation	128
Figure 54. Baseline simulation results, layer 2 hydraulic head contours (20m intervals)	129
Figure 55. Baseline simulation average flux (m ² /day) for segments 1-23 (defined in Figure 49).....	130
Figure 56. Population vs. withdrawals (mgd) in Roanoke County for the years 1982-1995.....	134

Figure 57. Location of Glenvar East and Glenvar New well – scenario 1.....	136
Figure 58. Pumping scenario 1 results, layer 2 hydraulic head contours (20m intervals)	138
Figure 59. Pumping scenario 1 average flux (m ² /day) for segments 1-23 (defined in Figure 49).....	139
Figure 60. Locations of wells added to baseline simulation for scenario 2	143
Figure 61. Pumping scenario 1 results, layer 2 hydraulic head contours (20m intervals)	144
Figure 62. Pumping scenario 2 average flux (m ² /day) for segments 1-23 (defined in Figure 49).....	145
Figure 63. General location of the Tinker Creek subwatershed in the Upper Roanoke River Basin.....	148
Figure 64. Pumping scenario 3 results, layer 2 hydraulic head contours (20m intervals) when population increase is concentrated completely in Tinker Creek	149
Figure 65. Locations of wells added to baseline simulation for scenario 3	150
Figure 66. Pumping scenario 3 results, layer 2 hydraulic head contours (20m intervals)	151
Figure 67. Pumping scenario 3 average flux (m ² /day) for segments 1-23 (defined in Figure 49).....	152
Figure 68. Zone defined to determine horizontal flow contribution from the west side of the study area.....	155

List of Tables

Table 1. List of packages in MODFLOW (McDonald and Harbaugh, 1988)	11
Table 2. Land use in the Upper Roanoke River Watershed	56
Table 3. Composite Sequence of Geologic and Geohydrologic Units, Upper Roanoke River Watershed (Waller, 1976)	63
Table 4. Input file for interpolation of boundary between layers 2 and 3	78
Table 5. Parameters estimated using UCODE	90
Table 6. Initial value and optimal value for estimated parameters during calibration with UCODE	94
Table 7. Summary of scaled composite sensitivities for all parameters	98
Table 8. Storage Values for the three hydrogeologic units	109
Table 9. Segment total discharge, length, and average flux for the transient simulation	122
Table 10. Individual well composition of combination wells	126
Table 11. Existing wells in Roanoke County pumping more than 10,000gal/day as of 1996 (DEQ, 1999)	127
Table 12. Segment total discharge, length, and average flux for baseline pumping simulation.	131
Table 13. Percent difference of average flux values for each segment for the baseline simulation with respect to the transient simulation.....	132
Table 14. Aquifer pumping capacities/possible yields (Waller, 1976)	134
Table 15. Future development scenarios simulated for the Upper Roanoke River Watershed ..	135
Table 16. Pumping rates for existing wells in Roanoke County pumping more than 10,000gal/day as of 1996 (DEQ, 1999) - future development scenario 1	137
Table 17. Segment total discharge, length, and average flux for pumping scenario 1	139
Table 18. Percent difference of discharge values for segments 1-23 between the baseline simulation and pumping scenario 1	140

Table 19. Pumping rates for existing wells in Roanoke County pumping more than 10,000gal/day as of 1996 (DEQ, 1999) - future development scenario 2.....	142
Table 20. Pumping rates for wells added to baseline simulation for scenario 2.....	143
Table 21. Segment total discharge, length, and average flux for pumping scenario	146
Table 22. Percent difference of discharge values for segments 1-23 between the baseline simulation and pumping scenario 2.....	147
Table 23. New pumping rates for wells added to baseline simulation for scenario 3.....	150
Table 24. Segment total discharge, length, and average flux for pumping scenario 3	152
Table 25. Percent difference of discharge values for segments 1-23 between the baseline simulation and pumping scenario 3.....	153
Table 26. Percent Difference of Stream Leakage with Respect to Baseline Simulation	161

Chapter 1

Introduction

1.1 Background

The quality and quantity of groundwater is an important public issue because it is estimated that 50% of the total population, and 95% of the rural households in the U.S. depend upon groundwater for drinking (Canter et al., 1988). Thus, it is important that groundwater is managed and protected as a key natural resource. Each year in the U.S. urban expansion claims another 420,070 acres of land (Lazaro, 1990). In fact, over 60% of the U.S. land surface has been altered for human "needs" (Cairns, 1995). Land-use change can significantly impact the hydrology of a natural system and we depend on groundwater as a plentiful resource. Therefore, it is important to understand how land development and urbanization effects the groundwater system.

The change of pervious to impervious land, a result of intense development associated with urbanization, has a significant impact on hydrology. Urbanization reduces the amount of infiltration into the groundwater system and can affect the quality of water discharged from a watershed. The groundwater flow regime is significantly impacted due to a reduction in recharge. Since recharge can be the driving force of groundwater flow, not only can this reduction change flow magnitude and direction, it can reduce the hydraulic heads of the system, affect the surface-water groundwater interaction and reduce the volume of water available for withdrawal. Reduced recharge can affect the ability of the system to serve as a reliable water supply. Pollutants that accumulate on impervious surfaces during dry periods are flushed into streams, rivers, lakes, and reservoirs during rainfall events and can degrade water quality. This can increase the maximum pollutant loads that the receiving natural systems eventually have to assimilate. Vegetation is sometimes completely stripped from the land during site development and the bare soil is exposed to the erosive forces of rainfall which could, in turn, increase the sediment loads in runoff during storm events. If the groundwater and surface water systems are hydrologically adjacent and interact dynamically, the pollution of one can cause reduction in quality of the other (Fetter, 1999). Furthermore, land subsidence can occur due to an increase in

withdrawal, which can reduce the water-producing qualities of the groundwater system and can cause structural damage to buildings.

It is important to keep in mind that cities, or concentrated land development areas, offer important opportunities for protecting the environment as well. If properly planned, dense settlement patterns can reduce pressures on land from population growth and can provide opportunities to increase energy efficiency. Recycling wastes is more feasible because of large quantities of materials, and the number of industries that can benefit from it is greater (Hardoy, 1992). The development of the proper infrastructure required to manage wastes may be easier and more cost effective to build and maintain, if it was concentrated in one area instead of being spread over a large area. Therefore, it is becoming increasingly important to more fully understand and characterize the effects that urbanization has on the environment. This understanding can lead to the proper planning and anticipation of impacts to provide a healthy, clean, and less intrusive environment for both the urban areas and the surrounding ecosystems. This understanding can be achieved through the use of mathematical models to predict the effects of development and urbanization on these ecosystems and perhaps appropriate measures can be implemented to minimize potential negative impacts.

Concern over water quality and the effects of urbanization on the hydrologic cycle has prompted the development of watershed monitoring programs and the use of comprehensive water quality models (Fauss, 1986). Monitoring programs are costly, but have allowed the development of databases that are an excellent source of information on watershed response to precipitation. Together with the use of comprehensive hydrologic models, the information collected through monitoring can be used to predict the impacts of land use changes on the subsurface flow system.

1.2 Goal and Objectives

The overall goal of this study was to determine the impact of land use activities on the subsurface flow regime in the Upper Roanoke River Watershed through groundwater modeling.

The specific objectives to achieve the goal of the study were to:

- 1) Select and apply an appropriate model to the Upper Roanoke River Watershed to determine the impacts of land use activities on the subsurface flow regime, and
- 2) Evaluate the model by comparing the model's results with the observed data available from the study area.
- 3) Perform sensitivity analyses on potential future groundwater withdrawals based on future growth projections for Roanoke County.

Chapter 2

Literature Review

2.1 Introduction

Urbanization refers to the change of land from an existing land use to one that supports a city or a town. This chapter introduces urbanization, and discusses recent trends in patterns of urbanization. It discusses both positive and negative impacts of urbanization, and more specifically, focuses on the impacts of urbanization on groundwater as a natural resource. Generally, impacts of urbanization on the environment are considered to be negative, however, these effects have not yet been fully understood. This chapter discusses the importance of characterizing the effects of urbanization on groundwater through the use of mathematical groundwater models. Perhaps a more complete understanding of these effects can allow for the proper planning and management of groundwater as a safe drinking water source.

2.2 Urban Growth

In 1995, more than 70 percent of the population in both Europe and North America was living in urban areas (U.N., 1995). In the United States, urban population growth has slowed to less than 1.3 percent per year (WRI, 1997). Much of the population shift now under way involves the movement away from centralized urban centers to vast, sprawling metropolitan regions, or to small intermediate-size cities. The physical dimensions of cities have changed along with population growth. Urban sprawl, sometimes referred to as “extended metropolitan regions” or “functional urban regions” include smaller urban centers and even rural areas outside of the urban core whose populations and activities are clearly part of the functioning city (U.N., 1996). The traditional urban downtown has been replaced by a multitude of interconnected suburbs, which makes the design and functionality of infrastructure difficult to maintain. When urban expansion takes place in traditional cities, the population is concentrated in small areas which potentially allows for efficient planning and maintenance of associated infrastructure. However, when urban sprawl takes place, sometimes the rate of growth exceeds the rate of proper planning, and the impacts of land use change are not entirely considered which could potentially be costly and harmful to the surrounding environment.

2.3 Positive Impacts of Urbanization

Historically, cities have been the driving force in economic and social development. They are centers of wealth and political power, as well as industry and commerce. Cities and towns also account for a disproportionate amount of the national income. The World Bank estimates that as much as 80 percent of future economic growth will occur in towns and cities in the developing world (Barton et al., 1994). Urbanization is also associated with a variety of other positive impacts such as higher incomes, improved health, higher literacy, and overall improved quality of life. Other benefits include access to information, diversity, creativity, and innovation. (WRI, 1997). These positive impacts however, are commonly over-shadowed by potential negative effects of urbanization on the environment.

2.4 Negative Impacts of Urbanization

The most acknowledged environmental problem associated with urbanization is the degradation of water quality (WRI, 1997). Cities use rivers, lakes, and coastal waters as receptacles for disposing wastes. The natural processes of water flow and associated biological processes occurring in these bodies of water help break down wastes. The increasing urban populations and the increasing amount of wastes they are producing have overtaxed the assimilative capacity of local rivers and lakes. Urban areas put tremendous pressures on the environment due to the heavy concentration of people, industry, buildings, transportation, and human activity. They provide higher potential for pollution through the concentration of industry and industrial pollutants; produce an abundance of waste to be disposed of; increase the amount and the rate of urban runoff; and as a result provide a higher potential for surface and ground water pollution.

2.4.1 Fuel/Energy Consumption

Since economic activities and urban inhabitants are clustered in urban areas, cities require vast quantities of resources. Advanced transportation networks allow resources to be tapped from distant areas so that urban communities are rarely confronted with the impacts of their resource consumption. (WRI, 1997). Urban energy demand and fossil fuel consumption continues to grow despite the potential for energy efficiency in cities. Along with population

growth, economic development, and industrialization, urbanization is one of the principal forces driving the global increase in energy demand (Gugler, 1988). Today's urban societies rely heavily on fossil fuels and electricity which may lead to a variety of negative environmental impacts as a result of urban growth. The increased transportation in and around cities increases the amount of pollutants deposited on pavement from vehicles, which eventually washes off during rainfall events and could potentially contaminate receiving waters.

2.4.2 Industrial Pollutants

There is a concentration of industrial pollutant sources associated with urban areas. Most large cities have severe water pollution problems due to chemical intensive-industries such as tanneries, metal plating operations, pulp mills, and refineries. Typical contaminants include organochlorides such as polychlorinated biphenols (PCBs) and dioxins, pesticides, grease and oil from automobiles and shipping traffic, acids and caustics, heavy metals such as cadmium and lead, sewage sludge, and a long list of synthetic organic compounds (Fetter, 1999). The concentration of industry in urban areas increases the potential for exceeding safe limits of such contaminants in water supplies through industrial effluent discharges to nearby water bodies.

2.4.3 Wastes

The increased level of consumption that occurs in urban areas leads to the generation of large quantities of wastes. The disposal of these wastes in landfills is common in the United States and Europe. However, if landfills are not properly managed, runoff and leachates can contaminate surface and ground water supplies. Landfills are also becoming increasingly expensive due to the rising costs of their construction and operation (Roy, 1994). Incineration is the second most common method of disposal in developed countries (WRI, 1997). However, incinerator ashes may contain hazardous materials including heavy metals and organic compounds such as dioxin (WRI, 1997) which can settle on surfaces and eventually be moved by runoff during rainfall events. The estimated population growth and expansion of urban areas makes the proper management of the associated increase in solid wastes management an important issue, because it too, could potentially be environmentally hazardous. An increased number of landfills enhances the potential for contaminated leachate to enter surface and groundwater that may eventually be used as a drinking water source.

2.4.4 Nutrient Loading

One of the most serious problems associated with urban effluents is excessive nutrient loading which can lead to eutrophication of natural waters (National Research Council, 1995). These excessive nutrients come from several sources, including upstream agricultural and urban areas, and human waste. Agricultural activities may increase in areas surrounding growing cities to provide food for the new inhabitants. An increase in the upstream agricultural activities in an area can increase the nutrient loads in receiving waters from agricultural runoff. However, the largest single source of nutrient loading in urban water is human waste (WRI, 1997). Human wastes contain large amounts of nitrogen and phosphorus (even after conventional treatment) which can lead to the nutrient-overloading problem if large amounts are concentrated in one area, as is the case in urban areas. Without a major restructuring of how urban waste-waters are handled, nutrient loads in waters seem certain to rise as urban populations increase and agricultural production expands to feed the urban residents. (Barnes et al, 1994).

2.4.5 Urban Runoff

Urban runoff also contributes to the water pollution problem. In 1990, a study found that a single year's runoff from Washington D.C., carried with it 3.8 million to 19 million liters of oil, 180 metric tons of zinc, 29 metric tons of copper, and 10 metric tons of lead (Faiz and Guatam, 1994). For some pollutants urban runoff rivals or exceeds the output from industrial sources and sewage treatment plants and is often much more difficult to track and control. Increases in runoff can also cause scouring of local waterways, which increases sedimentation in the receiving waters. The increased sediment load can contribute to pollution and can cause health problems for aquatic life.

2.5 Groundwater

Some cities rely heavily on groundwater as a resource due to excessively polluted surface water supplies. In fact, groundwater is fifty times as plentiful as surface water in the United States (Scott, 1985). However, in many natural systems, the groundwater and surface water systems are hydrodynamically coupled, and the pollution of one can lead to the pollution of the other (Fetter, 1999). Therefore, it is important to understand the impacts of urbanization on the groundwater system and how it effects the interaction between surface and ground water.

Understanding this relationship may lead to the prevention of groundwater pollution and prevent the exhaustion of groundwater as a reliable drinking water source.

Urbanization modifies the physical environment as it alters the natural surface by replacing a pervious soil-plant surface with artificial, impervious surfaces, and by the addition of a compact mass of buildings and roads. The extensive paving of urban areas reduces the amount of infiltration and evapotranspiration occurring within a system. This reduction of infiltration reduces the amount of recharge to the groundwater system, which can affect the flow characteristics of the system. The reduction in evapotranspiration occurs due to the replacement of vegetative surfaces with paved, impervious surfaces. Surface detention storage characteristics are also changed and street runoff collection systems and drainage conduits facilitate rapid removal of water from the surface (Lakshmanan and Chatterjee, 1977). All of these factors change the surface runoff regimes which in turn alter the groundwater recharge systems. Greater runoff peaks occur as soil permeability rates decrease. The cumulative effects of greater surface water volume, and improved underground drainage could accentuate localized peak flows and decrease base flow rates (McPherson, 1974).

2.6 Groundwater Models

The utilization of mathematical models to represent the three-dimensional simulation of groundwater flow is significant to hydrologic research. Models aid in the understanding of flow, transport of solutes, water budgets in the groundwater system, and thus, provide information for effective management (Anderson and Woessner, 1992). The development of a groundwater model can not only aid in the understanding of a flow system in a region, but the process will also identify additional data requirements which will increase understanding of the system.

Previously, most analyses using digital groundwater models were limited to two-dimensional cases, primarily because the computer processing power and storage were not sufficient to solve complicated three dimensional flow equations (Anderson and Woessner, 1992). Two-dimensional applications involved simulating strictly horizontal flow in an aquifer or vertical and horizontal flow in a vertical section. Then "Quasi-3-D" models were introduced which simulate aquifers as having strictly horizontal two-dimensional flow linked by connections of strictly vertical flow through aquitards. (Anderson and Woessner, 1992). Today,

solutions to complicated three-dimensional flow equations are no longer limited by technology as powerful computers allow simulation of true three dimensional groundwater flow systems.

2.7 MODFLOW

The USGS finite difference model, MODFLOW, has become an industry standard in groundwater modeling studies and is the most widely used and supported groundwater model today (Anderson and Woessner, 1992). It has also been extensively verified and produces numerically stable solutions (Anderson and Woessner, 1992), and therefore it was chosen for use in this study.

MODFLOW is a modular finite difference model that simulates groundwater in a three-dimensional environment. It was developed by the USGS and comprehensively models subsurface flow (McDonald and Harbaugh, 1988). The model contains separate subroutines or “modules” which are grouped into “packages” that simulate specific features of the hydrologic system to be simulated. The modular nature of the program allows the user to examine specific hydrologic features of the model independently (McDonald and Harbaugh, 1988). New packages can also be developed for additional capabilities without changing the existing packages. This feature, along with the input and output systems design allows for a great deal of flexibility. Table 1 lists the names of the packages included in the standard MODFLOW code, along with a brief description of each. Each program is described in detail in the discussion of the model.

A block-centered finite difference approach is used to simulate ground-water flow within the aquifer (McDonald and Harbaugh, 1988). Layers can be simulated as confined, unconfined, or a combination of the two. External stresses such as wells, areal recharge, drains, evapotranspiration, and streams can be simulated using the appropriate packages, as well as appropriate boundary conditions developed in a conceptual model.

The following section offers an explanation of the concepts and assumptions inherent in MODFLOW. They describe the derivation of the methods used in performing the numerical approximations within the model, and explain the notation conventions that will be referred to throughout this study. The information is primarily an overview of the information from the documentation manual, to better explain the concepts and assumptions made with the application

of MODFLOW. The documentation explains each concept introduced here in more detail (McDonald and Harbaugh, 1988).

2.7.1 Mathematical Model

The main equation that describes transient flow in an anisotropic porous medium when the coordinate system is oriented along the principal axes of anisotropy in three dimensions is (McDonald and Harbaugh, 1988):

$$\frac{\delta}{\delta x} \left(K_{xx} \frac{\delta h}{\delta x} \right) + \frac{\delta}{\delta y} \left(K_{yy} \frac{\delta h}{\delta y} \right) + \frac{\delta}{\delta z} \left(K_{zz} \frac{\delta h}{\delta z} \right) - W = S_s \frac{\delta h}{\delta t} \quad (1)$$

where:

- K_{xx} , K_{yy} and K_{zz} = values of hydraulic conductivity along the x, y and z coordinate axes, which are assumed to be parallel to the major axes of hydraulic conductivity (Lt^{-1}),
- h = potentiometric head (L),
- W = volumetric flux per unit volume and represents sources and/or sinks of water (t^{-1}),
- S_s = specific storage of the porous material (L^{-1}), and
- t = time (t).

The derivation of Equation 1 can be found in Fetter (1999). Equation 1 along with the specification of flow and/or head conditions at the boundaries, and initial head conditions constitute a mathematical representation of the aquifer system. Analytical solutions to Equation 1 are rarely possible, and therefore a variety of numerical solutions have been developed to obtain approximate solutions.

The finite-difference approach is a numerical approximation of the analytical solution to Equation 1. In this approach, the continuous system is replaced by a finite set of discrete points in space and time. The partial derivatives are replaced by terms calculated from the differences in head values at these points (McDonald and Harbaugh, 1988). The solution of the resulting multiple linear algebraic difference equations yields values of head at specific points in time, representing the time-varying head distribution that would be given by an analytical solution of the partial-differential equation of flow (McDonald and Harbaugh, 1988).

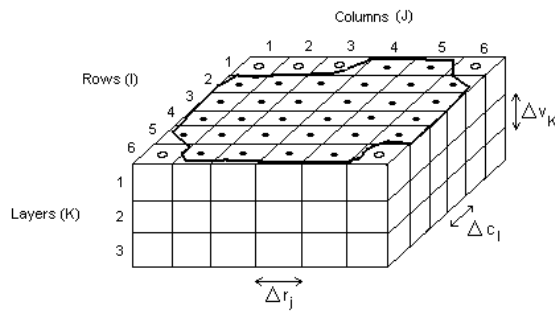
Table 1. List of *packages* in MODFLOW (McDonald and Harbaugh, 1988)

Package Name	Abbreviation	Package Description
Basic	BAS	Handles those tasks that are part of the model as a whole. Among those tasks are specification of boundaries, determination of time-step length, est. of initial conditions, and printing the results
Block-Centered Flow	BCF	Calculates terms of finite-difference equations which represent flow within porous medium; specifically, flow from cell to cell and flow into storage
Well	WEL	Adds terms representing flow to wells to the finite-difference equations
Recharge	RCH	Adds terms representing areally distributed recharge to the finite-difference equations
River	RIV	Adds terms representing flow to rivers to the finite-difference equations
Drain	DRN	Adds terms representing flow to drains to the finite-difference equations
Evapotranspiration	EVT	Adds terms representing ET to the finite-difference equations
General-Head Boundaries	GHB	Adds terms representing general-head boundaries to the finite-difference equations
Strongly Implicit Procedure	SIP	Iteratively solves the system of finite-difference equations using the Strongly Implicit Procedure.
Slice-Successive Overrelation	SOR	Iteratively solves the system of finite-difference equations using Slice-Successive Overrelaxation

2.7.2 Discretization

The ground-water system is divided into a mesh of blocks called cells. The cells are defined by rows (i), columns (j), and layers (k). The model was developed to represent a Cartesian coordinate system, and therefore the k index indicates changes along the vertical z axis, rows would be considered parallel to the x axis, and columns are parallel to the y axis. Figure 1 illustrates this discretization by showing the grid cells lined up in the coordinate system.

As stated above, MODFLOW uses a block-centered formulation of the finite difference equation. Thus, the discrete nodes at which heads are calculated are located at the center of each cell. The spacing of the nodes should be chosen so that the hydraulic properties of the system are uniform over the extent of the cell, because in assigning such properties, it is assumed that they are assigned to the whole cell (McDonald and Harbaugh, 1988).



Explanation

- Aquifer Boundary
- Active Cell
- Inactive Cell
- Δr_j Dimension of Cell Along Row Direction.
- Δc_i Dimension of Cell Along Column Direction.
- Δv_k Dimension of Cell Along Vertical Direction.

Figure 1. Discretized hypothetical aquifer system in MODFLOW (McDonald and Harbaugh, 1988).

2.7.3 Finite Difference Equation

The finite-difference equation for ground-water flow is developed based on the continuity equation: the sum of all flows into and out of a cell must equal the rate of change in storage within the cell. Figure 2 shows the three dimensional representation of a cell and its adjacent cells, and the corresponding subscript notation. The flow into cell i,j,k in the row direction from cell $i,j-1,k$, is given as:

$$q_{i,j-1/2,k} = KR_{i,j-1/2,k} \Delta c_i \Delta v_k \frac{(h_{i,j-1,k} - h_{i,j,k})}{\Delta r_{j-1/2}} \quad (2)$$

where:

- $h_{i,j,k}$ = head at node i,j,k ,
- $h_{i,j-1,k}$ = head at node $i,j-1,k$,
- $q_{i,j-1/2,k}$ = volumetric fluid discharge through the face between cells i,j,k and $i,j-1,k$ (L^3t^{-1}),

$KR_{i,j-1/2,k}$ = hydraulic conductivity along the row between nodes i,j,k and $i,j-1,k$ (Lt^{-1}),
 $\Delta c_i \Delta v_k$ = area of cell faces normal to the row direction, and
 $\Delta r_{j-1/2}$ = distance between nodes i,j,k and $i,j-1,k$.

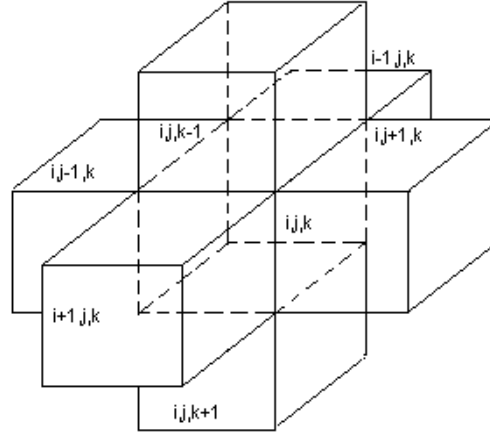


Figure 2. Cell i,j,k and indices for the six adjacent cells in MODFLOW (McDonald and Harbaugh, 1988).

The subscript $1/2$ does not represent a specific point between the nodes, rather it is meant to be the effective parameter for the entire region between the nodes, or the harmonic mean as described by Collins (1961) (McDonald and Harbaugh, 1988). Similar equations can be written for approximating flow into the cell through the remaining five faces. The expressions can be simplified by defining the “hydraulic conductance” or “conductance” as:

$$CR_{i,j-1/2,k} = KR_{i,j-1/2,k} \frac{\Delta c_i \Delta v_k}{\Delta r_{j-1/2}} \quad (3)$$

where:

$CR_{i,j-1/2,k}$ = conductance in row i and layer k between nodes $i,j-1,k$ and i,j,k (L^2t^{-1}),

Thus, conductance is the product of hydraulic conductivity and cross-sectional area of flow divided by the length of the flow path (or distance between the nodes) (McDonald and Harbaugh, 1988).

The application of continuity, and taking into account any external flow rates from any other sources and defining them as QS, yields:

$$q_{i,j-1/2,k} + q_{i,j+1/2,k} + q_{i-1/2,j,k} + q_{i+1/2,j,k} + q_{i,j,k+1/2} + q_{i,j,k-1/2} + QS_{i,j,k} = SS_{i,j,k} \frac{\Delta h_{i,j,k}}{\Delta t} \Delta r_j \Delta c_i \Delta v_k \quad (4)$$

where:

$q_{x,y,z}$ = cell-to-cell flow,

$QS_{i,j,k}$ = external flow rate from any other source,

$\Delta h_{i,j,k}/\Delta t$ = finite-difference approximation for the derivative of head with respect to time (Lt^{-1}),

$SS_{i,j,k}$ = specific storage of cell i,j,k (L^{-1}), and

$\Delta r_j \Delta c_i \Delta v_k$ = volume of cell i,j,k (L^3).

Substituting equation (2) for each cell into equation (4) yields:

$$\begin{aligned} & CR_{i,j-1/2,k} (h_{i,j-1,k} - h_{i,j,k}) + CR_{i,j+1/2,k} (h_{i,j+1,k} - h_{i,j,k}) \\ & + CC_{i-1/2,j,k} (h_{i-1,j,k} - h_{i,j,k}) + CC_{i+1/2,j,k} (h_{i+1,j,k} - h_{i,j,k}) \\ & + CV_{i,j,k-1/2} (h_{i,j,k-1} - h_{i,j,k}) + CV_{i,j,k+1/2} (h_{i,j,k+1} - h_{i,j,k}) \\ & + P_{i,j,k} h_{i,j,k} + Q_{i,j,k} = SS_{i,j,k} (\Delta r_j \Delta c_i \Delta v_k) \frac{\Delta h_{i,j,k}}{\Delta t} \end{aligned} \quad (5)$$

where:

CR, CC, and CV = the hydraulic conductivities along rows, columns, and layers,

$P_{i,j,k} h_{i,j,k}$ = all head-dependent fluxes entering or leaving the cell due to external sources, and

$Q_{i,j,k}$ = all external fluxes that are not head dependent.

In equation (5), the term QS from equation (4) is divided into fluxes that are head-dependent, and those that are not (McDonald and Harbaugh, 1988).

It is necessary to also represent the time derivative of head in terms of specific heads and times to transform it into the finite difference form. Figure 3 shows a hydrograph of head values at node i,j,k . The values for time are shown on the horizontal axis and the head values associated

with these times are also shown. The variable t_m is the time at which the flow terms of Equation 5 are evaluated, and t_{m-1} is the time that precedes t_m . The notation associate with the head terms is consistent with this convention. Then, an approximation to the time derivative of head at time t_m is given by:

$$\left(\frac{\Delta h_{i,j,k}}{\Delta t}\right)^m \cong \frac{h^m_{i,j,k} - h^{m-1}_{i,j,k}}{t_m - t_{m-1}} \quad (6)$$

where:

$$\begin{aligned} h^m_{i,j,k} &= \text{the head in the cell } i,j,k \text{ at the end of time step } m, \\ h^{m-1}_{i,j,k} &= \text{the head in the cell } i,j,k \text{ at the end of time step } m-1, \\ t_m &= \text{the time at the end of time step } m, \text{ and} \\ t_{m-1} &= \text{the time at the end of time step } m-1. \end{aligned}$$

Therefore, the derivative is approximated using the change in head at the node over a time interval over which the flow is evaluated. This is termed a “backward difference” approach to the finite difference equation, because it extends backwards in time. MODFLOW uses this method as opposed to a “forward difference” or any other approach because a “backwards difference” approach is always numerically stable-that is, “errors introduced at any time diminish progressively at succeeding times” (McDonald and Harbaugh, 1988). Equation 5 can be written in backward-difference form in the following way:

$$\begin{aligned} &CR_{i,j-1/2,k} (h^m_{i,j-1,k} - h^m_{i,j,k}) + CR_{i,j+1/2,k} (h^m_{i,j+1,k} - h^m_{i,j,k}) \\ &+ CC_{i-1/2,j,k} (h^m_{i-1,j,k} - h^m_{i,j,k}) + CC_{i+1/2,j,k} (h^m_{i+1,j,k} - h^m_{i,j,k}) \\ &+ CV_{i,j,k-1/2} (h^m_{i,j,k-1} - h^m_{i,j,k}) + CV_{i,j,k+1/2} (h^m_{i,j,k+1} - h^m_{i,j,k}) \\ &+ P_{i,j,k} h^m_{i,j,k} + Q_{i,j,k} = SS_{i,j,k} (\Delta r_j \Delta c_i \Delta v_k) \frac{(h^m_{i,j,k} - h^{m-1}_{i,j,k})}{(t_m - t_{m-1})} \end{aligned} \quad (7)$$

Equation 7 represents one equation and seven unknown heads at time m , and therefore cannot be solved independently. However, an equation of this type can be written for each active cell in the domain. Since there is only one unknown head for each cell, a system of “ n ” equations with “ n ” unknowns is created and can be solved simultaneously (McDonald and Harbaugh, 1988).

The initial head and boundary conditions defined by the user prior to the simulation become the

first values of head for the first iteration (McDonald and Harbaugh, 1988). As the time progresses, the head distribution for time m in the preceding time step becomes the head distribution for $m-1$ in the next time step. Therefore, the set of finite-difference equation is reformulated at each time step (McDonald and Harbaugh, 1988).

2.7.4 Iteration

MODFLOW utilizes iterative methods to solve the system of finite-difference equations for each time step. The calculation of head values at the end of a given time step is arbitrarily assigned a trial estimate for the head at each node at the end of that time step (McDonald and Harbaugh, 1988). A calculation procedure is then initiated that alters the estimated values and results in a new set of values which are closer in agreement with the solution to the equations. These interim head values take the place of the initial estimates and the procedure is repeated. Ultimately, the interim heads approach values that would exactly satisfy the set of equations (McDonald and Harbaugh, 1988).

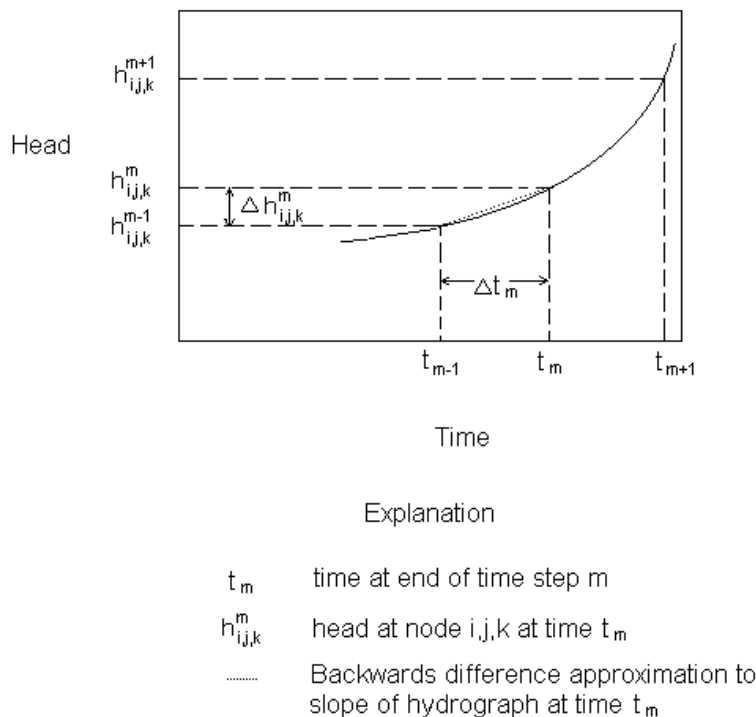


Figure 3. Hydrograph for cell i,j,k in MODFLOW (McDonald and Harbaugh, 1988).

Ideally, the iteration procedure should stop when the calculated heads are suitably close to the approximate solution. However, the actual solution is unknown, and instead, the changes in the computed heads occurring from one iteration to the next must be less than a certain “closure criterion” or “convergence criterion”, specified by the user (McDonald and Harbaugh, 1988)

2.7.5 Boundary Conditions

MODFLOW uses boundary conditions to represent the physical and hydraulic boundaries within a groundwater system. Physical boundaries are formed by the physical presence of an impermeable body of rock or large body of surface water. Hydraulic boundaries are invisible boundaries dependent upon hydrologic conditions. These may include groundwater divides and flow lines and can change with the changes of stresses on the system at a given time. MODFLOW can incorporate specified-head boundaries, specified-flux boundaries, and general-head boundaries during a simulation.

Specified head boundaries represent an inexhaustible supply of water. This means that the aquifer can potentially pull an infinite amount of water from this source without changing its head value. Therefore, they can accurately represent a large surface body of water that does not undergo a significant change in head, but they cannot accurately represent a body of water that does experience a large fluctuation in head.

Typically, specified-flux boundaries represent no-flow boundaries, but they can also represent constant flux boundary conditions where flow can be measured or estimated to be nonzero. No-flow boundaries can represent both physical conditions such as impermeable bedrock or impermeable fault zones, and hydraulic conditions like groundwater divides and streamlines. Care must be taken, however, in using this type of boundary condition for hydraulic conditions because they can change in time with the stresses on the system.

Finally, general-head boundaries are used whenever the head of a surface-water body or other known head is separated from the aquifer by material or deposits having different hydrogeologic properties than the aquifer. A separate package within the model simulates this type of boundary condition, and is discussed in the explanation of individual packages (McDonald and Harbaugh, 1988).

2.7.6 Program Structure

This section describes the overall design of the model program. The program consists of the main program and a number of highly independent subroutines called modules (McDonald and Harbaugh, 1988). The modules are grouped into “packages” that simulate specific features of the flow regime. The functions that must be performed for a typical simulation are shown in Figure 4. The period of the simulation is divided into stress periods. Each stress period is in turn, divided into time steps. Iterative solution methods are used to solve for the heads at the end of each time step. Thus, within a simulation, there are three nested loops: a stress period loop, within which there is a time-step loop, which contains an iteration loop (McDonald and Harbaugh, 1988).

Each rectangle in Figure 4 is called a procedure. The various procedures are implemented through individual modules. Modules can also be grouped by “packages”, where a package includes those modules required to incorporate a particular hydrologic process into the simulation (for example, the River Package). Each classification is useful in understanding the overall model structure. The package classification, for example indicates the modules which will be active in a given simulation, whereas, the procedure classification defines the specific function of the module in relation to the functions of other modules of the package. Figure 5 illustrates the classification according to both packages and procedure. The horizontal rows correspond to procedures, and the vertical columns correspond to the packages. An “X” is entered in each block of the matrix for which a module exists.

The following sections describe the function of each package included in the MODFLOW program. They also describe equations used in the formulation of each package, and assumptions made in their derivation.

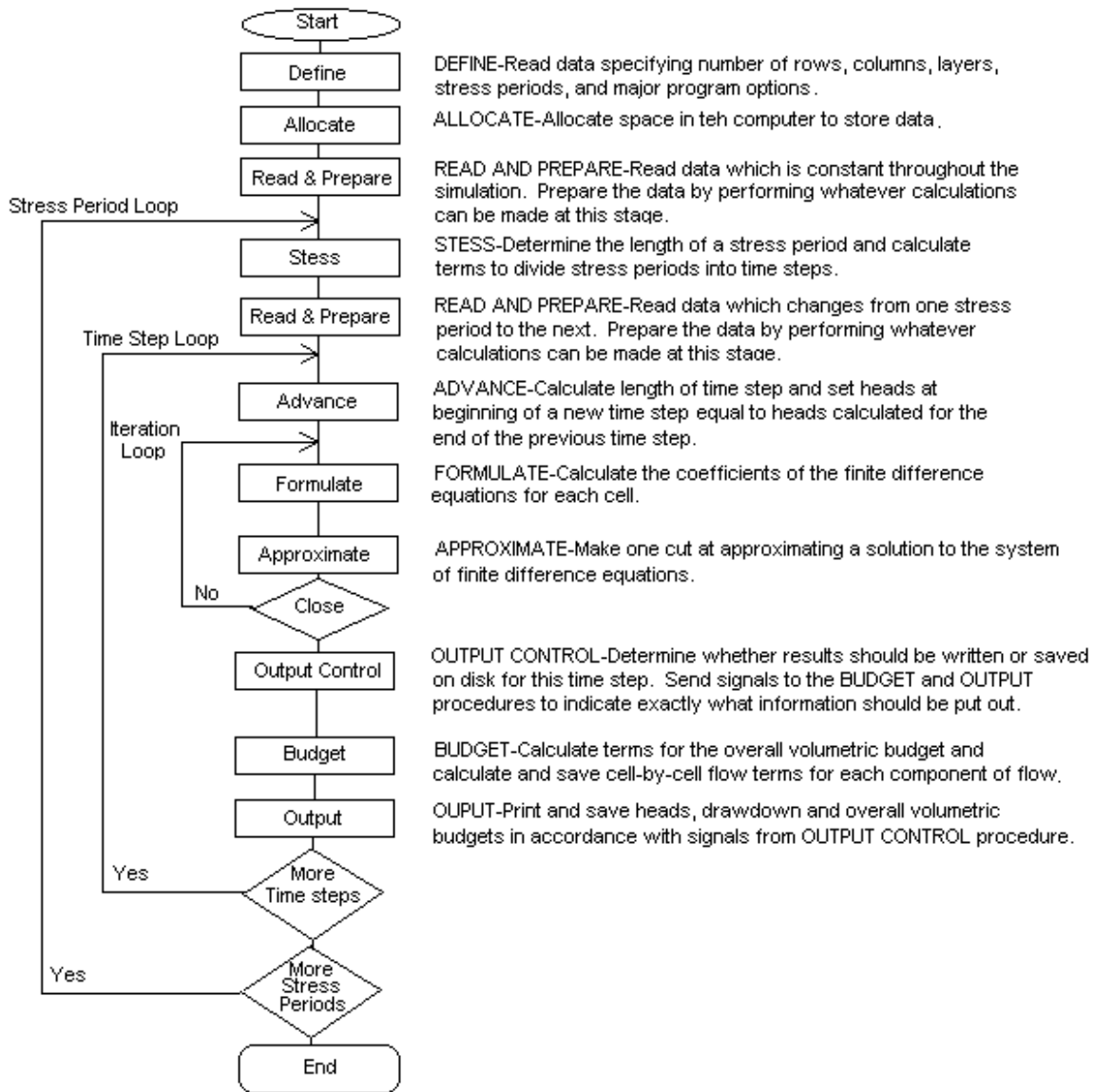


Figure 4. Overall MODFLOW program structure (McDonald and Harbaugh, 1988).

	Flow Component Packages								Solver Packages	
	Stress Packages									
	B A S	B C F	W E L	R C H	R I V	D R N	E V T	G H B	S I P	S O R
Define	X									
Allocate	X	X	X	X	X	X	X	X	X	X
Read & Prepare	X	X							X	X
Stress	X									
Read & Prepare			X	X	X	X	X	X		
Advance	X									
Formulate	X	X	X	X	X	X	X	X		
Approximate									X	X
Output Control	X									
Budget		X	X	X	X	X	X	X		
Ouput	X									

Figure 5. Organization of modules in MODFLOW by procedures and packages (McDonald and Harbaugh, 1988).

2.7.7 The Basic Package

The Basic Packages serves many different administrative purposes in the model. It reads input data sets that specify the number of rows, columns, layers, stress periods, the major options to be used, and the location of the input data for those options. It allocates memory for the model arrays, reads boundary condition data, reads and implements time discretization data, initializes head values, calculates an overall water budget and controls output structure according to user specification (McDonald and Harbaugh, 1988). This package is necessary for the model to run. The Basic Package deals with a number of arrays to organize the initialization data. The IUNIT array determines major options to be used, the IBOUND array determines the type of

boundaries used in the simulation and the domain and there is an initial head conditions array. The Basic Package also sets up the simulation stress periods and time steps, sets the output control options specifying the recording of results and determines the overall volumetric water budget.

2.7.7.1 The IUNIT Array

The primary role of the Basic Package with respect to the selection of major options and the designation of their input unit numbers is to read the IUNIT array. This determines whether or not a major option is to be used, and the unit number from which data for the option is to be read. There is an element in the IUNIT array for every major option used in the simulation.

2.7.7.2 The IBOUND Array

The IBOUND array, which is read in by the Basic Package indicates whether the head in each cell (1) varies with time (variable-head cell), (2) is constant (constant-head cell) or (3) allows no flow to take place within the cell (no-flow or inactive cell). The IBOUND array is specified by the user but can be modified by other packages if the state of the cell changes. Figure 6 shows an example of an IBOUND array. The different types of cells are shown as variable head cells, constant head cells, and no-flow cells.

2.7.7.3 Initial Conditions

Because the finite difference equation solved in MODFLOW is in the backward-difference form, a head distribution at the beginning of each time step is required to calculate the head values at the end of the time step (McDonald and Harbaugh, 1988).

The head distribution at the start of the time step is set equal to the head distribution at the end of the previous time step. For the first time step, "initial heads" are specified by the user. The Basic Package reads in the initial head distribution specified by the user.

2.7.7.4 Time Discretization

The simulation is divided into stress periods that are in turn, divided into time steps. A stress period is a time interval during which all external stresses are constant. Within each stress period, the time step form a geometric progression using a time step multiplier, or the ratio of the

length of each time step to that of the proceeding step (McDonald and Harbaugh, 1988). The user specifies the length of the stress period, the number of time steps the stress period contains, and the time step multiplier. Using these terms, the length of each time step is calculated for the simulation. Figure 7 illustrates the discretization of time in MODFLOW. It shows the stress periods that are in turn divided into time steps.

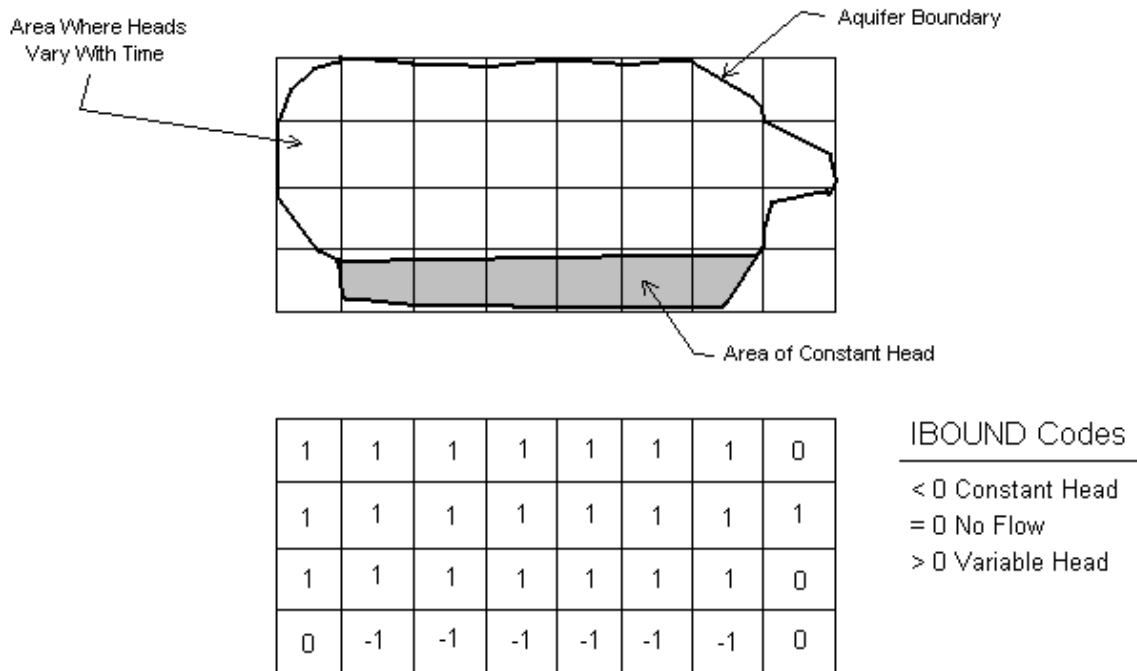


Figure 6. Example of the boundary layer (IBOUND) for a single layer in MODFLOW (McDonald and Harbaugh, 1988).

2.7.7.5 Output

The Basic Package contains the "Output Control" option which allows the user to control the frequency at which the heads are printed or saved to disk. The primary output of the program is head distribution, although it also provides a volumetric water budget and drawdown information if specified. If the Output Control is not utilized, a default option is used.

2.7.7.6 Budget Calculations

The individual flow components are calculated in the flow component packages and are stored in the one-dimensional array, VBVL. The array, VBVL, is passed to the Basic Package which sums and prints the budget entries determined from the other packages.

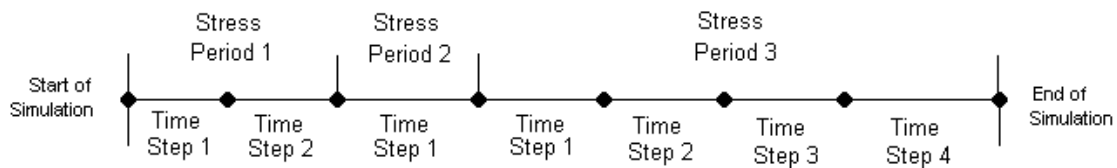


Figure 7. Division of simulation time into stress periods and time steps in MODFLOW (McDonald and Harbaugh, 1988).

2.7.8 The Block-Centered Flow Package

The Block-Centered Flow Package (BCF) calculates flow between adjacent cells by computing the conductance components of the finite-difference equation, and computes terms that determine the rate of water movement to and from storage (McDonald and Harbaugh, 1988). The calculations are made under the assumption that a node is located at the center of each model cell. This package is also necessary to run the program (McDonald and Harbaugh, 1988). The coefficients CV, CR and CC in the flow equation are referred to as "branch conductances" (Equation 5) The conductance terms along rows and columns (CR and CC) are called horizontal conductances and are calculated differently than conductance between layers or vertical conductance (CV). The BCF Package calculates these terms and also calculates a flow correction term that is added to the external source and storage.

2.7.8.1 Basic Conductance Equations

The hydraulic conductance combines grid dimensions and hydraulic conductivity into a single constant. Darcy's law defines one-dimensional flow in a prism of porous material.

$$Q = \frac{KA(h_2 - h_1)}{L} \quad (8)$$

where:

Q = flow (L^3/t),
 K = hydraulic conductivity of the material in the direction of flow (L/t),
 A = cross-sectional area perpendicular to the flow (L^2),
 h_2-h_1 = head difference across the prism parallel to flow (L), and
 L = length of the flow path (L).

Conductance, C, is defined as

$$C = \frac{KA}{L} \quad (9)$$

where

K = hydraulic conductivity of the material in the direction of flow (L/t),
 A = cross-sectional area perpendicular to the flow (L^2), and
 L = length of the flow path (L).

Figure 8 illustrates the idea of conductance through a cell. In the figure, the area perpendicular to flow is shown, and the length of flow is also illustrated.

Conductance is defined for both a particular prism of material and for a direction. The conductances in an anisotropic medium will differ in the three principal directions of hydraulic conductivity.

When a prism of porous material consists of two or more sub-prisms in series, as shown in Figure 9, the inverse of the equivalent conductance equals the sum of the inverses of the individual conductances. (McDonald and Harbaugh, 1988).

2.7.8.2 Horizontal Conductance

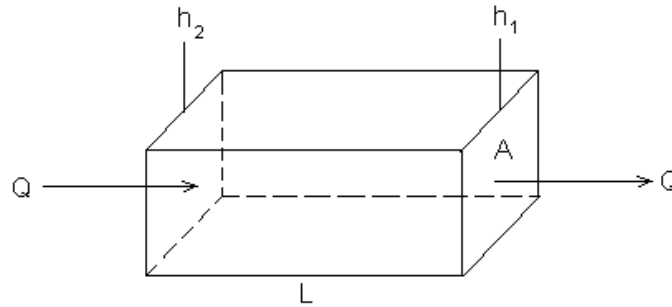
The finite-difference equations use equivalent conductances between nodes of adjacent cells, or "branch conductances". The horizontal conductance terms CR and CC are calculated between adjacent horizontal nodes where CR terms specify conductance between nodes in the same row, and CC terms specify conductance between nodes in the same column. To designate conductance between nodes, the subscript notation "1/2" is used. Figure 10 illustrates two cells along a row, along with the parameters defined in the equation.

Two assumptions are made in the Equation: (1) the nodes are in the center of the cells and (2) the transmissivity is uniform for each cell.

$$CR_{i,j+1/2,k} = 2DEL C_i \frac{TR_{i,j,k} TR_{i,j+1,k}}{TR_{i,j,k} DELR_{j+1} + TR_{i,j+1,k} DELR_j} \quad (10)$$

where

$TR_{i,j,k}$ = Transmissivity in the row direction in cell i,j,k ,
 $CR_{i,j+1/2,k}$ = Conductance in the row direction between nodes i,j,k and $i,j+1,k$,
 $DEL C_i$ = The distance between nodes i,j,k and $i+1,j,k$, and
 $DELR_j$ = The distance between nodes i,j,k and $i,j+1,k$.

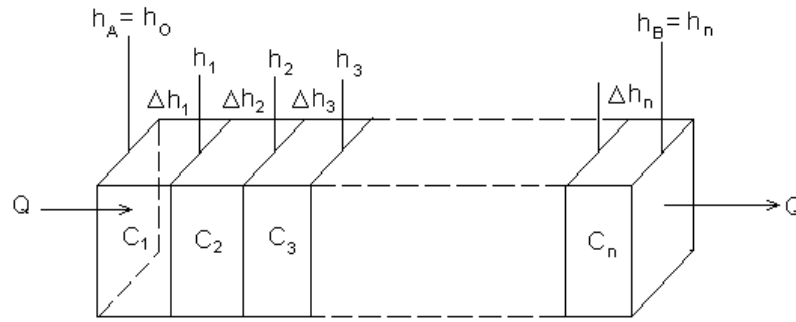


Explanation $Q = \frac{KA (h_2 - h_1)}{L}$

- K is Hydraulic Conductivity
- h_2 is the Head at the Left End of the Prism
- h_1 is the Head at the Right End of the Prism
- Q is the Flow Rate from the Left End to the Right End
- L is the Length of the Flow Path
- A is the Cross Sectional Area Perpendicular to the Direction of Flow

Figure 8. Prism of porous material illustrating Darcy’s law (McDonald and Harbaugh, 1988).

Horizontal conductance is considered to be constant for the simulation in a model layer which is confined. New values of horizontal conductance must be calculated as the head fluctuates if the layer is unconfined or potentially unconfined. These values are calculated at the start of each iteration. MODFLOW performs these calculations based on a user-specified layer-type flag, LAYCON. (McDonald and Harbaugh, 1988).



$$\frac{1}{C} = \frac{1}{C_1} + \frac{1}{C_2} + \frac{1}{C_3} + \dots + \frac{1}{C_n}$$

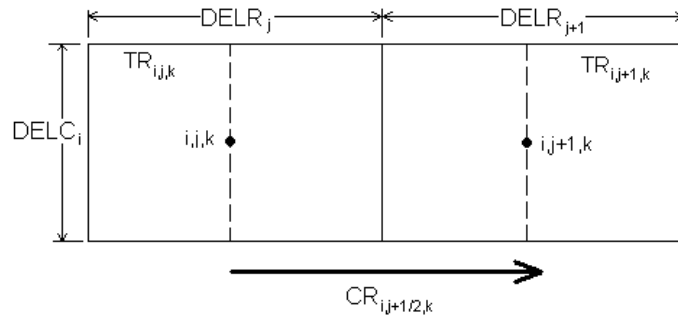
Explanation

- Q is the Flow Rate
- C_m is Conductance of Prism m
- h_m is Head at the Right Side of Prism m
- Δh_m is the Head Change Across Prism m
- C is the Conductance of the Entire Prism

Figure 9. Calculation of conductance through several prisms in series in MODFLOW (McDonald and Harbaugh, 1988).

2.7.8.3 Vertical Conductance

MODFLOW calculates the vertical conductance using data from an array (VCONT) that incorporates both thickness and vertical hydraulic conductivity (McDonald and Harbaugh, 1988). When running MODFLOW, rather than specifying a total thickness and vertical hydraulic conductivity, the user specifies the term VCONT. The VCONT values are calculated in different ways depending upon whether or not the nodes both fall within a single hydrogeologic unit.



$$CR_{i,j+1/2,k} = 2 \text{ DELC}_i \times \frac{TR_{ij,k} TR_{i,j+1,k}}{TR_{ij,k} \text{ DELR}_{j+1} + TR_{i,j+1,k} \text{ DELR}_j}$$

Explanation

$TR_{ij,k}$ is Transmissivity in the Row Direction in Cell i,j,k

$CR_{i,j+1/2,k}$ is Conductance in the Row Direction Between nodes i,j,k and $i,j+1,k$

Figure 10. Calculation of conductance between nodes using transmissivity and dimensions of cells in MODFLOW (McDonald and Harbaugh, 1988).

$$Vcont_{i,j,k+1/2} = \frac{K_{zi,j}}{\Delta z_{k+1/2}} \quad (11)$$

where:

$\Delta z_{k+1/2}$ = the vertical distance between the nodes, and

$K_{zi,j}$ = vertical hydraulic conductivity.

The vertical distance between the nodes of adjacent vertical cells is shown in Figure 11. When two adjacent model layers are used to represent two vertically adjacent hydrogeologic units, the expression for VCONT becomes:

$$Vcont_{i,j,k+1/2} = \frac{1}{\frac{(\Delta v_k)/2}{K_{zi,j,k}} + \frac{(\Delta v_{k+1/2})/2}{K_{zi,j,k+1}}} \quad (12)$$

where:

Δv_k = thickness of model layer k ,

Δv_{k+1} = thickness of model layer $k+1$,

$K_{z_{i,j,k}}$ = the vertical hydraulic conductivity of the upper layer in cell i,j,k , and
 $K_{z_{i,j,k+1}}$ = the vertical hydraulic conductivity of the lower layer in the cell $i,j,k+1$.

The thickness notation used in Equation 12 is illustrated in Figure 12. A third situation in which the node i,j,k and the node $i,j,k+1$ are within two aquifers separated by a semiconfining unit is represented in the following equation:

$$V_{cont_{i,j,k+1/2}} = \frac{1}{\frac{\Delta z_u / 2}{K_{zu}} + \frac{\Delta z_c}{K_{zc}} + \frac{\Delta z_L / 2}{K_{zL}}} \quad (13)$$

where:

Δz_u = thickness of the upper aquifer,

Δz_L = thickness of the lower aquifer,

K_{zu} = vertical hydraulic conductivity of the upper aquifer,

K_{zc} = vertical hydraulic conductivity of the semiconfining unit, and

K_{zL} = vertical hydraulic conductivity of the lower aquifer.

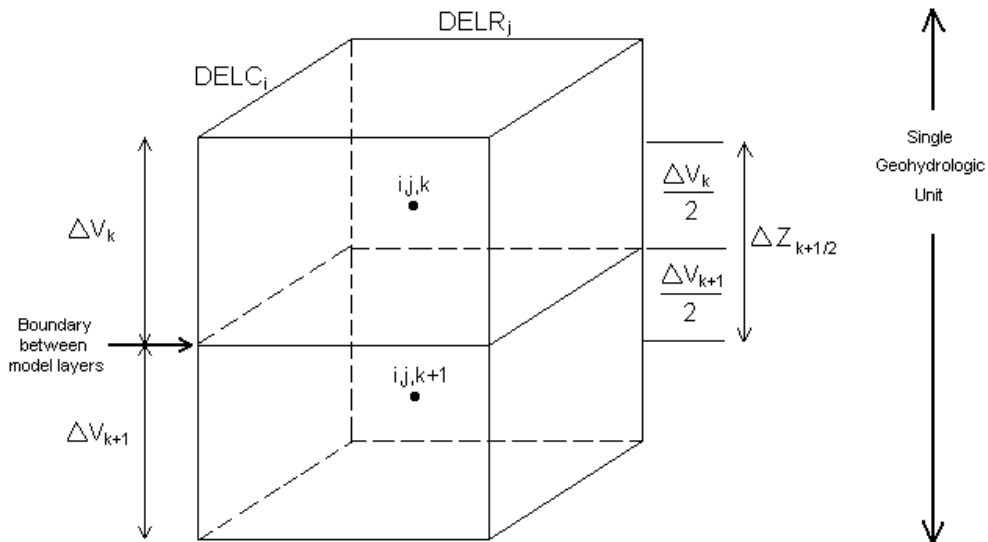


Figure 11. Diagram for calculation of vertical leakance, V_{cont} , between two nodes which fall within a single geohydrologic unit (McDonald and Harbaugh, 1988).

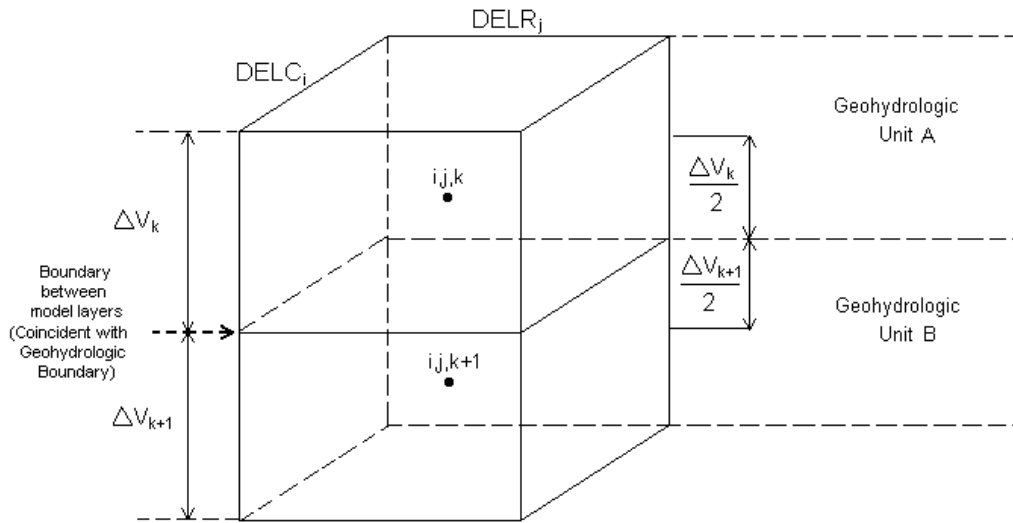
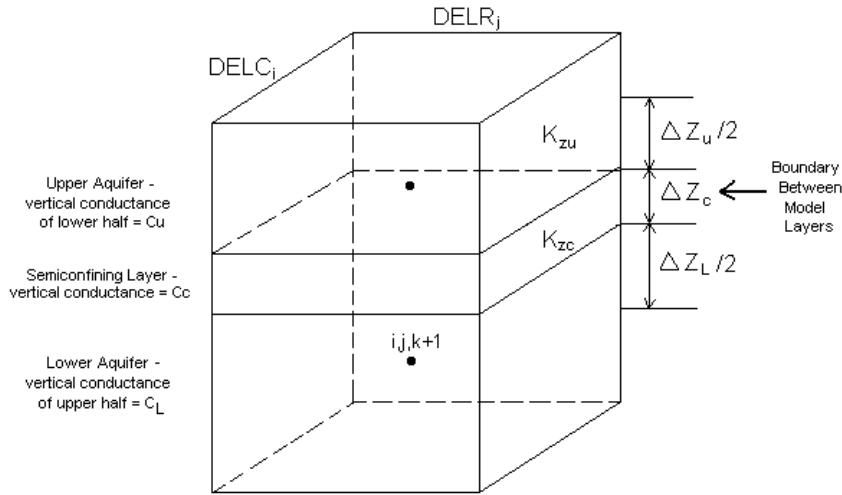


Figure 12. Diagram for calculation of vertical leakance, V_{cont} , between nodes located at the midpoints of vertically adjacent geohydrologic units (McDonald and Harbaugh, 1988).

Figure 13 illustrates the notation in Equation 13. It shows the different thicknesses of each layer and how they represent the total vertical thickness (McDonald and Harbaugh, 1988). In this situation, in effect the confining bed is treated simply as a vertical conductance between the two model layers and is not explicitly modeled. This formulation is frequently referred to as the "quasi-three-dimensional" approach, which also assumes that the storage within the confining unit is negligible (McDonald and Harbaugh, 1988). When the water level in cell $i,j,k+1$ has fallen below the top of the cell, two corrections must be made to the above equations to account for dewatering. (McDonald and Harbaugh, 1988).

2.7.8.4 Storage Formulation

MODFLOW distinguishes between layers in which storage coefficient values remain constant throughout the simulation and those in which the storage coefficient changes from confined to unconfined or vice-versa, depending upon the water table depth (McDonald and Harbaugh, 1988). This distinction is made through the parameter LAYCON which specifies if a layer is confined, unconfined, or a combination of the two.



$$VCONT_{ij,k+1/2} = \frac{1}{\frac{\Delta Z_u / 2}{K_{zu}} + \frac{\Delta Z_c}{K_{zc}} + \frac{\Delta Z_L / 2}{K_{zL}}}$$

Figure 13. Diagram for calculation of vertical leakage, Vcont, between two nodes located at the midpoints of aquifers which are separated by a semiconfining unit (McDonald and Harbaugh, 1988).

In the case when the storage coefficient is to remain constant during the simulation, the following equation is used:

$$\frac{\Delta V}{\Delta t} = SS_{i,j,k} (\Delta r \Delta c \Delta v) \frac{h^m_{i,j,k} - h^{m+1}_{i,j,k}}{t_m - t_{m-1}} \quad (14)$$

where:

- ΔV/Δt = rate of accumulation of water in the cell,
- SS_{i,j,k} = the specific storage of the material in cell i,j,k,
- Δr = the cell width,
- Δc = the cell length,
- Δk = the cell height,
- h^m_{i,j,k} = the head in the cell i,j,k at the end of time step m,
- h^{m-1}_{i,j,k} = the head in the cell i,j,k at the end of time step m-1,

t_m = the time at the end of time step m , and
 t_{m-1} = the time at the end of time step $m-1$.

The BCF requires the specification of dimensionless storage coefficient values. For a confined layer, the storage coefficient values are estimated by multiplying the specific storage by the thickness, and for unconfined layers, they are equal to the specific yield (McDonald and Harbaugh, 1988).

2.7.9 The River Package

The River Package simulates the effects of flow between groundwater and surface water systems. Terms representing seepage to or from the surface features are added to the groundwater flow equation for each cell affected by the seepage (McDonald and Harbaugh, 1988). The amount of seepage is dependent upon the head gradient between the stream and the ground-water regime. The streambed conductance and the head of the surface water body are required input parameters for the river package to make the appropriate calculations. The assumption is made that measurable head losses between the stream and the aquifer are limited to those across the streambed layer itself and the underlying model cell remains fully saturated (McDonald and Harbaugh, 1988). Figure 14 illustrates this concept. It illustrates how MODFLOW would represent an actual streambed. (McDonald and Harbaugh, 1988).

The flow between the stream and the groundwater system is then given by:

$$QRIV = CRIV(HRIV - h_{i,j,k}) \quad (15)$$

where

QRIV = flow between the stream and the aquifer (L^3/t),
HRIV = head in the stream (L),
CRIV = hydraulic conductance of the stream-aquifer interconnection (L^2/t), and
 $h_{i,j,k}$ = head at the node in the cell underlying the stream reach.

Equation 15 also assumes that the underlying cell remains fully saturated.

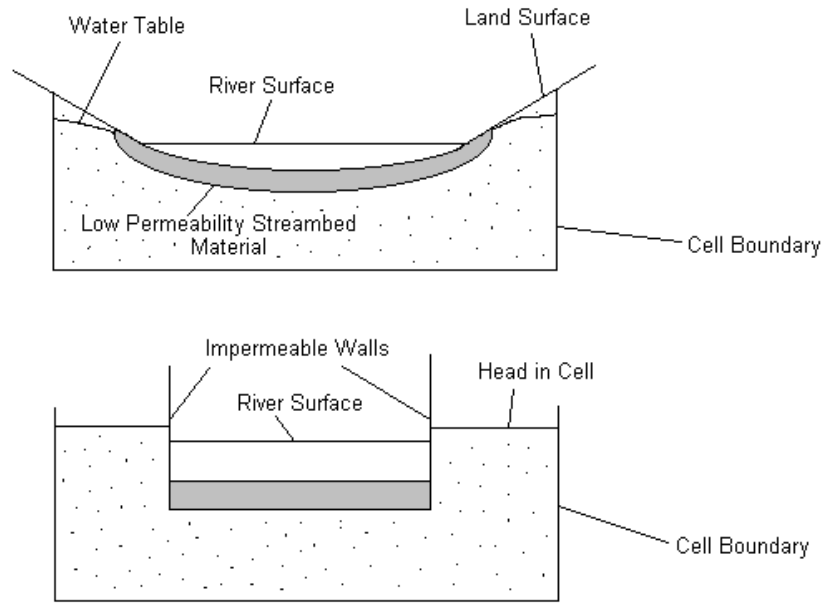


Figure 14. (a) Cross section of an aquifer containing a stream and (b) Conceptual representation of stream-aquifer interconnection in simulation (McDonald and Harbaugh, 1988).

The simplified model of stream-aquifer interaction utilized assumes that this interaction is independent of the location of the stream reach within the cell, and that the level of water in the stream is uniform over the reach, and constant over each stress period. This implies that the conditions of flow in the stream do not vary significantly during the stress period. If this assumption is satisfied, the application of the above equation is appropriate. If field measurements are available, they may be used to calculate the conductance of the river bed (CRIV), however, more often than not, the data are not available and the conductance value must be chosen more or less arbitrarily and adjusted during model calibration (McDonald and Harbaugh, 1988). If the water level in the aquifer falls below the bottom of the streambed layer, leaving an unsaturated interval beneath the reach, the head at its base will simply be the elevation of that point. If this elevation is designated RBOT, then the flow through the streambed layer is:

$$QRIV = CRIV(HRIV - RBOT) \quad (16)$$

where QRIV, CRIV, and HRIV are as defined above.

The further declines in head below RBOT produces no increase in flow through the streambed layer. Figure 15 illustrates the relationship given in Equation 16, it shows that as the water in the aquifer falls below the bottom of the streambed layer, the head will be the elevation at that point. Terms representing river seepage are added to the flow equation for each cell containing a river reach at the beginning of each iteration. (McDonald and Harbaugh, 1988).

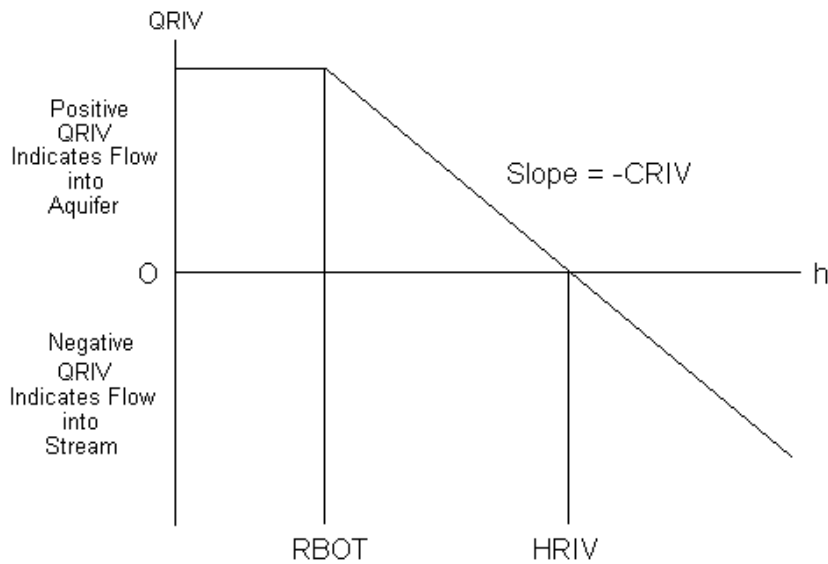


Figure 15. Plot of flow, QRIV, from a stream into a cell as a function of head, h, in the cell where RBOT is the elevation of the streambed and HRIV is the head in the stream (McDonald and Harbaugh, 1988).

2.7.10 The Recharge Package

The amount of recharge entering a groundwater system is perhaps the most difficult parameter to estimate, however, it plays a significant role in the system (McDonald and Harbaugh, 1988). The amount of recharge (infiltration) from precipitation depends on ET, soil moisture and soil storage capacity, thickness of the unsaturated zone, soil type and conditions, slope, and rainfall intensity and duration (McDonald and Harbaugh, 1988). Where recharge occurs depends on topography, altitude or elevation, hydrogeologic facies, and anthropogenic influences (McDonald and Harbaugh, 1988). There are many different methods to estimate

recharge, each with its own merit, however, it is important to be able to accurately represent the amount of recharge because it is the primary driving force of the groundwater movement in the system. The Recharge Package (RCH) simulates areally distributed recharge to the groundwater system (McDonald and Harbaugh, 1988).

Recharge applied to the model is defined as:

$$Q_{Ri,j} = I_{i,j} * DELR_j * DELC_i \quad (17)$$

where

Q = recharge flow rate applied to the model at horizontal cell location (i,j) (L^3/t), and
 $I_{i,j}$ = recharge flux (L/t) applicable to the map area $DELR_j * DELC_i$ of the cell.

There is no need to allow for recharge to occur simultaneously at multiple depths in the same vertical column because natural recharge enters the ground-water system through the ground surface, which corresponds to the top of the top-most layer. In the simplest situation, the top of the ground-water system will occur in layer 1; however, the vertical position of the top of the system may vary with horizontal location as the water-table rises and falls. The RCH (Recharge Package) can also potentially simulate recharge from sources other than precipitation. If it is necessary to represent recharge to more than one cell in a vertical column, the well package can be used to add water to the system. During each iteration, the recharge flow rate is added to the overall flow equation. (Equation 5) (McDonald and Harbaugh, 1988).

2.7.11 The Well Package

The Well Package is used to simulate water withdraw due to pumping wells or water injection due to injection wells at a specified rate during a given stress period. The volumetric flow rate is specified for each cell containing a well or group of wells and is independent of both the cell area and the head in the cell. The equations employed in this package assume that the features to be simulated are actual wells either discharging or recharging (McDonald and Harbaugh, 1988). Negative values of the flow rate Q indicate well discharge, while positive Q values indicate a recharging well. At each iteration step, the value of Q for each cell is added to the overall flow equation for that cell (Equation 5). The user can also specify where the well is screened. The drawdown that the model undergoes is dependent upon the discretization of the

model grid (McDonald and Harbaugh, 1988). Drawdown is taken over the area of the cell. A given volume of drawdown must be accomplished, and therefore if the cells are large in the vicinity of the well, less drawdown will occur in the model than if the cells were smaller, and the model output will not accurately represent drawdown in field conditions. The Well Package does not accommodate wells which are open to more than one layer of the model. This situation can be represented as a group of single layer wells with individual Q values (McDonald and Harbaugh, 1988). If this approach is used, the discharge must be divided according to the following equation:

$$\frac{Q_1}{Q_w} = \frac{T_1}{\Sigma T} \quad (18)$$

where:

Q₁ = discharge from layer 1 to a particular well in a given stress period,

Q_w = well discharge in that stress period,

T₁ = transmissivity of layer 1, and

ΣT = represents the sum of the transmissivities of all layers penetrated by the well.

This equation must be implemented by the user, externally to the program, for each multi-layer well, for each stress period.

2.7.12 The General-Head Boundary Package

The General-Head Boundary Package computes flow into or out of a cell from an external source provided in proportion to the difference between the head in the cell and the head assigned to the external source, similar to the RIVER, DRAIN and ET Package (McDonald and Harbaugh, 1988). General-head boundaries are used whenever the head of a surface-water body or other known head is separated from the aquifer by material or deposits having different hydrogeologic properties than the aquifer. If the conductance is set to a very high value, this boundary condition behaves like a constant-head boundary. However, the head can be changed for each stress period, unlike a constant-head boundary (McDonald and Harbaugh, 1988). Therefore, the conductance value results in a time lag for equilibrium conditions to be reached

between the boundary head and the head in the aquifer. The linear relationship between flow into the cell and head in the cell is established as:

$$Q_{bi,j,k} = C_{bi,j,k} (h_{bi,j,k} - h_{i,j,k}) \quad (19)$$

where:

$Q_{bi,j,k}$ = the flow into cell i,j,k from the source,
 $C_{bi,j,k}$ = the conductance between the external source and cell i,j,k,
 $h_{bi,j,k}$ = the head assigned to the external source, and
 $h_{i,j,k}$ = the head in cell i,j,k.

The GHB Package provides no limiting value of flow to bound the linear function in either direction, which makes it different from the RIVER, DRAIN, and ET Packages (McDonald and Harbaugh, 1988). Care must be taken to insure that unrealistic flows do not develop. The flow term found from this package is also added to the finite difference equation (Equation. 5) (McDonald and Harbaugh, 1988).

2.7.13 The Streamflow-Routing Package

The Streamflow Routing Package is a modification of the River Package (section 2.7.9). It is used to track the flow in one or more streams which interact with groundwater. The Streamflow Routing Package is not a true surface-water flow model but rather is an accounting program. It limits ground-water recharge to the available streamflow (Prudic, 1989). This routing package allows recharge to an aquifer to cease whenever and wherever flow in a stream ceases. This feature can become a definite advantage when simulating different time periods of varying streamflows and groundwater pumping.

Streams are divided into segments and reaches, each reach corresponding to individual cells in the finite-difference grid used to simulate flow (Prudic, 1989). A segment consists of a group of reaches connected in downstream order. Leakage is calculated for each reach on the basis of the head difference between the stream and aquifer and a conductance term, as in the River and General Head Boundary packages. The difference is that the water from upper reaches is incorporated into the head and thus effects the interaction downstream of the surface and ground water.

The Streamflow-Routing package does not include a time function for streamflow but rather the flow entering the modeled area is assumed to be instantly available to downstream reaches during each simulation time period (Prudic, 1989). This assumption is generally reasonable because of the relatively slow rate of ground-water flow. The package also assumes that leakage occurs instantaneously, which may not be reasonable if the streams and aquifers are separated by a thick unsaturated zone (Prudic, 1989).

2.7.14 Limitations of MODFLOW

There are limitations inherent in MODFLOW, just as in any simulation model. MODFLOW is strictly a saturated zone model, and does not model the unsaturated zone. The recharge value is assumed to be the actual volume of water that recharges the aquifer directly. The greatest limitations are those associated with representing the system as a finite-difference grid. Spatial discretization is sometimes limited by data availability, and error is introduced by assuming homogeneous characteristics within grid cells. Each package within MODFLOW uses equations that numerically limit the accuracy of the simulation. User input parameters may also introduce a significant amount of error, depending upon data availability and accuracy, and therefore, in analyzing model results, all limitations and overall assumptions must be considered.

2.7.15 Steady-State vs. Transient Models

MODFLOW can be run for “steady-state” or “transient” simulations. A steady-state simulation represents a cross-section in time, and produces one array of hydraulic head values for every cell. The model does not run for a given length of time, but it runs until the system reaches equilibrium, and the residuals have converged given the criterion specified in the Solver Package (McDonald and Harbaugh, 1988). A steady-state simulation is usually performed during the calibration procedure to develop an optimal parameter set. The optimal parameter set is then used for a transient simulation to solve a time-dependant problem, and the data are verified with available data for that time period. Sometimes the transient model will need to be re-calibrated to better match the observed data available for the transient simulation. However, if the steady-state model is adequately calibrated, usually, the re-calibration procedure just requires fine-tuning of the calibrated parameters, if necessary.

2.8 Applications of MODFLOW

MODFLOW has been applied to numerous systems in many different geologic settings for a variety of reasons. MODFLOW simulations are sometimes used to develop a better understanding of the groundwater flow system. For instance, in performing a modeling study, sometimes lack of data in a specific area can be identified, and effort can be made to collect more data to add to the knowledge of the flow system. The primary output from MODFLOW is a resulting hydraulic head distribution for a given simulation. This information can be used to manage existing problems in a groundwater system, evaluate the effects of proposed withdrawal rates from a system, or to evaluate the effects of urbanization on the flow system.

2.8.1 Managing Existing Problems in a Groundwater System

MODFLOW has also been applied to evaluate possible management strategies to alleviate existing problems in groundwater flow systems. In such an application, modeling offers an inexpensive way to evaluate whether or not preventative measures or management decisions will be effective.

Groundwater withdrawals in the Las Vegas Valley, Nevada totaled more than 2.5 million acre-ft between 1912 and 1981 (Morgan and Dettinger, 1994). Effects of heavy pumping are evident over large areas of the valley but are more pronounced near the major well fields. Secondary recharge from lawn irrigation and other sources is estimated to have totaled more than 340,000 acre-ft during 1972-81. Resulting rises in water levels in shallow, unconfined aquifers have caused widespread water-logging of soils, increased groundwater discharge, and potential for degradation of water quality in deeper aquifers by accentuating downward vertical hydraulic potential. MODFLOW was applied to the study area to evaluate possible management alternatives aimed at alleviating problems related to overdraft and water-logging while maximizing groundwater resources. The use of the model as a predictive tool was demonstrated by simulating the effects of using most municipal wells only during the peak demand season for the period 1972-81. The model determined that long-term rates of water level decline near the well fields would be less, but the magnitude of seasonal fluctuations would increase.

A case study in the North Carolina Coastal Plain was conducted using MODFLOW to determine the influence of advancing mining operations that are expected to increase stress on the aquifer system (Reynolds and Spruill, 1995). The Castle Hayne aquifer system is the most

productive in the North Carolina Coastal Plain. Though the aquifer provides water for numerous industrial, agricultural, and municipal/domestic water supplies, depressurization of the aquifer for phosphate mining has produced the most significant impact on its potentiometric surface. The results showed that the aquifer reaches steady state rapidly and is impacted over a large area as a result of the depressurization pumping while wellfield pumping has a relatively minor effect. These results will help to determine permitting decision with respect of withdrawal from the system.

MODFLOW was applied to the New Jersey Pinelands to determine alternate withdrawal strategies on groundwater flow patterns in the area (Modica, 1995). The model was developed to define groundwater flow patterns and residence times in a aquifer system typical of the New Jersey Coastal Plain, and to demonstrate the effects of alternative withdrawal strategies. Results of withdrawal simulations indicate that well-location strategies can alleviate the adverse effects of withdrawals on streams and that large scale regional withdrawals in confined aquifers can adversely affect streams although the effects are dispersed over numerous streams.

2.8.2 Evaluating Effects of Proposed Water Withdrawal

MODFLOW has also been frequently applied to determine the effects of increased water withdrawal, which is one of the primary results of urbanization. Since groundwater is relied on by an increasing number of people as a safe drinking water source, it is important that this increase in water demand does not deplete or lead to the contamination of the groundwater system. Therefore, using MODFLOW to simulate proposed increases in withdrawals serves as a key management practice to managing groundwater effectively.

An existing MODFLOW model was used to simulate changes in groundwater flow caused by hypothetical pumping in an area near the south-eastern part of Carson City, Nevada (Maurer, 1988). A total of five hypothetical pumping patterns were used in the model simulations. The simulations indicate that a maximum of 140 gal/min of induced flow from the Carson River could occur as a result of projected total pumpage of 1,700 gal/min after 10 years; the induced flow could increase 320 gal/min after 50 years. However, river losses were projected to decrease after 10 years and after 50 years when the locations of the pumping centers were moved farther away from the river.

A similar study was performed in East Carson Valley, Douglas County, Nevada (Maurer, 1988). An existing MODFLOW model was used to simulate changes in groundwater flow in response to hypothetical increases in groundwater pumpage. Pumpage scenarios that reflect State groundwater permits and pending applications were used in four different simulations to estimate the effect of hypothetical development of groundwater levels, storage, groundwater flow to the Carson River, and groundwater flow to the Carson River, and groundwater consumed by evapotranspiration over a 45-year period. The highest pumping rate caused water level declines as much as 15 ft, decreased water storage by 27,000 acre-ft, decreased groundwater to the Carson River by 4.3 ft³/sec, and reduced evapotranspiration losses by about 1,200 acre-ft.

A study was performed using MODFLOW to produce simulated effects of proposed groundwater pumping in 17 basins of East-Central and Southern Nevada (Schaefer and Harrill, 1995). The simulations indicate that the proposed pumping would cause water-level declines in many groundwater basins, decreases flow at several regional springs, and decreases discharge by evapotranspiration from the basins. Groundwater levels could ultimately decline several hundred feet in the basins scheduled to supply most of the pumped groundwater. The overall purpose of the study was to estimate potential effects of implementing the proposed water-rights applications filed by the Las Vegas Valley Water District.

A MODFLOW model was developed to simulate the effects of both modern-day (1988) and projected (2010) groundwater withdrawals on the Floridan aquifer system in the greater Orlando metropolitan area (Murray and Halford, 1996). Simulated drawdowns in the Upper Floridan aquifer ranged from 10 to 20 feet in central Orange County. The projected increase in withdrawals changed the entire flow system significantly, affecting spring discharge, river leakage, and capture zones. This simulation illustrates the importance of understanding such impacts to provide for the proper management measures to alleviate negative effects as a result of increased pumpage.

MODFLOW was also applied in the Pullman-Moscs Area, Washington and Idaho (Lum, et al. 1990). The model was used to assess the effects of changes in the rate of withdrawal of groundwater on the water levels in the hydrogeologic units and on streamflow in the area. The model results indicate that groundwater levels would stop declining if the pumpage rates were stabilized at a constant level. Levels will continue to decline into the foreseeable future, however, as long as groundwater pumpage continues to increase.

The public water supply in the Rockaway River Valley, Morris County, NJ, depends almost entirely on groundwater from wells in the valley-fill deposits (Gordon, 1993). A steady-state groundwater flow model was developed to quantify the effects of groundwater withdrawals on water levels. The purpose of the investigation was to examine aquifer response to current and predicted groundwater withdrawals in areas of proposed well sites and the effect of these withdrawals on groundwater discharge to the river. It was found that the anticipated increases in withdrawals of 11.5 million gallons per day by the year 2000, and 14.6 million gallons per day by the year 2040 would significantly affect water resources in the area. The baseflow to the Rockaway River above the Boonton Reservoir may not be sufficient to meet the minimum required reservoir outflow during extended periods of decreased recharge.

2.8.3 Evaluating the Effects of Land Development

MODFLOW has been applied to different sites to determine the combined effects of increased demand on groundwater as a water source and the decrease in recharge associated with urbanization. These studies include both the effects of increased withdrawal, an impact of urbanization, and sometimes of reduced recharge. The combination of these two effects of urbanization can be detrimental to the management of groundwater, and modeling these effects can aid in the planning of management procedures.

MODFLOW was applied to Carson Valley, a river-dominated basin in Douglas County, NV, and Alpine County, CA to simulate the effects of development on the groundwater system. The simulations show that surface water flow is the ultimate source of about 75% of pumped water for six scenarios of possible future groundwater development. Model simulations also indicate that changes from agricultural to urban land uses could decrease the loss of Carson River outflow to pumpage when streamflow is not used for flood irrigation in that area.

Intense development of the Miocene aquifer systems for water supplies along the Mississippi Gulf Coast has resulted in large water level declines that have altered the groundwater flow pattern in the area (Sumner, 1987). This study used MODFLOW to investigate the system response to increased withdrawal due to an increase in urban development. The simulation showed that drawdowns caused by large groundwater withdrawals along the coast have resulted in the gradual movement of the saltwater toward pumping centers.

MODFLOW was also applied to streams and springs in small basins typical of the Puget Sound Lowland, WA (Morgan and Jones, 1995). The model was calibrated to predevelopment conditions and then was used to simulate the effects of pumping on natural discharge to streams and springs. Simulations showed that increased well density caused greater water-level decline locally, but, at equilibrium, did not impact the extent of the area affected by reduction of natural discharge to streams and springs. The model also showed that decreased recharge in areas where development had created impervious surfaces had a direct effect on natural discharge rates to streams and springs. Increased recharge, however, increased natural discharge and offset the effects of water withdrawals from wells. The investigators concluded that further analyses of the time-dependent effects of withdrawals would provide additional insights.

MODFLOW was applied in the Portland Basin, Oregon and Washington (Morgan and McFarland, 1994). The model was used to test and refine the conceptual understanding of the flow system and estimate the effects of past and future human-caused changes to the groundwater system. Recharge under predevelopment conditions was 180 cu ft/sec more than in 1987-88 (post development conditions) due to greater pervious areas in the basin, as compared to post-development conditions. Simulation of the effects of the increased recharge and no well discharge indicates that water levels could have declined as much as 50 feet in response to municipal pumping. The combination of reduced recharge and increased pumpage could have reduced discharge to large rivers by 25 percent, and discharge to small rivers and streams by 16 percent, compared to the predevelopment conditions.

A study was performed on the upper Santa Cruz basin, AZ which used MODFLOW to simulate groundwater flow and potential land subsidence (Hanson and Benedict, 1993). The study evaluated predevelopment conditions, and potential water-level declines and land subsidence as a result of development. The results of projected simulations indicate that a maximum potential subsidence for 1987-2024 ranges from 1.2 feet for an inelastic specific storage of 0.0001 ft to 12 feet for an inelastic specific storage of 0.0015 ft. The simulations were made on the basis of pumpage and recharge rates from 1986 and by using a preconsolidation-stress threshold of 100 feet. A permanent reduction in aquitard storage can range from 1 to 12 percent of the potential loss of 3.9 million acre-feet in aquifer storage, which could significantly impact future groundwater supplies.

2.9 UCODE

The computer program, UCODE, was used for calibrating the steady-state MODFLOW model. UCODE performs inverse modeling, posed as a parameter estimation problem, using nonlinear regression (Hill and Poeter, 1998). Any application model or set of models that have numerical (ASCII or text only) input and output files, such as MODFLOW, can be used in conjunction with UCODE.

UCODE is designed to perform inverse regression using existing algorithms (called application models in the documentation) that can be executed in batch mode and use numerical input and output files. Specifically, the code was developed to: “(1) manipulate application model input files and read values from application model output files; (2) compare user-provided observations with equivalent simulated values derived from the values read from the application model output files using a weighted least-squares objective function; (3) use a modified Gauss-Newton method to adjust the value of user selected input parameters in an iterative procedure to minimize the value of the weighted least-squares objective function; (4) report the estimated parameter values; and (5) calculate and print statistics to be used to (a) diagnose inadequate data or identify parameters that probably cannot be estimated, (b) evaluate estimated parameter values, (c) evaluate how accurately the model represents the actual processes, and (d) quantify the uncertainty of model simulated values.” (Hill and Poeter, 1998). This section provides a brief overview of the information presented in the documentation (Hill and Poeter, 1998).

2.9.1 UCODE Program Structure

Figure 16 presents a flowchart of UCODE. The input files required to run UCODE are the universal, prepare, and extract files (one of each is needed for each UCODE run), the function file (optional, one may be used for each UCODE run), and template files (one or more needed for each UCODE run).

A problem is initialized by reading the following information: (1) solution control information, commands needed to execute the application model(s), and observations from the universal file; (2) instructions from the prepare file, template files, and perhaps a function file which are used to create application model input files with starting or updated parameter values;

and (3) instructions from the extract file for calculating simulated equivalents for each observation from numbers extracted from the application model output files (Hill and Poeter, 1998).

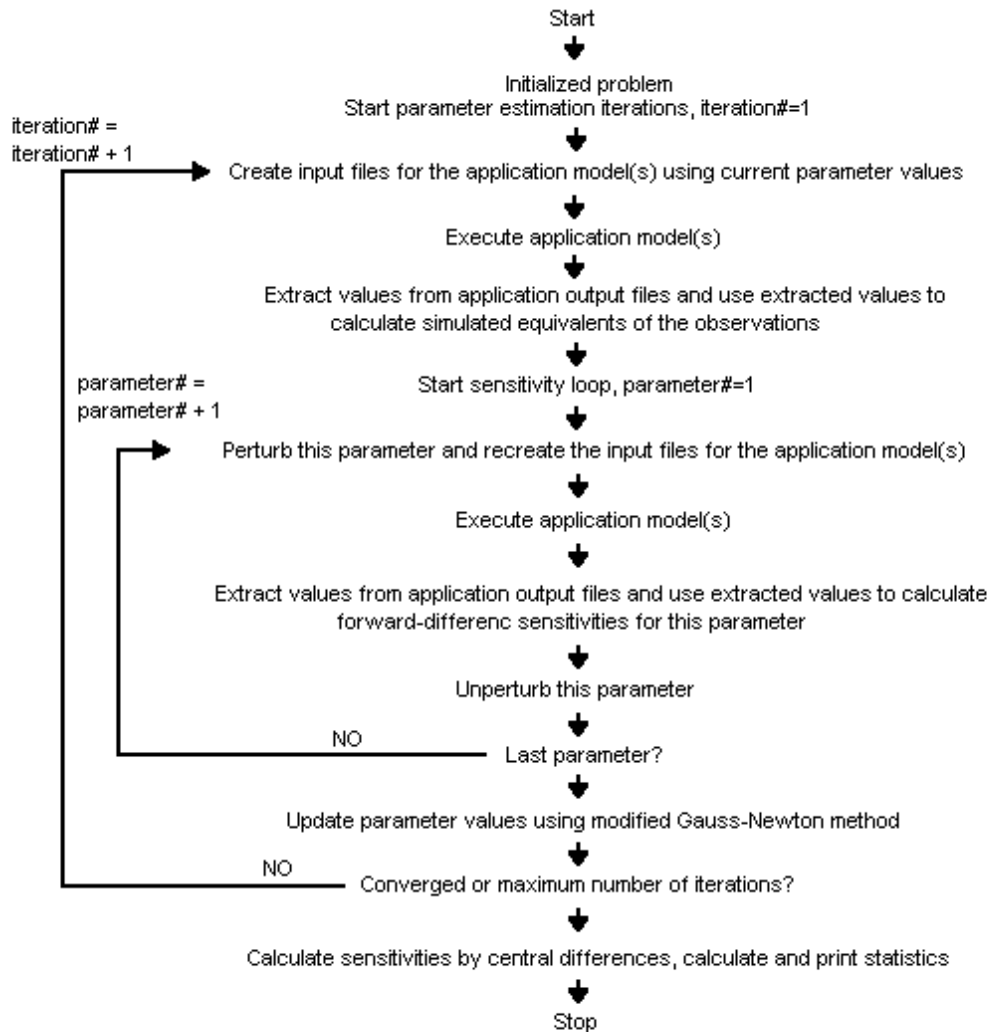


Figure 16. Flow chart of UCODE (Hill and Poeter, 1998).

To solve the nonlinear regression problems for which UCODE is designed, parameter estimation iterations are required. In UCODE, parameter estimation iterations begin by substituting the starting parameter values into template files using instructions from the prepare file to create application model input files (Hill and Poeter, 1998). The application model is then

executed. Next, for each observation, UCODE extracts one or more values from the application model output, using the instructions from the extract file, and calculates an equivalent simulated value to be compared to the observation (Hill and Poeter, 1998). The simulated values calculated at this step are referred to as “unperturbed simulated values” because they are calculated using the starting or updated parameter estimates. The unperturbed simulated values are subtracted from the observations, and these differences are called residuals (Hill and Poeter, 1998). The residuals are weighted, squared, and summed to produce the sum-of-squared-weighted residuals objective function, which is used by the regression to measure model fit of the observations (Hill, 1998, Eq.1).

The application model is executed once again for each parameter, and each time the value of one parameter is slightly different (perturbed) than its unperturbed value in order to calculate sensitivities of the simulated values to the parameters. Sensitivities are discussed the following section. The difference between the perturbed simulated values and the unperturbed simulated values are used to calculate forward-difference sensitivities. Alternatively, the sensitivities can be calculated using more accurate central-differences, but this added accuracy is rarely needed to perform parameter-estimation iterations (Hill and Poeter, 1998).

Both the calculated sensitivities and residuals are then used in a computer program which performs a single parameter estimation iteration (Hill and Poeter, 1998). UCODE is distributed with the nonlinear regression code MRDRIVE, which updates the parameter values using one iteration of the modified Gauss-Newton method as described by Hill (1998). The last step of the parameter-estimation iteration compares two quantities against convergence criteria: (1) the changes in the parameter values and (2) the change in the sum-of-squared-weighted residuals (Hill and Poeter, 1998). If the changes are too large and the maximum number of parameter-estimation iterations has not been reached, the next parameter-estimation iteration is executed (Hill and Poeter, 1998). If convergence is achieved because the changes in the parameter values are small, the parameter values are assumed to be the optimal parameter values - that is, the values that produce the best possible match between simulated and observed values, as measured using the weighted least-squares function (Hill and Poeter, 1998).

If convergence is achieved because the changes in the objective function are small, it is likely that the estimated parameters are optimal and further analysis is generally not needed (Hill and Poeter, 1998). If parameter estimation does not converge and the maximum number of

iterations has not been reached, the updated values are substituted into the template files, and the next parameter-estimation iteration is performed (Hill and Poeter, 1998).

When parameter estimation converges or the maximum number of iterations has been reached, sensitivities are calculated using the more accurate central-difference method. The additional accuracy is needed to achieve a sufficiently accurate parameter variance-covariance matrix (Hill, 1998, eq. 26), from which a number of useful statistics are calculated. The final parameter values are considered to be optimized if parameter estimation converges (Hill and Poeter, 1998).

2.9.2 Calculation of Sensitivities

A sensitivity for an estimated parameter is equal to the derivative of a simulated value, y' , associated with an observation, y , with respect to one parameter, b (Hill and Poeter, 1998), that is: $\delta y' / \delta b$. A sensitivity is calculated for each observation with respect to each parameter (Hill and Poeter, 1998). Sensitivities serve two purposes in inverse modeling. First, they are useful indicators of both the importance of the observation to the estimation of the different parameters and the importance of each parameter to the simulated values. Second, they are needed by the modified Gauss-Newton method to determine parameter values that produce best fit, as measured by a weighted least-squares objective function (Hill and Poeter, 1998). See Hill (1998, eq. 8-13 and Guideline 3) for additional discussion about sensitivities and their utility.

Either the forward- or central- difference approximation is used in UCODE to calculate sensitivities. For forward differences, each sensitivity (one for each observation with respect to each parameter) is calculated as:

$$\frac{\Delta y'}{\Delta b} = \frac{y'(b + \Delta b) - y'(b)}{(b + \Delta b) - (b)} \quad (20)$$

where:

$\Delta y'$ = the change in the simulated value caused by the parameter value change, Δb ,

b = a vector (or a list) of the values of the estimated parameters,

Δb = a vector in which all values are zero except for one which corresponds to the parameter for which sensitivities are being calculated, and

$y'(b)$ and $y'(b+\Delta b)$ indicate that the value of the simulated value, y' , is calculated using the parameter values represented by b or $(b+\Delta b)$.

The derivative is said to be "evaluated for the parameter values in b " which is important because for nonlinear problems, the sensitivities are different depending on the values in b (Hill and Poeter, 1998).

The size of the perturbation, Δb , is calculated as a user-specified factor times the unperturbed factor. If the unperturbed parameter value equals zero during the regression, the perturbation is calculated using the starting parameter value. Calculating the sensitivities for each parameter using either forward or backward differences requires that the application model be run once for the unperturbed parameters and an additional time for each parameter being estimated (Hill and Poeter, 1998).

Central-difference sensitivities are more accurate than forward-difference sensitivities, but require runs of the application model(s) in which the perturbed parameter is both increased and decreased, thus, increasing the execution time by about a factor of two (Hill and Poeter, 1998). Central-difference sensitivities are calculated as:

$$\frac{\Delta_2 y'}{\Delta_2 b} = \frac{y'(b + \Delta b) - y'(b - \Delta b)}{(b + \Delta b) - (b - \Delta b)} \quad (21)$$

where Δ_2 is used to denote the central-difference. Again, the derivative is said to be "evaluated for the parameter values in b ". The added accuracy of the central-difference approximation is always needed when the variance-covariance matrix is calculated. UCODE uses a statistical analysis based on information provided in Hill (1998). A brief discussion of these statistics is presented here.

The observations and prior information is weighted for the regression using diagonal weight matrices, as presented in Hill (1992). When a diagonal weight matrix is used, the scaled sensitivities, ss_{ij} are calculated as in Hill (1992):

$$ss_{ij} = \left(\frac{\delta y'_i}{\delta b_j} \right) b_j \omega_{ii}^{1/2} \quad (22)$$

where:

y'_j = the simulated value associated with the i th observation,

b_j = the j th estimated parameter,

$\frac{\delta y'_i}{\delta b_j}$ = the sensitivity of the simulated values associated with the i th observation with respect to the j th parameter, and is evaluated at b ,

\underline{b} = a vector which contains the parameter values at which the sensitivities are evaluated. Because the problem is nonlinear with respect to many parameters of interest, the value of a sensitivity will be different for different values of b , and

ω_{ii} = the weight of the i th observation.

Using the scaled sensitivities for all observations, composite scaled sensitivities are calculated for each parameter, and indicate the total amount of information provided by the observations for the estimation of one parameter (Hill, 1998). The composite scaled sensitivity for the j th parameter, css_j , is calculated as (Hill, 1992; Hill et al., 1998):

$$css_j = \left[\sum_{i=1}^{ND} (ss_{ij})^2 \Big|_b / ND \right]^{1/2} \quad (23)$$

where:

ND = the number of observations being used in the regression and the quantity in parentheses equals the scaled sensitivities of Equation 26 (Hill, 1998).

2.9.3 Weighted Least-Squares Objective Function

The objective function is a measure of fit between simulated and observed values that are being matched by the regression (Hill, 1998). During regression, defined parameters are calculated to minimize the objective function, creating an “optimized” set of parameters (Hill, 1998). The weighted least-squares objective function used in UCODE is expressed as:

$$S(b) = \sum_{i=1}^{ND} \omega_i (y_i - y'_i(b))^2 + \sum_{\eta=1}^{NPR} \omega_p (P_p - P'_p(b))^2 \quad (24)$$

where:

b = a vector containing values of each of the NP parameters being estimated,

ND = the number of observations (N-observations in UCODE documentation),

NPR = the number of prior information values (NPRIOR in UCODE),
 NP = the number of estimated parameters (N-PARAMETERS in UCODE),
 y_i = the i th observation being matched by the regression,
 $y'_i(b)$ = the simulated value which corresponds to the i th observation (a function of b),
 P_p = the p th prior estimate included in the regression,
 $P'_p(b)$ = the p th simulated value (restricted to linear functions of b in UCODE),
 ω_i = the weight for the i th observation, and
 ω_p = the weight for the p th prior estimate.

The simulated values related to the observations are of the form $y'_i(b)=f(b,\xi_i)$, where ξ_i are independent variables such as location and time, and the function may be nonlinear in b and ξ_i (Hill, 1998).

The differences $(y_i-y'_i(b))$ and $(P_p- P'_p(b))$ are called residuals, and represent the match of the simulated values to the observations. Weighted residuals are calculated as $\omega_i^{1/2}(y_i-y'_i(b))$ and $\omega_p^{1/2}(P_p- P'_p(b))$ and represent the fit of regression in the context of how the residuals are weighted (Hill, 1998).

2.9.4 Modified Gauss-Newton Optimization

The Gauss-Newton optimization method is an iterative form of standard linear regression (Hill, 1998). It works well only if modified by the addition of, for example, a damping parameter and a Marquardt parameter, as described below (Hill, 1998).

2.9.4.1 Normal Equations and the Marquardt Parameter

Normal equations are used to calculate parameter values that minimize the objective function (Hill and Poeter, 1998). Linear regression parameter values are estimated by solving the normal equations once, while nonlinear regression is iterative in that a sequence of parameter updates is calculated, solving linearized normal equations once for each update (Hill, 1998). Therefore, in nonlinear regression there are parameter-estimation iterations. The normal equations and the iterative process for the modified Gauss-Newton optimization method used in UCODE can be expressed as:

$$(C^T X^T_r \omega X_r C + \text{Im}_r) C^{-1} d_r = C^T X^T_r \omega (y - y'(b_r)) \quad (25a)$$

$$b_{r+1} = \rho_r d_r + b_r \quad (25b)$$

where

r = the parameter-estimation iteration number,

X_r = the sensitivity matrix evaluated at parameter estimates b_r , with elements equal to $\frac{\delta y'_i}{\delta b_j}$ (calculated by forward or central differences in UCODE),

ω = the weight matrix ,

$(X^T \omega X)$ = a symmetric, square matrix of dimension NP by NP that is an estimate of the Fisher information matrix, and which is used to calculate statistics described in the UCODE output,

C = a diagonal scaling matrix with element c_{jj} equal to $((X^T \omega X)_{jj})^{-1/2}$, which produces a scaled matrix with the smallest possible condition number (Forsythe and Strauss, 1955, Hill, 1990),

d_r = a vector with the number of elements equal to the number of estimated parameters, and is used to update parameter estimates,

I = an NP dimensional identity matrix,

M_r = the Marquardt parameter (Marquardt, 1963), and

ρ_r = a damping factor.

The Marquardt parameter is used to improve regression performance for ill-posed problems (Theil, 1963, Seber and Wild, 1989, Hill, 1998). Initially, $m_r=0$ for each parameter estimation iteration r (Hill, 1998). For iterations in which the vector d defines parameter changes that are unlikely to reduce the value of the objective function (as determined using condition described by Cooley and Naff, 1990), m_r is increased according to $m_r^{\text{new}} = 1.5m_r^{\text{old}} + 0.001$ until the condition is no longer met (Hill, 1998).

2.9.5 Convergence Criteria

Convergence criteria are needed for the modified Gauss-Newton iterative process. In UCODE parameter estimation converges if either one of two convergence criteria are satisfied (Hill, 1998). First, convergence is achieved when the largest absolute value of d_j^f/b_j^r , $j=1, NP$, is less than a user-defined convergence criterion. That is,

$$\left|d_j^r/b_j^r\right| < TOL \quad \text{for all } j=1, NP \quad (26)$$

where d_j^r is the j th element of d_r , the parameter change vector of equation (25); b_j^r , is the i th element of b_r , the vector of parameter values being changed in equation (25); and NP is the number of estimated parameters (Hill and Poeter, 1998). If b_j^r equals 0.0, 1.0 is used in the denominator. Preferably, this convergence criterion is satisfied by the final calibration model with TOL assigned a value no larger than 0.01 (Hill and Poeter, 1998).

Second, the nonlinear regression converges if the sum of squared objective function changes less than a user-defined amount (SOSR of UCODE) for three sequential iterations (Hill and Poeter, 1998). This convergence criteria often is useful early in the calibration process to avoid lengthy simulations that fail to improve model fit (Hill, 1998). A complete discussion of statistics included in the output of UCODE is found in Hill (1998) and Hill and Poeter (1998).

2.10 Visual MODFLOW

Visual MODFLOW is a pre and post processor developed by Waterloo Hydrogeologic (Guiguer and Franz, 1998). Visual MODFLOW was used in this investigation to create the input model files and to run the model. Visual MODFLOW also presents the output of simulations and has the ability to perform many other data manipulations specific to MODFLOW. Visual MODFLOW contains packages developed by Waterloo Hydrogeologic (Guiguer and Franz, 1998). Two of these packages used in this investigation are the WHS Solver package and the Calibration package. The WHS Solver package is an alternate method to iterate the finite difference approximations to the groundwater flow equation. The Calibration package allows the user to produce graphs to determine the performance of the model with respect to observations. This capability assists in the calibration process.

2.11 Summary of the Literature Review

Both positive and negative impacts are associated with urbanization. There are a variety of benefits that the people living in urban areas enjoy, however the negative environmental impacts tend to overshadow them. The degradation of water quality in urban areas is an important issue and as the population grows, only proper management and planning can minimize the impacts this growth will have on water as a natural resource. As the pattern of

urbanization changes, it is therefore necessary to understand how it affects the surrounding environment, especially the hydrologic cycle and its vulnerability to pollution. Perhaps with proper planning to minimize the negative impacts of urbanization, the positive impacts will once again become predominant.

Groundwater systems are effected by urbanization through increased withdrawal rates and reduced recharge. As previously discussed, since there is a concentration of people in urban areas, there is a large need for natural resources such as drinking water in these areas. Groundwater is the source of drinking water for many people in the United States, and if surface waters continue to become polluted, more people will rely on groundwater as a safer water supply. Increased withdrawal rates, combined with the increase in impervious surfaces associated with urban areas may eventually over-stress the groundwater system and in time deplete groundwater as a safe drinking water source. Therefore, understanding the effects of urbanization on the subsurface flow systems is critical to the efficient management of groundwater as a natural resource.

Groundwater flow models provide a useful tool to learn more about groundwater flow systems. Models are no longer limited by computing power and storage, and therefore can more accurately represent flow systems in three dimensions. When applied correctly, models can be used as predictive tools to assist in the management of groundwater as a natural resource.

The studies presented here are just a few of the numerous applications of MODFLOW, the USGS model used in this study, to determine the effects of future development scenarios, whether investigating withdrawal rates, reduced recharge, or a combination of the two. The primary reason for performing such investigations is to assure a sufficient quantity and quality of groundwater for future use. Excessive pumping could result in the depletion of groundwater as a safe drinking water source, which is why proper management and understanding of the pumpage effects on the groundwater flow system is necessary. A reduction in recharge rates as a result of increased impervious areas due to urbanization can further deplete the groundwater resources. Understanding the effects of urbanization is an important step in reducing the depletion of groundwater, and assuring safe and adequate water supplies from aquifers. Using a groundwater flow model such as MODFLOW can offer an inexpensive alternative to evaluate various management alternatives to better plan for the conservation of groundwater as a natural resource.

Chapter 3

Methodology

3.1 The Study Area

The Upper Roanoke River Watershed (URRW) comprises about 575 square miles of drainage area just below the Roanoke city limits (Figure 17). This area is expected to grow significantly in its transportation infrastructure, residential housing needs, and its industrial and commercial business base over the next decade (Harrington et. al., 1996). There is a need to assess the impacts of the potential growth on the environment, and account for them in a planning process. The city and county of Roanoke have just completed a comprehensive FEMA-sponsored planning of flood control and storm water management alternatives to be implemented over the next 25 years, however it does not address the in-stream impacts on water quality and biotic health of the Roanoke River (Dewberry & Davis, 1997). The Fifth Planning District Commission (FPDC) is the lead agency in the current Roanoke River Regional Stormwater Management Planning study.

The basin is oblong in shape and is located in the western part of Virginia within the Appalachian Valley and Ridge and Blue Ridge physiographic provinces (Figures 17 and 18). It encompasses most of Roanoke County and portions of Botetourt, Montgomery, and Floyd counties, and includes the cities of Roanoke and Salem and the towns of Vinton, Daleville, Lafayette, and Shawsville (Figure 18). The study area is bounded on the north by Tinker, Catawba, and Brush mountains, on the east by the Fincastle Valley and the Blue Ridge, on the west by the Roanoke River-New River drainage divide, and on the south by the Blue Ridge and Blue Ridge upland areas (Waller, 1976). There are several prominent topographic features within the study area: in the Roanoke area, Read-Coyner, Brushy, Mill, Roanoke, and Sugarloaf mountains and Green Ridge; in the Salem area, Fort Lewis and little Brushy mountains, and Twelve O-Clock Knob; in the western part of the area, Paris, Poor, Pilot, and Fishers View mountains and the Pedlar Hills (Waller, 1976). The highest elevation in the study area is Poor Mountain, with 3928 feet in elevation (Waller, 1976). The lowest elevation is at the mouth of Back Creek, 790 feet (Waller, 1976).



Figure 17. Location of study area in the state of Virginia (Waller, 1976).

3.1.1 Climate

The Upper Roanoke River Watershed is located in a zone of temperate climate, subject to seasonal variations and extremes in temperature and precipitation (Waller, 1976). The climate is classified as “mild” by the U.S. Weather Bureau (1970) since extremes of over 100° F in the summer and below 0° F in the winter are minimal. The mean annual temperature is 55.8°F (Roanoke Valley Convention & Visitors Bureau). The average January temperature is 34.5°F and the average July temperature is 75.6°F (Roanoke Valley Convention & Visitors Bureau). Subtropical and polar air masses commonly affect the climate, causing rapid and frequent weather changes due to pressure changes associated with the frontal movements (Waller, 1976). The average annual rainfall is 41.13 in/yr (Roanoke Valley Convention & Visitors Bureau). The average snowfall is 24.0 in/yr (Roanoke Valley Convention & Visitors Bureau).

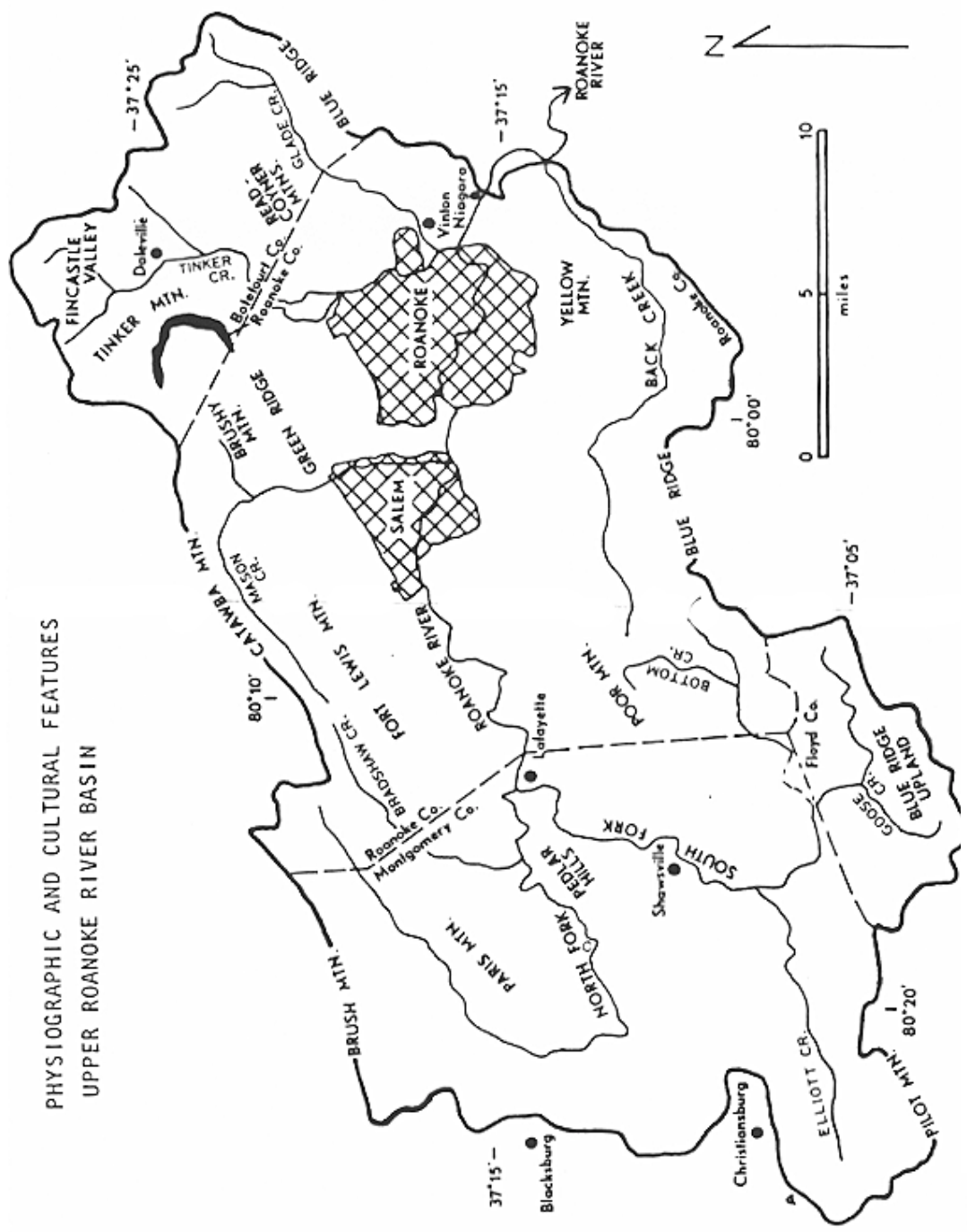


Figure 18. Physiographic and cultural features, Upper Roanoke River Basin (Waller, 1976)

Evapotranspiration is the process by which water is evaporated from wet surfaces and transpired by plants (Waller, 1976). Due to the relative stability of the factors that control it, Evapotranspiration has a narrow range of fluctuation from year to year in comparison to precipitation and runoff (Lee, 1942). Evapotranspiration accounts for the greatest amount of water loss from the Upper Roanoke River Watershed (Waller, 1976). Waller (1976) reported an annual Penman Potential Evapotranspiration of 25.08 inches, averaged for all of the sub-watersheds within the Upper Roanoke (April 1969-March 1970). Monthly potential evapotranspiration ranged from a low of 0.07 to 0.12 inches in December 1969 and January 1970 to a high of 4.79 to 5.61 inches in July 1969. The annual potential evapotranspiration ranged from a low of 24.52 inches in the Bottom Creek subbasin to 27.53 inches in the Tinker Creek subbasin. Waller (1976) estimated that approximately three-fourths of the annual precipitation in the basin was lost to evapotranspiration.

3.1.2 Land Use

The current land use of the study area was determined in general categories by the use of ArcView. The source of the data for this classification in the Virginia GAP Analysis Project from the Fish and Wildlife Information Exchange (FWIE, 1999). The original data came from LANDSAT Thematic Mapper Scenes which were classified by the FWIE (FWIE, 1999).

Table 2. Land use in the Upper Roanoke River Watershed.

Land Use	Area (ha)	% of Total Area
Forest	90,607	61.2%
Herbaceous/Agriculture	21,149	14.3%
Open Water	1,063	0.7%
Disturbed	17,826	12.0%
Mixed	17,436	11.8%

The “Mixed” land use category in Table 2 represents edge ecosystems, which are transition zones between forests and herbaceous areas. A reasonable assumption is to attribute half of the Mixed area to Forest and half to Herbaceous. The “disturbed” land use category in

Table 2 includes four subgroups: non-vegetated (mines, barrens, etc.), high intensity developed, residential/low intensity developed, and recent clear-cut (FWIE, 1999).

3.1.3 Population and Household Size

Roanoke County keeps separate records from the cities of Roanoke, Salem, and Vinton. However, most of the population within these cities are supplied by municipal water supplies. Therefore, the population increase in the County is the population that should be included in the groundwater development scenarios. The Demographic and Economic Profile for Roanoke County states that the population in 1970 was 53,817. In 1980, it increased to 72,945, which represents a population growth of approximately 35% (Harrington, et al. 1996). During the 1980s, the population growth slowed to 9%, and the population reached 79,294 according to the 1990 Census (Harrington, et al. 1996). In 1996, the population was estimated to be 83,100 (Harrington, et al. 1996). Based upon this historical trend and current building permit activity, the population will continue to grow at approximately 1% per year well into the next century (Harrington, et al. 1996). Figure 19 illustrates the population growth and projected growth from 1970 to 2010 (Harrington, et al. 1996).

The Roanoke County Demographic and Economic Profile also includes information about the Greater Roanoke Valley, which includes not only the County, but the cities as well. Figure 20 shows the population growth and projections for the Greater Roanoke Valley. However, since the population of the Greater Roanoke Valley that resides in the cities of Roanoke, Salem and Vinton is predominately served by municipal water supplies, the population increase of only the County is used in the future development scenarios.

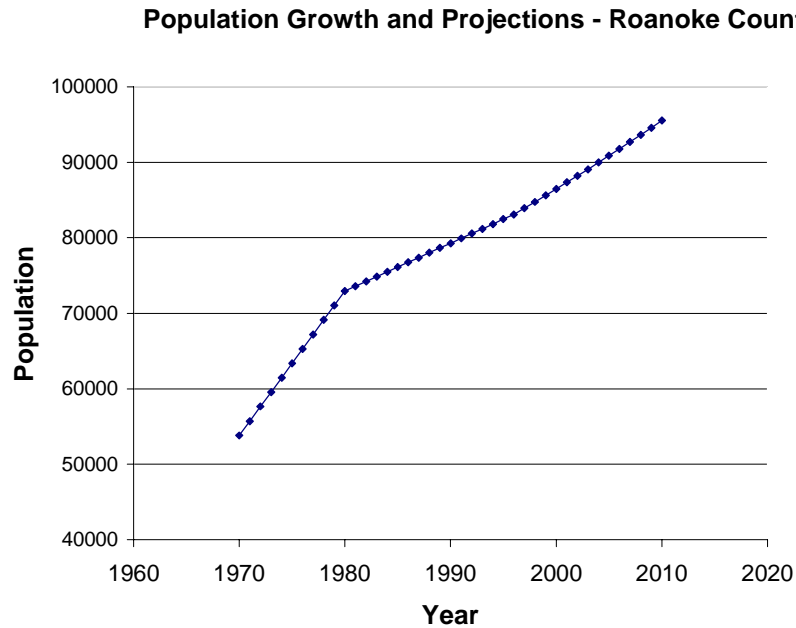


Figure 19. Population Growth and Projections – Roanoke County

The average household size is also an important statistic with respect to land use because it dictates the distribution of population and housing in future scenarios. The average household size in 1980 was 2.8, and in 1990 it was 2.54 (Harrington, et al. 1996). This number is projected to decline to 2.41 and 1.71 by the years 2000 and 2010 respectively (Harrington, et. al., 1996). As the total population increases and the average household size decreases, more housing units will be needed to accommodate the same number of people.

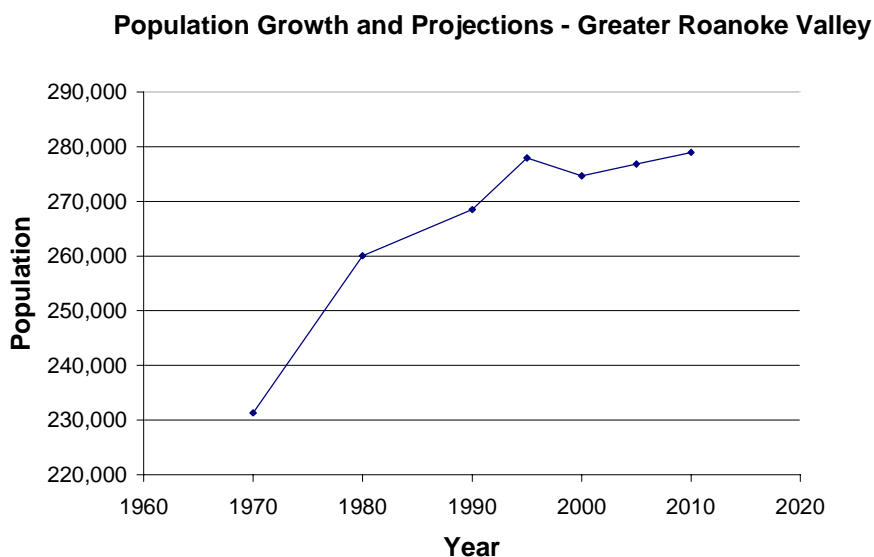


Figure 20. Population growth and projections – Greater Roanoke Valley.

3.1.4 Groundwater Use In the Study Area

Groundwater use in the study area is extensive with a minimum of 1000-2000 wells and springs used as sources of residential and commercial water supply (Roanoke County Health Dept., 1999). Groundwater use is concentrated in the Roanoke-Salem metropolitan area but domestic supplies are scattered throughout the study area. In the metropolitan area, most of the population is serviced by municipal sources, some of which are derived from groundwater. In the county areas surrounding the cities, groundwater is furnished by a large number of wells to most of the residential, industrial, and commercial users.

Almost all the water supplies to the Roanoke-Salem metropolitan area, including groundwater, are treated by the Roanoke and Vinton sewage treatment plants and discharged into the Roanoke River and Tinker Creek (Waller, 1976). Because of this area-wide sewage collection and treatment system, there are only a few septic systems in the metropolitan area, however, most rural areas in the watershed are served by septic systems (Waller, 1976). Therefore, groundwater, in most instances is protected except perhaps where there is a concentration of septic fields as in the rural areas.

3.1.5 Groundwater Level and Movement

The water table within the study area continuously fluctuates and reflects changes in recharge rates (Waller, 1976). There is a general seasonal fluctuation where there is a water level decline in April or May with the increase in evapotranspiration. During late August and into September, the water table tends to be the lowest. In November or December water levels begin to rise when evapotranspiration is low and after precipitation has recharged the system (Waller, 1976). During March, before evapotranspiration rates have increased and precipitation is high, the groundwater levels tend to be the highest. Water-level fluctuations can also be caused by changes in precipitation, overpumping, earth tides, and earthquakes. In the Valley and Ridge and Blue Ridge provinces, alluvial and colluvial deposits are commonly thin and the bedrock is well fractured, depending upon the depth. These characteristics allow natural recharge to be rapid and water levels to rise quickly (Waller, 1976). The recovery of water levels, as well as discharge from springs and seeps is also rapid for the same reason.

Average static water-level fluctuations due to seasonal climatic variations are generally less than short-term fluctuations caused by changes in precipitation (Gathright and Wilson, 1968). During a year with normal precipitation, recharge to the groundwater reservoir is approximately equal to the discharge from the reservoir so that the groundwater surface at the end of the year is about the same level as at the beginning of the year (LeGrand, 1967; Waller, 1976).

3.1.6 Geohydrologic Units

Geohydrologic units are defined as “bodies of rock (aquifers, confining units, or a combination of aquifers and confining units) that comprise a framework for a distinct hydrologic system” (Maxey, 1964; Pfankuch, 1969). Waller (1976) compiled information from the previous eighteen geologic studies that have been performed within the study area. These investigations resulted in detailed information on the geology of most of the study area with a minimum of overlap and conflicting data. Along with this information, in order to have as complete and accurate a geologic base map as possible at that time, an area in southeastern Roanoke County was mapped on a reconnaissance level (Waller, 1976). From this geologic base map and by grouping formations with similar characteristics, the investigator was able to determine three major geohydrologic units within the study area. A complete discussion of these

groupings can be found in Waller (1976). The resulting geohydrologic units are illustrated in Figure 21. These units were determined on the basis of hydrologic characteristics of the rock types present in the study area and the stratigraphic sequence of the bedrock units (Waller, 1976). The three units identified are:

- (1) The Precambrian and Cambrian metamorphics and clastics geohydrologic unit which contains the rocks of the Blue Ridge Complex and Chilhowee Group (Table 3). This unit underlies a portion of the eastern edge on the west slope of the Blue Ridge and the southern part of the study area (Figure 21) (Waller, 1976). This unit is relatively impermeable which serves as a poor to fair source of ground water unless wells are located near perennial streams or in fractured rocks along the Blue Ridge fault (Waller, 1976),.
- (2) The Cambrian and Ordovician carbonates geohydrologic unit which contains the rocks of the Shady Dolomite, Rome and Elbrook formations, Knox Group and the Middle Ordovician limestones (Table 3). This unit underlies the major valley areas in the central part of the study area and some upper valley areas (Figure 21) (Waller, 1976). This unit yields ground water from fractures and other openings that have been enlarged by solution (Waller, 1976). This unit is the most productive and most consistent geohydrologic unit in the Upper Roanoke River Basin (Waller, 1976).
- (3) The Ordovician to Mississippian clastics geohydrologic unit which contains the rocks of the Middle and Upper Ordovician shales, Devonian-Silurian sandstones and shales, and Mississippian-Devonian shales and sandstones (Table 3). This unit occurs as a body of rock in the center of the northern part of the study area (Figure 21) (Waller, 1976). This unit contains relatively impermeable rocks which are typically poor to fair sources of ground water (Waller, 1976).

Table 3. Composite Sequence of Geologic and Geohydrologic Units, Upper Roanoke River Watershed (Waller, 1976)

System	Formation	Thickness (ft)	Lithologic Description	Geohydrologic Unit
Mississippian	Unconsolidated Deposits	Variable	Alluvium, colluvium, and tufa	Ordovician to Mississippian Clastics
	Stroubles Formation Price Formation	1100 200-500	Sandstones, siltstones, and shales Quartzose sandstones, shales, and conglomerates	
Devonian	Chemung Formation	500-600	Sandstones, siltstones, and intercalated shales	Cambrian and Ordovician Carbonates
	Brallier Formation	1000-3000	Shales with interbedded siltstones and shales	
	Millboro Formation	200-900	Shales with siltstones	
	Needmore Shale	10-50	Clay shales and clay limestones	
	Huntersville Chert	10-50	Chert with interbedded shales, sandstones, and siltstones	
	Ridgeley Sandstone	10-80	Quartzose sandstones, locally conglomeratic	
	Keyser Sandstone	30-35	Quartzose sandstone	
Silurian	Tonolway Limestone	0-60	Limy Claystone	Cambrian and Ordovician Carbonates
	Keefer Sandstone	200-600	Orthoquartzite	
	Rose Hill Formation	40-70	Hematite-cemented sandstones and orthoquartzites	
	Tuscarora Sandstone	10-40	Orthoquartzite	
Ordovician	Martinsburg Formation	1000-15000	Calcareous shales with limestones	Cambrian and Ordovician Carbonates
	Bays Formation	40-900	Siltstones and sandstones	
	Liberty Hall Formation	900-1800	Calcareous shales with limestones	
Ordovician	Fetzer Limestone	0-25	Limestone (possible equivalent of Effna Limestone)	Cambrian and Ordovician Carbonates
	Effna Limestone	35	Limestone	
	Lincolnshire Limestone	0-50	Limestone	
	New Market Limestone	30	Limestone	
	Beekmantown Formation		Dolomite with limestone and chert	
	Chepultepec Formation	1900-3200	Limestone and dolomite	

Table 3. (Continued) Composite Geologic and Geohydrologic Units, Upper Roanoke River Watershed, Waller (1976)

Cambrian	Copper Ridge Dolomite	1000-1600 2000+	Dolomite with limestone and shales	Cambrian and Ordovician Carbonates Continued
	Elbrook Dolomite		Dolomite with limestones and shales	
	Rome Formation		Shales and siltstones with limestones and dolomites	
	Shady Formation		Dolomites with Shales	
PreCambrian	Erwin Quartzite	2500-3000	Orthoquartzites	Precambrian and Cambrian Metamorphics and Clastics
	Hampton Shale		Shales and siltstones	
	Unicoi Formation		Shalestones and quartzites with conglomerates, shales and basalts	
	Blue Ridge Complex		Undifferentiated gneisses and granites	

— Unconformity

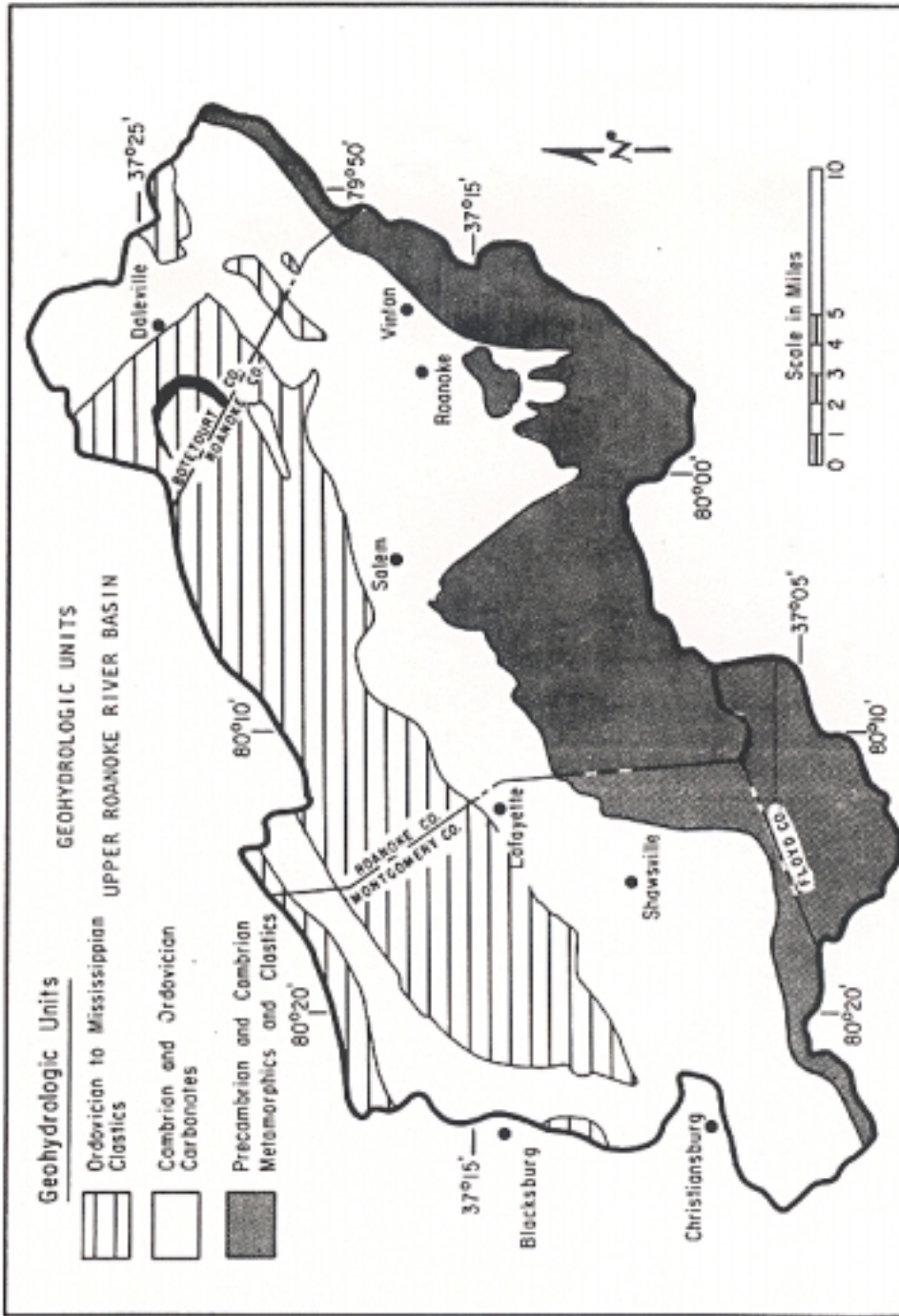


Figure 21. Geologic units of the Upper Roanoke River Basin (Waller, 1976).

The Quaternary unconsolidated deposits which overlie the three bedrock geohydrologic units were not considered as a geohydrologic unit in the Waller (1976) investigation because they are limited in areal extent and continuity. However, they will be considered as a geohydrologic unit in this modeling investigation because the water table may reside in these deposits.

Based on the available data within the Roanoke-Salem metropolitan area and from wells scattered throughout the basin, the groundwater surface is generally considered to be a subdued reflection of surface topography (Waller, 1976). The movement of groundwater is along angular fracture paths from areas of recharge to areas of discharge at springs and along the stream valleys. Due to the relief and stream dissection in most of the basin, the depth to groundwater is usually greater than 20 feet, but less than 100 feet, under most of the upland areas. In low-lying areas the depth to groundwater is commonly between zero and 10 feet below land surface, with hydraulic gradients not significantly different from the land surface gradients (Waller, 1976).

Quaternary unconsolidated deposits overlie the folded and faulted Precambrian and Paleozoic bedrock units in the Upper Roanoke River Basin (Waller, 1976). These deposits have generally not been utilized as a source of groundwater and it is difficult to determine their significance as a groundwater producing unit (Waller, 1976). Latta (1956) reported that only one well derives water from these deposits and that, therefore, they are relatively unimportant as a source of groundwater. He also stated that small to moderate supplies might be obtained in places, but that the deposits are too thin in most places to yield large quantities of water. Furthermore, there is a greater potential for water in these deposits to be contaminated due to their shallow depths.

In contrast to Latta's (1956) conclusions, Chen (1960) reported that the unconsolidated alluvial deposits along the larger creeks contain at least moderate to possibly large groundwater supplies. Chen (1960) also reported that the thick colluvial deposits fringing the ridges are good aquifers with a generally high rate of recharge. Where these colluvial deposits are wide and merge into residual and alluvial deposits, good well yields can be expected. Chen (1960) also reported that the unconsolidated deposits serve as a large recharge reservoir for underlying bedrock units and that the thickness, extent, and location of these deposits is important in selecting productive well sites (Chen, 1960).

The groundwater surface generally lies in the unconsolidated deposits several feet above the bedrock surface (Waller, 1976). Because these unconsolidated deposits are more porous than the underlying bedrock units, they serve as a recharge reservoir to the underlying aquifers (Waller, 1976).

These are the most current and the most complete geologic data that have been compiled for the study area to this date. These will be used to develop the conceptual model for the MODFLOW simulations. Although these generalizations were made in 1976, the assumption that they still hold true is reasonable due to the lag time it takes most regional groundwater systems to be effected by changes in recharge and withdrawals, and because no current data has been compiled.

3.1.7 Available Data

MODFLOW requires a variety of data as input, depending upon what packages are included in the simulation. For this study, the Basic Package, the Block-Centered Flow Package, the WHS Solver Package, the Output Control Package, the Recharge Package, the Calibration Package, the Well Package, the General Head Boundary Package and the Streamflow-Routing Package were used (McDonald and Harbaugh, 1988). The Evapotranspiration Package was not included in the model because it was assumed that surface water model simulations would account for this part of the water budget, and very little ET data exist for the area.

The Basic Package includes information about the aerial extent of the aquifers, and their location within the system (McDonald and Harbaugh, 1988). The input to this package defines the locations of the layers, and the aquifer boundaries. A complete discussion of the development of the grid is included in section 3.2.3.1 of this report. The grid was constructed from a variety of data including a 30 m Digital Elevation Model (USGS), well driller's logs in Roanoke and Montgomery Counties, and cross-sectional geologic data included in Waller (1976), and the Roanoke County Groundwater Report (Breeding, et. al.1976).

The Block-Centered Flow Package includes information about the hydraulic properties of each cell within the grid (model domain) (McDonald and Harbaugh, 1988). The properties include hydraulic conductivity, transmissivity, storage, and vertical conductance. Hydraulic conductivity and storage values were required as input for Visual MODFLOW. Transmissivity and vertical conductance values are calculated within Visual MODFLOW based upon the

thickness and extent of each layer. This internal calculation constrains the input values for transmissivity and vertical conductance because they are not defined by the user. The hydraulic conductivities and storage values were derived from a similar investigation performed in Pennsylvania, in a fractured bedrock aquifer system (Gburek, Fomar, and Urban, 1999). Section 3.2.3.5 of this report presents the hydraulic conductivities used as input for this model that were derived from both this investigation, and from flow information about the three geohydrologic units defined in Waller (1976). The storage values for each layer were also inferred from this study, and are included in the results presented for the transient simulations (section 4.2.1), since the storage values are not used in the groundwater flow equation for steady-state simulations.

The WHS Solver Package, a package specific to Visual MODFLOW (Guiguer and Franz, 1998) was used in this model. Details of this package and the methods of iteration it uses are included in the MODFLOW User's Manual (McDonald and Harbaugh, 1988). There were no physical data necessary as input for this package. The Output Control Package also does not require any physical data, but it simply controls the type and frequency of output for each simulation.

The Recharge Package requires a user-defined recharge flux for each cell within the model domain. This value can be set equal to zero if no recharge is occurring in a given location. Values of recharge are very difficult to either measure or estimate. Therefore, the original input values for recharge were estimated as a percentage of annual precipitation based on research performed in this area (Rutledge, Mesko, 1996). Since the model was built from information presented by Waller (1976), precipitation for the study year 1969-1970 was used as input to the model. Detailed information about the Recharge Package inputs for this model are discussed in section 3.2.3.6.

The Calibration Package, also a packages specific to Visual MODFLOW (Guiguer and Franz, 1998), aids in the manual calibration process, allows the creation of graphs within the Visual MODFLOW program and requires observed data as input. The geohydrologic data from 293 wells in the study area were collected by Waller (1976) using the groundwater files of the former Virginia Division of Water Resources (now the Bureau of Water Control Management of the Virginia State Water Control Board) the Virginia Department of Health, water-well completion reports, health permits, drillers' records, owners' records and reports from Latta (1956). Records were crosschecked by Waller (1976) to insure that data for each well were

accurate. Since domestic wells usually are pump tested until a specific yield is obtained and all other types of wells are usually pump tested for maximum yield, preference in data collection was given to non-domestic wells (Waller, 1976). The observed heads reported by Waller (1976) were used as observed head values to calibrate the model (Appendix B). A discussion of how the information was used is included in section 3.3.

The Well Package was used to add pumping scenarios to the calibrated model. The pumping information was compiled by the Department of Environmental Quality (DEQ) for Roanoke County. Population projections included in an Economic and Demographic Profile for Roanoke County were used to project future development scenarios (Harrington, et al., 1996). All wells were pumped in layer 2 of the model.

The rivers in this investigation were represented in two different ways, using two separate packages-the General Head Boundary Package, and the Streamflow-Routing Package. Both packages require detailed river information for input. The head of each river cell is a necessary input parameter. These values were digitized and interpolated from USGS 7.5' quadrangles of the study area. River bottom conductance values (Equation 9) are also necessary input, and are usually not known parameters due to the difficulty of measuring them. These values were determined in the calibration process, and were assigned an arbitrary initial value of 50m/d, based on initial model convergence. A complete discussion of the river input parameters is included in section 3.2.3.4.

Overall, there are not much current subsurface data available for the study area. A majority of the input information that was used to construct this model was compiled by Waller (1976). Cross-sections of the study area, and geohydrologic units were defined and flow characteristics were determined. Well information such as well yield and hydraulic head information was also included. Although these data are over 20 years old, the regional subsurface flow environment generally will not change much in this length of time due to the volume of water in a regional system. Therefore, the assumption that a majority of these data are still applicable is reasonable. A complete discussion of the input model data is included in section 3.2.3 of this report. The actual model input files are included in Appendix A. Current ground water use data is available from the City and County of Roanoke and is incorporated in the future development scenarios presented in section 4.3.2. The decision to use the 1976 data for the model construction was based on the fact that the data was compiled and field verified.

The field verification of the hydraulic heads took place, for all practical purposes, in a cross section of time, and therefore was ideal in the construction of a steady-state model. A more current nor complete compilation exists. The records that exist from the Roanoke County and Roanoke City seem to include well driller's logs and pumping information. However, the hydraulic heads must be measured in a well that is not being pumped, and the reported water table position included in well driller's records may not be accurate due to aquitards that may be present.

3.2 Conceptual Model

Developing a conceptual model is a method of organizing known information about the hydrogeologic system, and translating it into a simplified representation of complex hydrogeologic system. To mathematically model the groundwater flow within the study area, it is first necessary to conceptualize the system based on known data such as the direction of groundwater flow, identification of flow boundaries, hydrologic characteristics, and a variety of other data. The conceptual model is the key to developing an accurate representation of the natural system. The simplifying assumptions made in a conceptual model could govern the system's response, which could dramatically effect the model results. Therefore, it is necessary to learn as much as possible about the groundwater system before developing the conceptual model.

3.2.1 Model Assumptions

In order to simplify the modeling approach, several assumptions were made. Groundwater flow divides were assumed to generally coincide with surface-water and topographical divides. Many studies of local and regional groundwater systems (Faye and Mayer, 1990, Robinson and others 1997) especially those conducted for small basins, are based on this fundamental assumption. This assumption sometimes is violated as reported by Tiedeman (Tiedeman, 1998) and others in their study of fractured rock near Mirror Lake, New Hampshire. The boundaries in this investigation however, will be assumed to be no-flow boundaries that correspond to the surface-water drainage basin to minimize the variability in the input parameter set.

It was also assumed that the sediments that comprise the unconsolidated material in the top layer, and the system of fractures in the bedrock that supply a majority of wells in the area transmit water as an equivalent porous media. Darcy's Law can then be assumed to apply to groundwater flow, and the use of MODFLOW to simulate this flow system is thus appropriate. This assumption has been made by other investigations particularly in fractured or conduit-flow aquifers (Glenn and others, 1989, Nelson, 1989). It is valid due to the scale of the model. At a regional scale, the fractures in the system are assumed to represent the primary porosity of the system, and approximate the porosity of a continuous porous medium at a regional perspective.

The aquifer properties within each model cell (see discretization) are assumed to be homogeneous and isotropic. The model can simulate heterogeneity caused by changes in hydraulic properties by varying the hydraulic conductivities or transmissivities of the model cells. MODFLOW can simulate anisotropy in the horizontal direction, however, it is represented as one uniform value that is constant throughout a model layer (McDonald and Harbaugh, 1984). Different layers can have different values for anisotropy, but it cannot vary within a layer. Since anisotropy is constant for a given layer, the model does not adequately simulate geologic structures that could cause a barrier to groundwater flow in one direction and a conduit flow in another.

There are a number of faults in the study area that are not explicitly modeled (Figure 22). There are no data available to determine how these faults are affecting flow within the system, and therefore, in order to maintain simplicity in the model, they will not be included in the conceptual model framework. This assumption is made based on the lack of available data, and could significantly affect the model results. Since the system is comprised of fractured bedrock, the primary means of water movement is through these fractures that are influenced greatly by the fault system.

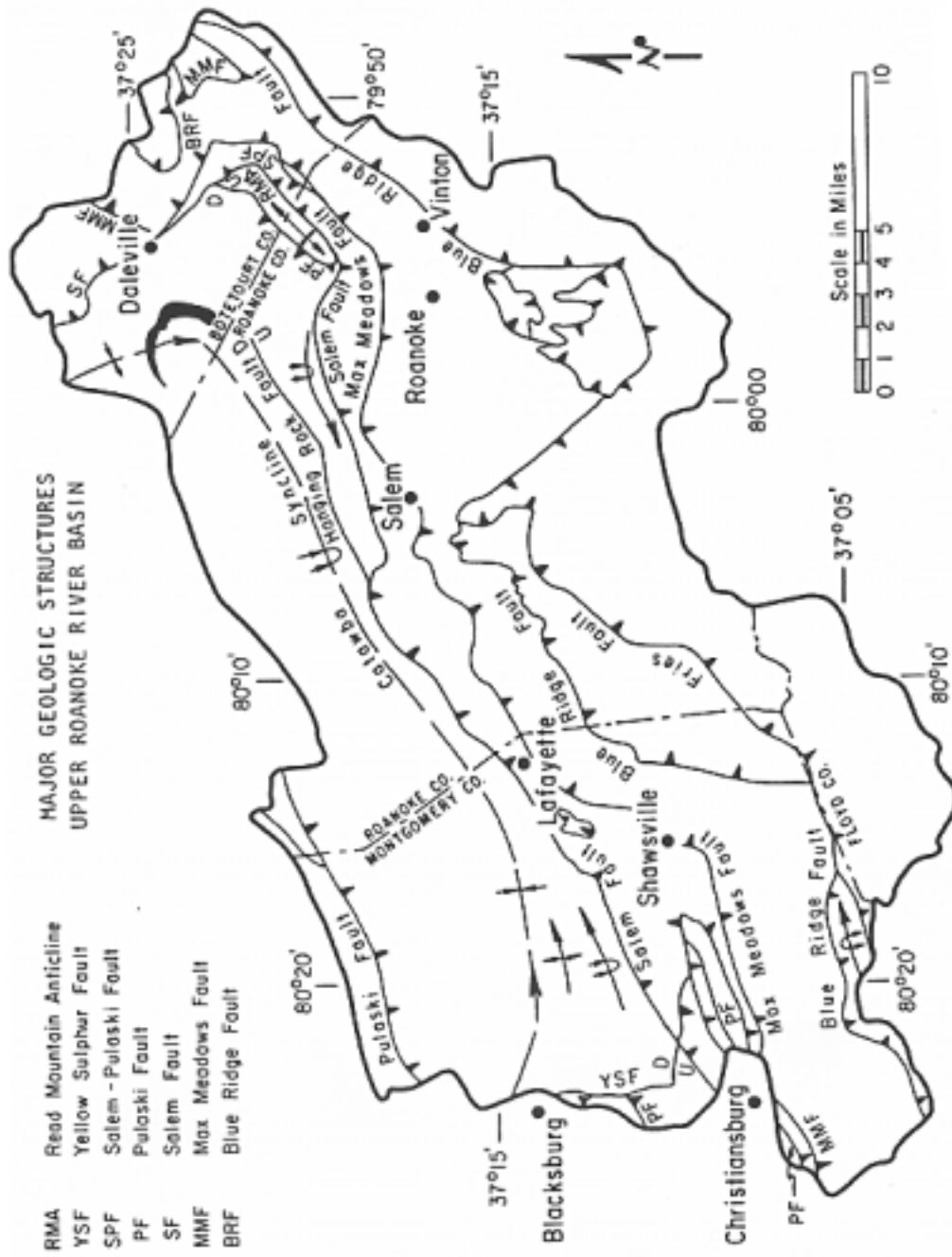


Figure 22. Major geologic structures of the Upper Roanoke River Basin (Waller, 1976).

Figure 23 shows a conceptual representation of the Upper Roanoke River Watershed. The sloping hydrogeologic units do not slope as steep as they appear in Figure 23, there is actually a vertical exaggeration factor of close to 1000 that distorts the conceptual model to illustrate the system. The conceptual representation was developed based on the cross-sectional geologic data reported by Waller (1976) and cross-sectional data included in the Roanoke County Groundwater Report (1976) (Figures 24 and 25). These cross sections were developed from field data collected along these sections of the County. The unconsolidated deposits that lie on top of the fractured bedrock in the study area will be represented in Layer 1. These unconsolidated deposits were assigned uniform hydrologic properties for the entire layer, based on the assumption that they serve only as a recharge reservoir to the fractured bedrock aquifers beneath. The following section discusses the details of the conceptual model, and assumptions made in its development.

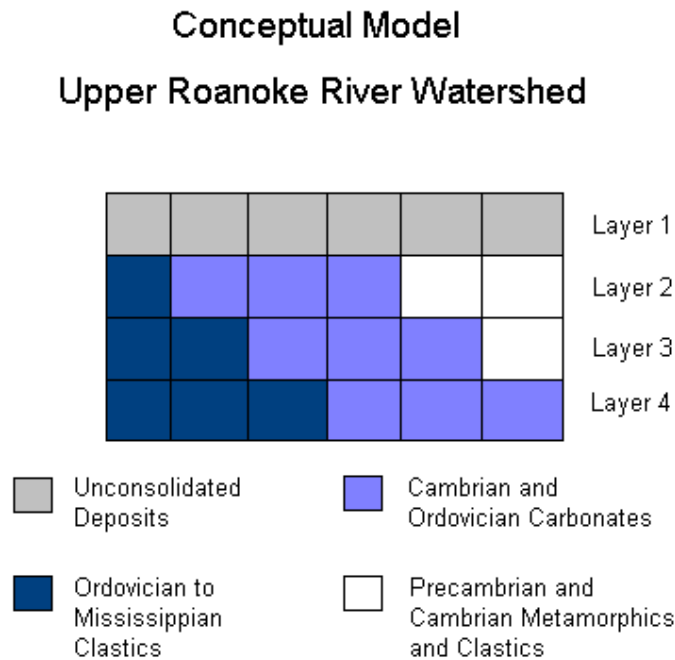


Figure 23. Conceptual model of the Upper Roanoke River Watershed (Vertical exaggeration factor of about 1000).

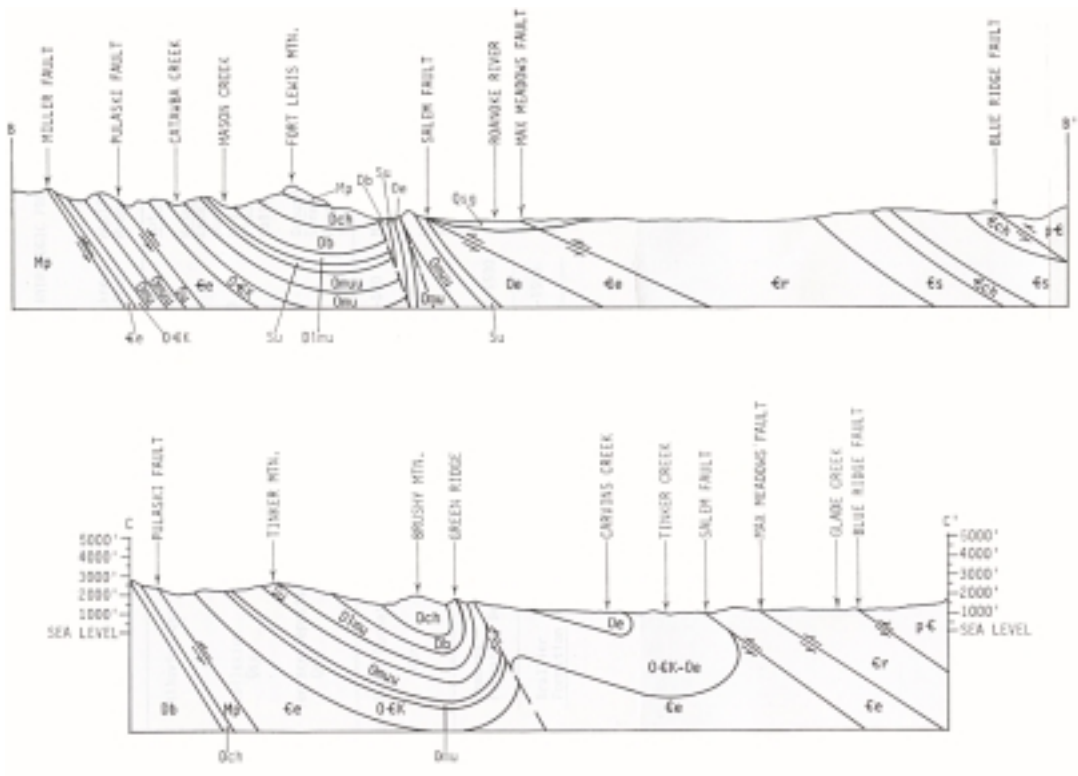


Figure 24. Cross-sectional view of Roanoke County (Breeding and Damson, 1976).

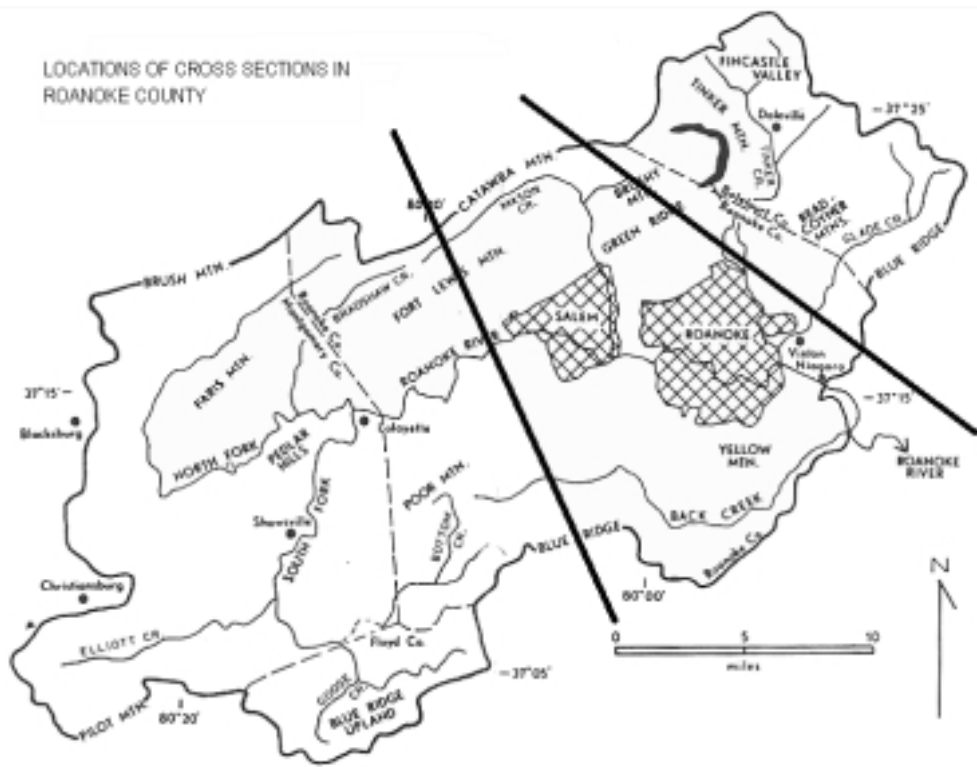


Figure 25. Location of cross-sections within Roanoke County (Breeding and Damson, 1976).

A majority of the productive wells in the study area were drilled directly into the bedrock with the goal of hitting a flowing fracture. Therefore, conceptually, a representative porous material is used to represent this system of water-producing fractures. The boundaries of the study area are represented as no-flow boundaries due to the lack of data and knowledge about the groundwater movement in the basin. This will allow the boundary conditions to change throughout the duration of the simulation. The land surface is represented using a DEM (Digital Elevation Model), and the groundwater surface was derived from the information reported by Waller (1976). A DEM is a file that contains the elevations of discrete points within an area based on the image resolution.

3.2.2 Representation of the System as a Four-Layer Model

Model layers are commonly separated on the basis of variability in the permeability values (Burbey and Prudic, 1991). Layer 1 (Figure 23) was used to simulate the unconsolidated deposits that act as a recharge reservoir to the underlying bedrock (Waller, 1976). The bedrock aquifers that are represented by Waller (1976) are a system of hydrogeologic units that are situated primarily in a downward-sloping position (Figure 24). This bedrock was simply divided into three layers in order to model vertical flow that may be occurring within the system. Layer 2 (Figure 23) represents relatively shallow flow, and Layer 3 (Figure 23) represents the deep flow that may be occurring. Layer four was added to the conceptual model to determine whether or not flow was occurring at greater depths. The actual depth to the base of deep flow is unknown, however a mathematical method presented by Hermance (1999) was applied to determine the theoretical depth of groundwater flow based on the maximum elevation in the watershed and the distance from that point to the outlet. The depth of the flow, d , can be estimated using:

$$d \leq \frac{\lambda_s}{2\pi} \quad (27)$$

where: λ_s = distance from maximum elevation to the watershed outlet (L)

d = theoretical maximum depth of groundwater flow (L)

This method indicates an estimated theoretical depth of 4533 m, given that the distance from maximum elevation to the watershed outlet is approximately 28,483.47m (calculated in ArcView from the 30m resolution DEM of the study area). The highest elevation in the study area was determined to be approximately 1197m, which would mean that the system would be modeled to a minimum depth of 3336 m below sea level. Most likely, water that is flowing in this deep aquifer system will not have much effect on the flow to and from waterways, and therefore it is not necessary to model the system to this depth. The bedrock aquifer system was thus represented in the model as three separate layers, Layer 2 (Figure 23) representing the shallow system, Layer 3 (Figure 23) representing the deeper system, and Layer 4 (Figure 23) to assess the depth of groundwater flow. This method also assumes that the material in the system is homogeneous and isotropic, which is not necessarily the case in the study area. The variability in hydraulic conductivity values in the system, especially those with small values, will greatly impede vertical flow. Therefore, the depth of flow calculated using this method is much larger than the actual depth of flow in the system.

3.2.3 Modeling Approach

A modeling approach similar to that used by Burbey and Prudic (1991) was employed in this study due to the lack of sufficient data from the study area. A steady-state model was first developed from the data presented by Waller (1976). Estimates of hydraulic properties of the various consolidated rocks are largely unknown, and were thus based on values available in the literature, presented later in this report. The steps taken to construct the groundwater flow model in MODFLOW were to create the model grid; adjust the data; develop initial hydraulic head data; determine necessary river input parameters and location of river cells; determine hydraulic conductivities; and determine recharge areas and rates.

3.2.3.1 Creating the Model Grid

The study area was divided into square cells of 0.0625 mi². This grid-cell size was chosen because the data are relatively sparse over much of the study area, and a smaller size was considered to be impractical. Previous regional studies have used grid cells up to and greater than 5 by 7 miles, as in the Carbonate Rock Province in the Great Basin (Burbey and Prudic, 1991) for a total study area of 92,000mi². And in studies developed for local smaller areas, as in

Woburn, Massachusetts, grid cells are as small as 20ft. by 20ft., for a total study area of 0.8mi² (Lima and Olimpio, 1989). In most watershed scale applications, grid cell sizes range from 0.0625 mi² to larger. Therefore, this grid cell size was chosen to attempt to represent the rivers at a small enough scale to accurately simulate the groundwater-surface-water interaction.

The elevation data used to create the model grid originated from a 30m resolution DEM of the study area (USGS). MODFLOW requires the model grid to be oriented along the principle directions of anisotropy (McDonald and Harbaugh, 1996). Due to lack of data, for the purpose of this study, the principle directions of anisotropy were assumed to correspond with the general direction of the faults in the area. This assumption is valid because the fractures in the rocks tend to be influenced by the fault network in fractured bedrock aquifer systems. This assumption has been made in other applications of MODFLOW that lacked specific flow data, such as the regional model of the Edwards Aquifer in Texas (Maclay, 1988), and the regional conceptual model of the Carbonate Rock Province in the Great Basin (Burbey and Prudic, 1991). An angle of 35 degrees from the orientation of the DEM was chosen to orient the grid in the assumed direction.

The elevation data in the DEM was 30m in resolution, and was oriented with the UTM NAD 1927 coordinate system. The data had to be resampled to the new resolution, 402.336m (0.25 miles) and the new orientation (35 degrees counter clockwise). In order to resample the elevation data to a resolution of 402.336m (square cells, 0.25 miles on each side), and align it in the assumed direction of anisotropy, a C++ program was written (Appendix C, Program 1). This program re-samples the data at the given resolution and the given orientation creating a new reference system in which the data will be represented for the remainder of modeling study. A grid was then created in Visual MODFLOW that consisted of 170 x 140 grid cells, 0.0625 mi² each, and 4 layers deep. The re-sampled array representing the elevation data (output from the C++ program) was then used to interpolate the land surface of the model. Although the boundaries of the watershed were originally against the boundaries of the grid, when the data was resampled at a new orientation, the boundaries of the watershed were no longer against the boundaries of the grid. This is the reason for the large amount of inactive cells (especially above and below the study area) within the model domain. These cells were included in the simulation because they include the origin of the new coordinate system. A watershed boundary in the form of a .DXF file, created and manipulated in ArcView was then used to turn off the cells that lie

outside the study area. The resulting grid is shown in Figure 26. This is a planimetric view of the study area divided into the user-defined grid cells.

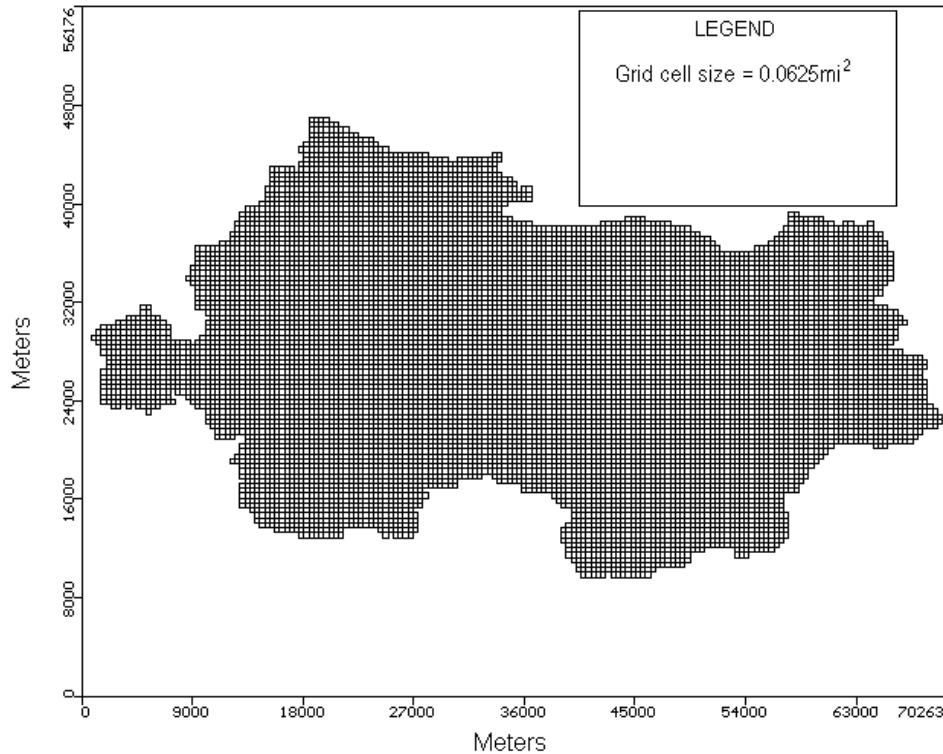


Figure 26. Model domain represented in Visual MODFLOW.

The boundary between layers 1 and 2 (Figure 23) essentially represents the bedrock surface. Well driller's logs from the Roanoke County Health Dept., located in Vinton, Virginia were inspected and information based on the reported depth to bedrock on a sample of 100 wells in Roanoke County was compiled. A bedrock surface was created using this information in ArcView GIS and exported as an ASCII file. The resampling C++ program (Appendix C, Program 1) was then used to create an ASCII file at the correct resolution and correct orientation to represent the bedrock surface. This file was used to interpolate the bedrock surface as the boundary between layers 1 and 2.

The boundaries between layers 2 and 3 and layers 3 and 4, and the bottom of layer 4 were created by inspecting the overall trend in topography, and slanting surfaces were created using interpolation in Visual MODFLOW. The layer between layers 2 and 3 sloped according to the input file in Table 4 that was used for interpolation.

Table 4. Input file for interpolation of boundary between layers 2 and 3

X Coordinate	Y Coordinate	Z Coordinate
0	0	250
0	56327.04 (140 x 402.336)	450
68397.12 (170 x 402.336)	0	150
68397.12 (170 x 402.336)	56327.04 (140 x 402.336)	250

The boundary between layers 3 and 4, and the bottom of layer 4 was interpolated so that both layer 3 and layer 4 were 100 m thick. Since the boundaries between the layers are not defined by the locations of the geohydrologic units due to their sloping nature, the divisions between these layers were arbitrarily defined. The constant 100m thickness of layers 3 and 4 will allow a direct correlation between hydraulic conductivity. The groundwater flow equation includes transmissivity as a variable, and transmissivity is thickness multiplied by hydraulic conductivity. Therefore, if the thickness is constant, the flow within these layers will be a reflection of the hydraulic conductivity. Cross sections of the study area in both the vertical and horizontal directions are shown in Figures 27 and 28. The trend in the boundaries between the 4 layers can be readily seen. Hydraulic conductivity input values are included in section 3.2.3.5.

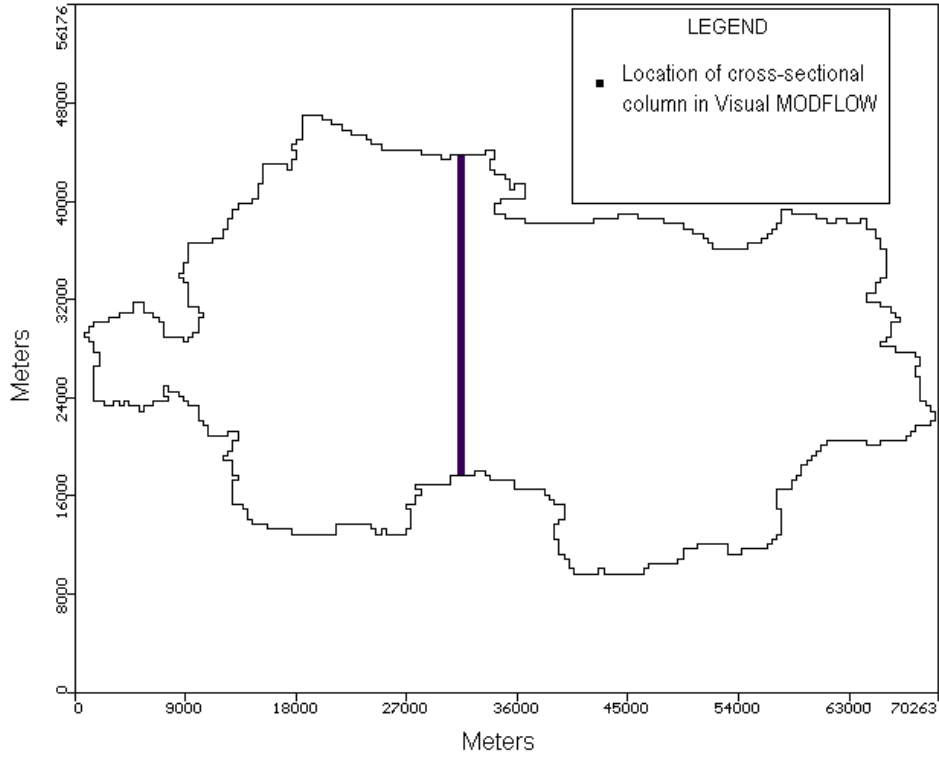


Figure 27A. Location of the cross-sectional column in Visual MODFLOW.

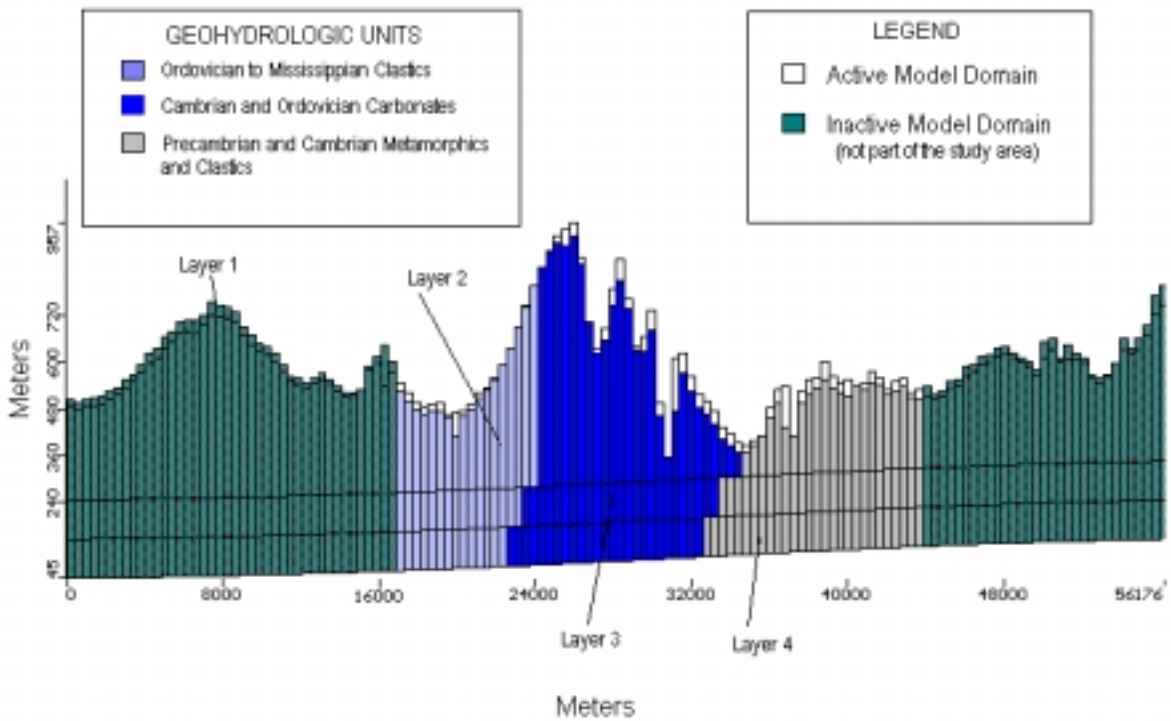


Figure 27B. Cross section of model domain along highlighted column in Figure 27A. (Vertical Exaggeration Factor of 20)

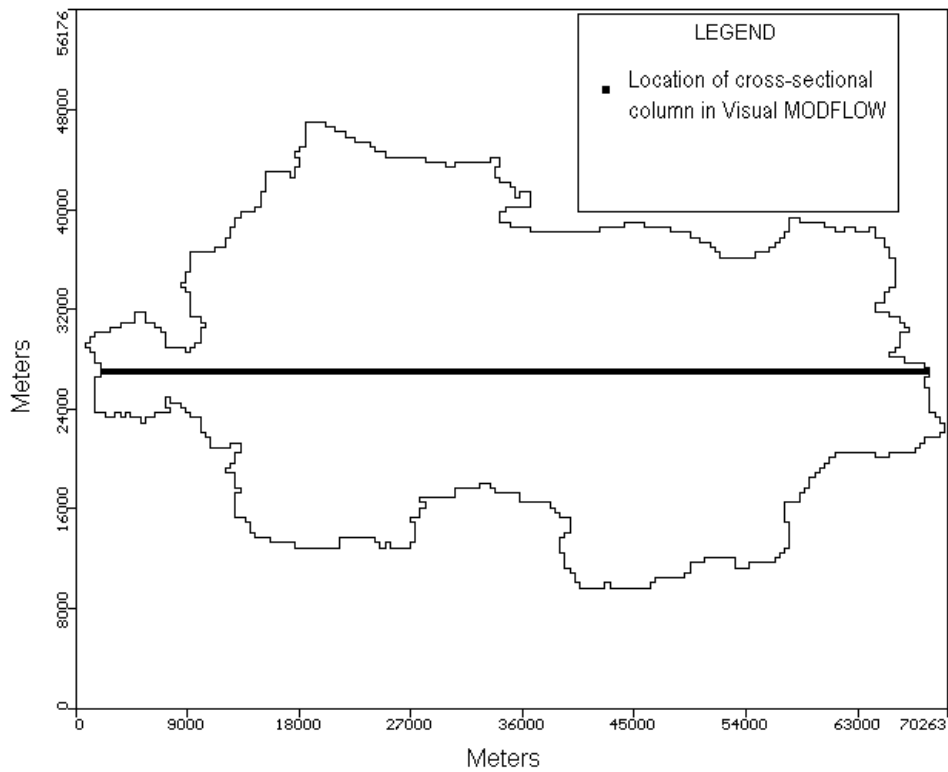


Figure 28A. Location of the cross-sectional row in Visual MODFLOW.

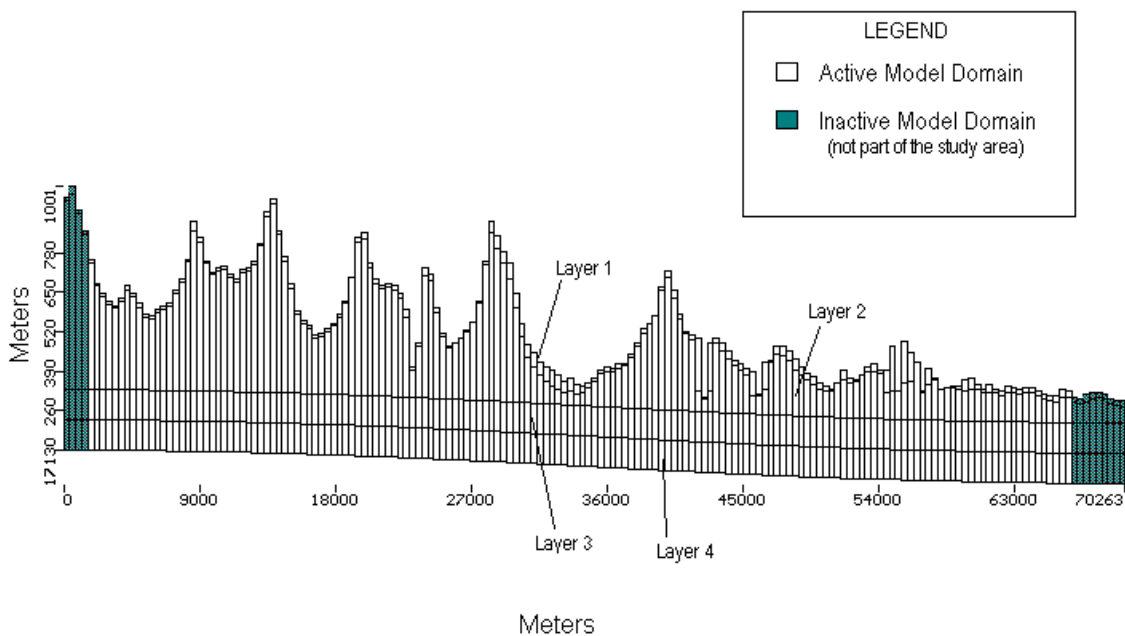


Figure 28B. Cross section of model domain along highlighted row in Figure 28A. (Vertical Exaggeration Factor of 20)

3.2.3.2 Data Refinement

Since the data were re-sampled at a different resolution and a different orientation, some of the data were distorted in the output file. This is due to the loss of detail in the original data. The data required adjustment since the reaches in some places were no longer found in valleys as dictated in the natural system. Therefore, it was necessary to insure that the cells directly adjacent to boundary cells representing reaches were assigned a higher elevation than the reach cells. Another C++ program (Appendix C, Program 2) was written to check the elevations of these adjacent cells and to correct them if they were lower than the elevations assigned to the reach cells. The altered cell were assigned elevations 2m higher than the elevations assigned to the adjacent river cells in order to insure the river cells were located in valleys.

3.2.3.3 Initial Hydraulic Head Data

It is necessary to assign initial head values to the cells before running MODFLOW, in order to iterative solve the groundwater flow equation (Equation 1). Therefore, a water table surface was created using ArcView GIS from the well information found in Waller (1976). Since the wells are primarily found in the Roanoke-Salem metropolitan area, the surface was “cropped” to an area that encompassed the wells and was output to an ASCII file. An identical cropping was done on the topographic data in the region to produce another ASCII file representing the elevation data. A regression analysis was then performed to produce a relationship between the water table data and the elevation data in SAS (Statistical Analysis Software) (Appendix D). Although the relationship between the elevations and the water table data was not very strong ($R^2=0.57$), this relationship was necessary to extrapolate the water table surface to the entire watershed since only data in the Roanoke-Salem metropolitan area was available. The resulting relationship was:

$$Head = -234.517 + 2.8685 * Elev - 0.004357 * Elev^2 + 0.0000022 * Elev^3 \quad (28)$$

where:

Elev = Elevation from the original DEM (m)

Head = Hydraulic head at that location (m)

The regression analysis output is included in Appendix D. The resulting array was then used as the input array to represent the initial head values for the model.

3.2.3.4 River Input Values

The General Head Boundary package (section 2.7.14) was used to represent the river reaches in the model. In representing the river cells using the General Head Boundary package, it was necessary to input the location of the cell (X, Y), the hydraulic head value, and a river bottom conductance value (equation 9). First, the reaches that were to be modeled were identified within the study area. Then, USGS 7.5-degree quadrangle maps were used to determine points along the reaches of known elevation. This was done by digitizing the maps using AutoCad to determine exact locations of points where the contour lines of the maps intersected the reaches to be modeled. These data points were located in the UTM NAD 1927 coordinate system of the original data, and therefore it was necessary to transform them into X,Y coordinates of the new coordinate system. Once these points were located in the model domain and assigned head values, an overlay of the rivers (.dxf file) (Figure 29) was used to locate the cells representing the reaches between the determined control points. The head values of the unassigned reach cells were then inferred from the topographic quadrangles or interpolated. The river bottom conductance of the initial data set was equal to a constant value of 50m/d for all river reach cells. The resulting input file created the general head boundaries used to represent the modeled reaches (Figure 30).

In order to represent the natural system, ideally it would be necessary to assign a different river bottom conductance value for each individual general head cell. However, since this would require a great amount of computing time during calibration, the system of reaches was divided into six separate sections depending on elevation and distance from the watershed outlet (Figure 31). Each individual section was assigned the same river bottom conductance value. To do this, another C++ program was written to alter the .GHB file (Appendix C, Program 3). The program determines the location of the reach cell (in X,Y coordinates) and based on defined location criteria, assigns it a value of river bottom conductance depending upon which section it is in.

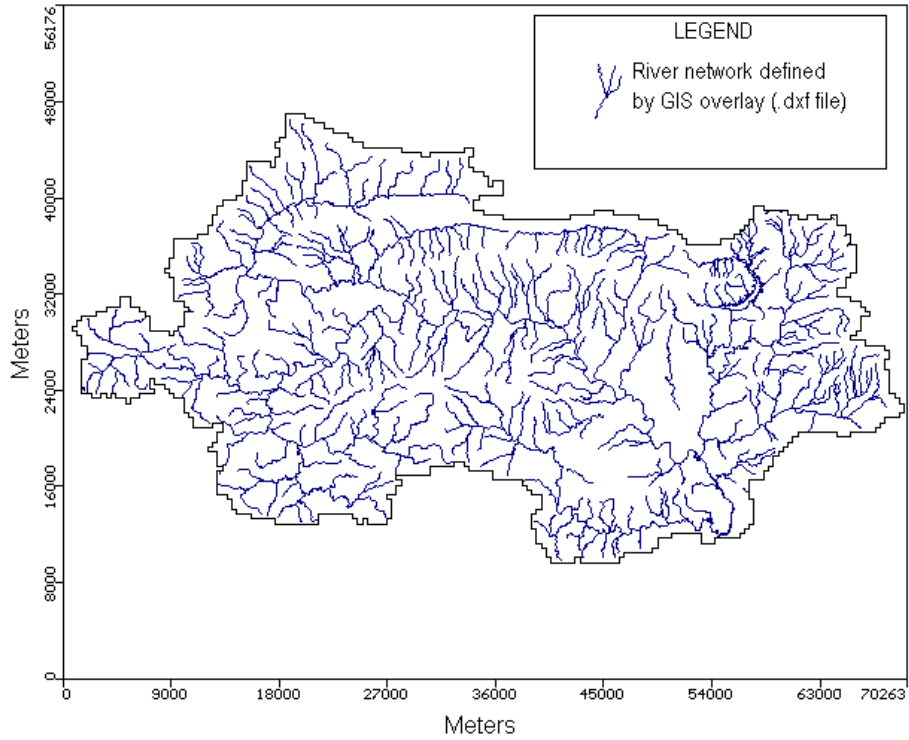


Figure 29. River overlay in Visual MODFLOW (.DXF file)

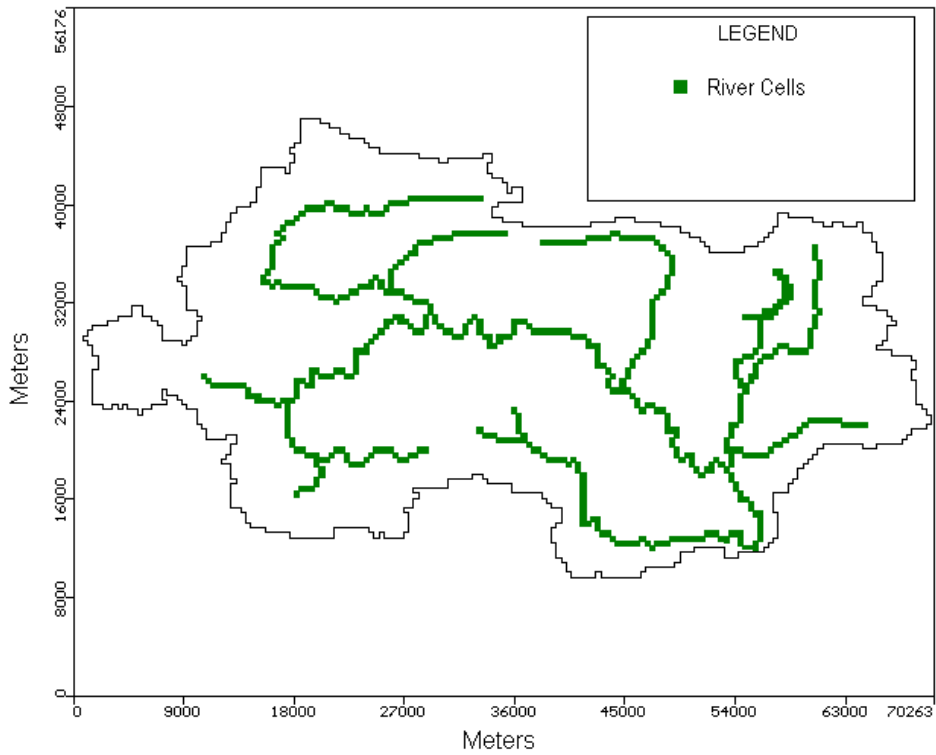


Figure 30. General-Head Boundaries represented in Visual MODFLOW.

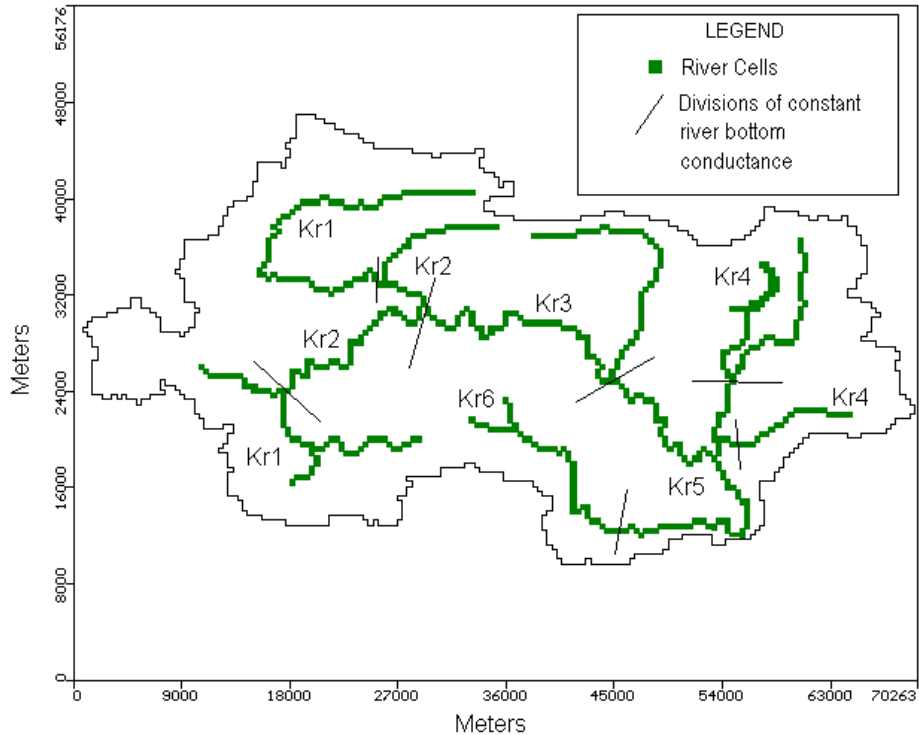


Figure 31. Sections of different river bottom conductance values represented in Visual MODFLOW.

3.2.3.5 Hydraulic Conductivities

The initial hydraulic conductivities were assigned according to the hydrogeologic units within the study area (Table 4). Hydraulic conductivities within cells were assumed to be isotropic, and therefore, the horizontal hydraulic conductivity was equal to the vertical hydraulic conductivity. This assumption was made due to the lack of subsurface flow data available from the study area. The values ranged from 20 m/d for layer 1; 1 m/d to 5 m/d for layer 2; 0.1 m/d to 0.5 m/d for layer 3; and 0.01 m/d to 0.05 m/d for layer 4. The order of magnitude of the initial hydraulic conductivities for all layers was modeled after a study performed in an east-central Pennsylvania watershed to characterize the geometry of its shallow layered and fractured bedrock (Gburek et al., 1999). In this study, hydraulic conductivity of the bedrock was determined by interval packer testing within boreholes (Gburek et al., 1999). This method of testing involves testing the hydraulic conductivities of an aquifer as a function of depth by isolating intervals of the well by packing them to create seals above and below the interval. The hydraulic conductivity of just that interval can then be determined. MODFLOW was applied to

the layer aquifer to determine watershed-scale aquifer parameters by calibrating the model against the observed data (Gburek et al., 1999). The hydraulic conductivity trends correspond with the assumption that there would be less fractures in deeper bedrock compared to shallow bedrock that may be exposed to weathering and dissolution. Within each layer, the Cambrian and Ordovician carbonates were assigned the highest hydraulic conductivity followed by the Ordovician to Mississippian clastics and the Precambrian and Cambrian metamorphics and clastics (Figure 21). A constant hydraulic conductivity was assigned to the entire top layer which represents the saprolite which primarily acts as a recharge reservoir to the ground water system (Waller, 1976). Figures 32, 33, and 34 show the layers of the model, and the distributions of the aquifer properties, dictated by the location of the hydrogeologic units.

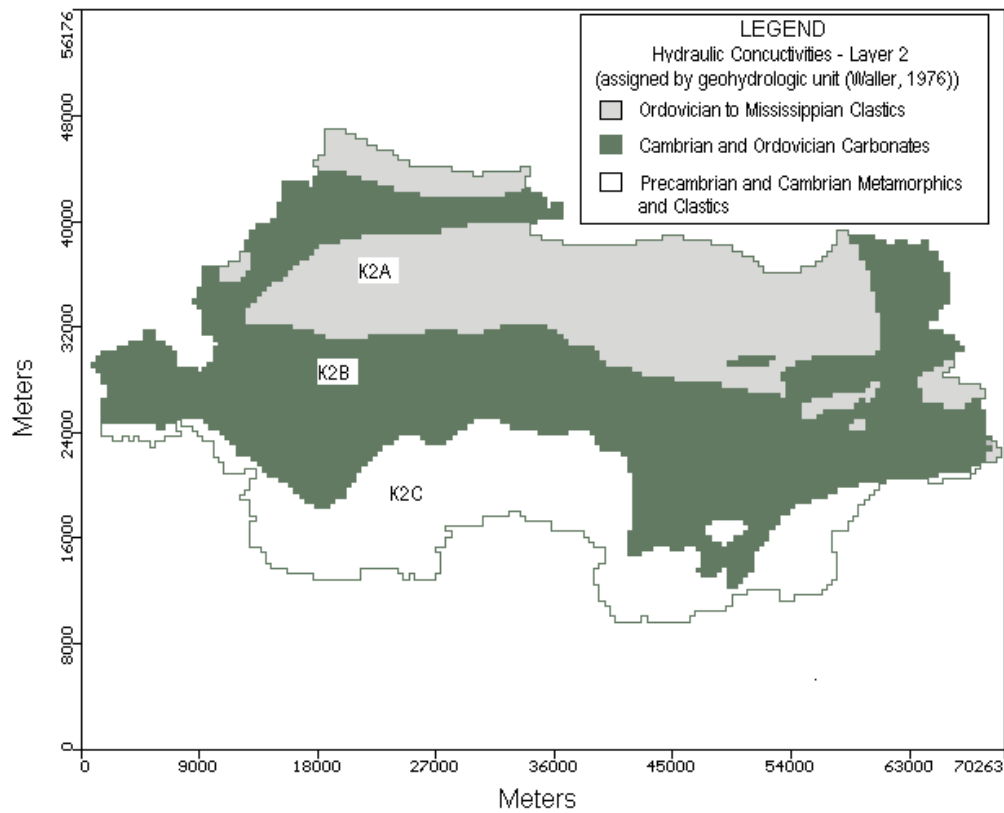


Figure 32. Distribution of hydraulic conductivity of layer 2.

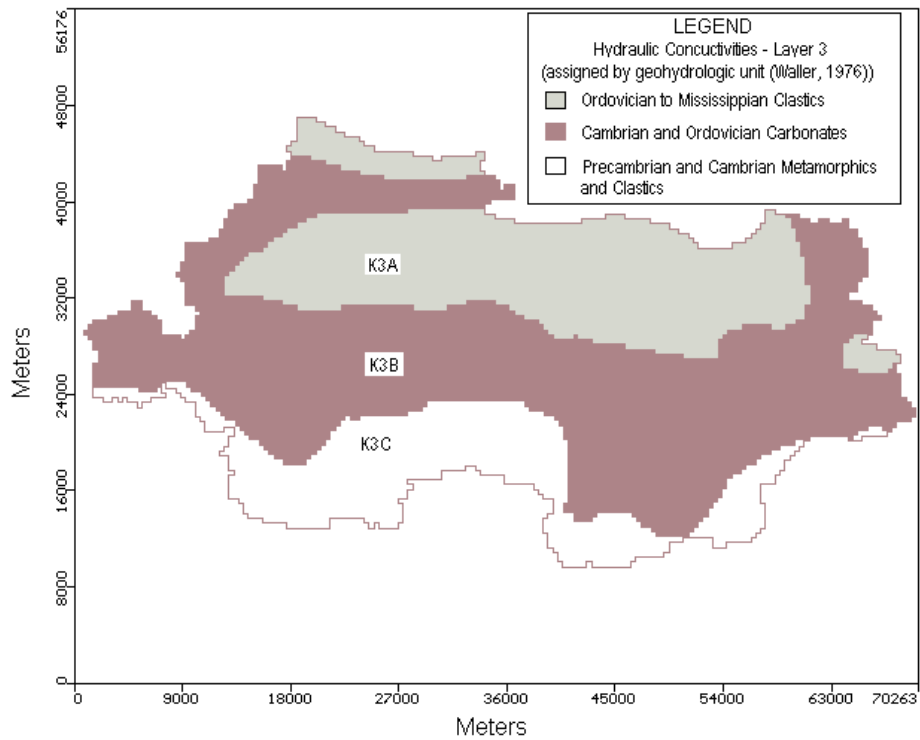


Figure 33. Distribution of hydraulic conductivity of layer 3.

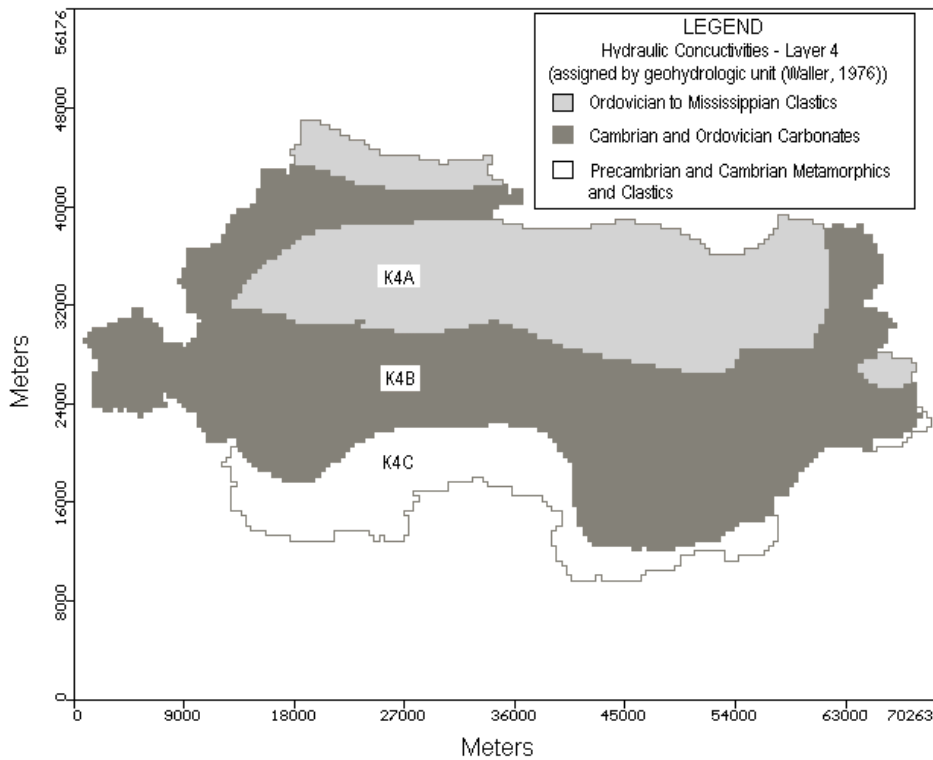


Figure 34. Distribution of hydraulic conductivity of layer 4.

3.2.3.6 Recharge

The study area was divided into two areas of recharge using a .DXF file to delineate the study area (Figure 35). Zone one represents the relatively flat areas within the watershed and zone two represents the relatively sloped topography within the watershed (Figure 36). These areas were determined by contours created from the original 30m resolution DEM within ArcView. Zone 1 is where the slope of the land is less than or equal to 15 degrees, and zone 2 is where the slope is greater than 15 degrees (Figure 36). This distinction was made under the assumption that recharge values in areas of greater slope would be less than recharge occurring in relatively flat areas due to differences in soils and less overall infiltration.

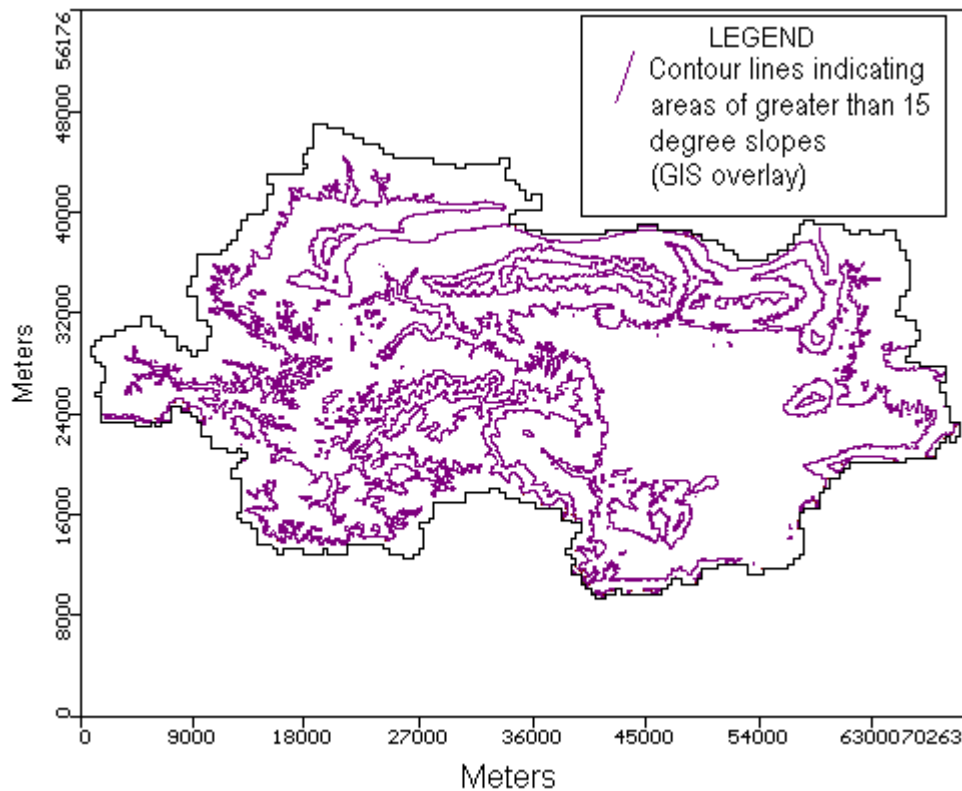


Figure 35. DXF overlay distinguishing recharge areas.

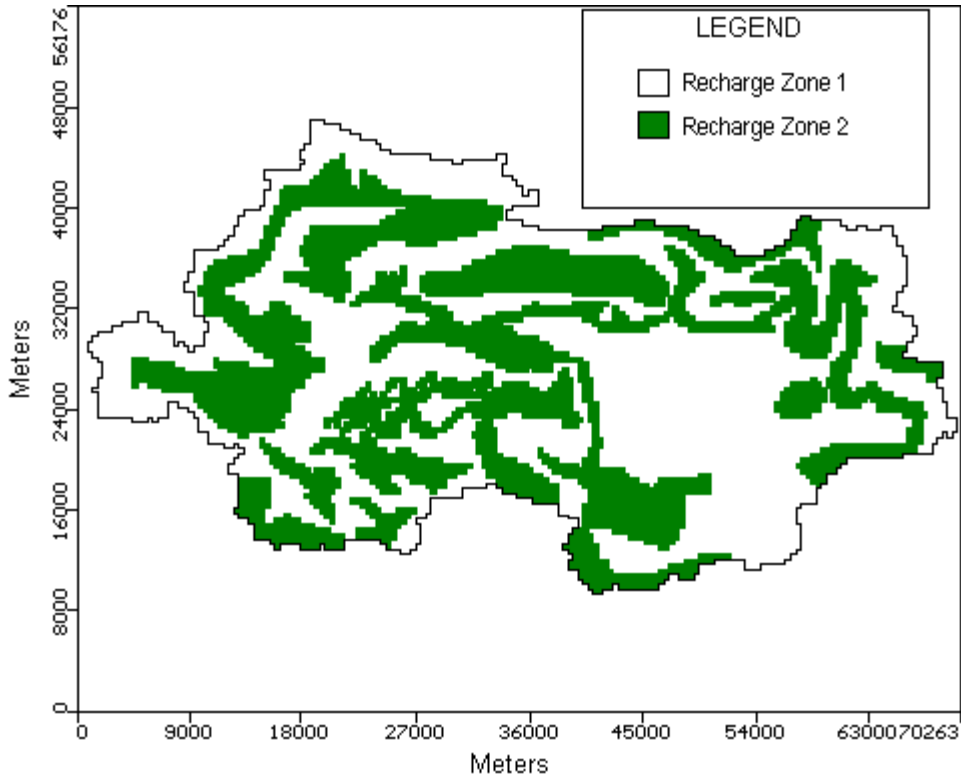


Figure 36. Recharge distribution in MODFLOW.

Similar distinctions have been made in previous studies performed in temperate areas. Ground-water recharge areas were determined according to topography in a study performed in the Upper Aquifer of the Rio Camuy to Rio Grande de Manati Area, Puerto Rico (Torres-Gonzalez et al., 1995). There were areas within the study area that were assumed to correspond to zones of different recharge values. For example, highland areas characterized by karst features with soils that are typically well drained comprised one zone, lowland areas characterized by blanket sands, dry valleys, marsh and swamp deposits with soils that are poorly drained comprised another zone, and alluvial sediments with soils that are moderately drained comprised another. Different recharge rates were also determined in a study that involved a model of the water-table aquifer in Vega Alta, Puerto Rico (Sepulveda, 1995). Different values of recharge were assigned according to topography, relief, topsoil and composition.

The initial data values for recharge area one and recharge area two (Figure 36), were assigned values of 9.8 in/yr and 2 in/yr respectively. The initial value for recharge area one was determined from a study that estimated the hydrologic characteristics in the Valley and Ridge, the Blue Ridge, and the Piedmont Physiographic Provinces based on analysis of streamflow

recession and base flow (Rutledge, Mesko, 1996). This study estimated 28-30% of precipitation would recharge the groundwater system in the Valley and Ridge Province. The initial value for recharge area two was assigned a value less than area one, and it was assumed that the optimal value would be determined during calibration.

3.2.4 Summary of the Conceptual Model

The model developed for use in this investigation is highly conceptual due to the lack of available and current data. There were many assumptions made in the development process which should be considered when interpreting the results. A lack of subsurface flow data and the influence of geologic formations forced the investigator to make generalizations about the system to avoid inferring too much detail from the limited available data.

3.3 Calibration

To use UCODE as the calibration code for this modeling study, it was necessary to create the following files: the universal file, the prepare file, the extraction file and the template files (Appendix E). The parameters that were estimated using UCODE are listed in Table 5. The initial values used during the calibration are also included in Table 5. A discussion of the initial values and calibrated values is also included. The initial values are important since the UCODE calibration does not guarantee an absolute solution to the parameter estimation. These values therefore, influence the calibration results. The template files constructed for the calibrations included the MODFLOW input files that contained these estimated variables: the Block-Centered Flow file (.BCF), the General Head Boundary file (.GHB), and the Recharge file (.RCH).

3.3.1 Calibration Data

In performing the calibration analysis and building the extract file required for UCODE, it was necessary to determine the calibration data points. Waller (1976) compiled information about 293 wells in the study area. These wells were primarily concentrated in the Roanoke-Salem Metropolitan area. Since the grid cells of the model are 0.25 mi^2 , if the wells were close together, they would be situated in the same cell. Therefore, it was necessary to determine what

MODFLOW cell they were in, and whether or not there was more than one well in each cell. If more than one well was located in a given cell, the head assigned to that cell was the average of the respective wells. The result of this analysis was 73 grid cells that were defined as known hydraulic heads (Figure 37).

Table 5. Parameters estimated using UCODE

Parameter	Description	Initial Value
Kr1	River bottom conductance – Section 1*	50 m/d
Kr2	River bottom conductance – Section 2*	50 m/d
Kr3	River bottom conductance – Section 3*	50 m/d
Kr4	River bottom conductance – Section 4*	50 m/d
Kr5	River bottom conductance – Section 5*	50 m/d
Kr6	River bottom conductance – Section 6*	50 m/d
K1	Hydraulic conductivity – Layer 1**	20 m/d
K2A	Hydraulic conductivity – Layer 2** Ordovician to Mississippian Clastics	3 m/d
K2B	Hydraulic conductivity – Layer 2** Cambrian and Ordovician Carbonates	5 m/d
K2C	Hydraulic conductivity – Layer 2** Precambrian and Cambrian Metamorphics and Clastics	1 m/d
K3A	Hydraulic conductivity – Layer 3** Ordovician to Mississippian Clastics	0.3 m/d
K3B	Hydraulic conductivity – Layer 3** Cambrian and Ordovician Carbonates	0.5 m/d
K3C	Hydraulic conductivity – Layer 3** Precambrian and Cambrian Metamorphics and Clastics	0.1 m/d
K4A	Hydraulic conductivity – Layer 4** Ordovician to Mississippian Clastics	0.03 m/d
K4B	Hydraulic conductivity – Layer 4** Cambrian and Ordovician Carbonates	0.05 m/d
K4C	Hydraulic conductivity – Layer 4** Precambrian and Cambrian Metamorphics and Clastics	0.01 m/d
RCH1	Recharge Flux – Recharge Area 1	6.8197e-4 m/d
RCH2	Recharge Flux- Recharge Area 2	1.3918e-4 m/d

* See Figure 31 for segment locations

** Horizontal and vertical hydraulic conductivity (cells assumed to be isotropic)

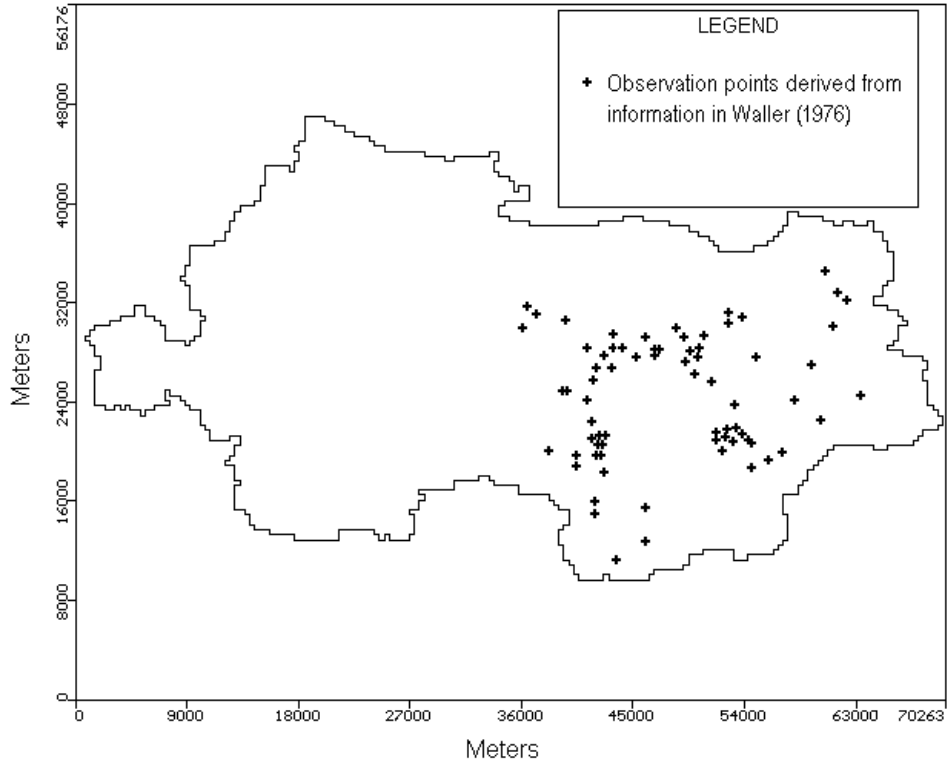


Figure 37. Location of known hydraulic heads used for calibration (Waller, 1976).

Waller (1976) field-verified the water level information included in his report. It was decided, therefore, that this information was reliable, whereas, if the water levels were taken from well drillers' logs, not only would the water levels reported be for a variety of different years, but they may not be as accurate depending upon the quality of the driller's work. Therefore, the steady-state model was only calibrated with the well data reported by Waller (1976). However, during transient simulations, the model output was compared to information in the drillers' logs to determine how well the model was representing the water table surface on the western part of the study area. The calibration results are presented in section 3.3.2.

The initial values of the river bottom conductances were determined through a trail-and-error analysis. At values much smaller, the model would not converge due to oscillation and stability problems. Therefore, the initial river bottom conductance values were assigned a arbitrary constant value of 50m/d, based on model convergence. Table 5 shows all of the initial values for the parameters that were estimated in the calibration process, using UCODE. All initial values were determined based on the discussion in section 3.2.3 in the discussion of the modeling approach.

UCODE performs a variety of different functions. For this investigation, since the problem is not well defined due to the fact that many of the parameters must be estimated, and not all of the functions of UCODE were completed. Parameter substitution, using the starting parameter values in the prepare, file was performed. The parameters were subsequently substituted and the sum-of-squared, weighted residuals objective function for many sets of variables was determined. The sensitivities and parameter variances, covariances and correlations were also calculated. UCODE then performed the regression. The model also has the ability to calculate the model linearity and predictions and their linear confidence and prediction intervals; however, this was not performed for this investigation. Linearity was not determined because it required perturbation of the parameters outside the stable range for the MODFLOW application model to converge, and therefore it was not possible to determine linearity.

All of the default parameter values outlined in Hill (1998) were used for this investigation, except for the convergence criteria. A parameter defined as “TOL” is a user-defined input value required in the input file. The TOL value, which sets the fractional amount between regression iterations that defines convergence, included in the universal file, was set equal to 0.1, not 0.01. This was necessary because UCODE would not converge when this variable was set equal to 0.01, which may be due to the fact that there was a limited amount of measured data that could be used to constrain the parameter estimation.

All of the observations were weighted the same since no information was included in Waller (1976) about the accuracy of each individual observation. A coefficient of variation of 0.5 was used to weight each of the observations included in the calibration. This value was assigned arbitrarily based on the assumed accuracy of the observations.

Although reasonable minimum and maximum values were used in the prepare file, these values were not used to constrain the perturbations of the parameter estimation iterations. Therefore, during the calibration process, UCODE would perturb the parameters outside reasonable limits for MODFLOW to converge, and the parameter estimation would abnormally terminate. It was necessary for the parameters to be constrained within acceptable limits. A statement of prior information was added to the prepare file to constrain the values of river bottom conductance, which was the parameter that would cause MODFLOW to not converge. The average of six values for the six sections of river, which defined the river bottom

conductance values, was constrained to 150m/d. This value was assigned purely from speculation of the magnitude of these values. This problem illustrates the fact that in order to properly estimate multiple parameters the problem must be very well defined. However, since the data were sparse in the study area, this was a reasonable assumption.

The value of perturbation that was assigned each of the 18 parameters (Table 5) that were estimated was originally set equal to 0.01, as recommended by the UCODE documentation (Hill, 1998). These values were later changed to 0.1 because too many of the calculated sensitivities were printed as zero. This was done based on a recommendation in the User's Documentation (Hill, 1998).

A majority of the other input parameters were assigned as the default values documented by Hill (1998). The important changes that were made are outlined above. This investigation did not provide an ideal application of a parameter estimation program (such as UCODE) due to the limited available data. Repeatedly, the User's Documentation states that the problem must be well defined for UCODE to predict accurate optimized parameter sets. Due to the uncertainty associated with this calibration, the optimized parameter set may not be a unique set of solutions to the problem, and may be a local minimum and not an absolute minimum. UCODE perturbs the parameter based on user-defined perturbations until convergence is reached, however, there is no guarantee that the initial estimate of the parameter caused the convergence of the model on an absolute minimum. Due to the lack of available data for this investigation, it was assumed that the output parameter set calculated by UCODE represents reasonable estimates for the system. The complete output from UCODE can be found in Appendix E.

3.3.2 Calibration Results

The optimized input parameter set obtained by the UCODE analysis was used to run the calibrated steady-state simulation. The optimized parameter set for the estimated parameters in UCODE is shown in Table 6. For the purpose of this investigation, it is assumed that the optimal parameter set in Table 6 represents the conditions for the calibration year. The transient simulations performed are only to demonstrate how such a model could be used, unless the model is validated with data from at least one more time period.

Table 6. Initial value and optimal value for estimated parameters during calibration with UCODE.

Parameter	Description	Initial Value	Calibrated Value
Kr1	River bottom conductance – Section 1*	50 m/d	19355.9 m/d
Kr2	River bottom conductance – Section 2*	50 m/d	0.1 m/d
Kr3	River bottom conductance – Section 3*	50 m/d	1445.8 m/d
Kr4	River bottom conductance – Section 4*	50 m/d	126.9 m/d
Kr5	River bottom conductance – Section 5*	50 m/d	2021.3 m/d
Kr6	River bottom conductance – Section 6*	50 m/d	212.1 m/d
K1	Hydraulic conductivity – Layer 1**	20 m/d	24.7 m/d
K2A	Hydraulic conductivity – Layer 2** Ordovician to Mississippian Clastics	3 m/d	0.390 m/d
K2B	Hydraulic conductivity – Layer 2** Cambrian and Ordovician Carbonates	5 m/d	0.893 m/d
K2C	Hydraulic conductivity – Layer 2** Precambrian and Cambrian Metamorphics and Clastics	1 m/d	0.0125 m/d
K3A	Hydraulic conductivity – Layer 3** Ordovician to Mississippian Clastics	0.3 m/d	0.242e-4 m/d
K3B	Hydraulic conductivity – Layer 3** Cambrian and Ordovician Carbonates	0.5 m/d	1.82 m/d
K3C	Hydraulic conductivity – Layer 3** Precambrian and Cambrian Metamorphics and Clastics	0.1 m/d	0.353e-3 m/d
K4A	Hydraulic conductivity – Layer 4** Ordovician to Mississippian Clastics	0.03 m/d	6.43 m/d
K4B	Hydraulic conductivity – Layer 4** Cambrian and Ordovician Carbonates	0.05 m/d	0.112e-2 m/d
K4C	Hydraulic conductivity – Layer 4** Precambrian and Cambrian Metamorphics and Clastics	0.01 m/d	0.708e-3 m/d
RCH1	Recharge Flux – Recharge Area 1	6.8197e-4 m/d	0.702e-3 m/d (9.8 in/yr)
RCH2	Recharge Flux- Recharge Area 2	1.3918e-4 m/d	0.537e-3 m/d (2 in/yr)

* See Figure 31 to determine location of sections

** Horizontal and vertical hydraulic conductivity (cells assumed to be isotropic)

3.3.2.1 River Bottom Conductance Values

The optimal river bottom conductance values estimated using UCODE (Table 6) vary drastically with respect to each other. It is important to remember that ideally, each river cell would be assigned an individual value for river bottom conductance. However, the river network was divided into six sections that were assigned constant river bottom conductance values (Figure 27). Therefore, these six river bottom conductance values are representative values or overall average values for each river reach. Therefore, the variation in order of magnitude is not surprising. Recall that the river bottom conductance equation is as follows:

$$CRIV = \frac{KLW}{M} \quad (29)$$

where:

- CRIV = the river bottom conductance (L/T),
- K = the hydraulic conductivity of the riverbed material (L),
- L = the length of the reach (L),
- W = the width of the reach (L), and
- M = the thickness of the riverbed (L).

Even though the cells in the model that represent reaches are 0.25mi wide, in reality, the reaches vary in width dramatically, from a meter or less in the headwaters to 10-30 meters at the outlet. A large range of values are acceptable for length (L, in Equation 29) since in reality, the river may meander causing the actual length of the river in a cell to be longer than the length of the cell. Even though the model represents the length of a reach as 0.25mi, in reality, the length of a reach could range from 0.25mi (if the reach was perfectly straight) to much greater values depending upon the actual curves in the river. The conductivity of the river bottom can vary in orders of magnitude due to the spatial variability of the river bottom material. In some places, the river bottom is very coarse, or sandy, and the hydraulic conductivity could be very large, however, in other places, it is very silty to clayey, and could have a very small hydraulic conductivity. The thickness of the material also varies dramatically in the study area. In some places, the bottom of the river is purely bedrock, making the thickness of the streambed material virtually zero. As the value of the thickness approaches to zero, the numerator goes to infinity, creating a huge range of acceptable values for the river bottom conductance (Equation 29).

Since the uncertainty and variability of the river bottom conductance is very large, typically in MODFLOW studies, it is used as a calibration parameter, as is the case in this

investigation. The justification of the optimized parameters is simple: the values are all acceptable, give the variability of the acceptable ranges of the variables that determine the river bottom conductance. The variability discussed here also shows that the optimized parameter set may not represent a unique set of parameters to create the desired output. However, once again, the availability of the data in the study area is the major constraint.

3.3.2.2 Hydraulic Conductivities

The hydraulic conductivity values found during the UCODE execution are most likely not representative of the natural system. They indicate that layer three is acting as a confining unit, thus restricting flow to the upper two layers. The hydraulic conductivity values in layer 3 ($K3A = 0.242e-4m/d$, $K3B = 1.82m/d$, $K3C = 0.353e-3m/d$) are more than two orders of magnitude smaller than the hydraulic conductivity values of layer 4 ($K4A = 6.43$, $K4B = 0.112e-2m/d$, $K4C = 0.708e-3m/d$). The system consists of fractured bedrock, and therefore, layer three is most likely not a confining unit. The hydraulic conductivities estimated using UCODE perhaps reflect the result of the assumption that the hydraulic conductivities within each model cell were isotropic. This assumption may not be valid for this system. Therefore, the values of hydraulic conductivities presented in Table 6 do not represent properties of the natural system, but instead, compensate for the assumption that the cells were isotropic.

The hydraulic conductivity values assigned to the three geohydrologic units also vary greatly from the original input parameters (before optimization). This is not at all surprising. Hydraulic conductivity values are understandably difficult to determine, even with the measured data. This is due to the fact that anisotropy and spatial variability of hydraulic conductivity is so great. Even if hydraulic conductivity values were measured, they could vary in depth and location so greatly that the measured values may not be representative of the system either.

The nature of the study area makes the values of the hydraulic conductivity even more difficult to determine. In essence, since the study area consists of fractured bedrock aquifers, the model is attempting to represent the system as a continuous porous medium with representative hydraulic properties. Since the system is fractured rock, it is not at all surprising that there are some values, $K4A$ (Table 6) for example, that are not at all consistent with the original conceptualization of the system. Conceptually, it was thought that there were more fractures near the land surface of the system and therefore, the hydraulic conductivities near the land

surface should be larger than those in lower layers. However, K4A represent a hydraulic conductivity in layer 4, and is larger than the values in layer 2. It could be that there are large fractures deep in the system which conduct water better than shallower layers. Therefore, given the nature of the aquifer system and the difficulty in obtaining accurate values, the values in Table 6 are all within an acceptable range.

A trend that assumed the Cambrian and Ordovician carbonates would have the largest hydraulic conductivities, followed by the Ordovician to Mississippian clastics and then the Precambrian and Cambrian metamorphics and clastics was originally assumed (Table 6). This assumption was based on characteristics of these geohydrologic units. Table 6 illustrates that this trend is only followed in layer 2. Again, this is not surprising given the nature of the system. There has been tremendous geologic activity in this area that has helped to form the aquifer system. In some places, this activity has folded new deposits under old deposits and formed multiple faults and geologic formations that are not explicitly represented by the model.

3.3.2.3 Sensitivity Analysis

During the execution of UCODE, the program calculates scaled composite sensitivities for all of the estimated parameters. Using the scaled sensitivities for all observations, composite scaled sensitivities are calculated for each parameter, and indicate the total amount of information provided by the observations for the estimation of one parameter (Hill, 1998). Section 2.9.2 presents the methods UCODE uses to calculate the sensitivities, the scaled sensitivities, and the composite scaled sensitivities.

The *scaled* sensitivity indicates the importance of an observation to the estimation of a parameter or, conversely, the sensitivity of the simulated value (at each observation) to the parameter (Hill and Poeter, 1998). The complete UCODE output includes the *scaled* sensitivities for all of the estimated parameters (Appendix E). However, the *scaled composite* sensitivity for a parameter (Table 7) is an indication of the information content of all the observations for the estimation of the parameter (Hill and Poeter, 1998). These values indicate an overall sensitivity for the estimated parameters to the set of observations (Hill and Poeter, 1998). Table 7 shows a summary of the scaled composite sensitivities calculated by UCODE.

Table 7. Summary of scaled composite sensitivities for all parameters
(refer to section 2.9.2 for explanation)

Parameter	Sensitivity	Parameter	Sensitivity	Parameter	Sensitivity
Kr1	1.277e-2	K1	1.378E-2	K3C	5.371E-3
Kr2	0.000	K2A	4.542E-3	K4A	3.902E-2
Kr3	3.532e-2	K2B	2.096E-3	K4B	7.756E-3
Kr4	7.399e-2	K2C	7.022E-3	K4C	4.899E-3
Kr5	1.496e-2	K3A	0.000	RCH1	0.371
Kr6	4.980e-2	K3B	3.843E-2	RCH2	0.206

The values for recharge have the highest scaled composite sensitivities. This was expected since recharge is the only input to the system, thus the results should be very sensitive to this parameter. Table 7 also indicates that the results are more sensitive to the streambed conductance values than most of the hydraulic conductivity values. This was also expected since the streambed conductance values govern the surface-water-groundwater interaction, and this is the only outflow path for the model. The hydraulic conductivity values closer to the surface (K1) have a higher sensitivity than some of the deeper values (K2A, K2B, K3B, K3C, K4B, K4C). This indicates that there is not much vertical flow occurring in the system, and therefore deep flow does not effect the results as much as shallow flow.

The sensitivities for both K3B and K4A are higher than the other hydraulic conductivity values (K2A, K2B, K2C, K3A, K3C, K4B and K4C). The estimated hydraulic conductivity values for these two parameters are also much higher than most of the other values of hydraulic conductivity (K2A, K2B, K2C, K3A, K3C, K4B and K4C, Table 6). Hydraulic conductivity is a property of a porous medium that describes how well the medium can conduct water. Therefore, the larger hydraulic conductivity values promote more flow than smaller hydraulic conductivity values. Thus, these values of higher hydraulic conductivity have a greater impact on the overall flow patterns of the groundwater flow system, and therefore, the groundwater flow system is more sensitive to these values than those that are smaller. These larger hydraulic conductivity values may indicate fracture zones in the system that are transmitting large volume of water, which could be the case in a fractured bedrock system.

In summary, Table 7 indicates that the model is the most sensitive to the recharge values, relatively sensitive to the streambed conductance values, and the least sensitive to the lower hydraulic conductivity values (Table 7). These sensitivities were only calculated for estimated parameters. Sensitivities for input parameters such as the initial hydraulic head array, cannot be

calculated because they are different for every cell in the system, however, through trial and error, it was determined that the model was also highly sensitive to the initial heads.

3.3.2.4 Recharge

The model was the most sensitive to the recharge input values (Table 7). This illustrates that the recharge is the driving force behind the movement of groundwater through the system since it is the only input to the system. Recharge values are generally difficult to determine for any model. Research has been conducted to estimate the recharge in a variety of areas, but the actual volume of water that recharges the aquifer system is difficult to quantify.

The recharge values that UCODE determined to be the optimal parameter values seem to be reasonable. The original input for recharge (zone1) was 9.8 in/yr, which corresponded to an estimation of recharge for the area of 28-30% of the annual precipitation (Rutledge, Mesko, 1996). The output parameter was 10.08 in/yr which is 27.7% of the 36.42in of annual precipitation for the calibration year. It is interesting to point out that the optimal recharge values correspond to previous reported values, however, this does not verify that the model is an accurate representation of the system due to the uncertainty in the other parameters.

3.3.3 Recalibration with Stream Routing

A re-evaluation of the objectives of the investigation led to using a different MODFLOW package to simulate the rivers in the model. It was decided that since the General-Head Boundary package does not account for water that is flowing from upstream to downstream cells in the model, the Streamflow-Routing package, which does route water through the river network, would be used instead. The utilization of the Streamflow-Routing package, however, made a recalibration necessary since the previous simulation was calibrated without streamflow-routing.

The General-Head Boundary Package computes flow into or out of a cell from an external source provided in proportion to the difference between the head in the cell and the head assigned to the external source, similar to the RIVER, DRAIN and ET Package (McDonald and Harbaugh, 1988, Section 2.7). General-head boundaries are used whenever the head of a surface-water body or other known head is separated from the aquifer by material or deposits having different hydrogeologic properties than the aquifer. However, the head can be changed for each stress period, unlike a constant-head boundary (McDonald and Harbaugh, 1988).

Therefore, the conductance value results in a time lag for equilibrium conditions to be reached between the boundary head and the head in the aquifer. The General-Head Boundary Package was initially used to simulate rivers in this investigation because the head changes for each stress period. Since the heads in the rivers were largely unknown, this was an advantage to assigning constant heads that do not change for each stress period. However, the General-Head Boundary Package does not route water from upper reaches to lower ones and therefore does not account for the higher volume of water in lower reaches. The volume of water that is routed from upper reaches can greatly influence hydraulic heads in the lower reaches, and thus affect the interaction between the surface-water system and the groundwater system.

One of the objectives of this study was to determine the effects of land-use change on the subsurface flow system. Changing the flow system not only affects the volume of groundwater available for withdrawal, but it can also effect the surface-water-groundwater interaction, which could impact surface water supplies as well. Therefore, understanding and correctly simulating the interaction of the surface-water system and the groundwater system is critical to determining the effects of land-use change on water resources, especially during low-flow conditions when baseflow from the groundwater may be the only source feeding surface streams. To meet this objective, it was determined that the surface-water-groundwater interaction would have to be simulated in a different way since the General-Head Boundary Packages neglects the routing of water through the river network, which could affect the surface water-groundwater interaction. Instead of using the General-Head Boundary Package to represent the river reaches within the model, it was determined that the Streamflow-Routing Package was more appropriate since it *does* account for the routing of water through the river network. However, the previous calibration performed with UCODE used the General-Head Boundary Package which does not include streamflow-routing, and therefore, the model had to be recalibrated with the streamflow-routing included.

The Streamflow-Routing package routes the water from the upper reaches to the lower reaches, which affects the head difference between the streams and the aquifers (Equation 8), and therefore effects the groundwater-surface-water interaction. A new input data set was developed to implement the Streamflow Routing Package (Appendix A). The only new information that is included in the new input file is information that defines the routing from one segment to the next, otherwise the information included in the previously calibrated GHB file was used. The

additional parameters are reach number, segment number, flow volumes, tributary information, and diversion information. The river network was divided into 218 segments, a new one starting every time there is a diagonal connection between river reaches, or when a tributary enters the network. Defining a “diversion” allows the user to specify that flow is occurring from one cell to another when the cells are not directly adjacent to one another. A diversion was specified every time there was a diagonal connection, and tributaries were specified every time segments join. There are 586 total cells that represent rivers in the study area. Once the appropriate file was created following the format specified in the Streamflow-Routing documentation (Prudic, 1989), the model was run with the new Streamflow-Routing Package instead of the General-Head Boundary Package.

The streambed conductance is the key parameter that governs the surface-water-groundwater interaction. Equation 8 illustrates the relationship between flow through a medium, the conductance of that medium, and the hydraulic head difference. Since the previous calibration did not include stream-routing, the optimal streambed conductance values estimated using UCODE reflect the head difference without taking into account routing. This head difference changed dramatically when routing was implemented, and the output from the simulation that included routing did not match the observed hydraulic heads used for the calibration. Therefore, it was determined that the model had to be recalibrated to match the observed data by changing the streambed conductance values.

This re-calibration was performed manually, without the use of UCODE because the *distribution* as well as the values of the streambed conductivities were changed throughout the calibration to determine the optimal parameter input set. The calibration consisted of changing the distribution and values of the streambed conductivities. A C++ program was developed to ease the process of changing the values and printing the changed values in the appropriate format (Appendix C).

The model was also determined to be highly sensitive to the initial head conditions. The original initial head array was developed from a regression analysis done on the wells in Waller (1976) (Figure 37) and the land elevations at those locations. However, there is a drastic change in topography near the center of the study area, east of the Roanoke County line. The land surface elevations in the western half of the study area are much higher and contain more drastic elevation changes than that of the Roanoke Valley. To determine if the relationship was

appropriate in the western half of the study area, information was collected from the Montgomery County Drillers' logs in the Montgomery County Health Department. A total of 21 observed hydraulic head values distributed throughout Montgomery County were added to the simulation. The observed hydraulic head values reported in the Drillers' logs were much higher than the values of the heads estimated from the regression equation at the same locations. For example, some of the highest elevations in the study area reach up to 900m, however, using Equation 24 to determine the hydraulic head at a location where the elevation is 900m only yields a hydraulic head of 421.763m. All of the observed hydraulic head values collected from the Montgomery County Drillers' logs are greater than this value. Therefore, it was assumed that since the topography varies greatly, a different relationship between hydraulic head and elevation may exist. A new regression analysis was performed using SAS (Statistical Analysis Software) on the information collected from the Montgomery County Drillers' logs, and the elevations at those locations. The new regression equation had an $R^2 = 0.66$. The regression results are included in Appendix D. Figure 38 shows the locations of both sets of wells included in Waller (1976) and the Montgomery County observation points.

A new data array was created for the entire study area based on the topography and the two regression equations relating land elevation to water table surface. The water table elevation equation determined using the first regression analysis was applied to the east half of the study area, and the equation obtained from the second regression was used to determine the water table elevations for the west half of the study area. This new data array was used as the input initial heads array necessary to run MODFLOW. The model was run using the new initial hydraulic head array, and using a trial-and-error process to determine the new distribution and magnitude of the streambed conductance values that best matched the observed hydraulic heads.

A graph of the final observed vs. calculated heads is in Figure 38. This figure illustrates the performance of the model with respect to matching the observed data from the observed hydraulic head values in Waller (1976) and the Montgomery County Health Department (Figure 39). The model does a relatively good job of matching the heads from the observed data in both the areas of high hydraulic heads and low hydraulic heads. A majority of the lower observed head values are in the Roanoke area, and a majority of the higher observed heads are in the Montgomery County side (west side) of the study area. Therefore, the model is performing relatively the same for both sides of the study area, although this is a broad generalization

because there are not as many observation points in Montgomery County. Also, the additional observation points in Montgomery County obtained from the Drillers' log may not be as accurate as the information that is presented in Waller (1976) since the author field verified his measurements. Also, drillers are sometimes not complete in their descriptions, and not accurate in their measurements.

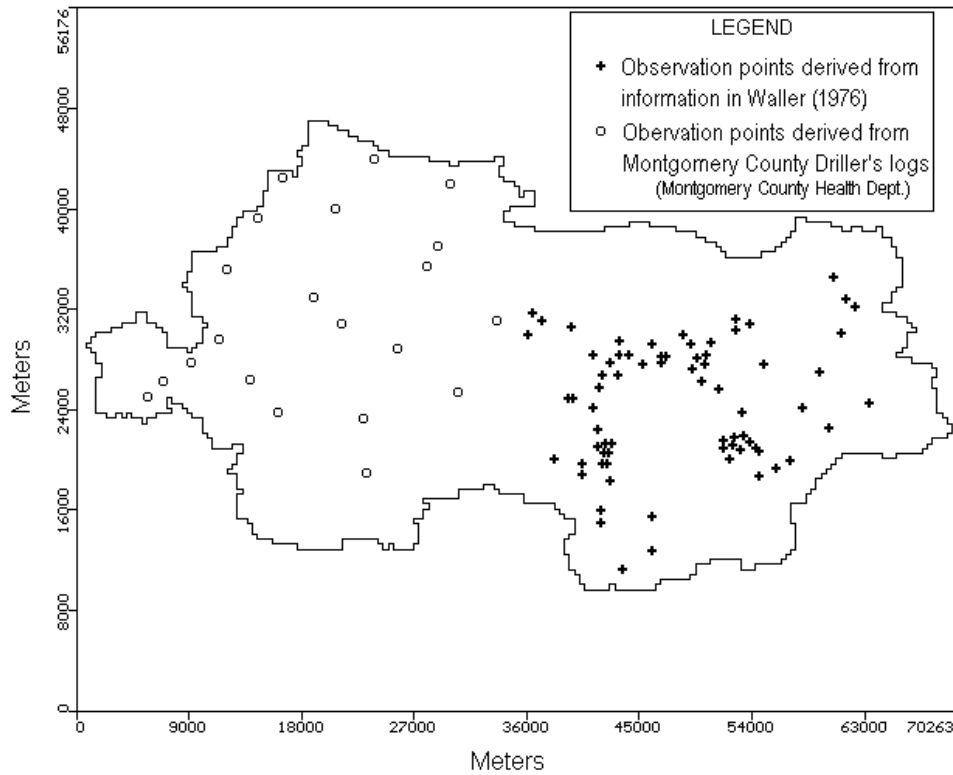


Figure 38. Observed well data locations within the study area (Waller (1976), and Montgomery Co. Health Dept.)

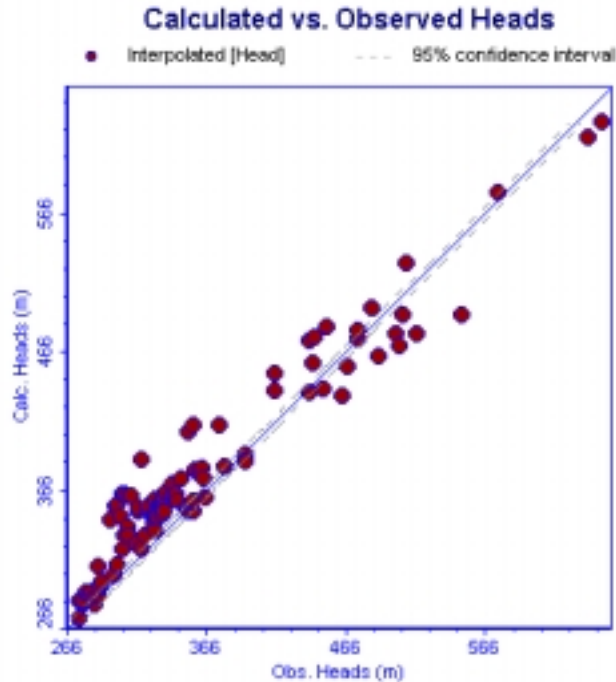


Figure 39. Observed vs. calculated hydraulic head values for observation points in Figure 38.

The distribution of streambed hydraulic conductivity values was changed during the calibration with streamflow-routing from that of the previous calibration (without streamflow-routing, Figure 31). New sections of constant streambed conductivity were created during the calibration process. The new sections of streambed conductivity are shown in Figure 40. The sections were developed during the calibration process to change the local head distributions in specific areas. Since UCODE was not used for the new calibration, a trial-and-error method was used to determine the values and distribution of the streambed conductance values to yield results that matched the observed hydraulic head values. The resulting streambed conductance values can be justified in the same manner as previous values (see Section 3.3.2.1 for a complete discussion of river bottom conductance value justification).

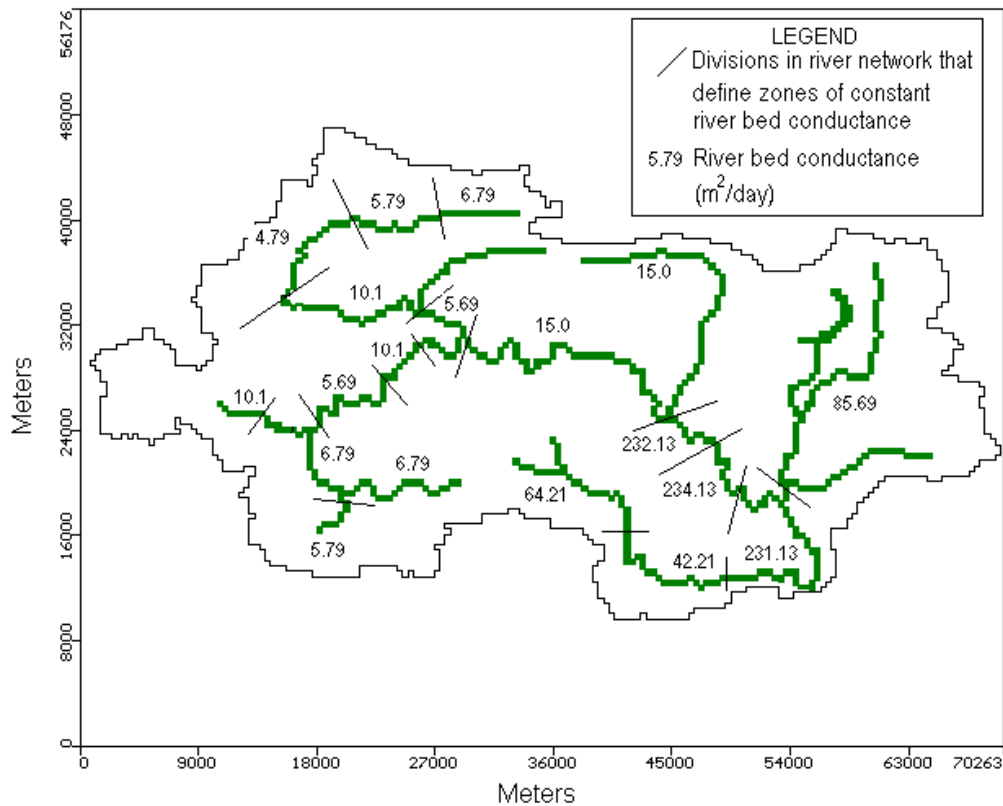


Figure 40. Sections of river assigned constant conductance values.

3.3.4 Summary of the Model Calibration

The groundwater flow model developed in MODFLOW to simulate the groundwater flow system of the Upper Roanoke River Watershed was calibrated to the observed hydraulic head values. Initially, it was calibrated with a USGS-developed parameter estimation program called UCODE. UCODE calibrated the groundwater flow model to observed hydraulic head information included in Waller (1976). The estimated parameters determined during UCODE execution were determined to be within acceptable ranges due to the large amount of uncertainty inherent in the groundwater flow model, and the parameters used in the equations used to calculate the estimated parameters. Upon re-evaluating the objectives of this investigation, a different MODFLOW package was substituted for the General-Head Boundary Package that was initially used to simulate the rivers within the system. The Streamflow-Routing Package was used in place of the General-Head Boundary Package because it includes the routing of water through the river network. This routing of water from upstream reaches to downstream reaches

was determined to be critical in simulating the surface-water-groundwater interaction within the system, which is necessary to meet the first objective of this study.

UCODE was utilized for the initial calibration of the Upper Roanoke River Watershed groundwater model. This initial calibration did not include streamflow-routing, and the rivers were simulated with the General-Head Boundary Package in MODFLOW. A total of 18 parameters were estimated using multiple inverse regression. Although the parameter estimation problem was not “well defined”, meaning there were not many known data included in the regression, the UCODE execution converged, and estimates for the eighteen parameters were determined. The values for the eighteen parameters calculated during the UCODE execution, were all determined to be within acceptable ranges.

A re-evaluation of the objectives of this investigation prompted the use of the Streamflow-Routing Package instead of the General-Head Boundary Package to include the routing of water through the river network. Routing water from upstream reaches to downstream reaches can significantly affect the head values of the downstream reaches, which, in turn, significantly affect the surface-water-groundwater interaction. To effectively determine the impacts of land-use change on the subsurface flow system, the surface-water-groundwater interaction must be accurately simulated. Therefore, the Streamflow-Routing Package was substituted for the General-Head Boundary Package to simulate the rivers in the study area.

The model was then recalibrated with the streamflow-routing included in the simulation. Data from the Montgomery County Health Department was added to the observed hydraulic head information from Waller (1976). The model was calibrated to match all of the observed hydraulic head values through a trial and error analysis. The only parameters that were changed during the calibration were the streambed conductance values and distribution.

The calculated parameters obtained during calibration may not accurately represent the system in future years. In order to determine if the estimated parameters accurately represent the system, a data set of current observed hydraulic heads would have to be compiled to validate the model for years other than 1969-1970. Observed hydraulic head data do not exist for any other year, and therefore this validation was not performed for this investigation. For all practical purposes, the parameter set calculated by UCODE represents a steady-state simulation during the study year. If this model were to be used as an actual management tool for future development scenarios, a parameter set that was validated with at least one more year of data would have to be

estimated. This illustrates a major problem with applying a distributed model such as MODFLOW to a natural system. A great deal of data are necessary to accurately represent the system. Ideally, a model such as MODFLOW would not be applied to a site such as the Upper Roanoke River Basin, due to a lack of data. However, to meet the objectives of this investigation, it is assumed that the input parameter set developed during the calibration procedure accurately represents the natural system.

Chapter 4

Results and Discussion

4.1 Introduction

The objectives of this study were to: (1) select and apply an appropriate model to the Upper Roanoke River Watershed to determine the impacts of land use activities on the subsurface flow regime, (2) evaluate the model by comparing its predictions with the observed data available from the study area, and (3) perform sensitivity analyses on potential future groundwater withdrawals based on future growth projections for Roanoke County. MODFLOW was used to develop a groundwater model of the Upper Roanoke River Watershed, and the results of the simulations performed by the model are presented in this chapter. The model was used to simulate present pumping conditions. The present condition simulation served as a basis for comparison for the three future development scenarios that were also simulated. The future development scenarios were developed based on projected population increase. A complete discussion of their development, results, and implications with respect to the flow system is also presented. Finally, a discussion of the overall conclusions about the groundwater flow system of the Upper Roanoke River Watershed and the impacts of future development on the subsurface flow system is included in this chapter.

4.2 Simulation Results

The model was calibrated for steady-state conditions. This model will be referred to as the “steady state model”. It represents a cross-section of time, and the simulation continued until equilibrium in the system was reached. Transient simulations were run to solve time-dependent problems, or to develop time-dependent scenarios to determine the cumulative results over a given length of time. The transient simulations, therefore, consisted of running the calibrated, steady-state model for a period of one year. During these transient simulations, no stresses were added to the system. If stresses were added to the system, it would be expected that the results would be different than those of the steady-state model since the added stresses could potentially alter flow direction and magnitude. The output for the one-year transient simulation is therefore, identical to the output from the steady-state model. Running the simulation for twenty years

produced the identical results as well. Only the results from the transient simulation will be presented and discussed since the results and discussion for the steady state model are identical.

4.2.1 Storage Values

During steady-state simulations, the right side of Equation 1 was set equal to zero. However, during transient simulations, this is not the case since the simulation takes place over a length of time, and $\delta h/\delta t$ is not equal to zero. Therefore, it is necessary to assign storage values to every cell within the model domain (Equation 1) during transient model simulations. These storage values were assigned based on the geohydrologic units defined in Waller (1976). The values reflect the hydraulic properties of the three units, and correspond to the trend of storage values reported in a study conducted in another layered, fractured aquifer system in Pennsylvania (Gburek et al., 1999). In that study, the storage values were reduced by one order of magnitude as the layers progressed down away from the land surface. This assumption is based on the notion that the number of fractures in the bedrock are greater near the land surface, and therefore the storage closest to the surface is larger than that of deeper material with fewer expected fractures. The smallest storage value reported by Gburek (1999) was 0.0001, and therefore, this value was assigned as a constant value to layer 4 (Table 8) (Gburek et al., 1999). Layer 1 (Not shown in Table 8) was assigned a constant value of 0.01, which also corresponds to the value used in the Pennsylvania study (Gburek et al., 1999). The values for layers 2 and 3 are based on the assumption that the Cambrian and Ordovician carbonates will have the most fractures due to dissolution (weathering of the carbonates), followed by the Ordovician to Mississippian clastics, and the Precambrian and Cambrian metamorphics and clastics. This trend was used to assign hydraulic conductivity values as well. It was assumed that the storage values for layers 2 and 3 would fall between the storage value of 0.01 for layer 1, and 0.0001 for layer 4 (Table 8).

Table 8. Storage Values for the three hydrogeologic units

Layer	Storage Value for *P&C M&C	Storage Value for *O-M Clastics	Storage Value for *C&O Carb
Layer 2	0.005	0.007	0.009
Layer 3	0.001	0.003	0.005
Layer 4	0.0001	0.0001	0.0001

*P&C M&C = The Precambrian and Cambrian metamorphics and clastics,

*O-M Clastics = The Ordovician to Mississippian clastics, and

*C&O Carb = The Cambrian and Ordovician carbonates.

4.2.2 Hydraulic Head Contours

The main output from a model such as MODFLOW is hydraulic head values for each cell in the model domain. A water table surface can be interpolated from these hydraulic head values. The water table is presented as contour lines representing an interpolated surface that indicates the hydraulic head of the model domain. This information is significant because the location of the water table indicates a variety of important observations about the flow system. A reduction in the elevation of the water table can indicate a depletion of groundwater resources. A depletion of groundwater resources could significantly impact the people that rely on groundwater as a primary drinking water source. The location of the water table also dictates the interaction between surface-water and groundwater, which could potentially influence surface water supplies. This information is key to managing groundwater effectively, and assuring a safe and sufficient groundwater supply.

The hydraulic head contours from the one-year transient simulation for each layer are shown in Figures 39, 40, 41, and 42. The steady-state results are not discussed because they are identical to the transient results. A discussion of these results and their implications to this investigation follows. This discussion includes the implications of dry cells, vertical flow, and flow direction within the groundwater system. The hydraulic head contours represent the overall trend of the water table on a regional scale, without the influence of stresses added to the system.

4.2.2.1 Dry Cells

A majority of Layer 1 “goes dry” (shown in dark areas, Figure 41), meaning that the water table resides below the bottom of these cells, and the cells no longer contain any available water. This means that the cells that are “dry” are no longer saturated. This result is consistent with the information reported in Waller (1976) which states that the water table commonly resides in the fractured bedrock, not in the overburden. Layer 1 conceptually represents the saprolite (overburden) that lies on top of the fractured bedrock aquifer system, and it is likely that the water table resides in layer 2 creating dry cells in layer 1. The dry cells are consistent with the information reported in Waller (1976) that the position of the water table would not reside in the saprolite (overburden) and therefore these cells were dry. Figure 41 shows that approximately 50% of layer 1 consists of dry cells, which means in these areas, the water table resides in layer 2. A majority of these dry cells occur in the west side of the study area where the

land surface elevations tend to be higher and change drastically. In areas such as this, the water table tends to be deeper than it is in the valleys where the topography changes more gradually and is lower in elevation (Waller, 1976).

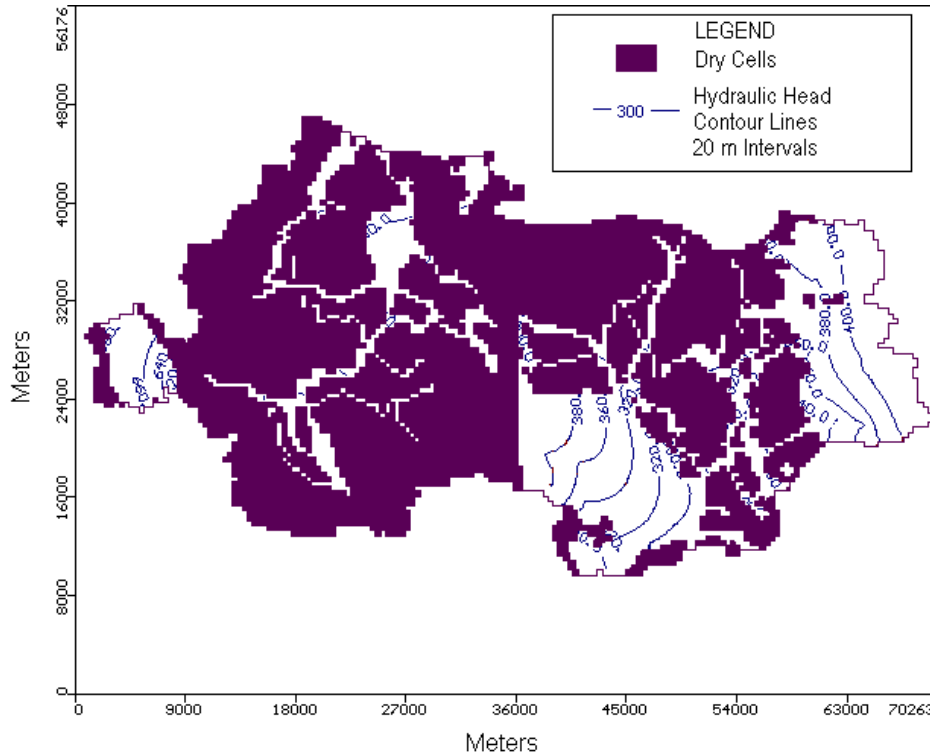


Figure 41. Transient simulation results, layer 1 hydraulic head contours (20m intervals)

The linear trend of dry cells that occurs in Figure 41 along approximately 36000m in the X direction is a result of the initial head array. Recall that the initial heads were assigned according to two separate regression equations, one for the east side of the study area, and one for the west side of the study area. These regression equations were developed based on the assumption that the difference in topography between the two sides would result in a different relationship between the water table and the land elevation surface. The linear trend of dry cells occurs along the boundary between the two regression equations that were used to create the initial heads. Although it is evident that the initial heads affect the dry cell distribution of layer 1, the distribution of hydraulic head values for layer 2 (Figure 42) does not appear to be affected by the initial head distribution, and therefore the results are still reasonable.

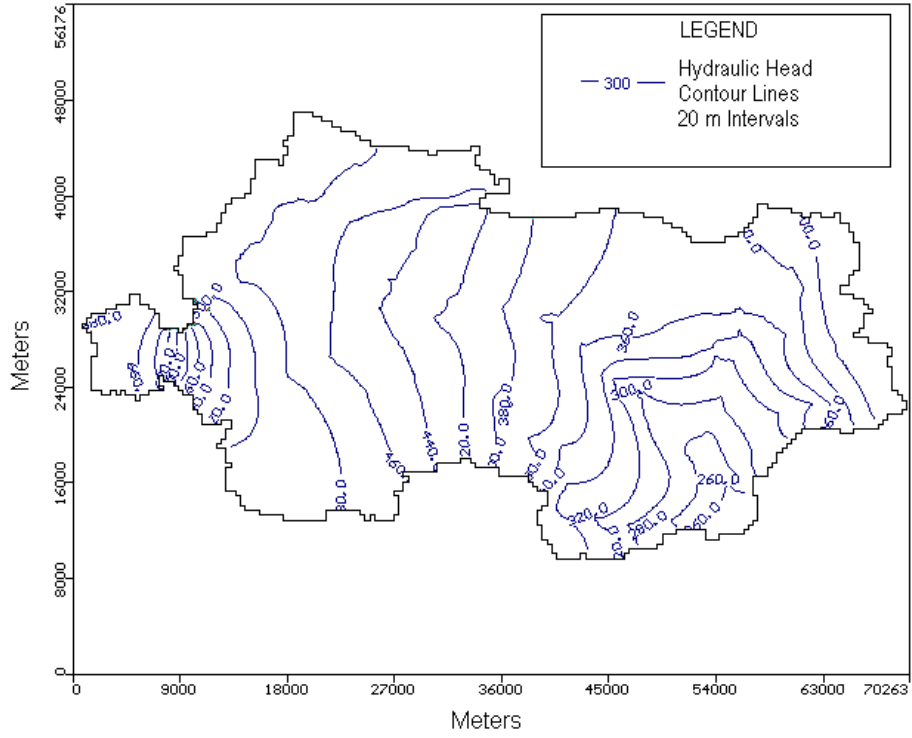


Figure 42. Transient simulation results, layer 2 hydraulic head contours (20m intervals)

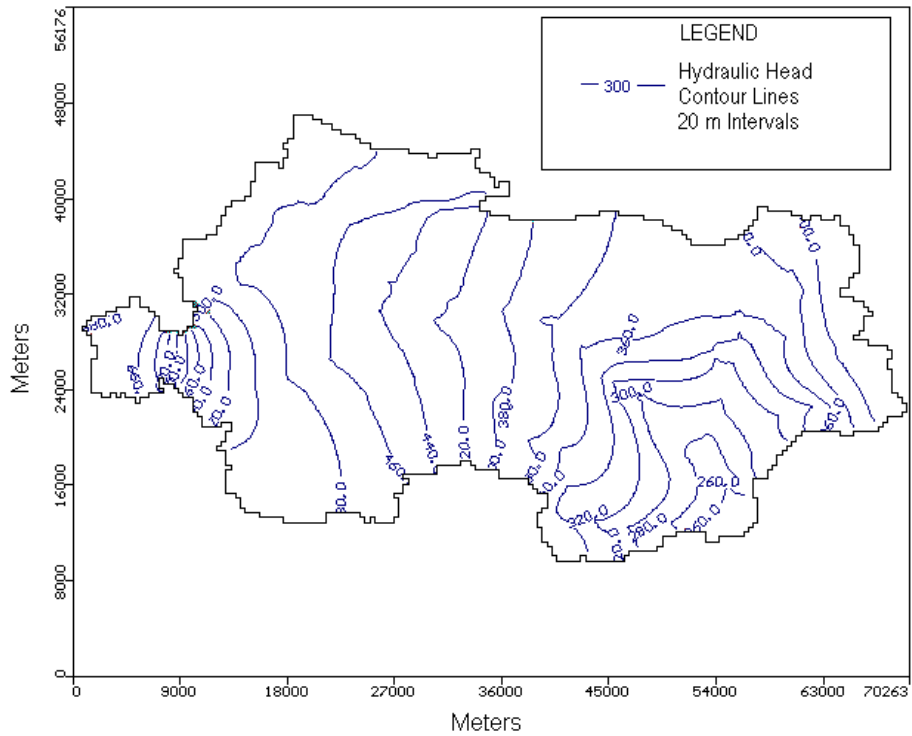


Figure 43. Transient simulation results, layer 3 hydraulic head contours (20m intervals)

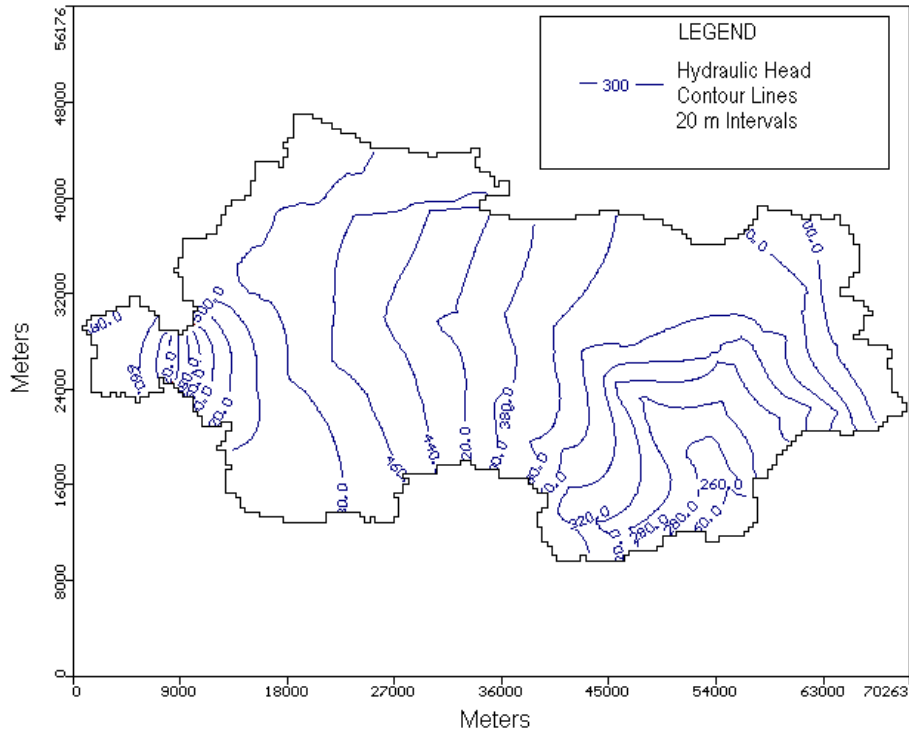


Figure 44. Transient simulation results, layer 4 hydraulic head contours (20m intervals)

In the lower-lying areas on the east side of the study area, there are less “dry” cells, which indicate that the water table resides in layer 1, and that these cells are still partially saturated. However, on the west side of the study area, where the land surface elevations are higher, the water table resides in layer 2, the fractured bedrock below the saprolite layer. This is also consistent with the fact that most of the productive wells in the study area are drilled into the underlying bedrock, and not in the saprolite (Waller, 1976), even in the lower-lying areas.

4.2.2.2 Vertical Flow

From the distribution of head values (Figures 40, 41, 42) for layers 2, 3, and 4, it is evident that there is almost no vertical flow occurring in the groundwater system. In a groundwater flow model such as MODFLOW, flow is calculated through the cell faces, and therefore is categorized as predominantly horizontal or vertical flow. Therefore, it is important to identify what type of flow is occurring in order to understand the flow system. Vertical flow represents flow between layers. If vertical flow was occurring, the hydraulic head distributions for each layer would be different. However, they are virtually the same. There are two possible

explanations for the absence of vertical flow in the system. The conceptualization of the model is such that the fractured bedrock aquifer system is represented as a “uniform porous medium”. This means that the model represents the system as a continuous porous medium, which is necessary in the application of Darcy’s Law, and the groundwater flow equation (Equation 1). In reality, the system consists of fractured bedrock, therefore the model attempts to assign hydraulic properties to the porous medium to simulate flow in the fractured rock. There are no deep fractures represented in the model. If deep flow occurs in the natural system, it is not accounted for in the model. The fault system could also promote vertical flow in the system, however, the faults are not represented in the conceptualization of the model for the study area. The hydraulic conductivity within each model cell was assumed to be isotropic, and therefore the horizontal conductivity was assumed to be equal to the vertical conductivity. This assumption may not have been valid since fractures promote predominantly horizontal flow. Therefore, the vertical flow within cells and therefore between layers is not accurately simulated. The hydraulic conductivity values estimated using UCODE indicate that layer 3 acts as a confining unit during the simulations, which restricts vertical flow to the upper two layers.

The second possible explanation for the absence of vertical flow in the simulation could be related to possible scale issues. One could argue that since recharge is entering the system, vertical flow must occur. Shallow vertical flow driven by recharge could be occurring in layer 2, however, given the depth of layer 2 which in some cases exceed hundreds of meters, this flow will most likely not reach the boundary between layer 2 and layer 3. The depth of the groundwater model is such that even if there was shallow vertical flow occurring in layer 2 (which is most likely the case) it does not go deep enough to occur in layer 3, or even deep enough to affect the head distribution of layer 2. The model is a regional flow model, and therefore, at the given scale, the model is not sensitive to the local vertical flow caused by recharge.

Since the model is not representing deep regional flow within the system, the flow is predominately horizontal. This may or may not be the case. However, since the conceptual model did not include any geologic formations that could influence flow, these results are reasonable. The fault system in the study area could play a significant role in conducting water throughout the system. However, without sufficient data about how these faults are affecting flow within the system, they cannot be accounted for in the model.

4.2.2.3 Model Performance Evaluation through Hydraulic Head Contour Comparison

Another method of evaluating the model performance is to compare the hydraulic head values simulated by the model to known hydraulic head values. Since there is not a complete map of observed hydraulic head values available, a map was created in ArcView GIS from the observed values in Figure 38. These observations were used to determine approximate known hydraulic head values for the entire study area through interpolation. The surface that was created is shown using contour lines in Figure 45. Figure 46 shows the hydraulic head results from the transient simulation. Intermediate contour lines were included to show the difference in the simulated water table elevations and the observed (interpolated) water table elevations. The 300m hydraulic head contour line matches well, meaning that the model matches the observed hydraulic head values well in the east side of the study area (Figures 45 and 46). The 420m contour line in Figure 46 closely matches the position of the 400m contour line in Figure 45. This indicates that the model is over-predicting the water table elevations in this area of the watershed. And finally, the 480m contour line in Figure 46 closely matches the position of the 500m contour line in Figure 45. This indicates that the model is under-predicting the water table elevations in this area of the watershed. These results indicate that the model is predicting the water table within approximately 20m of the observed location. It is difficult to draw absolute conclusions from these results however, since the observed hydraulic head map was interpolated from observation points and may not accurately represent the actual water table position. Figures 45 and 46 therefore, provide a visual comparison to the observed vs. simulated hydraulic head values.

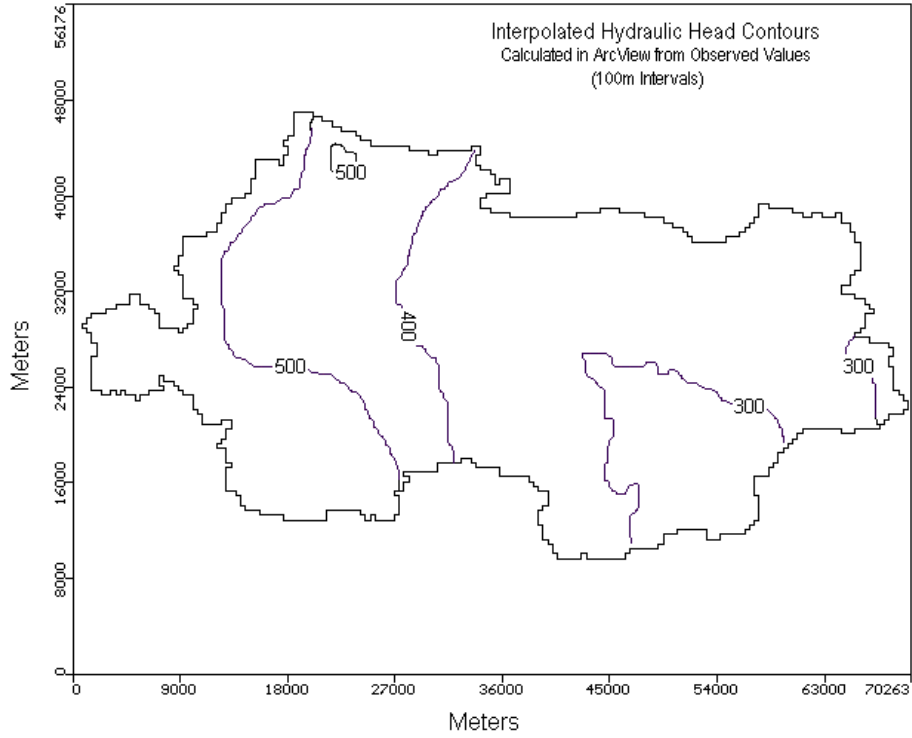


Figure 45. Interpolated hydraulic head surface from hydraulic head observations in Figure 39 (ArcView).

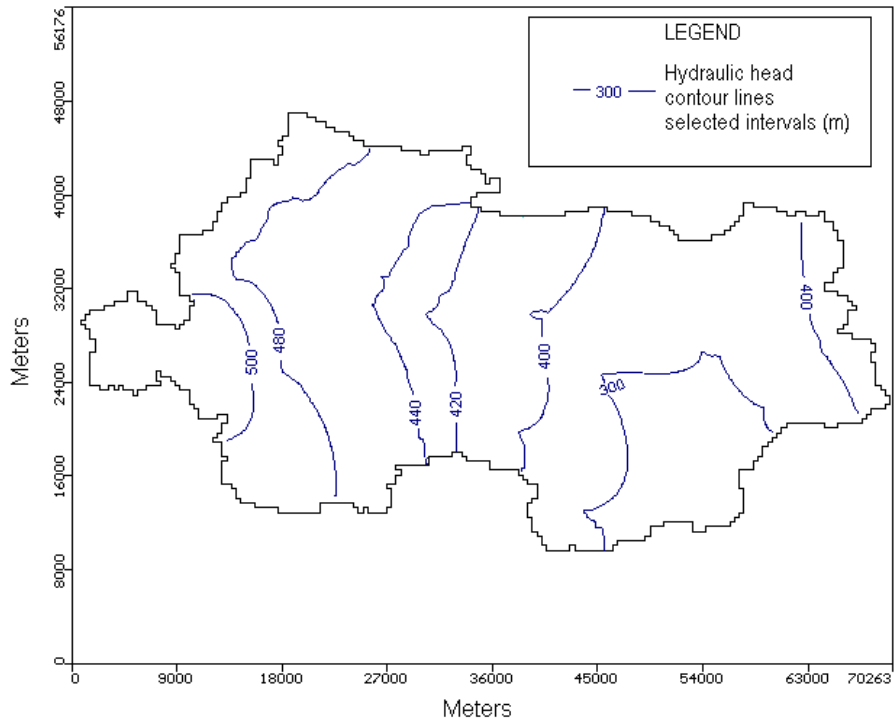


Figure 46. Transient simulation results, layer 2 hydraulic head contours (selected intervals, m)

4.2.3 Information on Horizontal Flow Direction

Determining the direction of horizontal flow within the groundwater system can indicate whether the surface-water flow divides for the sub-watersheds within the regional model correspond to the groundwater flow divides of the regional system. The flow direction can also be used to determine flow paths of possible contaminants in a system. Overall, the flow direction provides a better understanding of flow within the system.

Visual MODFLOW gives the user the ability to view the flow direction of each layer in the model. The flow direction is determined by the individual flux values calculated by solving Equation 1 for every node (cell) within the model domain. During the transient simulation (model calibrated for steady state conditions run for one year), since the system is not being stressed, the flow directions throughout the length of the simulation remain the same. The arrows in Figure 47 represents the direction of horizontal flow that is occurring within the layer 2. The flow direction figures for layers 3 and 4 are identical to Figure 47. Water within the system generally flows towards the outlet in the bottom right of the study area. Local flow tend to flow towards the reaches within the study area, which is expected since the local gradients near the streams induces flow from upland areas towards low areas where reaches reside.

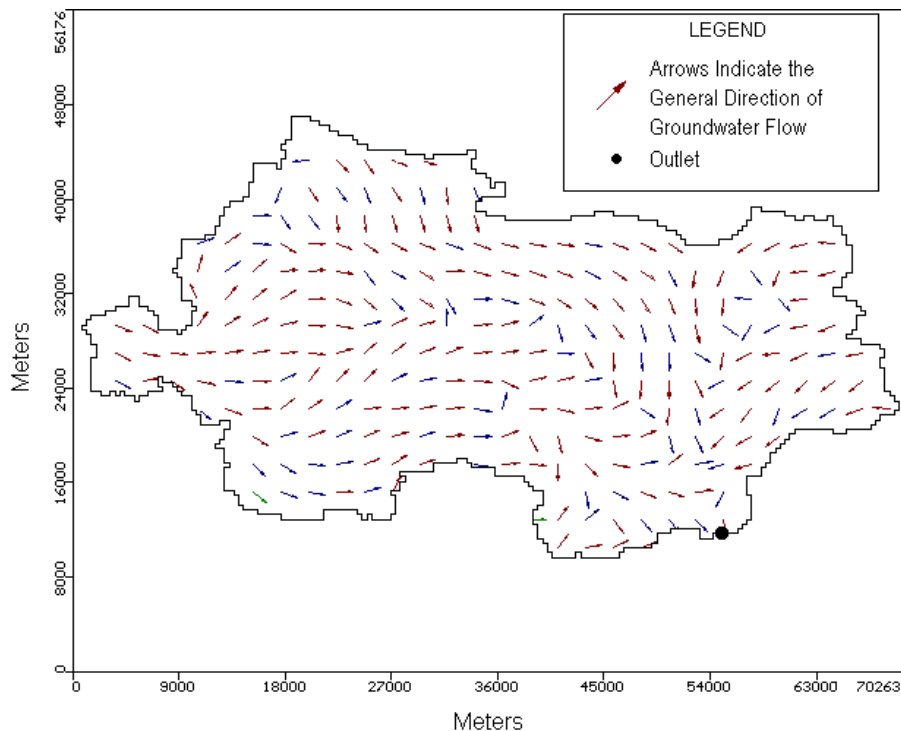


Figure 47. Transient simulation - general direction of horizontal flow in layer 2

4.2.4 Surface-Water-Groundwater Interaction

The gradients (head differences) between the surface-water system and the groundwater system induce flow from either the aquifer system into the surface-water system (streams/rivers) or from the streams into the aquifer system (Figure 48). If the river is contributing water to the aquifer system, the river is “losing” water (Figure 48). This means that the hydraulic head in the river is higher than that of the aquifer beneath it, and the water from the river flows from the higher hydraulic head (in the river) to the lower hydraulic head (in the aquifer). If the aquifer system is contributing water to the river, the river is “gaining” water from the subsurface flow system (Figure 48). This means that the hydraulic head in the aquifer below the river/stream is higher than that of the river, and therefore the water from the aquifer flows from the higher hydraulic head (in the aquifer) to the lower hydraulic head (in the stream).

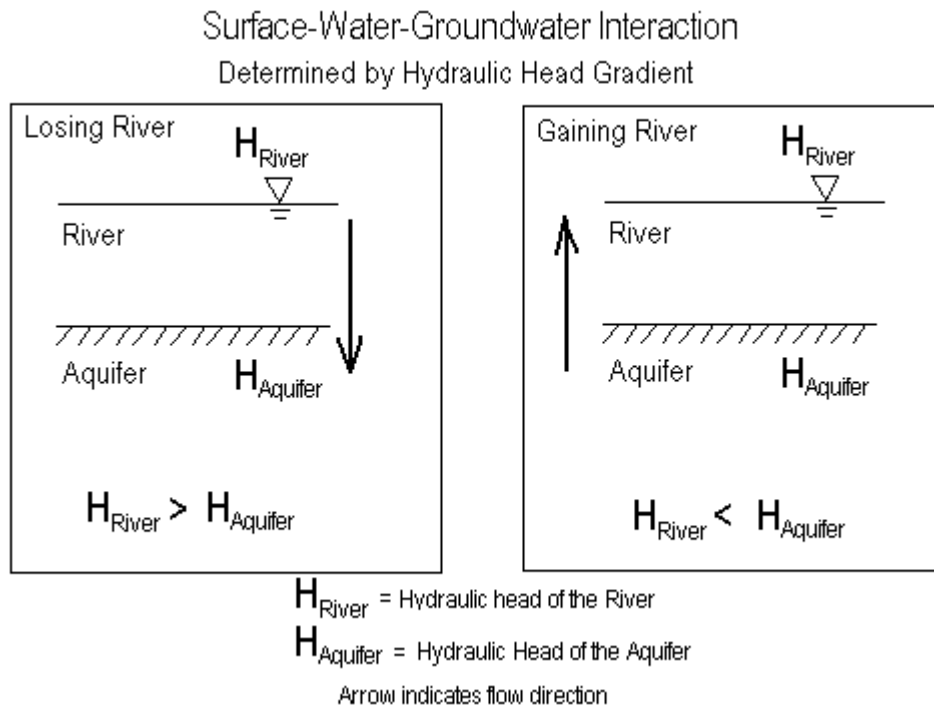


Figure 48. Surface-water-groundwater interaction dictated by the gradient between the two systems.

The interaction between the surface water system and the groundwater system shown in Figure 48, is key to understanding the influence of the groundwater system on the surface-water system, and vice versa. The location of gaining and losing streams in a watershed can aid in flood prevention, and can locate areas that may be sensitive to groundwater contamination. The systems are coupled dynamically through this gradient relationship (Fetter, 1998), and the impacts of urban development on one of the systems can directly impact the other.

MODFLOW calculates the volume of water exchanged between the surface-water and groundwater systems for each cell that is defined in the model as a river cell. Since there are 586 reach cells in the model, for the ease of reporting these values, an average discharge flux (m^2/day), for the segments shown in Figure 49, was estimated by dividing the reported total flux for a given segment (m^3/day) by the segment total length (m). A segment is defined as a length of continuous river cells that does not contain any tributaries (Prudic, 1989). A new segment is formed when tributaries join the main stem of the river network. There are 23 total segments represented in the model defined in the Streamflow-Routing input file. Segment 23 is the cell located at the outlet of the watershed. All of the other segments (1-22) are shown in Figure 49 by the divisions of the river network. Table 9 shows the cumulative discharge for each of the 23 segments, the total stream length of each segment, and the calculated average discharge flux for each segment. The average flux for a segment (Table 9) is an indication of the discharge that is occurring from the subsurface flow system into the rivers over that segment of river. The average flux magnitudes in Table 9 indicate the segments of river that are contributing a higher overall volume of water to the river network. The average flux values in Table 9 are negative because they are defined as “flow into the aquifer” (Prudic, 1989). Therefore, the negative sign is merely a sign convention indicating the flow direction is from the aquifers into the streams.

4.2.4.1 Explanation of Discharge Results

The results show that the streams are gaining practically everywhere in the system (Table 9, Figure 50). Since all of the values are negative, this shows that water is flowing out of the aquifer system, and is contributing to the surface flow.

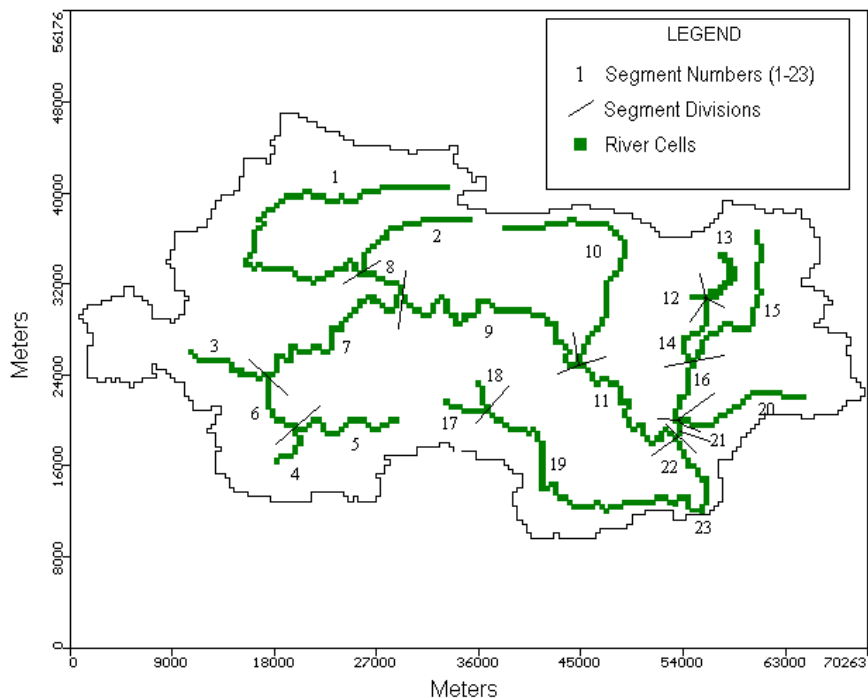


Figure 49. Segment numbers and locations (defined in Streamflow-Routing Package) (Prudic, 1989).

Figure 50 shows the respective locations of the average discharge values for each segment. The entire watershed is bound by no-flow boundary conditions. This was included in the model conceptualization due to the lack of surface flow data at the outlet. If this data were available, a specified-flow boundary would have been defined at the outlet to allow a given volume of water to flow out of the system. Since there is a no-flow boundary at the outlet, all of the water that would normally flow out of the system at the outlet, must leave the system through the river cells which is the only way water can leave the system in this model. This volume of water that would discharge at the outlet, plus the volume of water that would normally be discharged from the system through the river cells is the total amount of water that is leaving the system. Therefore, since a larger volume of water is forced to exit the system through the river cells, the distribution of the locations of discharge and recharge areas within the river has been distorted. Where there could be areas of losing streams, the extra volume of water that needs to be discharged, could alter these areas to become gaining streams instead. This may offer an explanation as to why the rivers are gaining (aquifers are contributing water to the streams) everywhere in the study area.

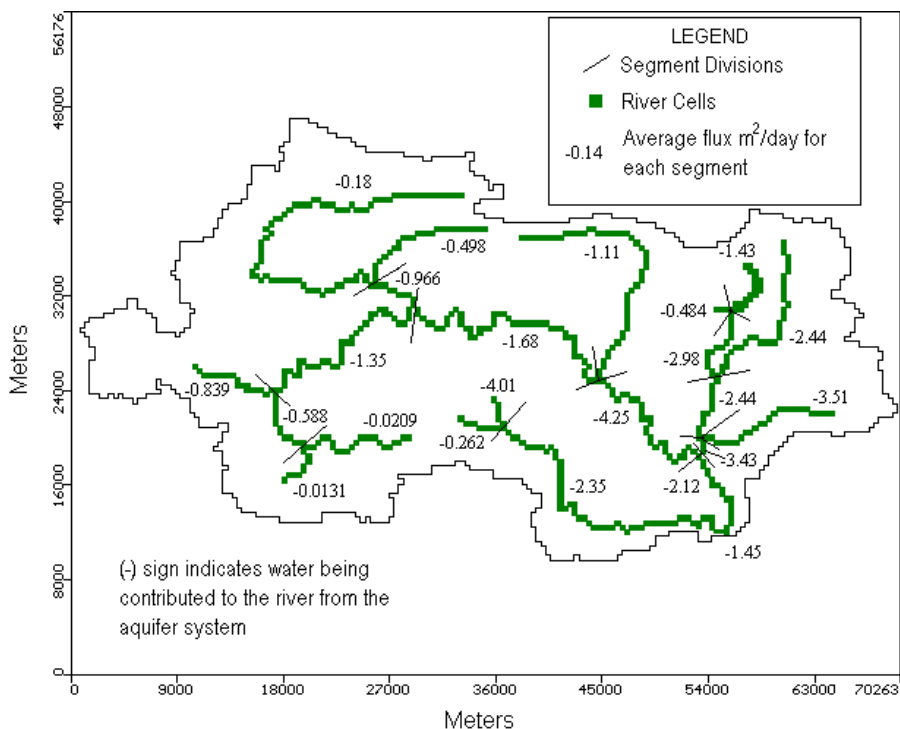


Figure 50. Transient simulation average flux (m^2/day) for segments 1-23 (Figure 49)

Another possible explanation for the streams to be gaining water from the aquifer system everywhere in the model may be due to the scale of the model. The model constructed for this investigation is not only strongly conceptual, due to the available data constraints, but it is also a regional model. It represents regional trends in the flow system, and therefore cannot be expected to show local details in the simulation results.

It would be expected that the streams would be gaining water from the aquifer system close to the outlet, but would be losing water to the aquifers in the higher elevations. This is expected to happen due to the lower position of the hydraulic heads with respect to the elevation in these higher areas. The water table tends to be closer to the land surface elevation in areas that are lower in elevation than those that contain drastic elevation changes.

Another explanation for the lack of local detail necessary to accurately simulate the stream-aquifer interaction is the large resolution of the model. An overall average elevation value was assigned to each new cell during the grid development to transform the DEM data for the surface elevations (30m resolution) to the resolution of the groundwater model (402.4m resolution). In changing the resolution in such a way, local details of the system were lost in

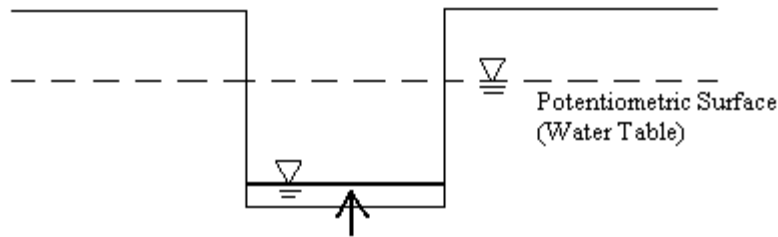
these average values. Also, since there are drastic changes in topography in the west part of the study area, it seems the model is representing an overall trend, but is failing to represent the local details of the surface-water-groundwater interaction (Figure 51). Figure 51 illustrates the notion that if more detail were included in the model, the local detail of the surface-water-groundwater interaction would be better simulated. The regional groundwater model (Figure 51) simulates an overall trend and is unable to simulate the detailed surface-water-groundwater interaction.

Table 9. Segment total discharge, length, and average flux for the transient simulation

Segment Number	Total Flow (m ³ /day)	Length(m)	Average Flux (m ² /day)
1	-5649	31387	-0.18
2	-5414	10864	-0.49
3	-6078	7243	-0.84
4	-42	3219	-0.01
5	-185	8852	-0.02
6	-3311	5633	-0.59
7	-23289	17303	-1.35
8	-3109	3219	-0.97
9	-37121	22132	-1.68
10	-67590	61164	-1.11
11	-54787	12876	-4.26
12	-389	804	-0.48
13	-9806	6840	-1.43
14	-19157	6438	-2.98
15	-34392	14084	-2.44
16	-13738	5633	-2.44
17	-842	3219	-0.26
18	-8070	2012	-4.01
19	-59668	25351	-2.35
20	-36736	10462	-3.51
21	-4144	1207	-3.43
22	-14530	6840	-2.12
23	-583	402	-1.45

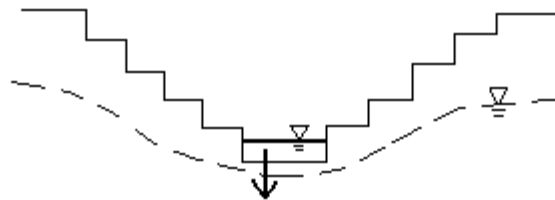
This is a scale issue because it cannot be expected for a regional groundwater-flow model, at a resolution of 402.4m by 402.4m cells to produce accurate detailed output about local phenomena in the system. If more accurate values are desired, local models with higher resolutions can be constructed using boundary conditions governed by this regional model.

Regional Groundwater Model Representation (Low Resolution)



Water is Flowing from the Aquifer System to the Stream

Local Groundwater Model Representation (Higher Resolution)



Water is Flowing from the Stream to the Aquifer System

Figure 51. Model resolution and its effects on detailed output

4.2.4.2 Discharge Trend

As stated above, it was expected that the streams that are farther away from the outlet would be losing water to the aquifer system and the streams closer to the outlet would be gaining water from the aquifer system. The results from the simulation (Table 9) show that this is not the case. The streams are gaining water from the aquifer system everywhere in the study area. The output does however, follow the expected trend. Figure 52 shows the trend of volume of discharge with respect to distance from the outlet. The overall trend shows that the segments that are farther away from the outlet are discharging less, and as the distance from the outlet decreases, the discharge increases. Because of this trend, it can be assumed that the model is still producing acceptable results, however, the magnitude of the discharge values is effected by model resolution and by the imposed no-flow boundary conditions.

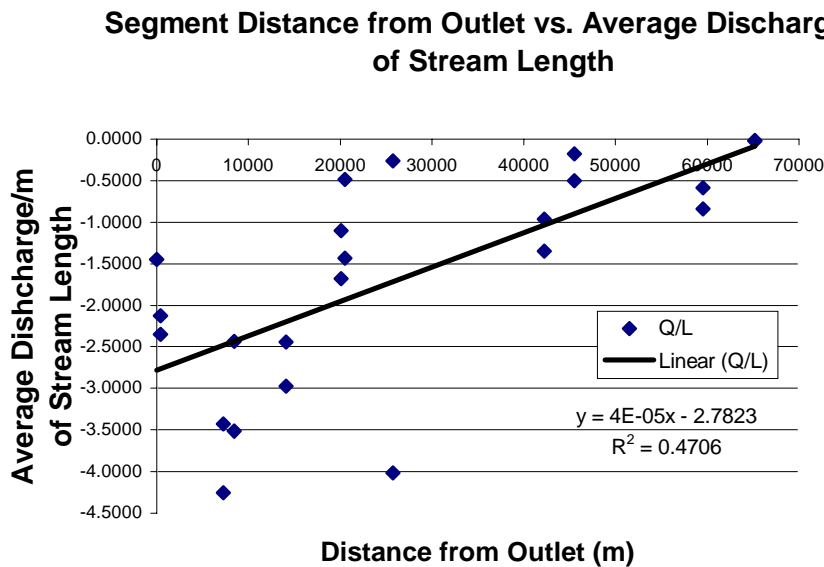


Figure 52. Trend of average discharge vs. distance from outlet

4.3 Model Application

To meet the first objective of this study, the model was applied to the watershed to account for land-use activities. Land use activities may effect the subsurface flow system in two ways. The first is by reducing the amount of recharge that enters the subsurface flow system. Increased development can lead to an increase in impervious areas within the watershed. These impervious areas reduce the amount of infiltration into the soil surface, and thus, reduce the volume of water recharging the subsurface system. The second way the subsurface flow system can be effected by land use change is by increasing the volume of water that is pumped from the system to account for the higher water demand associated with increased population. The latter involves a significantly larger volume of water and would potentially have much greater impacts on the system than a reduction in recharge. The lack of obvious vertical flow caused by recharge (as previously discussed) supports the idea that even though the model is more sensitive to recharge (Table 7) than any of the other estimated parameters, reducing it will not drastically affect the simulation results. Therefore, since the volume of water associated with reduced recharge is so much greater than the volume of water associated with increased withdrawal, increased pumping is the only impact that is taken into account during the model application. The recharge values determined during the calibration process were as inputs for model

application. These values are developed for a period with low precipitation (1969-1970, 36 in/yr of precipitation), and therefore, these scenarios represent extreme situations.

4.3.1 Baseline Simulation

A model representing current pumping conditions in the watershed is necessary before future development scenarios can be evaluated. This model simulation will be referred to as the “baseline simulation” since it will serve as a means of comparison for the future development scenarios. The baseline simulation consisted of adding pumping wells that represent current pumping rates to the transient simulation model.

Information about existing pumping was obtained from the Virginia Department of Environmental Quality. Any well that pumps more than 10,000gal/day is reported to the DEQ. Therefore, the data obtained in the baseline simulation only includes wells in the study area that were pumping over 10,000gal/day as of 1996 (the most current date that data were supplied).

It is assumed that the pumping that occurred in 1996 accounts for the population increase from 1970-1996. From 1970-1980, Roanoke County’s population increased from 53,817 to 79,294 according to the 1990 Census (Harrington et. al, 1996). In 1996, Roanoke County had a total population of 83,100, according to reported estimates. This information is just for Roanoke County, and as stated previously, does not include the population increase in the cities of Roanoke, Salem, and Vinton. However, a majority of the population that lives in the city utilizes municipal water sources, not groundwater. Therefore, the increase in population for the County was used in this investigation. A total increase of 29,283 people occurred from 1970-1996.

The well data supplied by the DEQ were used to develop an input file for the Well Package in the MODFLOW simulations. This package was used to simulate the pumping conditions for the year 1996. The supplied data was already organized into 4 Service Areas: North, South, East, and West. Each service area contained a unique number of wells and pumping was reported for each service area as a whole, not for each individual well within that service area. The average annual pumping rate was distributed uniformly to the wells within each service area. Some of the wells were clumped very close together, and were, therefore, represented in the model as a single well that pumps the equivalent volume of the group. Also, some of the wells in the southern part of the study area that pumped small amounts (less than 10m³/d) were combined into “combination wells” to minimize the number of wells that are

actually represented in the model, due to its large resolution. Table 10 shows the wells that were located within one mile of each other, and are represented as one “combination” well that pumps the combined pumping rate of each individual well included. Table 11 shows the names and numbers of wells in the four service areas (North, South, East, and West), and the x, y locations within the model domain. The most recent year of data was used as model input, which was 1996 for service areas South, East and West, and 1995 for the North service area. The 1995 data for the North service area were assumed to be sufficient to represent the pumping in 1996 as well. The locations of the wells are shown in Figure 53.

Table 10. Individual well composition of combination wells

Combination Well 1	Combination Well 2	Combination Well 3
Arlington Forest	Chesterfield Court	Oak Grove
Highfield	Craighhead-Utility Services	Castle Rock
Mount Vernon Forest	Pine Mountain	Hidden Valley
Scenic Hills		Crestwood Park
Brookwood		Longridge
Arlington Hills		Homewood
Laymans Lawn		
Starkey		
Belle Meade		
TOTAL WELLS = 19	TOTAL WELLS = 8	TOTAL WELLS = 21

Table 11. Existing wells in Roanoke County pumping more than 10,000gal/day as of 1996 (DEQ, 1999).

Service Area	Name	*X	*Y	Number of wells	Q (m ³ /day)
EAST	Labellevue	56600	23330	5	726
TOTAL				5	726
WEST	Wooded Acres	44528	31316	1	571
	Glen Forest	34176	30856	1	571
	Glenvar East	36708	31922	3	1713
	Andrew Lewis Place	50051	23096	1	571
TOTAL				6	3425
NORTH	Tinker Knoll	54342	28478	2	81
	Hollins	56623	28613	1	40
	North Ardmore	56375	27133	2	81
	BelleHaven-Brooklawn	53198	29234	6	242
	Carvins Meadow	54899	26282	1	40
	Burlington Heights	51937	27328	1	40
	North Lakes	48428	27823	5	202
TOTAL				18	726
SOUTH	Chesterfield Court	47975	12777	1	4
	Arlington Forest	45179	14626	1	4
	Oak Grove	47324	17592	5	22
	Farmingdale	46599	19533	1	4
	Castle Rock	45594	16910	4	18
	Highfield	45007	15471	2	9
	Mount Vernon Forest	44587	14836	1	4
	Scenic Hills	44386	14421	1	4
	Hidden Valley	45418	18853	7	31
	Brookwood	43572	14959	3	13
	Arlington Hills	45095	14499	2	9
	Craighead-Utility	47467	13113	5	22
	Hampden Hills	54444	11786	3	13
	Laymans Lawn	44925	14795	3	13
	Crestwood Park	46610	16237	1	4
	Southern Hills "B"	49240	13584	1	4
	Pine Mountain	47385	12437	2	9
	Green Haven Hills	48389	15060	1	4
	Longridge	45086	17246	2	9
	Starkey	45774	13868	5	22
	Belle Meade	46614	15139	1	4
	Homewood	44157	16947	2	9
TOTAL				54	239
TOTAL PUMPING IN 1996 (North, South, East and West Service Areas)					5116

*Location of each well in the model coordinate system (m)

The baseline simulation was run for a time period of 20 years. This length of time was chosen arbitrarily in order to assess the long-term results of pumping on the flow system. Twenty years was considered to be sufficient to determine the long-term effects. All scenarios that project future pumping were run for 20 years in order to make a direct comparison to the baseline simulation results to determine the long term impacts of increasing pumping rates.

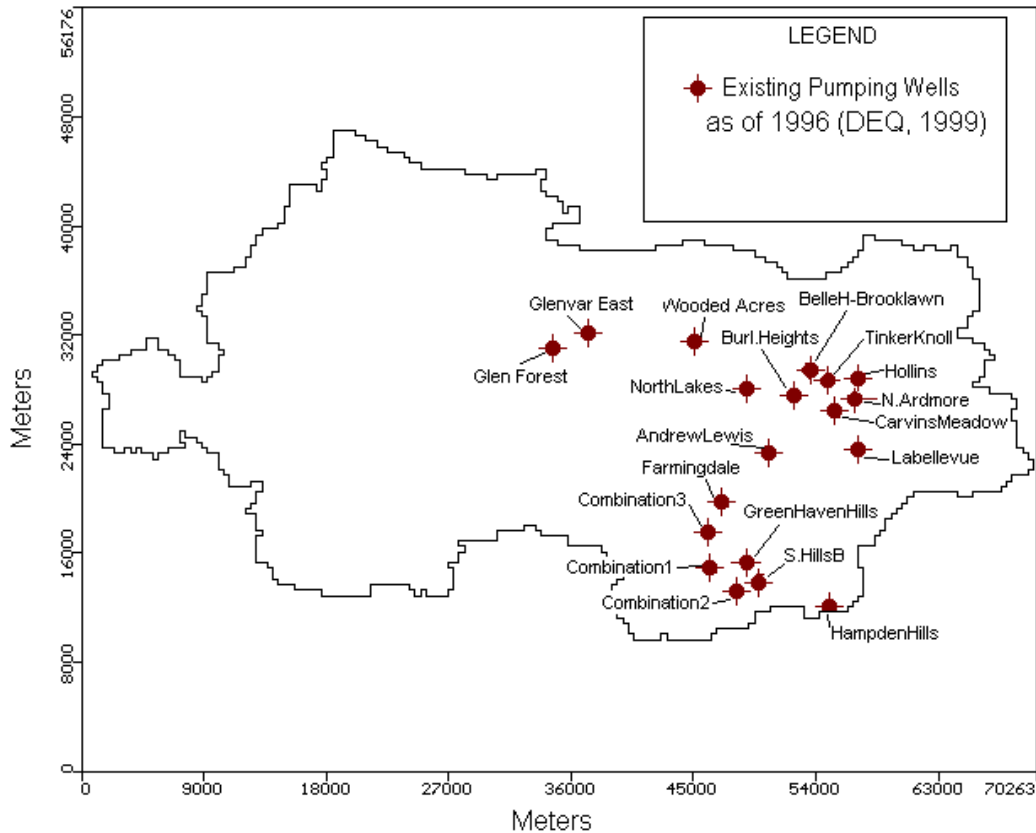


Figure 53. Roanoke County wells pumping as of year 1996 – baseline simulation

4.3.1.1 Baseline Simulation Results

The resulting hydraulic head contours for layer 2, from the baseline model simulation, are shown in Figure 54. It is difficult to detect a difference between the hydraulic head contours in Figure 54 and the hydraulic head contours shown in Figure 42, the transient simulation results which simulated no pumping wells. Comparing these contours with Figure 42, the layer 2 contours with no pumping, it is difficult to see a difference. There is a slight difference however,

in the discharge volume and locations. A total of 2,470,979,072m³ discharged from the aquifer system to the rivers (gaining) over a 20 year time period during the baseline simulation. When the transient model was run (with no pumping) for a 20-year period, the total discharge from the aquifer system to the rivers (gaining) was estimated to be 2,561,577,984m³. Therefore, the baseline simulation with induced pumping reduced the volume of water being discharged from the aquifer system into the rivers by 3.5%. This indicates that the hydraulic heads are slightly lower in the baseline scenario than in the transient simulation without pumping and apparently head difference drives the calculation of the flow (Equation 8). Therefore, even though there is no visible difference in hydraulic heads presented in Figures 52 and 40, the distribution output shows that there is a slight difference in the discharged water volume. There was also no difference between the contours of layer 2 with those of layers 3 and 4. Therefore, the only layer that is discussed here is layer 2. This implies that there is little or no vertical flow occurring since the hydraulic head contours between layers 2, 3, and 4 are virtually the same, and if vertical flow was occurring, the head distribution would be different (as discussed in a previous section).

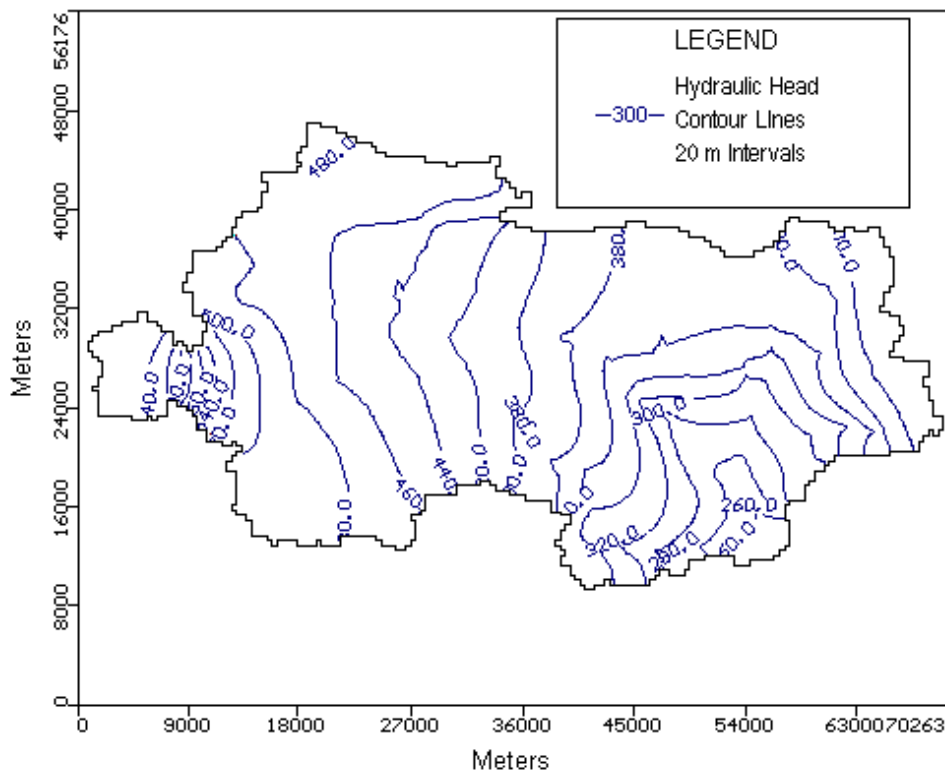


Figure 54. Baseline simulation results, layer 2 hydraulic head contours (20m intervals)

The distribution of discharges for each segment is presented in Figure 55. A list of discharges is presented in Table 12. The results from this simulation are presented in the same format than those presented from the transient model. The 586 values of discharge that were reported for each of the cells that represent rivers in the model were grouped in to the segments shown in Figure 49. The cumulative discharge for each segment is calculated, and divided by the total length of that segment to determine an average discharge flux for each segment (Figure 49). Figure 55 shows the locations of the average flux values (Table 12), for each of the 23 segments defined in Figure 49.

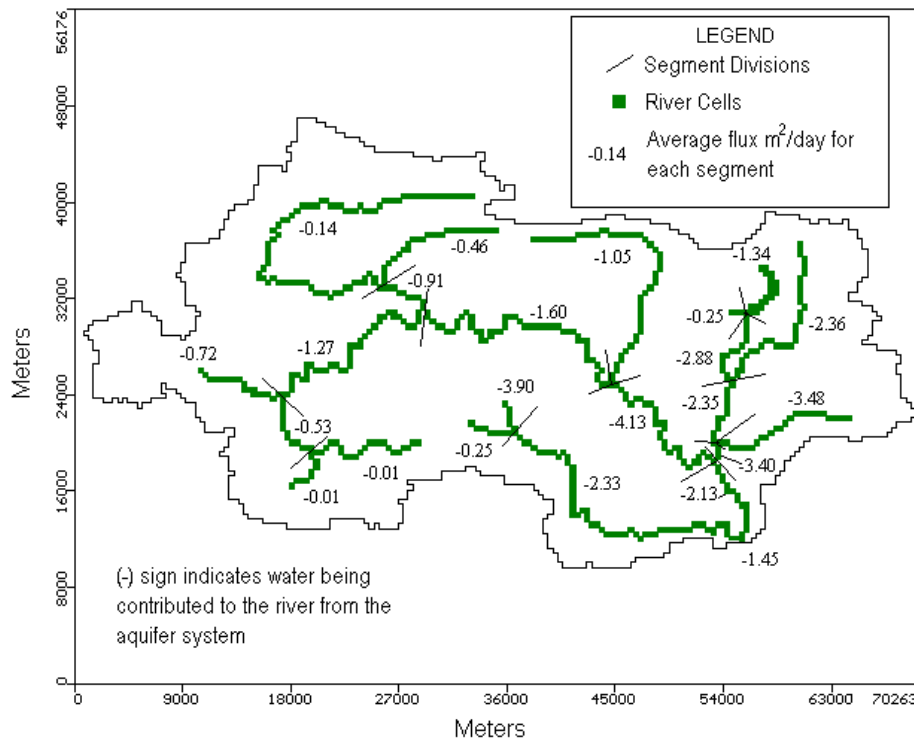


Figure 55. Baseline simulation average flux (m^2/day) for segments 1-23 (defined in Figure 49)

Table 13 shows the percent difference in average flux values between the baseline and the transient simulation. The higher percent difference occur predominantly in the segments that are located farther away from the outlet. Segments 1, 3, 4, 5, and 12 have the highest percent differences, with 19.8%, 14.0%, 45.6%, 30.7% and 48.4% respectively (Table 13). Segments 1, 3, 4, and 5 are all located in the west side of the study area where the land surface elevation tends

to be higher and varies more drastically (Figure 49). Segment 12 only consists of 3 river cells, therefore, if one value of discharge changes significantly, the overall average flux will also change significantly. These results indicate that the west side of the study area, which contains the higher elevations, and is further away from the outlet is more sensitive to pumping than the east side of the study area. Although there were not visible differences in the hydraulic head contours, the pumping affected the results enough to change the discharge values. These discharge changes occurred predominantly in segments that were far away from the outlet. The overall trend in the model domain occurs from the upper left corner of the basin, to the lower right corner, and therefore, more water is available near the outlet in the lower right corner. The Roanoke Valley area, near the outlet of the basin is not only receiving water from recharge, as is the rest of the basin, but the water from everywhere else in the basin if flowing there. Therefore, the areas farthest away from the outlet in the study area are the most sensitive to pumping, and the results presented here support that notion.

Table 12. Segment total discharge, length, and average flux for baseline pumping simulation.

*Segment Number	Total Flow (m ³ /day)	Length(m)	Average Flux (m ² /day)
1	-4530	31387	-0.14
2	-5040	10864	-0.46
3	-5225	7243	-0.72
4	-23	3219	-0.01
5	-128	8852	-0.01
6	-2995	5633	-0.53
7	-21920	17303	-1.27
8	-2927	3219	-0.91
9	-35485	22132	-1.60
10	-64128	61164	-1.05
11	-53203	12876	-4.13
12	-201	804	-0.25
13	-9152	6840	-1.34
14	-18562	6438	-2.88
15	-33201	14084	-2.36
16	-13244	5633	-2.35
17	-802	3219	-0.25
18	-7837	2012	-3.90
19	-59080	25351	-2.33
20	-36396	10462	-3.48
21	-4107	1207	-3.40
22	-14555	6840	-2.13
23	-582	402	-1.45

*See Figure 49 for segment locations

Table 13. Percent difference of average flux values for each segment for the baseline simulation with respect to the transient simulation

*Segment Number	Transient Simulation Average Flux (m ² /day)	Baseline Simulation Average Flux (m ² /day)	% Difference
1	-0.180	-0.144	19.807
2	-0.498	-0.464	6.908
3	-0.839	-0.721	14.034
4	-0.013	-0.007	45.626
5	-0.021	-0.014	30.676
6	-0.588	-0.532	9.519
7	-1.346	-1.267	5.878
8	-0.966	-0.909	5.854
9	-1.677	-1.603	4.407
10	-1.105	-1.048	5.121
11	-4.255	-4.132	2.890
12	-0.484	-0.250	48.357
13	-1.433	-1.338	6.669
14	-2.975	-2.883	3.106
15	-2.442	-2.357	3.463
16	-2.439	-2.351	3.596
17	-0.262	-0.249	4.751
18	-4.011	-3.895	2.881
19	-2.354	-2.330	0.985
20	-3.511	-3.479	0.926
21	-3.433	-3.402	0.893
22	-2.124	-2.128	-0.174
23	-1.449	-1.446	0.172
Average	-1.670	-1.607	9.941

* See Figure 49 for segment locations

4.3.2 Future Development Scenarios

To demonstrate how MODFLOW can be used as a management tool, three future pumping scenarios were developed to illustrate possible settlement trends, and determine the impacts these trends could potentially have on the subsurface environment in the Upper Roanoke River Basin. The scenarios were developed from historical pumping information supplied by the Virginia Department of Environmental Quality (DEQ) from the years 1982-1996, and from population projections for the year 2010 (DEQ, 1999). Three possible settlement patterns were developed, and the scenarios were run for 20 years to compare the results directly with the baseline simulation results.

In order to determine the necessary water demand to adequately serve the population increase, it was necessary to develop a relationship between population and pumping rates in Roanoke County. Historical pumping information obtained from the Virginia Department of Environmental Quality (DEQ) included all wells that pumped greater than 10,000gal/day in the county for the years 1982-1994. Historical pumping rates were plotted against the population for these years, and a relationship was determined (Figure 56). Although the relationship is not very strong ($R^2=0.22$), it is sufficient to supply a rough estimate of water use for the purposes of this analysis. A better relationship would probably be possible to determine if more data were included in the regression relationship. The ratio of water use to population was found for each year, and the ratios ranged from $1.5E-5$ to $2.5E-5$. Therefore, it was determined that the equation in Figure 56 was adequate to make a rough estimate since the value of 1.93mgd (calculated from the relationship in Figure 56) falls between the low estimate (1.43mgd) and the high estimate (2.39mgd) from the ratios.

If the population increases 1% per year from 1996 to 2010 as projected (Harrington et. al, 1996), the total population of Roanoke County will be a little over 95,500. Since the baseline simulation already accounts for a total population of 83,100 (in 1996), the future development scenarios will have to pump water for an additional 12,400 people to account for the projected population increase from 1996-2010.

The wells in the baseline simulation pump a total rate equal to 1.35mgd ($5,115m^3/day$). The relationship in Figure 57 determines that a total rate of 1.93mgd ($7,316m^3/day$) is necessary for the total projected population of 95,500 in 2010. The difference of 0.58mgd ($2200.79m^3/day$) is the rate of pumping that was added to the baseline run for each of the three development scenarios. Therefore, in each scenario, wells that have a total pumping rate equal to 0.58mgd ($2200.79m^3/day$) will be added to pump a total rate of 1.93mgd ($7,316m^3/day$) necessary for the 95,500 people.

In developing the scenarios, the aquifer pumping capacities of each geohydrologic unit (Waller, 1976) was also considered. Adding wells that pumps more than the expected yield from the aquifers caused the model to “go dry”; in other words, dry cells would appear throughout the model grid, indicating that over-pumping in one or more wells was occurring. This only occurred when wells were greatly exceeding the aquifer pumping capacities of the geohydrologic units. If the scenarios presented here were implemented, the well driller would have a general idea of the

yield to expect from a well given the location and the topography. Therefore, it is realistic to limit the amount of pumping that occurs in the wells in the following scenarios, based on the aquifer yield. The following table (Table 14) shows the general capacities of the three hydrogeologic units as presented in Waller (1976).

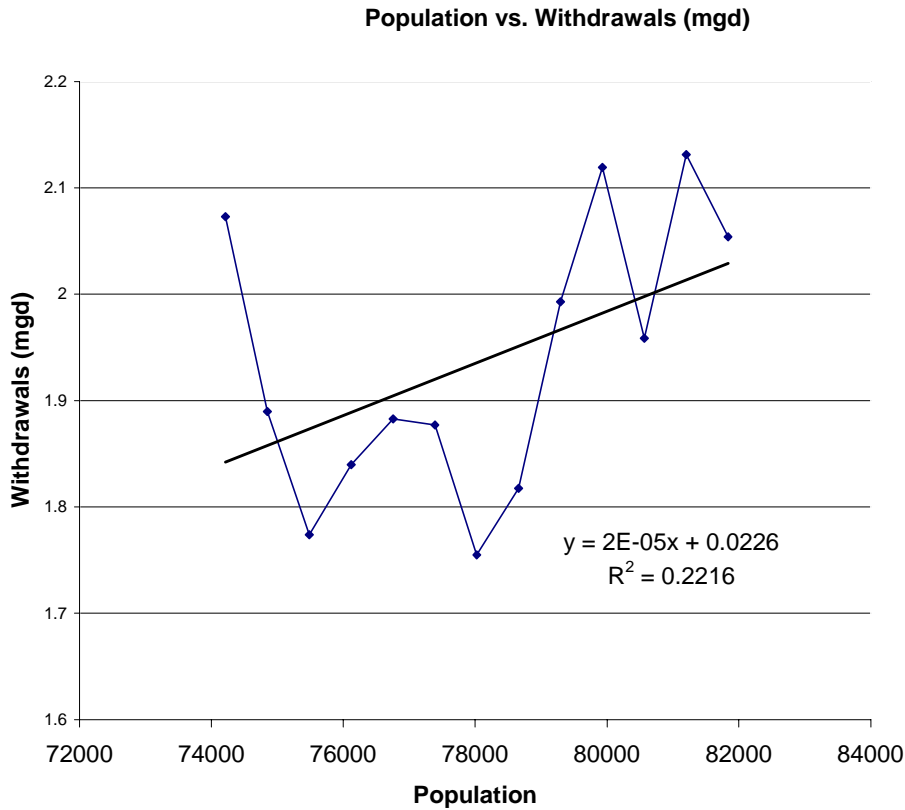


Figure 56. Population vs. withdrawals (mgd) in Roanoke County for the years 1982-1995

Table 14. Aquifer pumping capacities/possible yields (Waller, 1976).

Hydrogeologic Unit	Possible Yield	Comments
Ordovician to Mississippian Clastics	~400gpm (2180m ³ /day)	
Cambrian and Ordovician Carbonates	~1000-1500gpm (5450-8175m ³ /day)	
Precambrian and Cambrian Metamorphics and Clastics	~17gpm-400+gpm (92-2180+m ³ /day)	If located properly (near or in a fracture) can be highly productive

The future development scenarios and a description of each are given in Table 15. The following sections provide a detailed description of each scenario and the assumptions involved in developing them. A description of the addition of new pumping wells is included, along with the results of each scenario and a discussion of the implications such scenarios may have on future planning in the Upper Roanoke River Watershed.

Table 15. Future development scenarios simulated for the Upper Roanoke River Watershed

Scenario	Description
1 Roanoke County	The additional pumping was added proportionately to the existing wells in the baseline simulation – assumes projected population settles in or near already settled areas, and water demands in these areas increase
2 Roanoke + Montgomery County	Half of the additional pumping was added to existing well in the baseline simulation, and half was added in the west-side of the study area – assumes half of the projected population settles in or near settled areas, and half settles in Montgomery County
3 Roanoke + Tinker Creek	Half of the additional pumping was added to existing wells in the baseline simulation, and half was added to the Tinker Creek subwatershed – assumes half of the projected population settles in or near settled areas, and half settles in Tinker Creek based on County speculation of future areas of heavy development

4.3.2.1 Development Scenario 1

Development scenario 1 was developed to model the impacts of the increased population if most of the new developments occurred generally in the same areas of present development. To represent this phenomenon, the pumping rates of the wells that were included in the baseline simulation were increased proportionately. No new wells were added, but the pumping of the existing wells was increased. The new withdrawal rates are included in Table 16.

In the process of developing this scenario, the importance of taking into account the aquifer pumping capacity was evident. One well, Glenvar East, in the West service area caused the entire model to “go dry”. This was because, in increasing the pumping proportionately, the pumping rate of this well was increased to 2449m³/day, which exceeds the maximum yield of the

Ordovician to Mississippian clastics aquifer (Table 14). Therefore, a new well was added (Glenvar New) and the rate was divided evenly between the two wells. The added well is shown in Figure 57. The new pumping rate for both Glenvar East and Glenvar New was 1224m³/day. Glenvar New was added to the model, approximately 3 cells to the right of the Glenvar East well (1.5 miles), to ensure over-pumping in this one location would not occur.

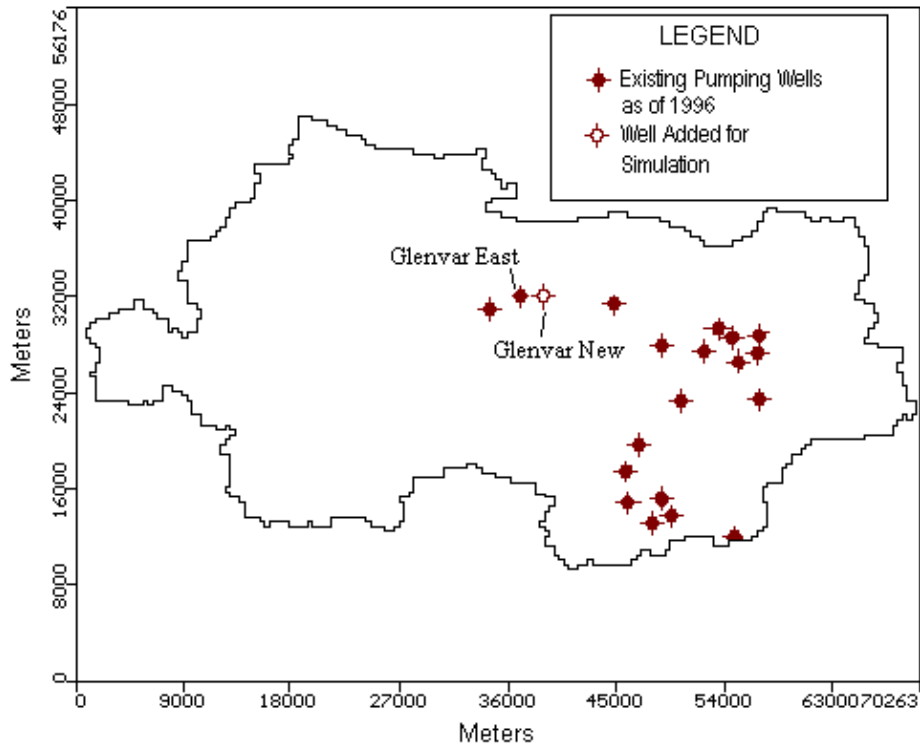


Figure 57. Location of Glenvar East and Glenvar New well – scenario 1

Table 16. Pumping rates for existing wells in Roanoke County pumping more than 10,000gal/day as of 1996 (DEQ, 1999) - future development scenario 1.

Service Area	Name	*X	*Y	Number of wells	Q (m ³ /day)
EAST	Labellevue	56600	23330	5	1039
TOTAL				5	1039
WEST	Wooded Acres	44528	31316	1	816
	Glen Forest	34176	30856	1	816
	Glenvar East	36708	31922	3	2449
	Andrew Lewis Place	50051	23096	1	816
TOTAL				6	4899
NORTH	Tinker Knoll	54342	28478	2	115
	Hollins	56623	28613	1	58
	North Ardmore	56375	27133	2	115
	BelleHaven-Brooklawn	53198	29234	6	346
	Carvins Meadow	54899	26282	1	58
	Burlington Heights	51937	27328	1	58
	North Lakes	48428	27823	5	288
TOTAL				18	1038
SOUTH	Chesterfield Court	47975	12777	1	6
	Arlington Forest	45179	14626	1	6
	Oak Grove	47324	17592	5	32
	Farmingdale	46599	19533	1	6
	Castle Rock	45594	16910	4	25
	Highfield	45007	15471	2	13
	Mount Vernon Forest	44587	14836	1	6
	Scenic Hills	44386	14421	1	6
	Hidden Valley	45418	18853	7	44
	Brookwood	43572	14959	3	19
	Arlington Hills	45095	14499	2	13
	Craighead-Utility	47467	13113	5	32
	Hampden Hills	54444	11786	3	19
	Laymans Lawn	44925	14795	3	19
	Crestwood Park	46610	16237	1	6
	Southern Hills "B"	49240	13584	1	6
	Pine Mountain	47385	12437	2	13
	Green Haven Hills	48389	15060	1	6
	Longridge	45086	17246	2	13
	Starkey	45774	13868	5	32
Belle Meade	46614	15139	1	6	
Homewood	44157	16947	2	13	
TOTAL				54	342
TOTAL PUMPING IN 1996 (North, South, East and West Service Areas)					7316

*Location of each well in the model coordinate system (m)

4.3.2.1.1 Scenario 1 Simulation Results

The results of this simulation were once again difficult to detect from the output hydraulic head contours (Figure 58), compared to the hydraulic head contours from the baseline simulation (Figure 54). However, the stream leakage (or discharge) values were slightly different, and there was an overall reduction in the discharge volume. This reduction was expected since more water was being extracted from the system, which lowered the hydraulic heads. The average discharge flux (m^2/day) is shown in Figure 59 for segment 1-23 (Figure 49), and Table 17 shows the values for each segment. The total stream leakage volume was $2,447,399,680 \text{ m}^3$, which is 0.95% different from the baseline simulation. Since the difference is less than 1%, this simulation illustrates that if the increase in population was to occur in and around existing cities and areas of current development, the impacts would be minimal.

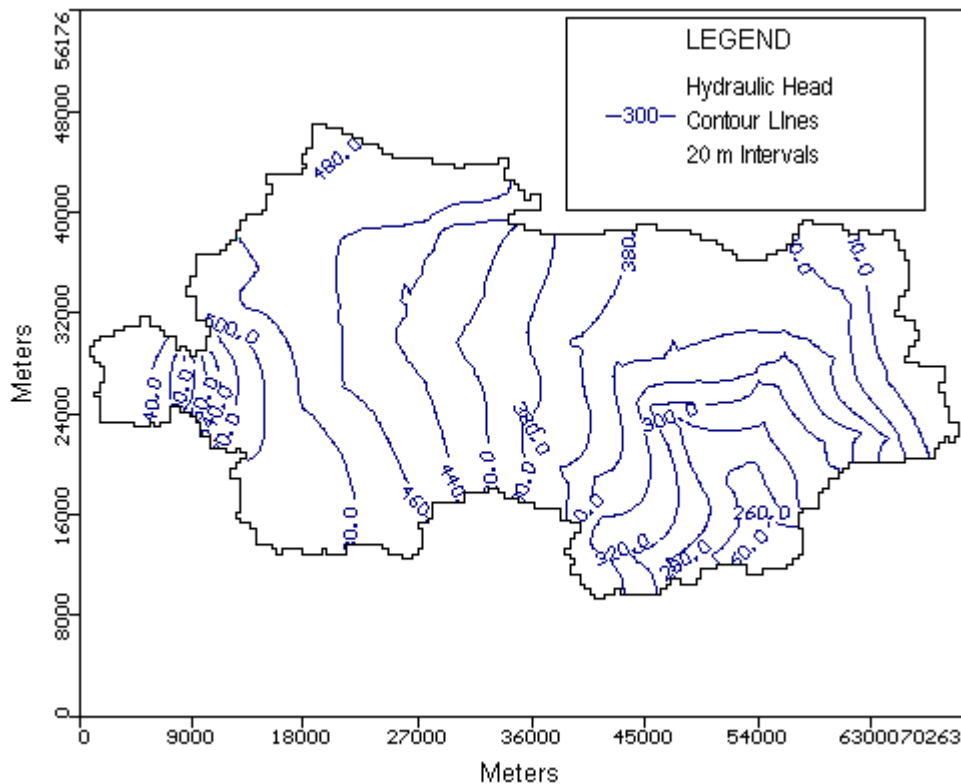


Figure 58. Pumping scenario 1 results, layer 2 hydraulic head contours (20m intervals)

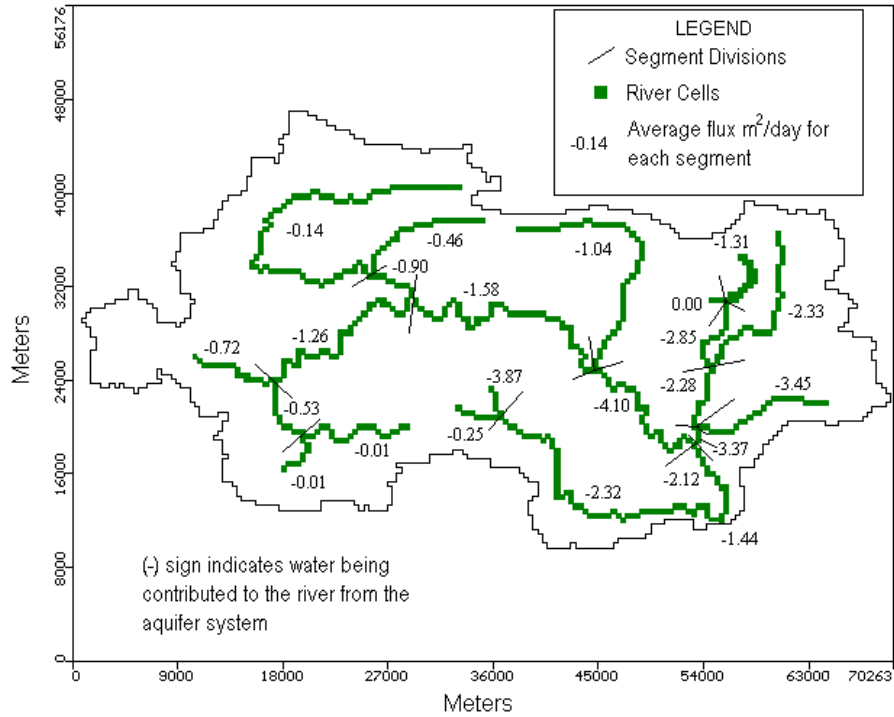


Figure 59. Pumping scenario 1 average flux (m^2/day) for segments 1-23 (defined in Figure 49)

Table 17. Segment total discharge, length, and average flux for pumping scenario 1.

*Segment Number	Total Flow (m^3/day)	Length(m)	Average Flux (m^2/day)
1	-4450	31387	-0.14
2	-4986	10864	-0.46
3	-5200	7243	-0.72
4	-21	3219	-0.01
5	-125	8852	-0.01
6	-2980	5633	-0.53
7	-21785	17303	-1.26
8	-2900	3219	-0.90
9	-35063	22132	-1.58
10	-63374	61164	-1.04
11	-52751	12876	-4.10
12	0	804	0.00
13	-8949	6840	-1.31
14	-18350	6438	-2.85
15	-32855	14084	-2.33
16	-12857	5633	-2.28
17	-794	3219	-0.25
18	-7793	2012	-3.87
19	-58916	25351	-2.32
20	-36090	10462	-3.45
21	-4068	1207	-3.37
22	-14479	6840	-2.12
23	-581	402	-1.44

*See Figure 49 for segment locations

The discharge distribution and results did not change significantly with respect to the baseline simulation. Only segments 4,5, and 12 changed more than 2% (Table 18). Again, segment 12 only contains 3 cells, and a change in discharge in one can drastically effect the total average discharge for the entire segment. The reaches that are further away once again generally had higher % differences compared to the discharges of these segments during the baseline simulation. This illustrates that even though the output from the simulation did not change significantly from the baseline simulation, the upland areas that are farthest away from the outlet, are again, more sensitive to pumping than the areas that are closer to the outlet.

Table 18. Percent difference of discharge values for segments 1-23 between the baseline simulation and pumping scenario 1

*Segment Number	Baseline Simulation Average Flux (m ² /day)	Scenario 1 Average Flux (m ² /day)	% Difference
1	-0.144	-0.142	1.760
2	-0.464	-0.459	1.071
3	-0.721	-0.718	0.478
4	-0.007	-0.007	5.217
5	-0.014	-0.014	2.456
6	-0.532	-0.529	0.521
7	-1.267	-1.259	0.616
8	-0.909	-0.901	0.922
9	-1.603	-1.584	1.189
10	-1.048	-1.036	1.177
11	-4.132	-4.097	0.851
12	-0.250	0.000	100.000
13	-1.338	-1.308	2.218
14	-2.883	-2.850	1.138
15	-2.357	-2.333	1.042
16	-2.351	-2.282	2.922
17	-0.249	-0.247	0.998
18	-3.895	-3.873	0.568
19	-2.330	-2.324	0.279
20	-3.479	-3.449	0.841
21	-3.402	-3.370	0.950
22	-2.128	-2.117	0.523
23	-1.446	-1.444	0.172
Average	-1.607	-1.444	5.561

*See Figure 49 for locations of segments.

The results of this scenario indicate that the areas of existing development within Roanoke County are relatively insensitive to increased pumping. If the projected increase in population settles completely in and around existing development areas, the subsurface system will not become significantly more stressed. The groundwater available in these areas is sufficient to supply the assumed volume of water necessary to serve the proposed population increase without depleting the system of available water. In fact, the increased pumping may not cause detectable changes in the position of the groundwater table or overall stream discharge.

4.3.2.2 Development Scenario 2

The second development scenario was designed to simulate the effects of withdrawal due to the projected population increase from 1996-2010, if half of the population increase was to settle in Montgomery County (west side of the study area) and half near the existing areas of development in Roanoke County. Therefore, from the 0.58mgd (2200m³/day) of pumping added to the rates of the baseline simulation, half of it was pumped from new wells in Montgomery County (1100 m³/day), and half was added to the already-pumping wells in Roanoke County proportionately (1100.395 m³/day). Originally, the entire increase in population was assumed to settle in Montgomery County, and the entire rate of 0.58mgd (2200m³/day) was pumped from the west side of the study area. However, when this was situation simulated, the entire left side of the study area went dry. This indicates that it is not feasible for the entire projected population increase to settle in this half of the study area unless they are supplied with surface water instead of groundwater. Otherwise, there is not enough groundwater available to satisfy the new water demand associated with the population increase. Therefore, the scenario presented here was developed in an attempt to determine a better estimate of how much pumping the west side of the study area can sustain without causing drastic over-pumping, and dry cells. The configuration of the added new wells was determined on a trial and error basis to minimize the amount of dry cells that resulted from the simulation. The new pumping rates for the existing Montgomery County wells are shown in Table 19, to account for half of the new pumping (which correspond to half of the population increase). Figure 60 shows the locations of the wells included in this scenario, and Table 20 summarizes the pumping rates of the added wells.

Table 19. Pumping rates for existing wells in Roanoke County pumping more than 10,000gal/day as of 1996 (DEQ, 1999) - future development scenario 2.

Service Area	Name	*X	*Y	Number of wells	Q (m ³ /day)
EAST	Labellevue	56600	23330	5	882
TOTAL				5	882
WEST	Wooded Acres	44528	31316	1	694
	Glen Forest	34176	30856	1	694
	Glenvar East	36708	31922	3	2081
	Andrew Lewis Place	50051	23096	1	694
TOTAL				6	4161
NORTH	Tinker Knoll	54342	28478	2	98
	Hollins	56623	28613	1	49
	North Ardmore	56375	27133	2	98
	BelleHaven-Brooklawn	53198	29234	6	294
	Carvins Meadow	54899	26282	1	49
	Burlington Heights	51937	27328	1	49
	North Lakes	48428	27823	5	245
	TOTAL				18
SOUTH	Chesterfield Court	47975	12777	1	5
	Arlington Forest	45179	14626	1	5
	Oak Grove	47324	17592	5	27
	Farmingdale	46599	19533	1	5
	Castle Rock	45594	16910	4	22
	Highfield	45007	15471	2	11
	Mount Vernon Forest	44587	14836	1	5
	Scenic Hills	44386	14421	1	5
	Hidden Valley	45418	18853	7	38
	Brookwood	43572	14959	3	16
	Arlington Hills	45095	14499	2	11
	Craighead-Utility	47467	13113	5	27
	Hampden Hills	54444	11786	3	16
	Laymans Lawn	44925	14795	3	16
	Crestwood Park	46610	16237	1	5
	Southern Hills "B"	49240	13584	1	5
	Pine Mountain	47385	12437	2	11
	Green Haven Hills	48389	15060	1	5
	Longridge	45086	17246	2	11
	Starkey	45774	13868	5	27
Belle Meade	46614	15139	1	5	
Homewood	44157	16947	2	11	
TOTAL				54	290
TOTAL PUMPING IN 1996 (North, South, East and West Service Areas)					6216

*Location of each well in the model coordinate system (m)

Table 20. Pumping rates for wells added to baseline simulation for scenario 2

Well	Pumping Rate (m ³ /day)
New 1	300
New 2	300
New 3	50
New 4	100
New 5	200.785
New 6	50
New 7	50
New 8	50
Total	1100.785

Once again, the Glenvar East well exceeded the maximum pumping capacity of the aquifer (Table 14), and the pumping rate (2081 m³/day) was divided into 2 separate wells, and Glenvar New was added (Figure 60). The new pumping rate for both Glenvar New and Glenvar East was 1040 m³/day.

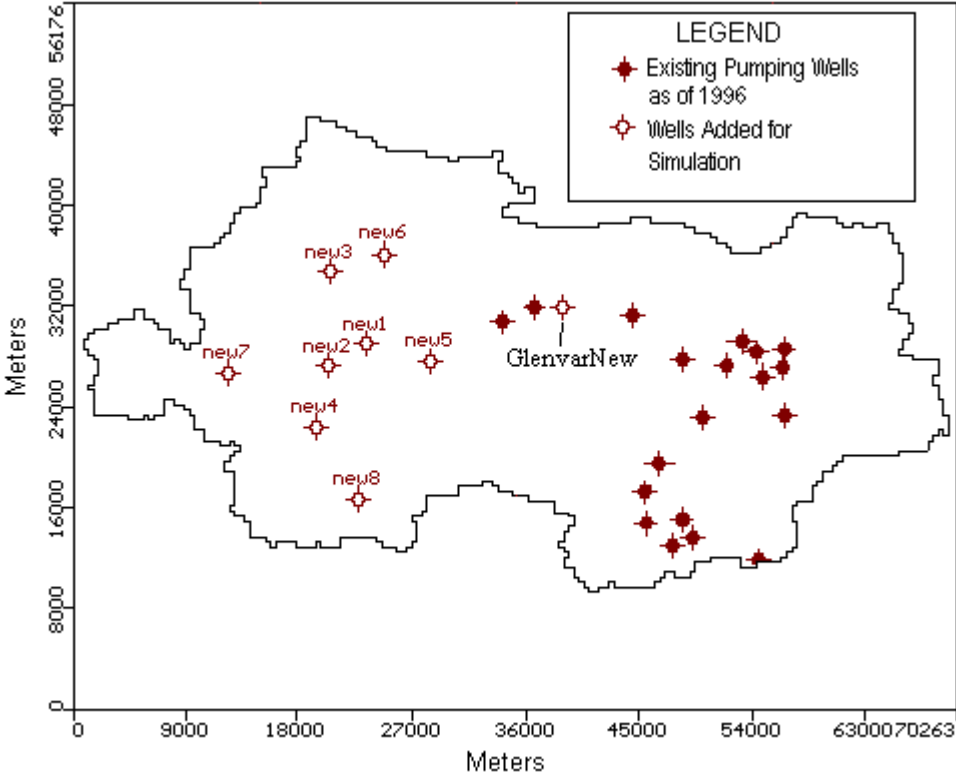


Figure 60. Locations of wells added to baseline simulation for scenario 2

4.3.2.2.1 Scenario 2 Simulation Results

The hydraulic head output contours for layer 2 are shown in Figure 61. The results of this scenario illustrate the sensitivity of the model to pumping in the west-side of the study area. Several different combinations of pumping rates were attempted however, a majority of them produced a large amount of dry cells. The scenario presented here produced dry cells as well, although the amount was minimal. The contours differ greatly from the baseline scenario. The hydraulic heads were reduced drastically, indicating that this area cannot support drastic increases in population that would use groundwater as the primary water source.

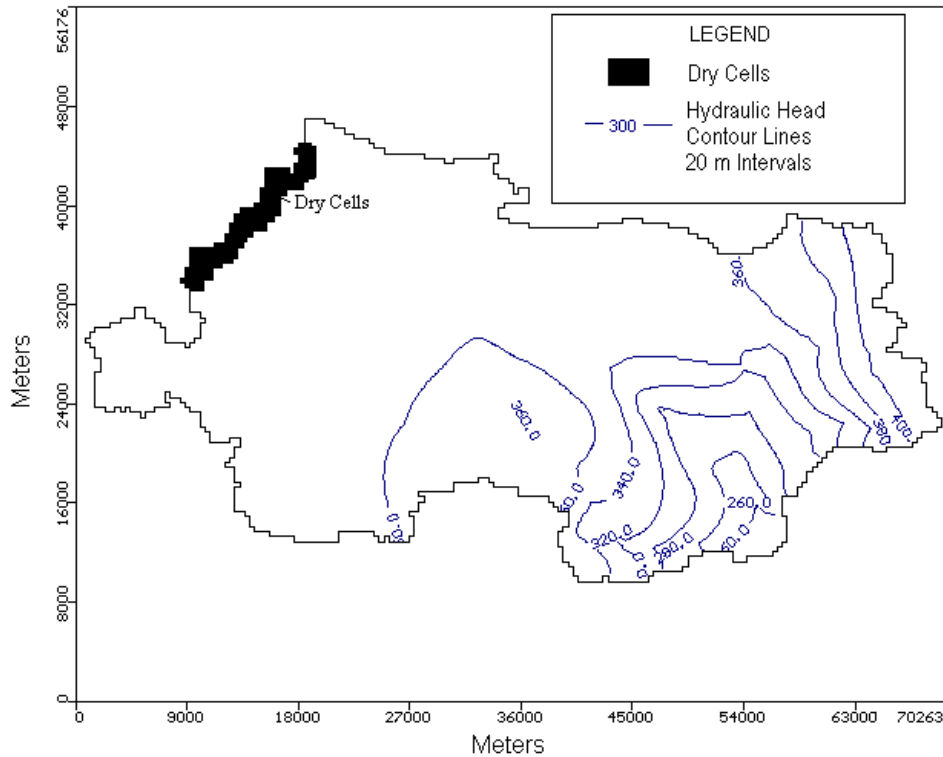


Figure 61. Pumping scenario 1 results, layer 2 hydraulic head contours (20m intervals)

This pumping scenario also drastically affected the discharge distribution. Since the hydraulic heads in the west-side of the study area were reduced, it appears some of the rivers in that area would go dry (Figure 62), and the discharge in those rivers was equal to zero, which indicates that there was no water in the rivers at all. Table 21 contains a list of the discharge values for each segment. The segments of river that went dry are shown in Figure 62, where the

average flux is equal to zero. This happened in the west- side of the study area, where the heads were drastically reduced. These results illustrate that if a large amount of pumping were to take place in the part of Montgomery County, groundwater resources in that area would be depleted drastically.

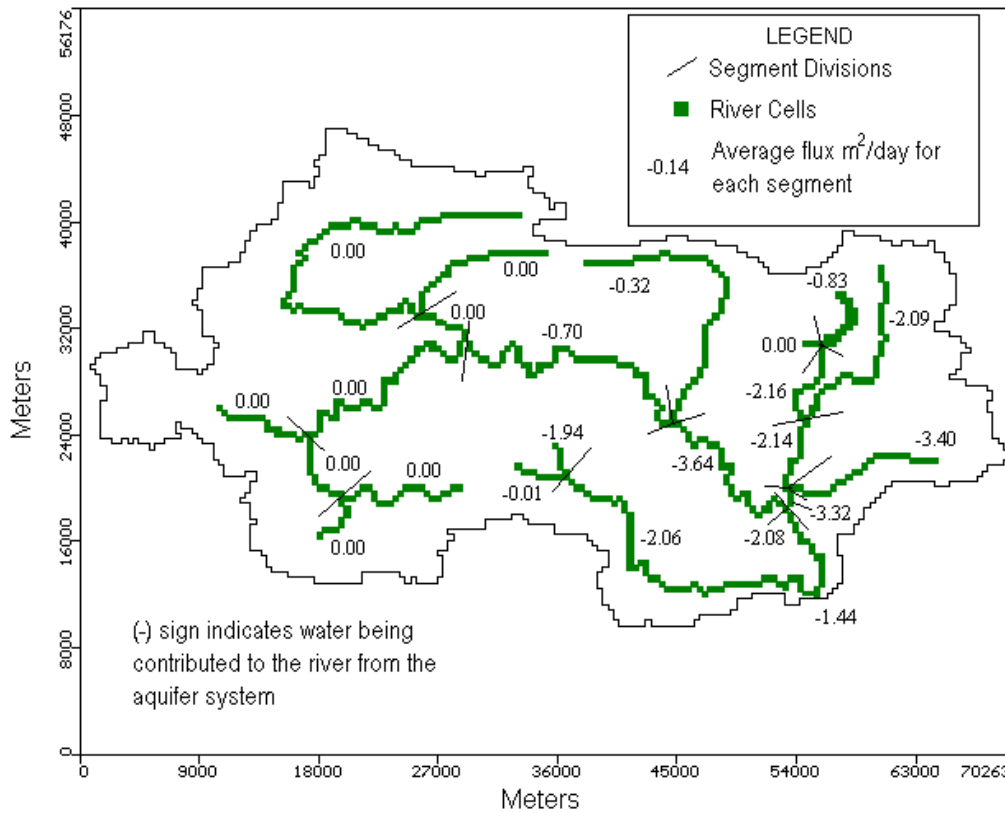


Figure 62. Pumping scenario 2 average flux (m²/day) for segments 1-23 (defined in Figure 49)

Table 21. Segment total discharge, length, and average flux for pumping scenario 2.

*Segment Number	Total Flow (m ³ /day)	Length(m)	Average Flux (m ² /day)
1	0	31387	0.00
2	0	10864	0.00
3	0	7243	0.00
4	0	3219	0.00
5	0	8852	0.00
6	0	5633	0.00
7	0	17303	0.00
8	0	3219	0.00
9	-15600	22132	-0.70
10	-19405	61164	-0.32
11	-46923	12876	-3.64
12	0	804	0.00
13	-5695	6840	-0.83
14	-13915	6438	-2.16
15	-29397	14084	-2.09
16	-12060	5633	-2.14
17	-19	3219	-0.01
18	-3911	2012	-1.94
19	-52190	25351	-2.06
20	-35624	10462	-3.40
21	-4002	1207	-3.32
22	-14231	6840	-2.08
23	-579	402	-1.44

*See Figure 49 for segment locations

Table 22 shows the percent difference in the average flux values for segments 1-23 (Figure 49) between the baseline simulation and scenario 2. These results reflect the results illustrated in Figures 58 and 59. The hydraulic heads in the west side of the study area were the most affected by the additional pumping, therefore, the discharge distributions in these areas are also the most effected (as shown by the high percent differences in Table 22). The segments that went completely dry (indicated by an average flux value of zero in Table 21) have a percent difference of discharge equal to 100% (Table 22). This is because discharge has ceased since the rivers are completed dry. These results are very drastic and illustrate a depletion of groundwater resources in the west side of the study area that is so severe, the surface water system has also been depleted.

Table 22. Percent difference of discharge values for segments 1-23 between the baseline simulation and pumping scenario 2.

*Segment Number	Baseline Simulation Average Flux (m ² /day)	Scenario 2 Average Flux (m ² /day)	% Difference
1	-0.144	0.00	100.00
2	-0.464	0.00	100.00
3	-0.721	0.00	100.00
4	-0.007	0.00	100.00
5	-0.014	0.00	100.00
6	-0.532	0.00	100.00
7	-1.267	0.00	100.00
8	-0.909	0.00	100.00
9	-1.603	-0.70	56.03
10	-1.048	-0.32	69.73
11	-4.132	-3.64	11.81
12	-0.25	0.00	100.00
13	-1.338	-0.83	37.78
14	-2.883	-2.16	25.03
15	-2.357	-2.09	11.44
16	-2.351	-2.14	8.94
17	-0.249	-0.01	97.54
18	-3.895	-1.94	50.09
19	-2.33	-2.06	11.64
20	-3.479	-3.40	2.13
21	-3.402	-3.32	2.55
22	-2.128	-2.08	2.23
23	-1.446	-1.44	0.49
Average	-1.607	-1.136	55.976

*See Figure 49 for segment locations

4.3.2.3 Development Scenario 3

The third development scenario was designed to simulate the effects of withdrawal due to the projected population increase from 1996-2010, if the population was to settle predominately in the Tinker Creek sub-watershed. Although the demographic and economic Profile for Roanoke County does not include specific locations of development, there has been some speculation that new developments will concentrate in this area. Tinker Creek is located in the northeast of the study area (Figure 63). When all of the projected increased population settled in Tinker Creek, and the pumping in the 5 wells added up to $2200\text{m}^3/\text{day}$, a large area of the west side of the study area went dry (Figure 64).

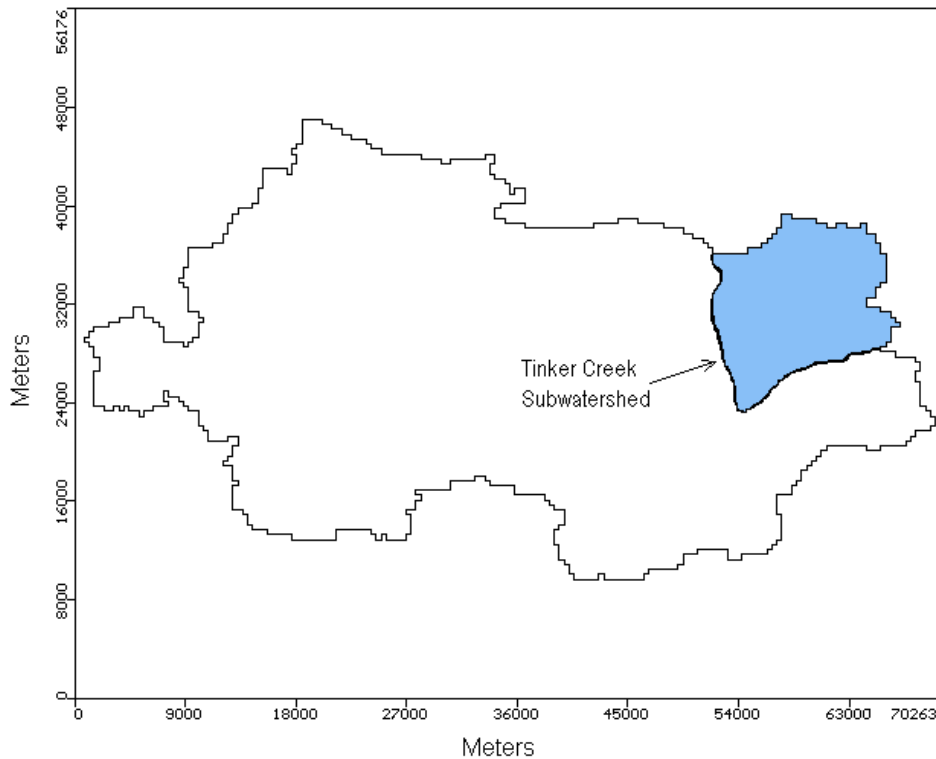


Figure 63. General location of the Tinker Creek subwatershed in the Upper Roanoke River Basin.

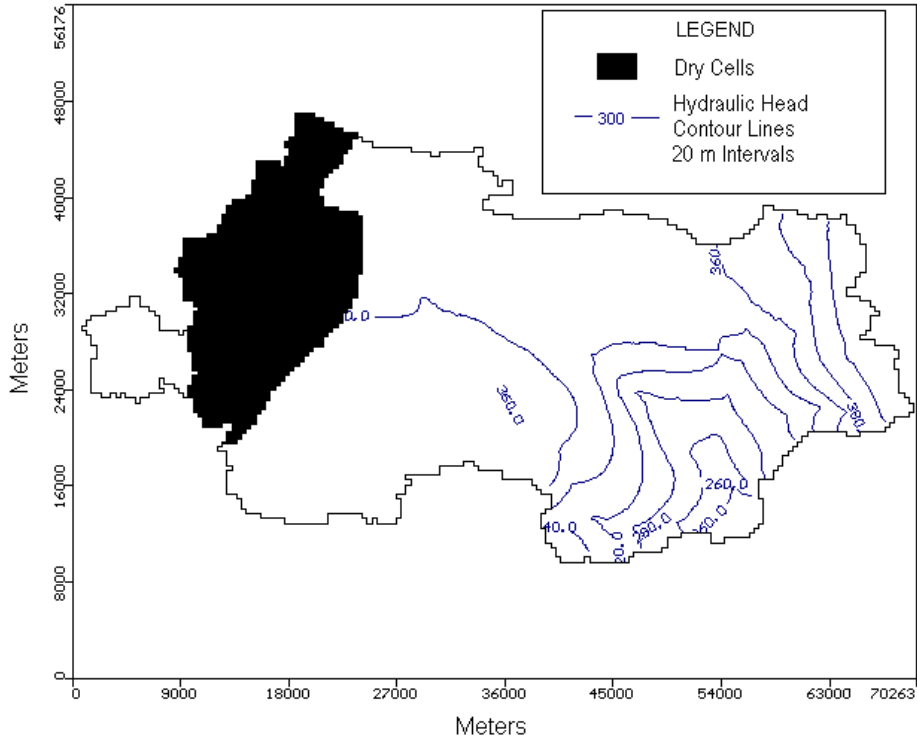


Figure 64. Pumping scenario 3 results, layer 2 hydraulic head contours (20m intervals) when population increase is concentrated completely in Tinker Creek

From these results, it can be assumed that locating the entire population increase in this area is not feasible unless a percentage of the inhabitants are served by municipal water supplies. If groundwater is the only source of water for this additional population, then the Tinker Creek sub-watershed does not have enough available groundwater to adequately supply the volume of water necessary to meet the increased water demand. It also supports the notion that the west side of the study area is more sensitive to pumping than any other area in the watershed, and groundwater resources of this area will be depleted first.

To determine the impacts of concentrating the increased population in Tinker Creek, half of the increased population was assumed to settle in and around the existing developed areas, as in scenario 2, and half was assumed to settle in Tinker Creek. Therefore, from the 0.58mgd (2200m³/day) of pumping that was added to the study area, half of it was pumped from new wells in Tinker Creek (1100m³/day), and half was added to the already-pumping wells in Roanoke County, proportionately (1100m³/day). The pumping rates for the existing wells were the same as the rates in scenario 2, and are listed in Table 20. The Glenvar New well was also added and pumped the same rate as in scenario 2 to avoid over-pumping the aquifer. This well

was previously discussed in scenario 2. The extra pumping was concentrated in Tinker Creek by adding 5 new wells. This number was determined arbitrarily to distribute the pumping to more than one well, and to not exceed the aquifer pumping capacities. A number of different pumping combinations were attempted, and the results were virtually identical to those presented here. The pumping rates of these new wells are presented in Table 23, and the locations of the new wells are shown in Figure 65.

Table 23. New pumping rates for wells added to baseline simulation for scenario 3

Well	Pumping Rate (m ³ /day)
New 1	250
New 2	250
New 3	100.785
New 4	250
New 5	250
Total	1100.785

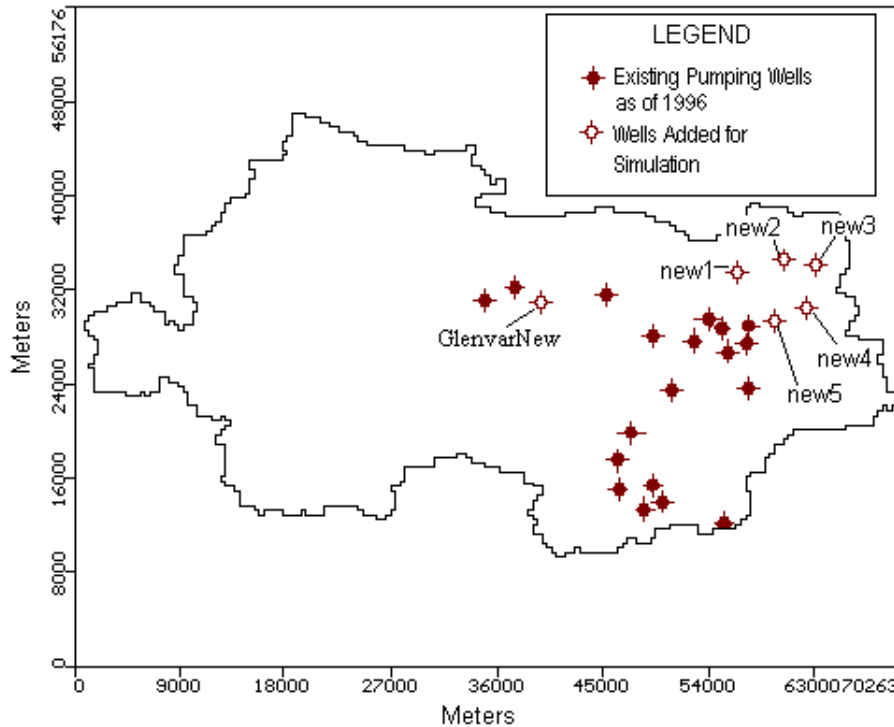


Figure 65. Locations of wells added to baseline simulation for scenario 3

4.3.2.3.1 Scenario 3 Simulation Results

The resulting hydraulic head contours from this simulation, again, do not differ much from the baseline simulation (Figure 66). However, the discharge values are slightly different. The total discharge (stream leakage) for this simulation was 2,450,760,960 m³, a difference from the baseline simulation of 0.82%. Again, since the difference in stream leakage volumes (discharge) is less than 1%, and the assumption can be made that this pumping scenario produces minimal impacts on the sub-surface flow system. The discharge distribution is shown in Figure 67. Table 24 shows the average discharge flux for each segment (Figure 49).

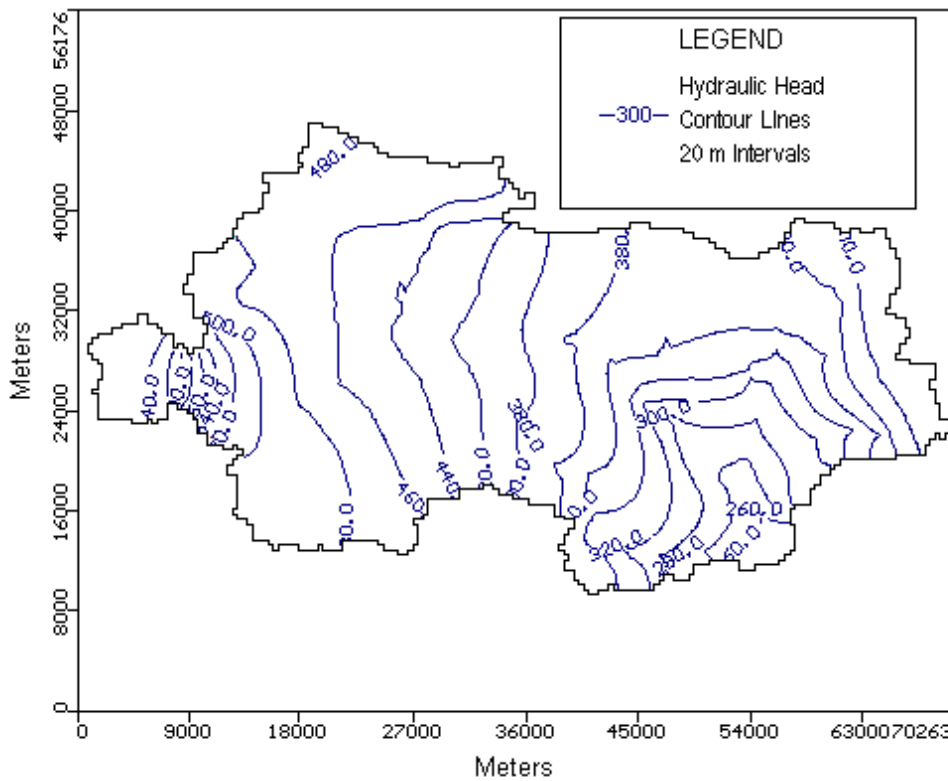


Figure 66. Pumping scenario 3 results, layer 2 hydraulic head contours (20m intervals)

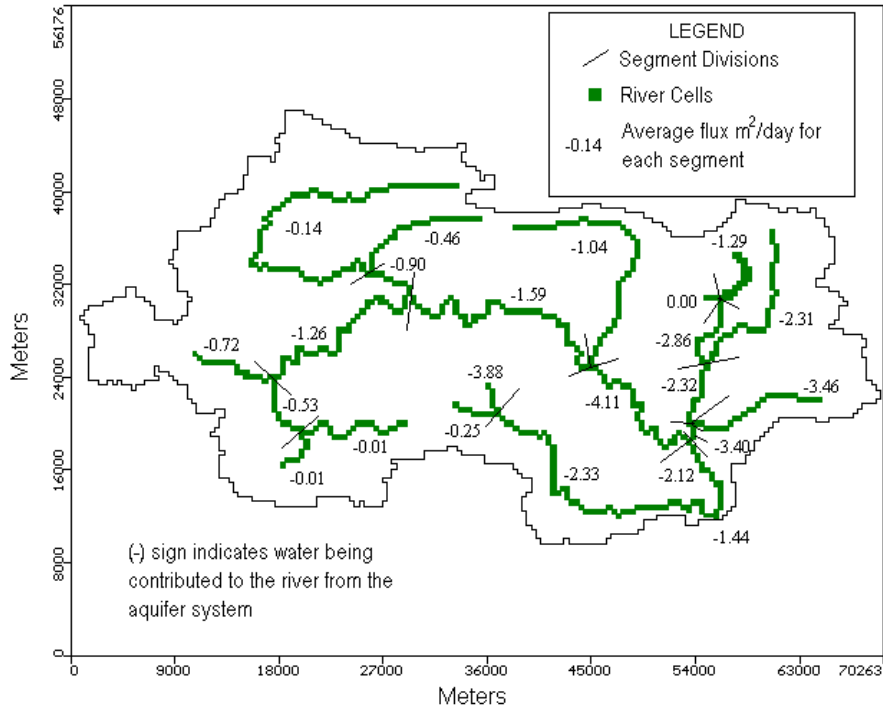


Figure 67. Pumping scenario 3 average flux (m^2/day) for segments 1-23 (defined in Figure 49)

Table 24. Segment total discharge, length, and average flux for pumping scenario 3

*Segment Number	Total Flow (m^3/day)	Length(m)	Average Flux (m^2/day)
1	-4487	31387	-0.14
2	-5008	10864	-0.46
3	-5209	7243	-0.72
4	-22	3219	-0.01
5	-126	8852	-0.01
6	-2988	5633	-0.53
7	-21838	17303	-1.26
8	-2911	3219	-0.90
9	-35155	22132	-1.59
10	-63564	61164	-1.04
11	-52911	12876	-4.11
12	0	804	0.00
13	-8824	6840	-1.29
14	-18387	6438	-2.86
15	-32527	14084	-2.31
16	-13052	5633	-2.32
17	-796	3219	-0.25
18	-7801	2012	-3.88
19	-58956	25351	-2.33
20	-36190	10462	-3.46
21	-4101	1207	-3.40
22	-14522	6840	-2.12
23	-581	402	-1.44

*See Figure 49 for segment locations

When all of the increase population was added to the Tinker Creek subwatershed however, the model cells on the west side of the study area went dry, meaning the groundwater resources of these areas were depleted (Figure 64). This implies that there is a maximum amount of groundwater that this area of the watershed can supply without depleting groundwater resources on the west side of the watershed. This maximum amount of additional pumping from Tinker Creek is between the pumping rate occurring in this scenario, 1100m³/day, and the total amount of additional pumping required to serve the projected additional population, 2200m³/day. Therefore, although the results of this simulation show that the Tinker Creek area can sufficiently supply the additional pumping of 1100m³/day without a significant impact on the rest of the watershed, there is a limit to the volume of groundwater this area can supply before causing drastic impacts.

Table 25. Percent difference of discharge values for segments 1-23 between the baseline simulation and pumping scenario 3.

*Segment Number	Baseline Simulation Average Flux (m ² /day)	Scenario 3 Average Flux (m ² /day)	% Difference
1	-0.144	-0.143	0.72
2	-0.464	-0.461	0.66
3	-0.721	-0.719	0.26
4	-0.007	-0.007	0.60
5	-0.014	-0.014	0.00
6	-0.532	-0.531	0.27
7	-1.267	-1.262	0.39
8	-0.909	-0.904	0.52
9	-1.603	-1.588	0.91
10	-1.048	-1.039	0.84
11	-4.132	-4.109	0.56
12	-0.250	0.000	100.00
13	-1.338	-1.290	3.59
14	-2.883	-2.856	0.94
15	-2.357	-2.310	2.02
16	-2.351	-2.317	1.45
17	-0.249	-0.247	0.70
18	-3.895	-3.877	0.45
19	-2.330	-2.326	0.19
20	-3.479	-3.459	0.57
21	-3.402	-3.397	0.14
22	-2.128	-2.123	0.24
23	-1.446	-1.444	0.15
Average	-1.607	-1.584	5.050

*See Figure 49 for segment locations

The percent differences in the discharge output for segments 1-23 between the baseline simulation and scenario 3 are listed in Table 25. The simulated discharge fluxes were not affected significantly from the baseline scenario. There are only three segments, 15, 13, and 12 in which the percent difference of discharge flux between the baseline simulation and scenario 3 was greater than 1. These results support the idea that this pumping scenario did not significantly affect the subsurface system. All three of these segments are located near the Tinker Creek area, indicating that the head values in this area, the area where the additional pumping was located, were reduced more than the heads in other regions of the study area. This implies that there is some local effects of concentrated pumping in this area, however, when large amounts of pumping occurs (as when all of the population was concentrated in Tinker Creek, Figure 64), the regional effects are visible in the west side of the study area first. This supports the result that this part of the study area is most sensitive to regional pumping within the watershed.

4.4 Zone Budget Analysis

All three of the development scenarios illustrated that the west side of the study area was the most sensitive to large withdrawals that could occur in the basin. Although some minor local changes in discharge values occurred, it seems if large withdrawals were going to impact the regional system, the response would first occur in the western part of the study area, farthest from the outlet. The upper left corner of the basin, where the highest land surface elevations occur, and therefore where the largest gradients exist, is also the first area of the watershed where dry cells appear. Dry cells indicate that the groundwater resources have been depleted, and the cells no longer contain any available water. The cells in the northwest of the study area, where the dry cells occur, are only fed by recharge from precipitation and are not receiving horizontal flow from anywhere else in the system. The lower-lying areas that are located down gradient and close to the outlet (southeast) are fed not only by recharge from precipitation, but also by horizontal flow from other areas in the watershed. To determine the sensitivity of the hydraulic heads in the southeast to the horizontal flow from the northwest, a zone budget analysis was performed.

To determine how much horizontal flow the west side of the study area contributes to the east side of the study area, a zone budget analysis was performed on the baseline simulation. An

identical analysis was performed on pumping scenario 2 since it produced the most extreme system response. Defining a “zone” within MODFLOW allows the user to monitor the flow budget of a group of cells within the model domain. A horizontal zone, four layers deep, was defined along the center of the basin as shown in Figure 68. In defining this area as a “zone”, the fluxes into and out of this area are calculated during the MODFLOW simulation, determining a cumulative flow budget for that group of cells. Since the zone was included in all four of the layers, it created a horizontal zone barrier in the middle of the study area. All of the horizontal flow occurring through this vertical barrier was calculated during the zone budget analysis to determine the volume of water that flowed horizontally from the west side of the study area to the east. Comparison of the output of the zone budget analysis from the baseline simulation and pumping scenario 2 will determine if the horizontal flow contribution affects the hydraulic head results.

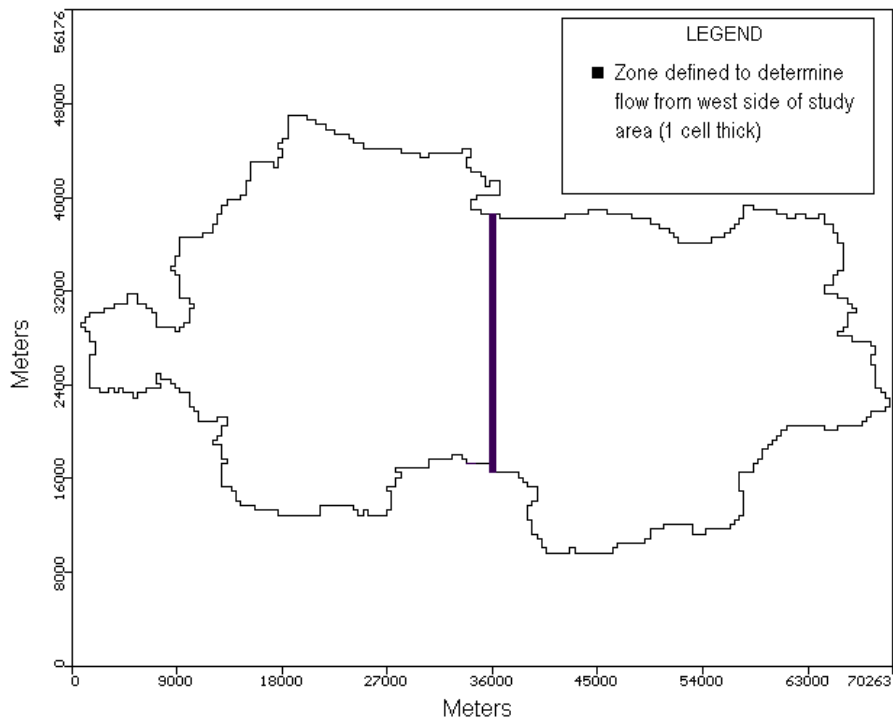


Figure 68. Zone defined to determine horizontal flow contribution from the west side of the study area

The output from the zone budget analysis determined that the east side of the study area is relatively insensitive to the horizontal flow from the west side of the basin. During the baseline simulation, the west side of the study area contributed 35,832 m³/day to the east side of the study area for all three of the stress periods. During the second pumping scenario simulation, the west side of the study area initially contributed 35,578 m³/day during the first stress period (the first year of the simulation). However, this value was reduced to 8,135 m³/day by the third stress period due to the drastic reduction in head values in the west side of the basin (Figure 61). These head values reduced the gradient that drives flow to the outlet, and thus reduced the horizontal flow during the simulation. The hydraulic head contours in the east side of the basin were not drastically different (Figure 61) from those in the baseline simulation (Figure 54). This result implies that the east side of the study area is not very sensitive to the pumping occurring on the west side of the study area, nor to the horizontal flow that the west side of the area is contributing to the east side.

The zone budget analysis illustrated that when the horizontal flow contribution to the east side of the watershed was reduced, the hydraulic heads in the east side of the study area were not affected. Therefore, the groundwater resources in the Roanoke Valley (east side of the basin) would not be significantly affected when the increased pumping rates associated with the projected population increase are located anywhere in the watershed. However, the analysis indicates that the west side of the study area was very sensitive to pumping, and if increased withdrawals affect the regional flow system of the Upper Roanoke River Watershed, these upland areas would be the first depleted. This depletion occurs because the upland areas in the watershed receive recharge from precipitation only, and do not receive horizontal flow from any other areas in the study area. Also, since the highest land elevations occur in these areas, the hydraulic gradient to the outlet is greater, causing more horizontal flow from these areas than other areas in the watershed.

4.5 Summary of the Results and Discussion

The groundwater model developed for this investigation was applied to the Upper Roanoke River Watershed understand the flow system and its potential response to future urban development. Information from the Virginia Department of Environmental Quality about current pumping conditions within the watershed was collected. These pumping wells were simulated

with the Well Package of MODFLOW to determine current conditions (baseline simulation). Three future development scenarios were developed from population projections for the year 2010 to represent different possible settlement patterns. The results of the three future scenarios were compared to the results of the baseline simulation to determine the long-term impacts of increased pumping on the subsurface flow system.

The Virginia DEQ supplied information about the pumping rates and locations of wells pumping water from the system in excess of 10,000gpd. The most current year of data supplied was 1996. These data were used to develop a MODFLOW input file for the Well Package to simulate current pumping conditions. This simulation (the baseline simulation) was run for a period of 20 years to determine the long-term impacts of current pumping. The results from this simulation were reported, and were used as a reference to assess the impacts of increased pumping simulated on the future scenarios.

Three future pumping scenarios were developed from population projections for the year 2010. The following future scenarios were simulated:

- 1) The additional pumping was added proportionately to the existing wells in the baseline simulation – assumes projected population settles in or near already settled areas, and water demands in these areas increase
- 2) Half of the additional pumping was added to existing well in the baseline simulation, and the other half was added in the west-side of the study area – assumes half of the projected population settles in or near settled areas, and half settles in Montgomery County
- 3) Half of the additional pumping was added to existing wells in the baseline simulation, and the other half was added to the Tinker Creek subwatershed – assumes half of the projected population settles in or near settled areas, and half settles in Tinker Creek based on County speculation of future areas of heavy development

Each scenario was simulated for a period of 20 years to determine the long-term impacts of the pumping increase. The results of each scenario were compared to the results of the baseline simulation. Table 26 presents a summary of the total discharge volume for each development scenario and the percent difference from the baseline simulation.

Table 26. Percent Difference of Stream Leakage with Respect to Baseline Simulation

Simulation	Total Stream Leakage (m ³)	Percent Difference
Baseline	2,470,979,072	
Scenario 1	2,447,399,680	0.95
Scenario 2	1,768,409,728	28.43
Scenario 3	2,450,760,960	0.82

The results from the future development scenarios demonstrated that the west side of the study area is more sensitive to pumping in the basin than any other area. If pumping were to affect the regional system, it would affect the groundwater resources in the northwest areas of the study area first. Therefore, although local variations in the flow system may occur, the regional response will first occur in these upland areas.

A zone budget analysis was performed to determine whether or not the hydraulic head values in the east side of the study area closest to the outlet were sensitive to the horizontal flow contribution from the west side of the study area. The results from this analysis illustrate that the hydraulic head values near the outlet are not sensitive to the horizontal flow contribution from the west side of the study area. Therefore, even if the groundwater resources in the west side of the study area are depleted, and the horizontal flow contribution from the west to the east is drastically reduced, the groundwater resources in the east will not be affected. However, the groundwater resources in the west are the most sensitive to pumping and will be the first to be depleted in the region.

The results of the simulations demonstrate how a groundwater model could potentially be helpful in evaluating the impacts of settlement patterns on the subsurface flow system. Learning about the flow system, and modeling its response could avoid adverse effects on the groundwater system, and could help maintain the system as a reliable source of water for years to come.

Chapter 5

Summary and Conclusions

A groundwater flow model of the Upper Roanoke River Watershed was developed using MODFLOW to determine the impacts of land use activities on the subsurface flow system. The model was developed from information found in previous geologic investigations that were performed in the study area. The conceptual model was based primarily on information found in Waller (1976), who compiled the previous investigations conducted in the study area. The model cells had dimensions of 402.4m (0.25mi) by 402.4m (0.25mi). The model consisted of four layers. The top layer represented the unconsolidated deposits that act as a recharge reservoir to the fractured bedrock aquifer system. The bottom three layers represent the fractured bedrock aquifer system. Layer 2 simulates the shallow flow in the system, and all of the pumping wells are located in this layer. The bottom two layers simulate deep regional flow and possible deep vertical flow. Three hydrogeologic units were represented in the model, as defined by Waller (1976). The hydraulic properties were assigned in a sloping pattern to represent the sloped geologic formations. No subsurface flow or hydraulic property data exist for the Upper Roanoke River Watershed and therefore, hydrologic properties were assigned using average values found in the literature.

The model was applied under the following assumptions:

- 1) Flow through the fractures is approximately equivalent to flow through a porous medium,
- 2) Darcy's Law is applicable from a regional perspective,
- 3) Hydraulic properties are homogeneous and isotropic for an area that is represented by a model cell,
- 4) Groundwater flow divides correspond to surface-water or topographic divides,
- 5) Evapotranspiration is not explicitly simulated and the recharge input values already reflect evapotranspiration losses, and
- 6) Faults and geologic formations in the system that may influence flow are not explicitly simulated due to a lack of data determining their influence, and the calibrated hydraulic properties account for the influence of these possible formations.

MODFLOW is a finite-difference, three-dimensional groundwater flow model developed by the United States Geological Survey. It is extensively used and verified in numerous groundwater flow studies for many different purposes. A three-dimensional grid was developed

to represent the flow system of the Upper Roanoke River Watershed. No-flow boundaries were assumed around the whole perimeter of the study area, due to the lack of available flow data. The model was calibrated using UCODE, a universal code for inverse modeling. The model was calibrated to observed hydraulic head information from 1969-1970. A total of 18 parameters were estimated using UCODE, including hydraulic conductivities, river bottom conductance values, and recharge rates.

Current pumping well data were obtained from the Virginia Department of Environmental Quality (DEQ, 1999) and these data were used to create an input for the Well Package in MODFLOW. The model was then run for 20 years to determine the long-term effects that pumping at these current rates may have on the flow system. This simulation (“baseline simulation”) served as a basis for comparison for future development scenarios.

Three future scenarios were developed based on the projected population of Roanoke County for the year 2010. Pumping was increased from the present conditions to represent the additional pumping necessary for the increased population. The three future scenarios represent distinctly different pumping patterns in the study area to determine the possible impacts of future development in various locations. Development scenario 1 simulated the impacts of the increased population if the population increase settled generally in areas of existing development. Development scenario 2 simulated the impacts of the increased population if half settled in areas of present development and the other half in the western half of the watershed. Development scenario 3 simulated the impacts if half of the population increase settled in areas of present development and the other half settled in the Tinker Creek sub-watershed.

Each of the three future scenarios were simulated for a period of 20 years as well to determine long term effects from the increased pumping associated with the increase in population. The results of the scenarios were compared to the results of the simulation that represents current pumping conditions, and general conclusions were made about the regional flow system.

Conclusions

The following conclusions could be drawn from this study:

- 1) The calibrated recharge values indicate that approximately 28% of the total precipitation recharges the aquifer system, which is consistent with previous estimates performed in the general location of the study area.
- 2) The Cambrian and Ordovician carbonates geohydrologic unit was found to generally have the highest hydraulic conductivity in each layer which reflects the notion that due to dissolution, this geohydrologic unit contains more fractures or perhaps greater fracture apertures than the other two units. The hydraulic conductivity of the Cambrian and Ordovician carbonates ranged from 0.893m/d in layer 2 to 0.00112m/d in layer 4.
- 3) The streambed conductance values reflected both the variation in streambed thickness, which ranges from nonexistent in some areas to several feet thick in others, and streambed material which ranges from sandy material with relatively high conductivity values to silty material with lower hydraulic conductivity values. The streambed conductance values range from 4.79 m²/d in the upland reaches to 234.13 m²/d in reaches closer to the outlet.
- 4) The most sensitive areas in the basin to increased water withdrawal are the upland areas where the land surface elevations are the highest. These areas occur in the northwest region of the study area where there is no horizontal flow contribution from other places in the watershed. Therefore, if increased withdrawals are so great as to impact the regional system, the west- side of the study area will be affected before all other areas in the watershed.
- 5) If the increase in population that is projected for 2010 in Roanoke County settles generally in areas of existing development, the groundwater flow system of the study area would not be significantly impacted. The volume of water discharged from the streams would be reduced by 0.95% from the baseline scenario, and the hydraulic head values in the study area would not change significantly.

- 6) If 50% of the increased population projected for 2010 settled in areas of existing development, and the other 50% settled in the western half of the study area, the groundwater system would be significantly impacted. The volume of water discharged from the streams would be reduced by approximately 28.4% from the baseline scenario and the hydraulic head values in the western half of the study area would be significantly reduced.
- 7) If 50% of the increase in population that is projected for 2010 settled in areas of existing development, and the other 50% settled in the Tinker Creek sub-watershed, the groundwater system would not be significantly impacted. The volume of water discharged from the streams would be reduced by 0.82% from the baseline scenario and the hydraulic head values in the study area would not change significantly.
- 8) Flow in the system is predominantly horizontal. There is no deep vertical flow from possible deep fractures. There may be shallow vertical flow occurring that is driven by recharge, however this flow is not being simulated in the model due to its resolution. This may be a result of the assumption that hydraulic conductivity of the model cells were isotropic and therefore the horizontal hydraulic conductivity was assumed to be equal to the vertical hydraulic conductivity. This may not be a valid assumption within all natural systems.
- 9) In general, the simulation of horizontal flow follows the overall trend of the hydraulic gradient from west to east, which also follows the overall topographic trend. Therefore, upland regions in the province are recharging down-gradient areas.
- 10) Simulations indicate that the hydraulic head values in the eastern part of the study area closest to the outlet are relatively insensitive to horizontal recharge contribution from the upland areas in the west.

The groundwater flow model developed for this investigation is a conceptualization of the study area for only 1969-1970. If the model were to be used for management and planning purposes, it would first need to be validated with current data, and perhaps re-calibrated. Sub-surface data from the study area is necessary to implement a ground water flow model of this

scale. The model presented in this study is a conceptual model of the system because average values of hydraulic properties were assigned, and no subsurface flow data existed. If the model could be applied with more confidence, it would serve as an efficient management tool to planning and accounting for impacts of land-use change on the subsurface flow system.

Chapter 6

Recommendations for Future Studies

The groundwater flow model used in this study simulates subsurface flow of the Upper Roanoke River Watershed. Although this model offers a conceptualization of regional flow within the system, if it were to be used as a management tool to support decisions with regard to future land-use change, the model would have to be further validated with field data. Since data were not available, the assumption was made that the calibrated input parameters accurately represented the system. More subsurface flow data need to be collected in order to validate the model presented in this investigation. This validation would greatly improve the model's predictive capability and would minimize uncertainty in the model results.

The groundwater flow model was greatly simplified since geologic formations such as the fault system in the study area were not explicitly simulated, and the simulation of evapotranspiration was not included. Data need to be collected as to how the geologic formations affect groundwater flow in the system. These geologic formations could then be explicitly modeled perhaps changing the model to more accurately represent the natural system. Measured evapotranspiration data may also need to be collected in order to include them in the simulation.

The development of this groundwater flow model was part of a larger investigation which included other subgroups. An effort to integrate all of the models developed in this larger investigation needs to be continued. The surface water subgroup is modeling the surface hydrology with HSPF. A system of computer programs has been written to transform the HSPF output into recharge input to the groundwater model developed for this investigation. The interaction between the two models is included in Appendix E. Work to transform the MODFLOW output from this investigation to a form that is helpful to decision makers and to other subgroups participating in the larger investigation must be undertaken.

The interaction between the surface water system and the groundwater system is not simulated with sufficient detail to determine local changes in the flow system. The model resolution is that of a regional model. The resolution would have to be smaller in order to simulate this interaction accurately. Therefore, the implementation of the Telescoping Mesh Program needs to be completed. The Telescoping Mesh Program is a new MODFLOW package

that can define local groundwater models within the framework of a regional flow model. This allows the boundaries of the local model to be dictated by the regional model, and the local model can simulate the surface water-groundwater interaction at a smaller resolution. This implementation is key to accurately determining impacts of land use change on the interaction of the surface water system and the groundwater system.

Chapter 7

References

Anderson, M.P., and W. W. Woessner. 1992. *Applied Groundwater Modeling: Simulation of Flow and Advective Transport*. Academic Press, Inc., San Diego, CA.

Barnes, D. F. 1994. *Urban Energy Transitions, Poverty, and the Environment: Understanding the Role of the Urban Household Energy in Developing Countries*. The World Bank Washington D.C.

Breeding, N.K. and J.W. Dawson. Roanoke County Groundwater. Virginia State Water Control Board, Bureau of Water Control Management, Richmond, Virginia, Planning Bulletin 301, July, 1976.

Burbey, T.J. and D.E. Prudic. 1991. *Regional Aquifer-System Analysis—Great Basin, Nevada-Utah*. USGS Professional Paper 1409-D.

Cairns, J. Jr., 1995. Urban Runoff in Integrated Landscape Context, In *Stormwater Runoff and Receiving Systems Impact, Monitoring, and Assessment*, Ed. E.S. Herricks, CRC Press, Inc., Carnegie Commission of Science, Technology, and Government, Environmental Research and Development, Strengthening the Federal Infrastructure, Task Force on Organization of Federal Government R & D program, New York, 1992.

Canter, L.W., R.C. Knox, and D.M. Fairchild. 1988. *Groundwater Protection*. Lewis Publishers, Inc. Chelsea, Michigan. pp. 49-66.

Chen, Ping-fan. 1960. *Geology and Mineral Resources of the Goose Creek Area Near Roanoke, Virginia*: unpublished Ph.D. dissertation, VPI&SU, Blacksburg, Va.

Collins, R. E. 1961. *Flow of Fluids Through Porous Materials*. Reinhold Publishing Corp.: New York.

Department of Environmental Quality (Virginia). 1999. Personal Communication.

Dewberry & Davis. 1997. *Roanoke Valley Regional Stormwater Management Plan*.

Faiz, A. and S. Gautam. 1994. *Motorization, Urbanization, and Air Pollution*. The World Bank: Washington, D.C.

Fauss, L.M. 1986. *Linking the Effects of Land Use Change with Water Quality and Discharge: An Integrated Approach*. M.S. Thesis in Environmental Science and Engineering.

Faye, R.E. and G.C. Mayer. 1990. *Ground-water flow and stream-aquifer relations in the northern coastal plain of Georgia and adjacent parts of Alabama and South Carolina*: USGS Water-Resources Investigations Report 88-4143.

- Forsythe, G.E. and Strauss, E.G., 1995. On best conditioned matrices: American Mathematical Society proceedings, v. 10, no.3, p. 340-345.
- Freeze, R.A. and J.A. Cherry. 1979. Groundwater. Prentice-Hall, Engelwood Cliffs, New Jersey.
- Fish and Wildlife Information Exchange (FWIE). Personal Communication, 1999.
- Gburek, W.J., G.J. Folmar, and J.B. Urban. 1999. *Field Data and Ground Water Modeling in a Layered Fractured Aquifer*. Ground Water, v. 37, No. 2, pp. 161-320.
- Glenn, S.L., Armstrong, C.F. Kennedy, Craig, Doughty, Paula, and Lee, C.G. 1989. Effects of open pit mining dewatering on ground- and surface-water supplies, Ridgeway, South Carolina, in Daniel, C.C., III., White, R.K., and Stone, P.A., eds., Proceedings of a Conference on Ground Water in the Piedmont of the Eastern United States, Charlotte, N.C., October 16-18, 1989: Clemson, S.C., Clemson University.
- Gordon, A.D. 1993. *Hydrogeology of, and Simulated Ground-Water Flow In, the Valley-Fill Aquifers of the Upper Rockaway River Basin, Morris County, New Jersey*. USGS Water-Resources Investigations Report 93-4145.
- Gugler, J. 1988. Overurbanization Reconsidered in the Urbanization of the Third World. Oxford University Press: Oxford, United Kingdom.
- Guiguer, N. and T. Franz. 1998. Visual Modflow User's Manual. Waterloo Hydrogeologic: Waterloo, Ontario, Canada.
- Harrington, T., J. Hartley, and G. Mitchell. 1996. Roanoke County Demographic and Economic Profile. Roanoke County Planning Department.
- Hanson, R.T. and J.F. Benedict. 1993. *Simulation of Ground-Water Flow and Potential Land Subsidence, Upper Santa Cruz Basin, Arizona*. USGS Water-Resources Investigations Report 93-4196.
- Hardoy, J.E., D. Milton and D. Satterthwaite. 1992. Environmental Problems In Third World Cities. Earthscan: London.
- Hernance, J.F. 1999. A Mathematical Primer on Groundwater Flow-An Introduction to the Mathematical and Physical Concepts of Saturated Flow in the Subsurface. Upper Saddle River, N.J.: Prentice Hall.
- Hill, M.C. 1998. *Methods and Guidelines for Effective Model Calibration*. USGS Water-Resources Investigations Report 98-4005.

- Hill, M.C. 1992. *A Computer Program (MODFLOW-P) for Estimating Parameters of a Transient, Three-Dimensional, Ground-Water Flow Model Using Nonlinear Regression*. USGS Open-File Reports 91-484.
- Latta, B.G. 1956. Public and Industrial Ground-Water Supplies of the Roanoke-Salem District, Virginia: Va. Geol. Surv. Bull. 69.
- Lazaro, T.R., 1990. *Urban Hydrology-A Multi-Disciplinary Perspective*, Technomic Publishing Co., Inc., PA.
- Lee, C.H. 1942. Transpiration and total precipitation: in Meiner, O.E., 1942, *Hydrology*: Dover Publ., New York.
- LeGrand, H.E. 1954. *Geology and Groundwater in the Statesville Area, North Carolina*. N.C. Division of Mineral Resources Bull. 68.
- Lima, V. and J.C. Olimpio. 1989. *Hydrogeology and Simulation of Ground-Water Flow at Superfund-Site Wells G and H, Woburn, Massachusetts*. USGS Water Resources Investigations Report 89-4059.
- Lum, W.E., Smoot, J.L. and D.R. Ralston. 1990. *Geohydrology and Numerical Model Analysis of Ground-Water Flow in the Pullman-Moscow Area, Washington and Idaho*. USGS Water-Resources Investigations Report 89-4103.
- Maclay, R.W., and L.F. Land. 1988. *Simulation of Flow in the Edwards Aquifer, San Antonio Region, Texas*. USGS Water Supply Paper 2336-A, pp. A1-A48).
- Marquardt, D.W. 1963. An algorithm for least-squares estimation of nonlinear parameters: *Journal for the Society of Industrial and Applied Mathematics*, v. 11, no. 2, p. 431-441.
- Maurer, D.K. 1988. *Simulated Changes in Ground-Water Flow Caused by Hypothetical Pumping in East Carson Valley, Douglas County, Nevada*. USGS Open-File Report 87-765.
- Maurer, D.K. 1988. *Simulated Changes in Ground-Water Flow Caused by Hypothetical Pumping in Southeastern Carson City, Nevada*. USGS Open-File Report 87-769.
- Maxey, G.B. 1964. Hydrostratigraphic units: *Journal of Hydrology*, vol. 2, pp. 124-29.
- McDonald, M.G. and A.W. Harbaugh. 1984. A Modular Three-Dimensional Finite-Difference Ground-Water Flow Model. USGS Techniques of Water-Resources Investigations, Book 6, Chapter A1.
- McPherson, M.B. 1974. *Hydrological Effects of Urbanization*. Paris: UNESCO Press.
- Modica, E. 1995. *Simulated Effects of Alternate Withdrawal Strategies on Ground-Water-Flow Patterns, New Jersey Pinelands*. USGS Water-Resources Investigations Report 95-4133.

Morgan, D.S. and M.D. Dettinger. 1990. *Ground-Water Conditions in Las Vegas Valley, Clark County, Nevada: Part II. Geohydrology and Simulation of Ground-Water Flow*. USGS Open-File Report 90-179.

Morgan, D.S. and J.L. Jones. 1995. *Numerical Model Analysis of the Effects of Ground-Water Withdrawals on Discharge to Streams and Springs in Small Basins Typical of the Puget Sound Lowland, Washington*. USGS Open-File Report 95-470.

Morgan, D.S. and W.D. McFarland. 1994. *Simulation Analysis of the Ground-Water Flow System in the Portland Basin, Oregon and Washington*. Open File Report 94-505, USGS.

Murray, L.C. Jr. and K.J. Halford. 1996. *Hydrogeologic Conditions and Simulation of Ground-Water Flow in the Greater Orlando Metropolitan Area, East-Central Florida*. USGS Water-Resources Investigations Report 96-4181.

National Research Council. 1995. Academia de la investigacion Cientifica, A.C., and Academia Nacional de Ingenieria, A.C. *Mexico City's Water Supply: Improving the Outlook for Sustainability*. National Academy Press: Washington, D.C.

Nelson, A.B. 1989. Hydraulic relationship between a fractured bedrock aquifer and a primary stream, North Carolina Piedmont, in Daniel, C.C., III., White, R.K., and Stone, P.A., eds., *Proceedings of a Conference on Ground Water in the Piedmont of the Eastern United States*, Charlotte, N.C., October 16-18, 1989: Clemson, S.C., Clemson University.

Pfannkuch, H.O. 1969. *Elsevier's Dictionary of Hydrogeology*: Elsevier Publ., New York, p. 168.

Poeter, E.P. and M.C. Hill. 1998. *Documentation of UCODE, A Computer Code for Universal Inverse Modeling*. USGS Water-Resources Investigations Report 98-4080.

Prudic, D.E. 1989. *Documentation of a computer program to simulate stream-aquifer relations using a modular, finite-difference, ground-water flow model*. USGS Open-File Report 88-729.

Reynolds, J.W. and R.K. Spruill. 1995. *Ground-Water Flow Simulation for Management of a Regulated Aquifer System: A Case Study in the North Carolina Coastal Plain*. *Groundwater*, Sept-Oct 1995 v33 n5 p741(8).

Roanoke County Health Department, Vinton, Virginia. Environmental Division. Personal Communication, 1999.

Roanoke Valley Convention & Visitors Bureau, Roanoke, Virginia. 1999. Available at: <http://www.visitroanoke.com>, 1999.

Robinson, J.L., C.A. Journey, and J.B. Atkins. J.B. 1997. *Ground-water resources of the Coosa River basin in Georgia and Alabama—Subarea 6 of the Apalachicola-Chattahoochee-Glnt and Alabama-Coosa-Tallapoosa River basins*: USGS Open-File Report 96-177.

Roy, P. K. *Lucknow*: 1994. *Slow Death of a Water Source*. The Hindu Survey of the Environment.

Rutledge, A.T., and Mesko, T.O., 1996, *Estimated hydrologic characteristics of shallow aquifer systems in the Valley and Ridge, the Blue Ridge, and the Piedmont Physiographic Provinces based on analysis of streamflow recession and base flow*. U.S. Geological Survey Professional Paper 1422-B, 58 p.

Schaefer, D.H. and J.R. Harrill. 1995. *Simulated Effects of Proposed Ground-Water Pumping in 17 Basins of East-Central and Southern Nevada*. USGS Water Resources Investigations Reports 95-4173.

Seber, G.A.F., and C.J. Wild. 1989. *Nonlinear Regression*, John Wiley & Sons, NY, p. 768.

Sepulveda, N. 1995. *Three-Dimensional Ground-Water Flow Model of the Water-Table Aquifer in Vega Alta, Puerto Rico*. USGS Water-Resources Investigations Report 95-4184.

Storm, E.W. and M.J. Mallory. 1994. *Hydrogeology and Simulation of Ground-Water Flow in the Eutaw-McShan Aquifer and in the Tuscaloosa Aquifer System in Northeastern Mississippi*. Water Resource Investigations Report 94-4223, USGS.

Sumner, D.M., Wasson, B.E. and S.J. Kalkhoff. 1987. *Geohydrology and Simulated Effects of Withdrawals on the Miocene Aquifer System in the Mississippi Gulf Coast Area*. USGS Water Resources Investigations Report 87-4172.

Theil, H., 1963. On the use of incomplete prior information in regression analysis: *American Statistical Association Journal*, v.58, no. 302, p. 401-414.

Tiedeman, C.R., D.J. Goode, and P.A. Hsieh. 1998. Characterizing a Ground Water Basin in a New England Mountain and Valley Terrain. *Ground Water*, Vol. 35, No. 4.

Torres-Gonzalez, S., M. Planert, and J.M. Rodriguez. 1995. *Hydrogeology and Simulation of Ground-Water Flow in the Upper Aquifer of the Rio Camuy to Rio Grande de Manati Area, Puerto Rico*. USGS Water Resources Investigations Report 95-4286.

United Nations (U.N.) 1996. Centre for Human Settlements (Habitat), *An Urbanizing World: Global Report on Human Settlements*. Oxford University Press: Oxford, United Kingdom, and New York.

United States Weather Bureau. 1970. Local climatological data—Roanoke, Virginia, annual summary: U.S. Weather Bureau.

World Resources Institute (WRI). 1997. *World Resources 1996-97*. World Resources Institute for the United Nations Development Programme, United Nations Environment Programme, and the World Bank.

United Nations (U.N.) 1995. Population Division, World Urbanization Prospects: The 1994 Revision. U.N.: New York.

Waller, J.O. 1976. Influence of Geology on the Water Resources of the Upper Roanoke River Basin. Dissertation for Doctor of Philosophy in Geological Sciences, Virginia Tech.

Appendices

Appendix A – Model Files

This appendix contains all of the files necessary to run the baseline model simulation. To run the transient model simulation, the same files are necessary, however, the Well Package should not be included in the simulation. The following is a list of the files included on the CD in the file folder labeled “Appendix A”. Some of the files on the CD are not defined here, however, are necessary to run the Visual MODFLOW simulations.

Baseline.BAS – Basic file necessary to run MODFLOW

Baseline.BAT – Batch file that runs MODFLOW independent of Visual MODFLOW

Baseline.BCF – Block-Centered Flow file necessary to run MODFLOW

Baseline.BGT – Binary file that contains flow information for every cell in the model domain

Baseline.BUD – Binary file that contains flow information for every zone defined in the zone budget

Baseline.CLB – Input file that contains input calibration information

Baseline.DDN – Output file that contains drawdown information

Baseline.GHB – General-Head Boundary input file for MODFLOW

Baseline.HDS – Binary file that contains hydraulic head output information

Baseline.LST – Output list file from MODFLOW

Baseline.M**- All files with the extension that begins with “M” are specific to Visual MODFLOW

Baseline.OC – Output control necessary to run MODFLOW

Baseline.RCH – Recharge input file necessary to run MODFLOW

Baseline.STR – Streamflow-Routing input package for MODFLOW

Baseline.V**- All files with the extension that begins with “V” are specific to Visual MODFLOW and translate the graphic information into MODFLOW input files- they are necessary to run the Visual MODFLOW simulation

Baseline.WHS – Solver Package necessary to run MODFLOW for this investigation

All other files are necessary for configuration settings within Visual MODFLOW.

Appendix B – Observed Hydraulic Heads

Hydraulic Head Observations from Waller (1976) Used for Calibration with UCODE

Observation Name	X Location in Model Coordinate System (m)	Y Location in Model Coordinate System (m)	Hydraulic Head Observation (m)
w11	60934.7	31547.5	357.5
w116	48744.3	29596.7	342
w122	49158.9	28844.8	343.8
w123	49696.1	27864.7	345.9
w125	50287.8	27653.7	333.8
w126	50372.6	27231.2	329.8
w132	51834.1	28271.5	335.3
w14	60637.7	33575.7	379.5
w142	56967	23389.3	320.4
w151	59545.2	22587.8	307.2
w179	43125	28030.1	306
w183	45572.7	26070.7	309.4
w185	46696.4	26658.7	304.8
w186	46357.3	28623.5	312.7
w188	46907.6	26975.7	316.9
w189	47203.1	27419.6	316.7
w193	49021.1	25751.4	329.2
w195	49569.9	26850.4	327.7
w201	50500.6	24949.3	316.1
w211	52487.6	23260.1	300.2
w22	61864.5	31294.4	393.8
w221	56081.6	19585.6	290.8
w232	33340.8	31067.3	375.8
w233	34376.4	30560.7	352.9
w242	37905.1	30004.9	320
w251	43003.1	26829.9	301.8
w252	42209	26077.3	307.5
w253	41055	26845.8	341.4
w261	43912.5	25089.4	297.8
w264	43662.3	26830.3	300.5
w274	46655.7	23848.5	288.3
w281	50333.2	21948.9	290.2
w282	49699.7	21272.4	283.8
w283	50207	20934.6	280.4
w284	50249.3	20723.4	282.9
w291	50228.7	19730.3	277.4
w2910	51791.9	20428.4	275.2
w2911	52100.4	20369.4	276.8
w2913	52650.6	18831.5	274.3
w295	50769.3	20377.1	284.9
w298	50862.1	20681.5	288

Hydraulic Head Observations from Waller (1976) Used for Calibration with UCODE
(continued)

Observation Name	X	Y	Hydraulic Head Observation (m)
w301	54290	19314.1	286.5
w331	32411.4	30771	356.3
w341	40849.6	23760.9	361.5
w342	41162.2	23845.6	348.1
w3510	43001.1	22621.1	335.6
w3514	42895	23423.9	329.8
w3517	42387.5	24311	309.4
w354	42600.2	21606.7	336.8
w361	44105.3	20238.3	356.6
w362	43995.2	20677.8	324.6
w363	43593.7	20762.1	324.6
w365	44523.5	20509	330.1
w366	45048.2	19097.9	327.2
w391	41215.6	18977.5	365.8
w393	41181.5	19476.2	344.4
w4012	44165	19283.4	334.1
w408	42622.4	19578.3	329.8
w409	43205.8	19080	352
w41	60724.6	29307.6	364.2
w412	45155.3	16427.3	321.6
w421	37149.7	20293.8	394.1
w431	41461.5	17422.6	352.7
w433	41440.7	16704.2	331.3
w441	46154.3	13199.3	301.8
w452	43991.4	11710.7	306.3
w61	53498.3	29726.1	346.3
w610	54724.1	29093	336.2
w64	53456.5	28838.7	334.7
w72	56077.7	26727.2	310.3
w82	59204.9	26475.4	356.6
w91	62967	24702.7	363.6

Hydraulic Head Observations from the Montgomery County Health Department, Well Driller Logs (1999)

Observation Name	X	Y	Hydraulic Head Observation (m)
G108	8674.81	27967.8	575
G109	11483.2	26341.4	510
G110	14677	24342	485
G121	6240.64	24345.3	650
G2	21994.2	19903.3	475
G28	16749.7	42845.1	516.8
G3	6670.14	25546.5	640
G30	20765.7	40027.2	444.3
G32	29198	42019.3	504.9
G33	28794.1	36436.7	415.6
G4	23217.9	43615.3	502.2
G41	15489	41290.4	501.7
G45	23951.5	36425.5	467
G53	28797.5	26347.9	463.8
G59	25164.9	29965.6	450
G6	12689.3	35194.4	452.6
G7	21534.8	30379	442.2
G80	11490.9	31605.6	506.9
G81	14700.3	28789.8	550
G97	17490.3	23921.5	475
G98	20721.9	22316.5	440

Appendix C – C++ Programs

All of the C++ programs used to manipulate the input data for the model development are included on the CD in the file folder labeled “Appendix C”. Within this folder, there are four separate folders labeled: “gridprogram”, “headsprogram”, “krprogram”, and “segmentsforrouting”. A description of each program is included below. The files included on the CD are the *.cpp files, or the actual program files that can be viewed in any C++ editor.

- Gridprogram – C++ program written to resample the original data array for land surface elevation (30m resolution) to the necessary resolution of 402.4m. This program re-samples the data at the new resolution at a 35 degree CCW angle from the UTM NAD 27 coordinate system of the original data. The program was written to meet the requirement within MODFLOW that the model domain must be aligned along the principle direction of anisotropy.
- Headsprogram – C++ program written to be run with the output data set from the Gridprogram. In the process of re-sampling, it was possible for river cells to not necessarily be located in valleys as they are in the natural system. Since the re-sampling program averages the elevations of all of the cells included in the new cell, the land surface was distorted. This program reads a list of the river cells, and makes the necessary adjustments to assure that these cells are located in valleys, and that the cells immediately adjacent to them have higher land surface elevations.
- Krprogram – C++ program written to divide the General-Head Boundaries into six sections depending upon their location in the model domain. This was necessary to avoid separating the 586 river cells manually. This program divides the 586 river cells into the six sections through user defined locations.
- Segmentsforrouting – C++ program written to assist in the creation of the Streamflow-Routing input file. Visual MODFLOW has the ability to run the Streamflow-Routing module, however, does not support the creation of the input file within the graphical user interface. Therefore, it was necessary to create the file by hand. The river network had to be divided into “segments” and “diversions” as defined in the Streamflow-Routing Package manual (Prudic, 1989). This program was written to avoid this file creation manually, and categorized all of the river cells into segments and diversions, and included the appropriate routing information necessary.

Appendix D – Regression Analysis

REGRESSION ANALYSIS – INITIAL HEADS FOR ROANOKE COUNTY

SIMPLE LINEAR REGRESSION

General Linear Models Procedure

Dependent Variable: SURF

Source	DF	Sum of Squares	Mean Square	F Value	Pr > F
Model	3	2792651.50310191	930883.83436730	1297.55	0.0001
Error	2936	2106338.29221681	717.41767446		
Corrected Total	2939	4898989.79531873			
	R-Square	C.V.	Root MSE		Surf Mean
	0.570046	7.746310	26.78465371		345.77308201

Source	DF	Type I SS	Mean Square	F Value	Pr > F
DEM	1	1778104.96457519	1778104.96457519	2478.48	0.0001
DEM*DEM	1	787034.73446708	787034.73446708	1097.04	0.0001
DEM*DEM*DEM	1	227511.80405966	227511.80405966	317.13	0.0001

Source	DF	Type III SS	Mean Square	F Value	Pr > F
DEM	1	466296.41387527	466296.41387527	649.97	0.0001
DEM*DEM	1	315059.08730617	315059.08730617	439.16	0.0001
DEM*DEM*DEM	1	227511.80405966	227511.80405966	317.13	0.0001

Parameter	Estimate	T for HO: Parameter=0	Pr > T	Std Error of Estimate
INTERCEPT	-234.5173001	-12.23	0.0001	19.18209786
DEM	2.8684550	25.49	0.0001	0.11251308
DEM*DEM	-0.0043563	-20.96	0.0001	0.00020788
DEM*DEM*DEM	0.0000022	17.81	0.0001	0.00000012

REGRESSION ANALYSIS – INITIAL HEADS FOR MONTGOMERY COUNTY (WEST SIDE OF STUDY AREA)

SIMPLE LINEAR REGRESSION

General Linear Models Procedure

Dependent Variable: head

Source	DF	Sum of Squares	Mean Square	F Value	Pr > F
Model	3	90687.3091	30229.1030	14.05	<.0001
Error	22	47342.6937	2151.9406		
Corrected Total	25	138030.0027			

R-Square	Coeff Var	Root MSE	head Mean
0.657012	10.28917	46.38901	450.8527

Source	DF	Type I SS	Mean Square	F Value	Pr > F
elev	1	57145.23532	57145.23532	26.56	0.0001
elev*elev	1	16197.40904	16197.40904	7.53	0.0119
elev*elev*elev	1	17344.66470	17344.66470	8.06	0.0095

Source	DF	Type III SS	Mean Square	F Value	Pr > F
elev	1	10010.53519	10010.53519	4.65	0.0422
elev*elev	1	14413.92367	14413.92367	6.70	0.0168
elev*elev*elev	1	17344.66470	17344.66470	8.06	0.0095

Parameter	Standard Estimate	Error	t Value	Pr > t
Intercept	1007.351474	366.2855826	2.75	0.0117
elev	-4.176092	1.9362283	-2.16	0.0422
elev*elev	0.008313	0.0032122	2.59	0.0168
elev*elev*elev	-0.000005	0.0000017	-2.84	0.0095

Appendix E – UCODE files

The files created for the UCODE execution are included on the CD in the file folder labeled “Appendix E”. An explanation of the files follows:

Baseline._** - All files with an extension that begins with _ contain UCODE output information specific to phases executed with UCODE.

Baseline._OT – Output file that contains all of the output information for the UCODE execution. All sensitivities and output iteration information is included in this file.

Baseline.EXT – Extract file necessary to run UCODE. A user-defined file that navigates through the MODFLOW output to extract the output hydraulic head values to match observation data.

Baseline.PRE – Prepare file necessary to run UCODE. A user-defined file that defines the parameters estimated and perturbed during UCODE execution.

Baseline.UNI – Universal file necessary to run UCODE. A user-defined file that contains guidelines for UCODE execution. This file also defines universal parameters included in the parameter estimation, and the observed data used for the calibration.

The folder labeled “templates” contains the template files used in the execution of UCODE. These files are necessary to create the new input files when UCODE performs perturbations on the estimated parameters.

Appendix F – MODFLOW and HSPF Interaction

This investigation is a component of a larger multidisciplinary project funded jointly by the EPA and NSF. The other subgroups involved were the Agricultural Economics, Surface Hydrology, Hydraulics, Biology, and GIS subgroups. A list of various land-use patterns resulting from the changes occurring in the watershed has been developed by the investigators. These land use patterns will be representative of projected urban development and associated commercial and industrial development in the watershed.

The Surface Hydrology subgroup is using HSPF (Hydrologic Simulation Program—Fortran) to model the surface hydrology of the watershed. They simulated the effects of the land use patterns on the surface flow. In addition to simulating runoff, HSPF contains a rough representation of the subsurface hydrology as well. The simulations have provided an estimation of subsurface contribution to the aquifer system, or the recharge component in MODFLOW. The surface simulations however, have been concentrated only in the Back Creek Subwatershed (figure AF1). Therefore, an estimation of recharge will be used for areas that occur outside of Back Creek until surface water simulations have been conducted for all of the subwatersheds within the Upper Roanoke River Watershed.

There are problems associated with the use of HSPF output as direct input for the MODFLOW simulations. HSPF uses both a different spatial and temporal scales than MODFLOW. These scale differences occur due to the nature of the two models.

The different spatial scales of the models are associated with the fact that HSPF is a lumped parameter model and MODFLOW is a distributed model. HSPF simulates an area of land as a single unit, assigning parameters that apply everywhere within that given area. Therefore, the output resulting from the surface simulation will be a volume of water that is recharging the aquifer system. However, MODFLOW is a discrete model, representing the system as a number of discrete cells. The HSPF output will have to be subdivided to various cells that are within the Back Creek boundary. This redistribution of the lumped recharge values currently is being conducted through the use of a C++ program to ensure that the impervious areas are represented in the MODFLOW simulation as well. Automation of this redistribution would require a program to link the two models and to translate the output of one to the input to the other which is beyond the scope of this project.

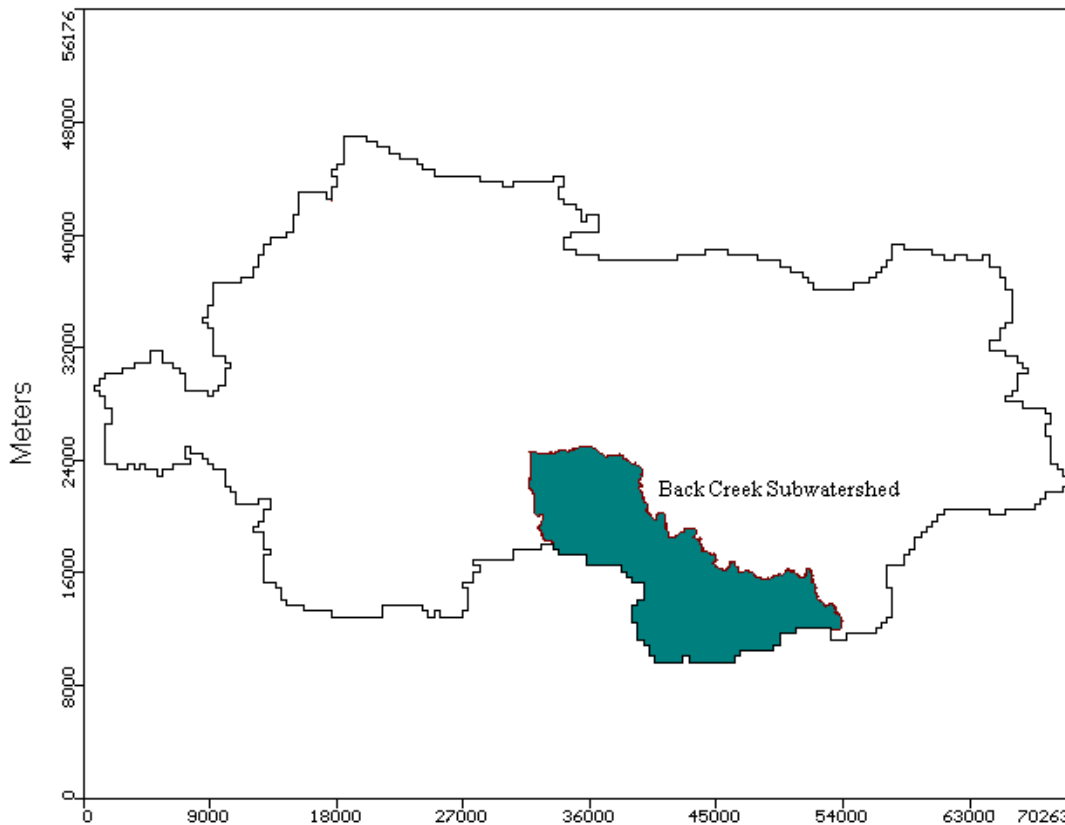


Figure AF1. Back Creek Subwatershed within the Upper Roanoke River Watershed

HSPF and MODFLOW also operate on different time scales. HSPF is a continuous model that is run on an hourly time-step in this study. Surface runoff occurs more quickly than groundwater runoff or baseflow, and therefore it is appropriate to use such a short time-step. However, since MODFLOW simulates groundwater flow, it is typically not run on an hourly basis. Groundwater reacts more slowly to changes in recharge and other parameters that change the stresses on the system because groundwater flow is much slower than surface water flow. MODFLOW simulations are divided into user specified “stress periods” which represent the duration of a constant stress acting on the system, such as a pumping well at a specific rate for a specified period of time. These “stress periods” are then divided into time-steps, however, a weekly time-step is more appropriate for a groundwater flow model at this scale than the hourly time-scale used in the HSPF model. Therefore, the HSPF output, must be lumped into a larger time-step for MODFLOW simulations in order to maintain consistency between the two models.

HSPF includes a simulation of the subsurface flow regime with a system of simplified user input parameters. It represents storage and runoff in the unsaturated zone as well as the saturated zone. The parameter used as the input to MODFLOW is the parameter AGWI (active groundwater inflow) which represents water that is entering the saturated zone. HSPF has a simple saturated-zone model, however, MODFLOW represents the system more accurately and should provide the subsurface contribution to nearby streams more accurately.

There are some inconsistencies with the conceptualization of this methodology. The groundwater surface, represented in MODFLOW changes dynamically throughout the simulation. The fluctuation of the water table changes the storage capacities of the unsaturated zone, and the volumes of interflow leaving this zone. However, this information is not taken into account during the HSPF simulations. This overlap of HSPF and MODFLOW can only be overcome if the models run simultaneously and exchange information about the position of the water table dynamically throughout a simulation. This inconsistency cannot be overcome without significant effort to create an interface between the models, a task that is beyond the scope of this report. Therefore, the change in the unsaturated storage due to water table fluctuations is ignored. Figure AF2 shows the interaction between the two models.

MODFLOW AND HSPF INTERACTION

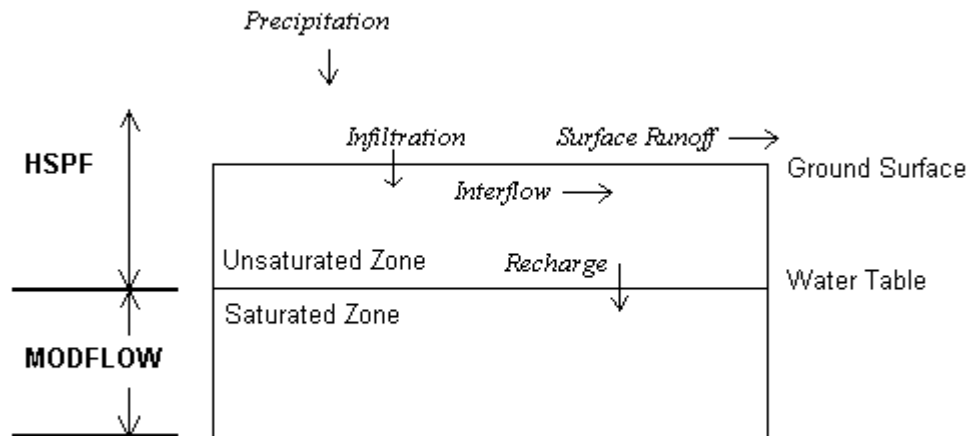


Figure AF2. MODFLOW and HSPF Interaction

During the transient simulations, when the output from HSPF is being used as input to MODFLOW, the recharge values conceptually account for a decrease in the amount of pervious land within the watershed. However, the subsurface flow regime is affected by urbanization in two ways: a decrease in recharge due to an increase in impervious areas (represented in the HSPF recharge values), and an increase in withdrawal due to the increase in population and associated water demand.

Vita

Victoria Ann Barone

Victoria Ann Barone was born on December 21, 1975 in Littleton, NH. After spending her childhood living all over the country, her family settled in Woodbridge, Virginia. She graduated from Woodbridge Senior High School with an advanced degree in May 1994. She entered Virginia Polytechnic Institute and State University as a General Engineering student in August 1994. In the spring of 1995, she decided to pursue a degree in Biological Systems Engineering. She was identified as a candidate for a program within the university that allows advanced students to earn both a Bachelor's degree and a Master's degree in 5 years, and was accepted as a graduate student in the Biological Systems Engineering Department during the fall of 1997. She graduated Magna Cum Laude with a Bachelor's degree in Biological Systems Engineering in May 1998. She completed her work and received her Master's degree in January 2000.